August 2016

First Major Appearance of Brachiopod-Dominated Benthic Shelly Communities in the Reef Ecosystem during the Early Silurian

Cale A.C. Gushulak
The University of Western Ontario

Supervisor
Dr. Jisuo Jin
The University of Western Ontario

Joint Supervisor
Dr. Rong-yu Li
The University of Western Ontario

Graduate Program in Geology

A thesis submitted in partial fulfillment of the requirements for the degree in Master of Science

© Cale A.C. Gushulak 2016

Recommended Citation

Gushulak, Cale A.C., "First Major Appearance of Brachiopod-Dominated Benthic Shelly Communities in the Reef Ecosystem during the Early Silurian" (2016). *Electronic Thesis and Dissertation Repository*. 3972.
https://ir.lib.uwo.ca/etd/3972

Abstract

The early Silurian reefs of the Attawapiskat Formation in the Hudson Bay Basin preserved the oldest record of major invasion of the coral-stromatoporoid skeletal reefs by brachiopods and other marine shelly benthos, providing an excellent opportunity for studying the early evolution, functional morphology, and community organization of the rich and diverse reef-dwelling brachiopods. Biometric and multivariate analysis demonstrate that the reef-dwelling *Pentameroides septentrionalis* evolved from the level-bottom-dwelling *Pentameroides subrectus* to develop a larger and more globular shell. The reef-dwelling brachiopods in the paleoequatorial Hudson Bay Basin were more diverse than contemporaneous higher latitude reef-dwelling brachiopod faunas, with ten distinct community associations recognized in the Attawapiskat Formation. The absence or paucity of hurricane-grade storms in the paleoequatorial Hudson Bay Basin is interpreted as a major factor in the evolutionary success of the reef-dwelling brachiopods in the Attawapiskat Formation.

Keywords

Reef-dwelling brachiopods, early Silurian, paleoecology, evolution, Laurentia

Co-Authorship Statement

A more succinct version of Chapter 3 "The Paleolatiudinal morpho-gradient of *Pentameroides* in Telychian Laurentia" has been published by Gushulak, C.A.C., Jin, J., and Rudkin, D.M. in the Canadian Journal of Earth Sciences under the title "Paleolatitudinal morpho-gradient of the early Silurian brachiopod *Pentameroides* in Laurentia." J. Jin provided assistance with the interpretation of results and editing of the manuscript while D.M. Rudkin provided additional information on the geology of the Attawapiskat Formation and editing the manuscript.

Acknowledgments

I would not have been able to finish this thesis without the support and encouragement from many people. First, I would like to thank my supervisors Dr. Jisuo Jin and Dr. Rong-yu Li. Dr. Jin's advice and support over these last two years have been an immense help to me. Although not in London, I always appreciated Dr. Li's support from Manitoba and friendly meetings when I was back home.

I would like to thank Dr. Paul Copper for kindly making his fossil collections from Manitoulin and Anticosti islands freely available during this project. I also thank Mr. David Rudkin and Mr. Peter Fenton from the Royal Ontario Museum for their guidance and assistance in field work on Akimiski Island and the James Bay lowlands. Mr. Rudkin is thanked again for his input on Chapter 3 of this thesis and the subsequent publication. I also thank the territorial government of Nunavut for allowing access to Akimiski Island. Logistics and funding support for the Hudson Bay lowlands fieldwork were provided by the Ontario Ministry and Natural Resources and the Natural Sciences and Engineering Research Council of Canada.

I would like to thank my lab-mates Nikole Bingham-Koslowski, Shuo Sun, and Colin Sproat. It has been great working with you over the past two years. Special thanks to Colin for dealing with my rants and explaining how cameras work.

I thank the Western Taekwondo Club for accepting me into their family with open arms and being great friends during my time at Western. Apologies are given if I have kicked any of you too hard, graduate work can be stressful.

Finally, I need to thank my family for their continuing and unwavering support of academic goals. Without your encouragement I would not have had the courage to move across the country and complete this degree.

Table of Contents

List of Tables

List of Figures

List of Equations

List of Appendices

Chapter 1 – Introduction

1.1 Introduction

The early Silurian (Llandovery) was a time of intense climatic, oceanic, and biological change from cool temperatures, low sea-level, and extinction recovery fauna to a stable greenhouse environment (Rong et al. 2006; Haq and Schutter 2008; Finnegan et al. 2011; Harper et al. 2014). The preceding Ordovician Period experienced super-greenhouse conditions during its Early and Middle epoches due to extremely high levels of atmospheric carbon dioxide (Berner 1990; Berner and Kothavala 2001), but cooled during the Late Ordovician, terminating in a short-lived but intense glaciation (Brenchley et al. 1994; Finnegan et al. 2011; Harper et al. 2014). This initial warmth, combined with rampant sea floor spreading and a high degree of continental dispersal resulted in the highest sea levels of the Phanerozoic (Hallam 1992; Miller et al. 2005; Haq and Schutter 2008) which created expansive intracratonic seas over much of modern North America (Laurentia), Europe (Baltica/Avalonia), Siberia, and China. (Miller et al. 2005). The organisms that came to inhabit these tropical seas, especially the predominant marine benthic invertebrates (e.g. corals, brachiopods, bryozoans, bivalves, trilobites, echinoderms), became highly specialized to their specific environment, resulting in a high degree of endemicity (Sheehan and Coorough 1990; Jin et al. 2014; Candela 2014). The diversity of these environments declined sharply at the end of the Ordovician when approximately 85% of all marine species went extinct due to climate cooling and a dramatic fall in sea level (Raup and Sepkoski 1982; Hambry 1985; Alroy et al. 2008;

Alroy 2010; Finnegan et al. 2011; Harper et al. 2014). By the end of this biological

catastrophe low temperatures, sea-level, and biodiversity typified global marine

environments (Munnecke et al. 2010). Organisms that did survive this extinction event

quickly evolved and diversified by middle Llandovery time and dispersed widely in the

epeiric seas that re-flooded the interiors of tropical continents. The rapid expansion of

marine organisms in the early Silurian resulted in a notably higher degree of

cosmopolitanism compared to the highly endemic Late Ordovician faunas (Berry and

Boucot 1973; Sheehan and Coorough 1990; Rong et al. 2007).

One ecosystem of particular importance during this time was represented by

coral-stromatoporoid reefs, which first evolved during the Late Ordovician (Copper et al.

2013), and were the first metazoan-built reefs that became associated with highly diverse,

brachiopod-dominated, benthic communities (Chow and Stearn 1988; Jin et al. 1993; Jin

2002). The early Silurian benthic shelly communities of North America (Laurentia) and

Europe (Baltica) were dominated by large-shelled pentameride brachiopods in both the

level-bottom (carbonate or siliciclastic) and reefal ecosystems. The taxonomy and

paleoecology of these brachiopods have been studied for several decades, resulting in a

comprehensive understanding of the taxonomic composition and community organization

of early Silurian level-bottom communities (Ziegler 1965; Ziegler et al. 1968; Johnson

1977, 1980; Jin et al. 1993; Watkins 1998; Jin and Copper 2000; Jin 2008). Despite the

large amount of previous work on the Llandovery level-bottom brachiopods, reef-

dwelling brachiopods have been little-studied from a paleoecologic viewpoint. The goal

of this thesis is to examine the functional morphology, community structure, and

diversity of specific lineages of reef-dwelling brachiopods from the early Silurian of

Laurentia and Baltica and compare them to contemporaneous level-bottom species and communities. Examination of the differences and connections between the brachiopods of level-bottom and reef environments during a period of climatic and faunal recovery will help us gain a better understanding of the middle Paleozoic reef ecosystem.

1.2 The Silurian World

The Llandovery (444–433 Ma) was the first epoch of the Silurian Period and immediately followed the latest Ordovician (Hirnantian) glaciation and mass extinction event. The early part of the Llandovery experienced fluctuating warm and cool episodes, due to small-scale glaciations (much smaller than those of the Hirnantian) in what is now South America and North Africa (Hambrey 1985; Grand and Caputo 1992; Azmy et al. 1998; Sheehan 2001; Finnegan et al. 2011). By the end of the epoch, however, climate conditions had improved sufficiently for the recovery faunas to reach their pre-extinction levels of diversity.

1.2.1 Paleogeography and Tectonism

The configuration of the Earth's continents during the Silurian was markedly different than that of today (Fig. 1.1). Earth's landmass area was dominated by the supercontinent Gondwana which consisted of modern day South America, Africa, Antarctica, Arabia, India, Australia, and much of Southern Europe (Torsvik and Cocks 2013). This
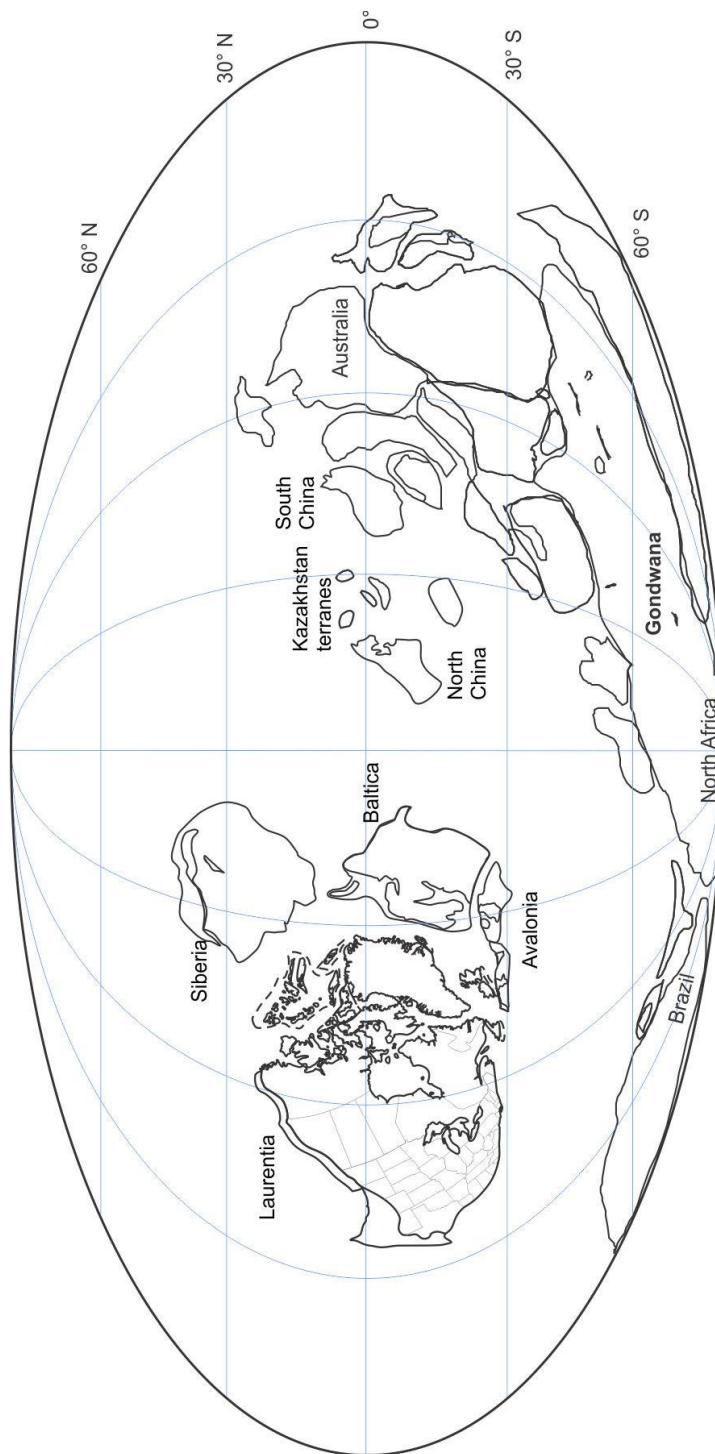
Figure 1.1: Global paleogeography during the Llandovery (440 Ma). Major continents and continental blocks are labelled. Modified from Torsvik and Cocks 2013, Domeier 2016.

supercontinent covered the South Pole and stretched north past the Equator in the Eastern

Hemisphere.

The tropical regions of the planet had much less landmass and consisted of

subcontinental blocks and island chains (now part of North and South China and Central

Asia), as well as a few larger continents (Siberia, Baltica, and Laurentia) in the tropical

Western Hemisphere. Laurentia consisted of the majority of modern day North America

and Greenland, with additional peri-continental terranes such as Scotland and the

northern part of Ireland, and Baltica (now most of northern and central Europe with the

addition of Novaya Zemlya). By the beginning of the Silurian, Baltica had collided with

the small continent Avalonia (which now makes up England and Wales, the southern part

of Ireland, Newfoundland, Acadia, and Maine), and was moving towards Laurentia

(Torsvik and Cocks 2013). The Northern Hemisphere was dominated by a semi-global

ocean with no significant land masses occurring above 40° north.

Laurentia was rotated ~80° clockwise compared to modern North America's

orientation, with the modern eastern margin facing south. The continent was almost

entirely tropical, extending from 10° north to 30° south of the Equator itself, passing

through modern day North Greenland, the Arctic Archipelago, Manitoba, Wyoming,

Utah, and Nevada (Torsvik and Cocks 2013; Jin et al. 2013). The tectonic character of the

continental margins were different as the southeastern (modern eastern) margin of

Laurentia was tectonically active and had been the location of the Taconic orogeny

during the Ordovician (van Staal et al. 2007). During the Silurian this margin was an

active subduction zone, resulting in Laurentia and Baltica to move towards each other

and subsequently colliede and suture by the mid-Devonian. This tectonic event, called the

Caledonian orogeny, began at the eastern margin of the Laurentia (modern Greenland) and progressed towards the south and west until Laurentia, Baltica, and Avalonia combined to form one continent known as Laurussia by Middle Devonian time (McKerrow et al. 2000). This culminated in the final closure of the Iapetus Ocean, a body of water which had formed when Laurentia broke off from Rodinia several hundred million years earlier (Powell et al. 1993). There was significantly less exposed land in early Silurian Laurentia than in modern day North America, with shallow tropical seas in intracratonic basins occupying up to 65% of the Laurentian craton (Johnson 1987).

1.2.2 Climate and Sea Level

The Early–Middle Ordovician was a predominantly super-greenhouse world. High levels of carbon dioxide which increased temperature combined with rapid and extensive sea floor spreading which displaced large volumes of ocean water resulted in the highest sea levels of the Phanerozoic (Johnson 2006; Haq and Schutter 2008). These conditions came to an end in the Late Ordovician when the climate cooled, terminating in the Hirnantian glaciation (Brenchley et al. 1994; Sheehan 2001; Finnegan et al. 2011). The cause of these glaciations is debated, but it is likely that atmospheric carbon drawdown lowered global temperatures enough to cause the glaciations. Suggested causes of this carbon drawdown range from increased weathering rates for silicate rocks caused by the Taconic Orogeny (Kump et al. 1999) to extensive carbonate production and organic carbon burial in the shallow epeiric seas (Patzkowsky et al. 1997). The temperature fall resulting from this carbon drawdown was dramatic, with tropical sea temperature falling by approximately 5°C in the Hirnantian (Finnegan et al. 2011).

Global-scale cooling manifested dramatically in the formation of large-scale ice caps over the South Pole (modern day Brazil and North Africa), thought to have exceeded the Pleistocene glaciations in terms of ice volume (Finnegan et al. 2011). The formation of these ice caps caused global sea level to fall drastically, with some estimates claiming a greater than 120 m short-term fall (Haq and Schutter 2008). This regression caused the draining of intracratonic seas and the extinction of many groups of shallow marine organisms that formerly inhabited these environments (Hallam and Wignall 1999; Barash 2013; Harper et al. 2014).

During the Llandovery and early Wenlock, the world was still experiencing episodic but minor icehouse conditions that typified the Late Ordovician (Brenchley et al. 1991; Brenchley et al. 1994; Sheehan 2001; Calner 2008; Finnegan et al. 2011), but there was an overall rise in sea-level and temperature, punctuated by fluctuations, during this epoch (Fig. 1.2; Azmy et al. 1998; Johnson 2006; Haq and Schutter 2008; Munnecke et al. 2010; Clayer and Desrochers 2014; Trotter et al. 2016). By the end of the Llandovery, tropical ocean surface temperatures had reached approximately 33°C while long-term sea-level had risen by 80 m since the low-stand at the end of the Ordovician (Haq and Schutter 2008; Cummins et al. 2014). This warming trend reached its zenith in the middle Telychian before entering a cooling trend in the late Telychian, culminating in an early Wenlock glaciation (Calner 2008; Lehnert et al. 2010). The cause of this cooling trend is currently being investigated, but rapidly changing oxygen isotopic ratios across this time suggest short term dramatic climatic alterations (Lehnert et al. 2010). These cooler temperatures may have triggered increased reef growth as modern-day hermatypic corals reject their zooxanthellae photosymbiotes in extreme warmth. If this phenomenon
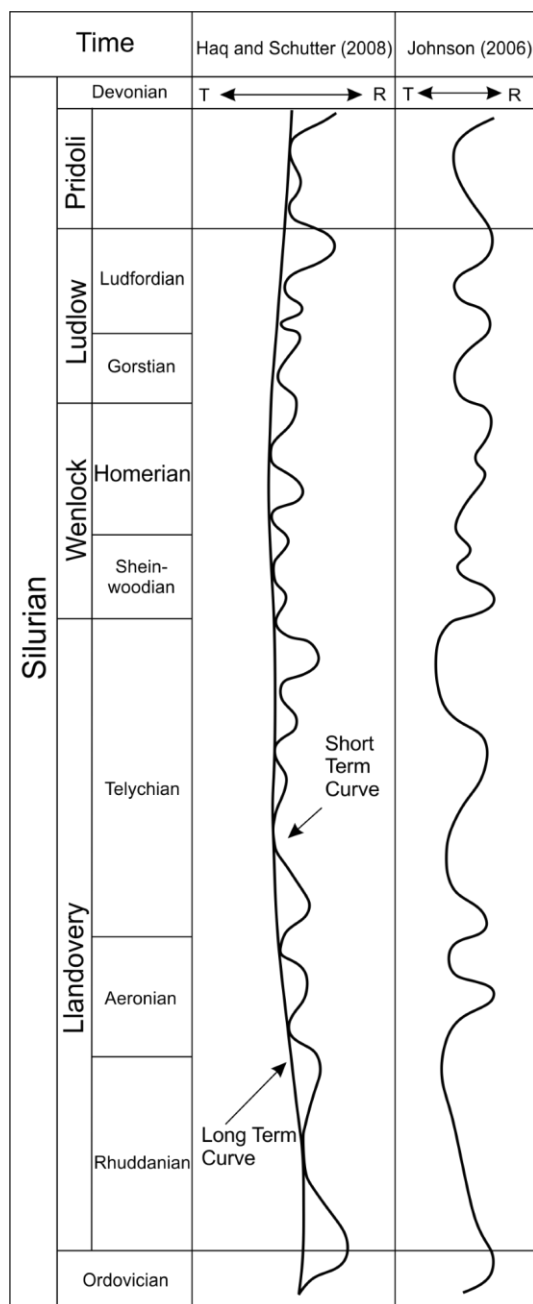
Figure 1.2: Simplified sea-level curve for the Silurian. T: transgression, high sea-level; R: regression, low sea-level. Data from Haq and Schutter 2008 and Johnson 2006. Modified from Johnson 2010.

occurred in the Paleozoic then an overall cooler climate that is similar to modern oceans may have provided optimum climatic conditions for the proliferation of coral reef growth in the late Llandovery (Trotter et al. 2016).

1.2.3 Oceanic Circulation and Chemistry

Ocean chemistry and circulation were in flux during the Late Ordovician and early Silurian due to the intense climatic changes. High-latitude ocean cooling initiated a thermally driven ocean circulation system. This, although typical of modern oceans, constituted a major change from the poor circulation of earlier Ordovician oceans (Hammarlund et al. 2012; Harper et al. 2014). This resulted in anoxic water from the deep ocean upwelling onto the continental shelves that ultimately triggered a secondary extinction event in the latest Ordovician (Hallam and Wignall 1999; Hammarlund et al. 2012).

The Silurian has been thought to have been relatively stable in terms of ocean chemistry, but new data suggests that the Silurian was equally chemically volatile as other time periods throughout earth history. Three positive oxygen excursions (Early Aeronian, Late Aeronian and Early Wenlock) and four carbon excursions (Early Wenlock, Late Wenlock, Late Ludlow, and Silurian–Devonian boundary) appear throughout the Silurian suggesting that changes to the global atmosphere-ocean system were much more common in the Silurian than previously thought (Azmy et al. 1998; Calner 2005, 2008; Munnecke et al. 2010). Changes in oxygen isotope composition within the Llandovery suggests periods of small-scale glaciations and sea-level fall as

they correlate to glacially deposited diamictites from South America (Gran and Caputo 1992; Azmy et al. 1998). The carbon excursions of the Silurian appear to correlate with minor extinctions of planktonic and nektonic organisms; chiefly graptolites and conodonts (Calner 2005, 2008). These minor Silurian extinction events are the Ireviken Event (Early Wenlock), the Mulde Event (Late Wenlock), and the Lau Event (Late Ludlow; Fig. 1.3; Munnecke et al. 2003; Calner 2005, 2008).

1.2.4 Silurian Recovery Fauna

The end Ordovician mass extinction was the second largest mass extinction of the Phanerozoic, as up to 85% of all marine species went extinct (Raup and Sepkoski 1982), although recent data suggested that the severity was somewhat lower (Alroy et al. 2008; Alroy 2010). The reason for the intense loss of biodiversity stems from the stepwise nature of this extinction event. First, cool temperatures and a sea level regression restricted the ecospace available to the highly endemic organisms adapted to the shallow intracratonic tropical seas which resulted in their extinction (Sheehan and Coorough 1990; Servais et al. 2010). During the latest Ordovician, the Hirnantian fauna, which originated from high latitude, cool water regions, invaded the tropics as the tropical organisms died out (Rong and Harper 2002; Harper and Rong 2008). This fauna, however, was to be adversely affected by the second-pulse extinction when the Gondwana ice cap decayed during climate warming and sea level rose during the latest Hirnantian and into the early Silurian (Munnecke et al. 2010; Harper et al. 2014). The lineages that survived the entire extinction event did so on the continental margins where seas were not completely drained or rendered largely anoxic. These marginal refugia
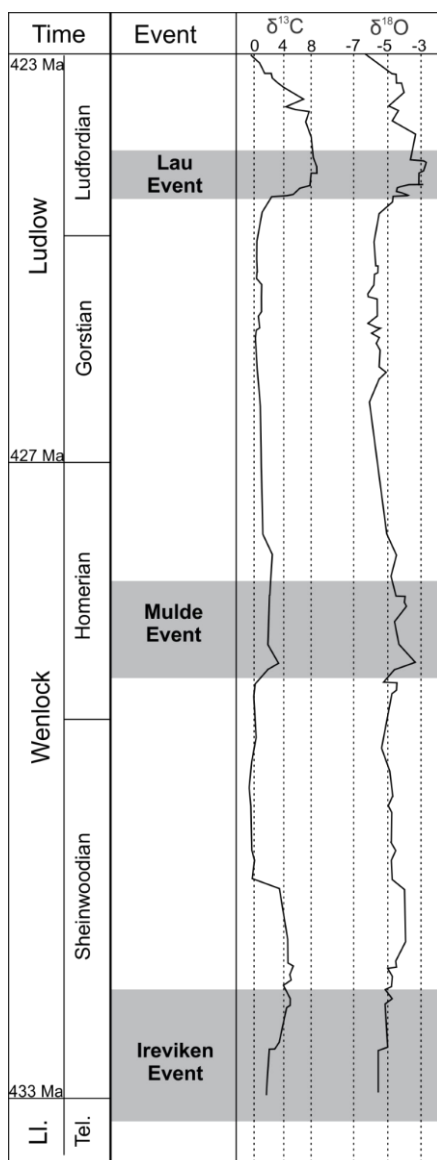
Figure 1.3: $\delta^{13}C$ and $\delta^{18}O$ curves during the Silurian with major geochemical events highlighted. Values are measured in (‰). Ll: Llandovery, Tel: Telychian. Modified from Calner et al. 2004.

acted as focal points for faunal recovery after the extinction events in the Llandovery (Jin et al. 2007).

The early Silurian fauna shares many of the typical characteristics of recovery faunas including low diversity, composed of generalist taxa, small body sizes, and a low degree of community zonation (Copper 1988; Erwin 1998; Rong et al. 2006). Compared to their Late Ordovician counterparts, the Llandovery faunas are known for their high degree of cosmopolitanism and large-scale biogeographical provinces (Berry and Boucot 1973; Sheehan 1975; Sheehan and Coorough 1990). For example, the Aeronian pentameride brachiopod faunas can be separated into distinct Laurentian and South China faunas, while the remainder of the world's brachiopods form a third faunal province (Rong et al. 2007). In addition, the earliest Silurian fauna (pre-Telychian) consists of a much smaller number of taxa than the pre-extinction Late Ordovician fauna due to the extinction of approximately 100 species of bryozoans, 50 genera of trilobites, and 150 genera of rhynchonelliformean brachiopods (51% of genera during the first stage of extinction, 41% in the second stage; Rong et al. 2006) by the end Ordovician (Servais et al. 2010), indicating a protracted interval (~ 5 million year) of post-extinction recovery. Several brachiopod taxa that survived one or more extinction pulses did not recover during the Silurian (51 Hirnantian genera, 13 Rhuddanian genera) adding to the great taxonomic loss of this extinction event (Rong et al. 2006).

Despite the great taxonomic losses of the end Ordovician mass extinction, ecologically the extinction was minor (Sheehan 2001; McGhee et al. 2012). The short trophic chains dominated by filter feeding organisms that had developed in the Ordovician remained virtually unchanged into the earliest the Silurian (Droser et al.

1997; Munnecke et al. 2010). Ecological stability across the extinction event is shown in reef recovery because these generally fragile systems recovered relatively quickly within the span of 3–4 million years with the first Silurian-type patch reefs reappearing in the mid-Aeronian in Laurentia and South China (Copper 1994, 2001; Copper and Jin 2012; Wang et al. 2014). By the end of the Telychian reefs had spread throughout the paleotropics and had become invaded by highly diverse, brachiopod-dominated, benthic faunas (Suchy and Stearn 1993; Jin et al. 1993; Watkins 1998, 2000).

1.3 Brachiopods and their Importance as Paleoecological Indicators

Brachiopods are a large and diverse group of lophophore-bearing, double-valved, marine, sessile animals which have a continuous range from the Cambrian to today. In modern ecosystems brachiopods are predominantly found in deep oceans, or cool- to cold-water shallow seas as they have been largely excluded from shallow tropical carbonate or reefal environments by modern bivalve molluscs (Richardson 2002). In the Paleozoic, however, brachiopods were common, often dominant, components of the suspension filter feeders in tropical carbonate level-bottom and reefal ecosystems (Watkins 2000). Rhynchonelliform brachiopods formed a major part of the 'Paleozoic fauna' (Sepkoski 1984) and experienced significant diversification during the Ordovician as part of the Great Ordovician Biodiversification Event (GOBE; Servais et al. 2010; Harper et al. 2013). Despite being heavily affected by the end Ordovician mass extinction, brachiopods as a group recovered well and became important components of the Silurian and Devonian coral-stromatoporoid reef systems (Watkins 2000; Cocks and Rong 2007). Following the late Devonian mass extinction and the destruction of these

reef systems, brachiopods still flourished in the generally cooler conditions of the Carboniferous and Permian periods (Schubert and Bottjer 1995; Shen et al. 2006). At the end of the Paleozoic the Permo-Triassic mass extinction finally reduced the brachiopods to a minor component in tropical shallow marine communities in the Mesozoic and Cenozoic (Shen et al. 2006) when the morphologically and physiologically more complex bivalves took over these niches (Sepkoski 1984; Sepkoski and Miller 1985). The complexity of the bivalves, however, did not directly contribute to their modern success. It has instead been shown that the bivalves are more successful in modern environments simply because they did better during the Permo-Triassic extinction and were therefore more diverse at the start of the Mesozoic (Gould and Calloway 1980). Reasons for the bivalves' success during the extinction event include their resistance to turbidity or their infaunal mode of life, although the issue is still a matter of controversy. Overall the brachiopods are one of the most successful groups of animals in the Phanerozoic with their simple and conservative body plan (two valves protecting internal organs and a pair of lophophores used for feeding and respiration) remaining stable since their origin.

As one of the predominant fossil groups during the Paleozoic, brachiopods are important tools for paleoecological and paleobiogeographical investigations. The sessile nature of brachiopods means that they must be perfectly adapted to the conditions of the habitat following larval settlement on the sea floor. Evolutionarily, this causes brachiopods to have a wide variety of outer morphological characteristics (shell size, globosity, convexity, and shell-substrate relationships, etc.) that vary according to characterisitcs of their surrounding environment. This relationship between morphology and environment has been used widely for interpreting water depth, storm frequency,

water energy level, and water temperature based on the paleogeography and shell characteristics of brachiopods (e.g. Ziegler 1965; Ziegler et al. 1968; Rudwick 1970; Boucot 1975; Johnson 1980, 1987; Brett et al. 1993).

1.3.1 Pentameride Brachiopods in the Silurian

Pentameride brachiopods (Order Pentamerida Schuchert and Cooper, 1931) are characterized by generally large, biconvex, impunctate shells, with a short hinge line and a spondylium in the ventral valve (Carlson et al. 2002). This order is divided into two suborders, the Syntrophiidina Ulrich and Cooper, 1936, which first appeared in the middle Cambrian, and the Pentameridina Schuchert and Cooper, 1931, which first appeared in the Late Ordovician, but became very diverse and ecologically important in the early Silurian following the end Ordovician mass extinction (Johnson 1997). Despite existing through the entire GOBE, pentamerides did not become exceptionally diverse during this time as other brachiopod groups, such as the orthides and strophomenides (Harper et al. 2013).

By the early Silurian, the Suborder Pentameridina diversified into four superfamilies: Pentameroidea M'Coy, 1844, Stricklandioidea Schuchert and Cooper, 1931, Clorindoidea Rzhonsnitskaia, 1956, and Gypiduloidea Schuchert and LeVene, 1929. The evolution of these groups has been well studied with several proposed evolutionary lineages such as *Virdita–Virgiana*, *Pentamerus–Pentameroides*, *Stricklandia–Costistricklandia*, and *Microcardinalia–Plicostricklandia*. Other common

or important genera in this group include *Clorinda* and *Gypidula* (Williams 1951; Johnson 1979; Baarli 1988; Jin and Copper 2000).

These pentameride brachiopods became widespread in the intracratonic and pericratonic seas ranging from equatorial to subtropical, shallow to relatively deep (continental shelf margin), and level-bottom to reefal settings. They occur in great abundance in Llandovery strata of Laurentia (Jin et al. 1993; Watkins 1994, 1998; Jin and Copper 2000, 2010; Jin 2008; Jin and Popov 2008), Baltica (Cocks 1982; Baarli 1988; Baarli and Johnson 1988; Watkins 2000; Dahlqvist and Bergström 2005), Avalonia (Williams 1951; Ziegler 1965; Ziegler et al. 1968; Watkins and Boucot 1975; Lawson 1999), Siberia (Sapelnikov 1961, 1985; Sapelnikov et al. 1999), Kazakhstan (Sapelnikov and Rukavishnikova 1975; Modzalevskaya and Popov 1995; Nikitina et al. 2015) and China (Rong et al. 2004, 2005, 2007). Despite being very successful in the Silurian, pentameride diversity went through a drastic decline during the Devonian as strophomenides, rhynchonellides, and spirifierides went through episodes of diversification (Copper 2003; Gourvennec 2000; Zapalski et al. 2007). The Order Pentamerida, along with the atrypide brachiopods went extinct during the Frasnian–Fammenian mass extinction during the Late Devonian (Copper 1986, 1998).

1.4 Silurian Level-Bottom Brachiopod Communities

One of the best paleoecologic models based on early Silurian brachiopod fauna is the five brachiopod community zones first recognized by Ziegler (1965) from the Welsh borderlands that were subsequently expanded by Boucot (1975) into the five benthic

assemblages (BAs) related to water depth. Each benthic assemblage is made up of a specific fauna, characterized by brachiopods, but also by other fossil groups such as trilobites, corals, and nautiloids. In addition, Boucot (1975) expanded the time range of these zones from the early Silurian to include the Late Ordovician through to the Devonian. The five widely used brachiopod communities, interpreted to occur in zones parallel to shoreline, from the intertidal to continental shelf-margin, include the *Lingula* community, the *Eocoelia* community, the *Pentamerus* community, the *Stricklandia* community, and the *Clorinda* community (Fig. 1.4). These five communities or BAs have been shown to be largely applicable to early Silurian level-bottom environments in Avalonia, Baltica, and Laurentia (Ziegler et al. 1968; Johnson 1977, 1980; Baarli 1987, 1988; Watkins 1998; Baarli et al. 1999; Jin 2008).

Despite the usefulness of this model for studies of level-bottom communities it has been shown that it cannot be applied directly to reefal settings. For example, in the Attawapiskat Formation's reefal and inter-reefal facies members of the *Eocoelia*, *Pentamerus*, and *Clorinda* communities are intermixed while the *Stricklandia* community is not present (Jin et al. 1993; Jin 2003, 2005). This may be due to the high substrate heterogeneity, a higher degree of ecological tiering due to vertical relief or other complex ecological factors within the reef ecosystem. The more complex nature of reef-dwelling brachiopod community structure is investigated and addressed in Chapter 4 of this thesis.
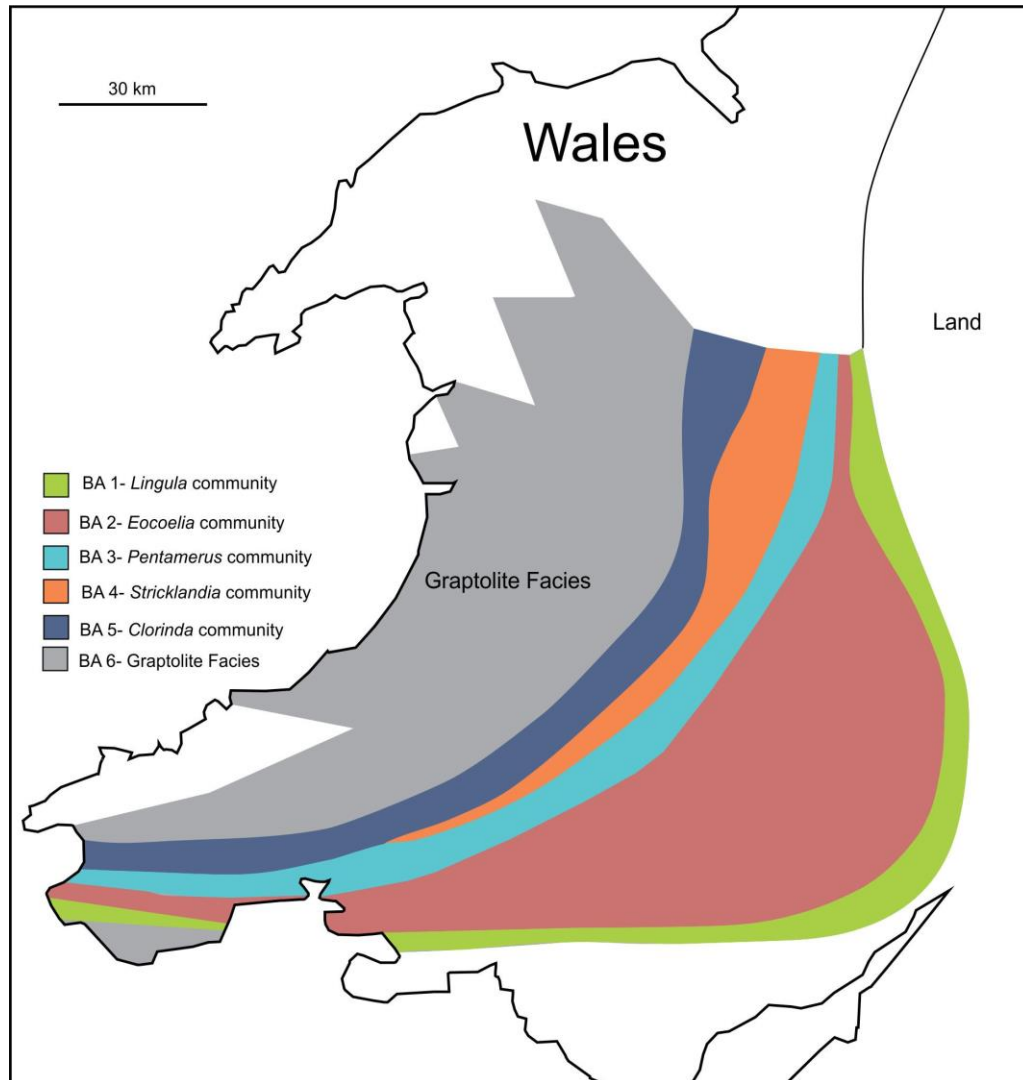
Figure 1.4: Five brachiopod level-bottom community zones from the early Silurian of the Welsh Borderlands. Modified from Ziegler 1965.

1.5 The Reef Environment

Today, the tropical reef environment usually supports highly diverse and complex benthic shelly communities. In the fossil record, the first appearance of reef-dwelling benthic shelly communities of high alpha- (community level) and beta- (between communities) diversity is found in the coral-stromatoporoid reefs of early Silurian age (Jin et al. 1993; Copper 2002). Prior to the Silurian, reefs were typically formed by sediment-binding calcimicrobes, with bryozoan components in the Middle Ordovician and archaeocyathids in the early Cambrian (Rowland and Gangloff 1988). Small coral-stromatoporoid skeletal framework reefs were locallyt present during the Late Ordovician, such as those in the upper Vaureal Formation (upper Katian) and the upper Ellis Bay Formation (Hirnantian) on Anticosti Island, Quebec (Long and Copper 1987; Desrochers et al. 2010; Copper et al. 2013) but, due to their limited ecological importance, they were not heavily affected by the end Ordovician mass extinction (<10 genera loss for stromatoporoids; Servais et al. 2010). Nevertheless, the reef ecosystem as a whole was constricted due to the sea level fall and corals and stromatoporoids did not reorganize into large-scale and geographically widespread reefs until the mid-Aeronian (Copper 2001; Copper and Jin 2012; Wang et al. 2014).

It has been suggested that the initial recovery of reefs after the mass extinction event may have occurred as early as the Rhuddanian as coral-stromatoporoid bioherms are found within the Manitoulin Formation of Manitoulin Island, Ontario (Brunton and Copper 1994; Stott and Jin 2007). The age of this formation, however, has been recently debated as Bergström et al. (2011) suggest that the Manitoulin Formation is latest Hirnantian age based on isotopic carbon composition. This interpretation has some merit

as Hirnantian-aged coral-stromatoporoid patch reefs are found in the Ellis Bay Formation on Anticosti Island and do not appear in the Rhuddanian Becscie Formation directly above (Long and Copper 1987; Desrochers et al. 2010). These two locations suggest the possibility that coral-stromatoporoid reefs survived until the very latest Ordovician.

The first patch reefs with unequivocal early Silurian reef-builders and associated shelly faunas occur in the mid-Aeronian East Point Member of the Meniér Formation on Anticosti Island (Copper 2001; Copper and Jin 2012). These reefs were formed by tabulate and rugose corals and stromatoporoids characteristic of early Silurian age, with encrusting cyanobacteria and green algae. Invertebrate benthic communities are represented by common crinoids and Silurian brachiopods (e.g. *Pentamerus*, *Stegerhynchus*) in the reef and inter-reef facies (Jin and Copper 2000; Copper and Jin 2012), but these communities are not highly diverse. Late Aeronian patch reefs have also been found in South China (Wang et al. 2014). The timing of the recovery is likely related to increasing global temperatures and sea-level due to the simultaneous recovery of the reef ecosystem across zoogeographical provinces. It is clear by the relatively low levels of brachiopod diversity in these Aeronian reefs that they represent the initial step of reef recovery in the tropical and subtropical environments.

Coral-stromatoporoid reefs fully recovered by the end of the Telychian. The coral-stromatoporoid barrier and fringing reefs of the Attawapiskat Formation in the Hudson Bay and Moose River basins, for example, completely encircle modern day Hudson Bay in subcrop and show the first invasion of highly rich and diverse shelly benthic invertebrate communities into the reef ecosystem in Earth history (Suchy and Stearn 1993; Jin et al. 1993). Therefore, the Attawapiskat reefs provide an excellent

opportunity for studying the evolution of complex reef ecosystems and reef-dwelling

shelly organisms. These Hudson Bay reefs disappeared by the beginning of the Wenlock

when a global regression resulted in the Hudson Bay Basin becoming restricted and

evaporitic for several million years (Sanford 1987; Suchy and Stearn 1993). Globally,

however, the reef ecosystem continued to flourish and expand throughout the remainder

of the Silurian and the Devonian (Copper 2002). During the Devonian, super-greenhouse

conditions caused the coral-stromatoporoid reefs to form the largest reef tracts with the

most expansive distribution of any reef building organisms in life history (Copper 2002).

These reefs went totally extinct during the Late Devonian (Frasnian–Fammenian) mass

extinction and the reef ecosystem would not fully recover until the Triassic Period, after

the Permo-Triassic mass extinction altered marine ecology structures (Copper 1986,

1994; Rowland and Gangloff 1988).

1.6 The Cause of Tropical Biodiversity

The tropical regions are typified by high levels of biological diversity in both

terrestrial and marine settings throughout Phanerozoic Earth history. The cause for this

has been heavily debated, but can generally be divided between two competing

hypotheses: the cradle hypothesis and the museum hypothesis (Pianka 1966; Jablonski

1993). The cradle hypothesis suggests that the generally favourable climatic or

environmental conditions of the tropics promotes a higher speciation rate and therefore

higher diversity than higher latitude environments (Jablonski 1993; Moreau and Bell

2013). Alternatively, the museum hypothesis argues that tropical biodiversity is caused

by greater species longevity in the tropics compared to higher latitudes, combined with a

higher immigration rate, where organisms from higher latitudes migrate into the tropics and become more successful than their higher latitude counterparts (Moreau and Bell 2013). The paleocontinent of Laurentia straddled the Equator during the Ordovician and Silurian, with rich and well-preserved faunas ranging from paleoequatorial to subtropics, thus offering a great opportunity for examining the validity or relative merit of either hypothesis as tropical marine environments by examing the re-establishment of marine faunas that were heavily affected by the end Ordovician mass extinction across various sedimentary basins across the paleolatitudes.

1.7 Overall Objectives of the Thesis Projects

The Llandovery was a time of recovery in terms of climate, sea-level, and marine faunas, and marked the first appearance of highly diverse benthic invertebrate communities as a part of skeletal reef ecosystems. In order to achieve a better understanding of this important event in life history, this thesis examines the paleoecology of specific North American and European reef-dwelling brachiopod communities of Llandovery age. The objectives of this thesis are to:

1. Examine the functional morphology of both reef-dwelling and level-bottom inhabiting species of the brachiopod genus *Pentameroides* in order to assess which, if any, morphological characteristics are the results of adaptations to the reef ecosystem.

2. Examine the diversity levels of several reef-dwelling brachiopod communities from latest Ordovician (Hirnantian) to early Silurian (Wenlock) in Laurentia and

Baltica to understand how reef-dwelling communities recovered after the Late Ordovician mass extinction events.

3. Investigate the community structures of the diverse and abundant reef-dwelling brachiopod fauna of the Attawapiskat Formation to gain a better understanding of this oldest known major invasion of reef ecosystem by benthic shelly organisms, and to explore the evolutionary relationships between level-bottom and reef-dwelling brachiopod communities.

4. Attempt to shed some light on relative merit of the museum vs. the cradle hypotheses of tropical biodiversity in regards to the early Silurian reef-dwelling brachiopod faunas and to discuss how they fit in the large-scale evolutionary framework.

1.8 Organization of the Thesis

Chapter 1 provides a general background on the early Silurian in respect to climate, sea-level, paleogeography, ocean chemistry, and fauna. It examines the importance of brachiopods as tools to assess paleoecology as well as the brachiopod dominated level-bottom and reef ecosystems of this time.

Chapter 2 describes the geological settings of the reefal and level-bottom brachiopod communities examined in this thesis and discusses the importance of these study areas.

Chapter 3 describes the morphology of the abundant reef-dwelling brachiopod species *Pentameroides septentrionalis* from the Attawapiskat Formation, Akimiski

Island, James Bay, Nunavut and compares it to the morphology of level-bottom inhabiting *Pentameroides subrectus* from the Fossil Hill Formation, Manitoulin Island, Ontario, and the Jupiter Formation, Anticosti Island, Quebec in order to determine which morphological features or evolutionary factors allowed for the transition from the level-bottom settings in mid–high tropics to the paleoequatorial reef environment.

Chapter 4 describes the diversity levels of several reefal and level-bottom brachiopod dominated communities throughout Laurentia and Baltica ranging from Hirnantian to Wenlock in age. In addition, the community structures of the reef-dwelling Attawapiskat Formation brachiopods will be analyzed. This study will provide quantitative biodiversity data for examining the recovery of the reef ecosystem following the end Ordovician mass extinction as well as the community organization of the reef dwelling brachiopods.

Chapter 5 discusses the paleoecological implications of the findings of chapters 3 and 4 in a broader evolutionary context including the importance of latitude in paleoecology and the possible cause of high levels of biodiversity in the early Silurian tropics.

References

Alroy, J. 2010. Geographical, environmental and intrinsic biotic controls on Phanerozoic
     marine diversification. Palaeontology, 53(6): 1211–1235.

Alroy, J., Aberhan, M., Bottjer, D.J., Foote, M., Fürsich, F.T., Harries, P.J., Hendy,
     A.J.W., Holland, S.M., Ivany, L.C., Kiessling, W., Kosnik, M.A., Marshall, C.R.,
     McGowan, A.J., Miller, A.I., Olszewski, T.D., Patzkowsky, M.E., Peters, S.E.,
     Villier, L., Wagner, P.J., Bonuso, N., Borkow, P.S., Brenneis, B., Clapham, M.E.,
     Fall, L.M., Ferguson, C.A., Hanson, V.L., Krug, A.Z., Layou, K.M., Leckey, E.H.,
     Nurnburg, N., Powers, C.M., Sessa, J.A., Simpson, C., Tomasovych, A., and
     Visaggi, C. C. 2008. Phanerozoic trends in the global diversity of marine
     invertebrates. Science, 321: 97–100.

Azmy, K., Veizer, J., Bassett, M.G., and Copper, P. 1998. Oxygen and carbon isotopic
     composition of Silurian brachiopods: implications for coeval seawater and
     glaciations. Geological Society of America Bulletin, 110(11): 1499–1512.

Baarli, B.G. 1987. Benthic faunal associations in the Lower Silurian Solvik Formation of
     the Oslo-Asker Districts, Norway. Lethaia, 20(1): 75–90.

Baarli, B.G. 1988. Bathymetric co-ordination of proximality trends and level-bottom
     communities: A case study from the Lower Silurian of Norway. Palaios, 3(6): 577–
     587.

Baarli, B.G. and Johnson, M.E. 1988. Biostratigraphy of key brachiopod lineages from
     the Llandovery Series (Lower Silurian) of the Oslo Region. Norsk Geologisk
     Tidsskrift, 68: 259–274.

Baarli, B.G., Keilen, H.B., and Johnson, M.E. 1999. Silurian communities of the Oslo region. *In* Paleocommunities – a case study from the Silurian and Lower Devonian. Cambridge University Press. *Edited by* Boucot, A.J., and Lawson, J.D. p. 327–349.

Barash, M.S. 2013. Interaction of the reasons for the mass biota extinction events in the Phanerozoic. Oceanology, 53: 739–749.

Bergström, S.M., Kleffner, M., Schmitz, B., and Cramer, B.D. 2011. Revision of the position of the Ordovician–Silurian boundary in southern Ontario: regional chronostratigraphic implications of δ13C chemostratigraphy of the Manitoulin Formation and associated strata. Canadian Journal of Earth Sciences, 48(11): 1447–1470.

Berner, R. 1990. Atmospheric carbon dioxide levels over Phanerozoic time. Science, 249(4975): 1382–1386.

Berner, R.A., and Kothavala, Z. 2001. GEOCARB III: a revised model of atmospheric CO_2 over Phanerozoic time. American Journal of Science, 301(2): 182–204.

Berry, W.B.N., and Boucot, A.J. 1973. Glacio-eustatic control of Late Ordovician–Early Silurian platform sedimentation and faunal changes. Geological Society of America Bulletin, 84: 275–284.

Boucot, A.J. 1975. Evolution and extinction rate controls. Elsevier, New York.

Brenchley, P.J., Romano, M., Young, T.P., and Storch, P. 1991. Hirnantian glaciomarine diamictites-evidence for the spread of glaciation and its effect on Upper Ordovician faunas. *In* Advances in Ordovician Geology, Geological Survey of Canada Paper, Volume 90. *Edited by* Barnes, C.R., and Williams, S.H. p. 325–336.

Brenchley, P.J., Marshall, J.D., Carden, G.A.F., Robertson, D.B.R., Long, D.G.F.,
   Meidla, T., Hints, L., and Anderson, T.F. 1994. Bathymetric and isotopic evidence
   for a short-lived Late Ordovician glaciation in a greenhouse period. Geology, 22(4):
   295–298.

Brett, C.E., Boucot, A.J., and Jones, B. 1993. Absolute depths of Silurian benthic
   assemblages. Lethaia, 26(1): 25–40.

Brunton, F.R., and Copper, P. 1994. Paleoecologic, temporal, and spatial analysis of
   Early Silurian reefs of the Chicotte Formation, Anticosti Island, Quebec,
   Canada. Facies, 31(1): 57–79.

Calner, M. 2005. Silurian carbonate platforms and extinction events – ecosystem changes
   exemplified from Gotland, Sweden. Facies, 51: 584–591.

Calner, M. 2008. Silurian global events–at the tipping point of climate change. *In* Mass
   Extinction. Springer Berlin Heidelberg, Berlin. *Edited by* Elewa, M.A.T. p. 21–
   57.

Calner, M., Jeppsson, L., and Munnecke, A. 2004. The Silurian of Gotland—Part I:
   Review of the stratigraphic framework, event stratigraphy, and stable carbon and
   oxygen isotope development. Erlanger geologische Abhandlungen,
   Sonderband, 5: 113–131.

Candela, Y. 2014. Evolution of Laurentian brachiopod faunas during the Ordovician
   Phanerozoic sea level maximum. Earth-Science Reviews, 141: 27–44.

Carlson, S.J., Boucot, A.J., Rong, J.Y., Blodgett, R.B., and Kaesler, R.L. 2002.
   Pentamerida. Treatise on Invertebrate Paleontology. Part H, Brachiopoda
   (revised), 4: H921–H928.

Chow, A.M., and Stearn, C.W. 1988. Attawapiskat patch reefs, Lower Silurian, Hudson
Bay Lowlands, Ontario. Canadian Society of Petroleum Geologists Memoir, 13:
273–270.

Clayer, F., and Desrochers, A. 2014. The stratigraphic imprint of a mid-Telychian
(Llandovery, Early Silurian) glaciation on far-field shallow-water carbonates,
Anticosti Island, Eastern Canada. Estonian Journal of Earth Sciences, 63(4): 207–
213.

Cocks, L.R.M. 1982. The commoner brachiopods of the latest Ordovician of the Oslo–
Asker District, Norway. Palaeontology, 25(4): 755–781.

Cocks, L.R.M., and Rong, J. 2007. Earliest Silurian faunal survival and recovery after the
end Ordovician glaciation: evidence from the brachiopods. Earth and
Environmental Science Transactions of the Royal Society of Edinburgh, 98: 291–
301.

Copper, P. 1986. Frasnian/Famennian mass extinction and cold-water oceans: Geology,
14: 835–839.

Copper, P. 1988. Ecological succession in Phanerozoic reef ecosystems: is it
real?. Palaios, 3: 136–151.

Copper, P. 1994. Ancient reef ecosystem expansion and collapse. Coral reefs, 13: 3–11.

Copper, P. 1998. Evaluating the Frasnian–Famennian mass extinction: Comparing
brachiopod faunas. Acta Palaeontologica Polonica, 43: 137–154.

Copper, P. 2001. Reefs during multiple crises towards the Ordovician–Silurian boundary: Anticosti Island, eastern Canada, and worldwide. Canadian Journal of Earth Sciences, 38: 153–171.

Copper, P. 2002. Silurian and Devonian reefs: 80 million years of global greenhouse between two ice ages. *In* Phanerozoic Reef Patterns, SEPM Special Publication No. 72. *Edited by* Kiessling, W., Flugel, E., and Golonka, J. p. 181–238.

Copper, P. 2003. Radiations and extinctions of atrypide brachiopods: Ordovician– Devonian. *In* Brachiopods. *Edited by* Brunton, C.H.C., Cocks, L.R.M., and Long, S.M. p. 201–211.

Copper, P., and Jin, J. 2012. Early Silurian (Aeronian) East Point coral patch reefs of Anticosti Island, Eastern Canada: first reef recovery from the Ordovician/Silurian mass extinction in eastern Laurentia. Geosciences, 2: 64–89.

Copper, P., Jin, J., and Desrochers, A. 2013. The Ordovician–Silurian boundary (late Katian–Hirnantian) of western Anticosti Island: revised stratigraphy and benthic megafaunal correlations. Stratigraphy, 10(4): 213–227.

Cummins, R.C., Finnegan, S., Fike, D.A., Eiler, J.M., and Fischer, W.W. 2014. Carbonate clumped isotope constraints on Silurian ocean temperature and seawater $\delta18O$. Geochimica et Cosmochimica Acta, 140: 241–258.

Dahlqvist, P., and Bergström, S.M. 2005. The lowermost Silurian of Jämtland, central Sweden: conodont biostratigraphy, correlation and biofacies. Transactions of the Royal Society of Edinburgh: Earth Sciences, 96(1): 1–19.

Desrochers, A., Farley, C., Achab, A., Asselin, E., and Riva, J.F. 2010. A far-field record of the end Ordovician glaciation: the Ellis Bay Formation, Anticosti Island, Eastern Canada. Palaeogeography, Palaeoclimatology, Palaeoecology, 296(3): 248–263.

Domeier, M. 2016. A plate tectonic scenario for the Iapetus and Rheic oceans. Gondwana Research, 36: 275–295.

Droser, M.L., Bottjer, D.J., and Sheehan, P.M. 1997. Evaluating the ecological architecture of major events in the Phanerozoic history of marine invertebrate life. Geology, 25(2): 167–170.

Erwin, D.H. 1998. The end and the beginning: recoveries from mass extinctions. Tree, 13: 344–349.

Finnegan, S., Bergmann, K., Eiler, J.M., Jones, D.S., Fike, D.A., Eisenman, I., Hughes, N.C., Tripati, A.K., and Fischer, W.W. 2011. The magnitude and duration of Late Ordovician–Early Silurian glaciation. Science, 331: 903–906.

Gould, S.J., and Calloway, C.B. 1980. Clams and brachiopods – ships that pass in the night. Paleobiology, 6: 383–396.

Gourvennec, R. 2000. The evolution, radiation and biogeography of early spiriferid brachiopods. Records of the Western Australian Museum Supplement, 58: 335–347.

Grahn, Y., and Caputo, M.V. 1992. Early Silurian glaciations in Brazil. Palaeogeography, Palaeoclimatology, Palaeoecology, 99(1): 9–15.

Hallam, A. 1992. Phanerozoic sea-level changes. Columbia University Press, New York.

Hallam, A., and Wignall, P.B. 1999 Mass extinction and sea-level changes. Earth-Science Reviews, 48: 217–250.

Hammarlund, E.U., Dahl, T.W., Harper, D.A., Bond, D.P., Nielsen, A.T., Bjerrum, C.J., Schovsbo, N.H., Schonlaub, H.P., Zalasiewicz, J.A., and Canfield, D.E. 2012. A sulfidic driver for the end-Ordovician mass extinction. Earth and Planetary Science Letters, 331: 128–139.

Hambrey, M.J. 1985. The Late Ordovician—Early Silurian glacial period. Palaeogeography, Palaeoclimatology, Palaeoecology, 51(1): 273–289.

Haq, B.U., and Schutter, S.R. 2008 A chronology of Paleozoic sea level changes. Science, 322: 64–68.

Harper, D.A., and Rong, J., 2008. Completeness of the Hirnantian brachiopod record: spatial heterogeneity through the end Ordovician extinction event. Lethaia, 41(2): 195–197.

Harper, D.A., Rasmussen, C.M.Ø, Liljeroth, M., Blodgett, R.B., Candela, Y., Jin, J., Percival, I.G., Rong, J., Villas, E., and Zhan, R. 2013. Biodiversity, biogeography and phylogeography of Ordovician rhynchonelliform brachiopods. Geological Society, London, Memoirs, 38(1): 127–144.

Harper, D.A., Hammarlund, E.U., and Rasmussen, C.M.Ø. 2014. End Ordovician extinctions: a coincidence of causes. Gondwana Research, 25: 1294–1307.

Jablonski, D. 1993. The tropics as a source of novelty through geologic time. Nature, 364: 142–144.

Jin, J. 2002. Niche partitioning of reef-dwelling brachiopod communities in the Lower Silurian Attawapiskat Formation, Hudson Bay Basin, Canada. IPC 2002, Geological Society of Australia, Abstracts No. 68: 83–84.

Jin. J. 2003. The Early Silurian Brachiopod *Eocoelia* from the Hudson Bay Basin, Canada. Palaeontology, 46: 885–902.

Jin, J. 2005. Reef-dwelling gypiduloid brachiopods in the Lower Silurian Attawapiskat Formation, Hudson Bay region. Journal of Paleontology, 79(1): 48–62.

Jin, J. 2008. Environmental control on temporal and spatial differentiation of Early Silurian pentameride brachiopod communities, Anticosti Island, eastern Canada. Canadian Journal of Earth Sciences, 45: 159–187.

Jin, J., and Copper, P. 2000. Late Ordovician and Early Silurian pentamerid brachiopods from Anticosti Island, Québec, Canada. Palaeontographica Canadiana, 18: 1–140.

Jin, J., and Copper, P. 2010. Origin and evolution of the early Silurian (Rhuddanian) virgianid pentameride brachiopods—the extinction recovery fauna from Anticosti island, eastern Canada. Bollettino della Società Paleontologica Italiana, 49: 1–11.

Jin, J., and Popov, L.E. 2008. A new genus of Late Ordovician–Early Silurian pentameride brachiopods and its phylogenetic relationships. Acta Palaeontologica Polonica, 53(2): 221–236.

Jin, J., Caldwell, W.G.E., and Norford, B.S. 1993. Early Silurian brachiopods and biostratigraphy of the Hudson Bay lowlands, Manitoba, Ontario, and Quebec. Geological Survey of Canada, 457.

Jin, J., Copper, P., and Renbin, Z. 2007. Species-level response of tropical brachiopods to environmental crises during the Late Ordovician mass extinction. Acta Palaeontologica Sinica, 46: 194–200.

Jin, J., Harper, D.A.T., Cocks, L.R.M., McCausland, P.J.A., Rasmussen, C.M.Ø., and Sheehan, P.M., 2013. Precisely locating the Ordovician equator in Laurentia. Geology, 41: 107–110.

Jin, J., Sohrabi, A., and Sproat, C. 2014. Late Ordovician brachiopod endemism and faunal gradient along palaeotropical latitudes in Laurentia during a major sea level rise. GFF, 136(1): 125–129.

Johnson, M.E. 1977. Succession and replacement in the development of Silurian brachiopod populations. Lethaia, 10: 83–93.

Johnson, M. E. 1979. Evolutionary brachiopod lineages from the Llandovery series of eastern Iowa. Palaeontology, 22: 549–567.

Johnson, M.E. 1980. Paleoecological structure in early Silurian platform seas of the North American midcontinent. Palaeogeography, Palaeoclimatology, Palaeoecology, 30: 191–216.

Johnson, M.E. 1987. Extent and bathymetry of North American platform seas in the early Silurian. Paleoceanography, 2: 185–211.

Johnson, M.E. 1997. Silurian event horizons related to the evolution and ecology of pentamerid brachiopods. *In* Paleontological events: stratigraphic, ecological, and

evolutionary implications. *Edited by* Brett, C.E., and Baird, G.C. Columbia
University Press, New York. p. 162–180.

Johnson, M.E. 2006. Relationship of Silurian sea-level fluctuations to oceanic episodes
and events. GFF, 128(2): 115–121.

Johnson, M.E. 2010. Tracking Silurian eustasy: Alignment of empirical evidence or
pursuit of deductive reasoning?. Palaeogeography, Palaeoclimatology,
Palaeoecology, 296(3): 276–284.

Kump, L.R., Arthur, M.A., Patzkowsky, M.E., Gibbs, M.T., Pinkus, D.S., and Sheehan,
P.M. 1999. A weathering hypothesis for glaciation at high atmospheric pCO_2
during the Late Ordovician. Palaeogeography, Palaeoclimatology, Palaeoecology,
152(1): 173–187.

Lawson, J.D. 1999. Review of UK Silurian Associations. *In* Paleocommunities – A Case
Study from the Silurian and Lower Devonian. Cambridge University Press. *Edited
by* Boucot, A.J., and Lawson, J.D. Boucot, and J. D. p. 355–369.

Lehnert, O., Männik, P., Joachimski, M.M., Calner, M., and Frýda, J. 2010.
Palaeoclimate perturbations before the Sheinwoodian glaciation: A trigger for
extinctions during the 'Ireviken Event'. Palaeogeography, Palaeoclimatology,
Palaeoecology, 296(3): 320–331.

Long, D.G.F., and Copper, P. 1987. Stratigraphy of the Upper Ordovician upper Vaureal
and Ellis Bay formations, eastern Anticosti Island, Quebec. Canadian Journal of
Earth Sciences, 24(9): 1807–1820.

M'Coy, F. 1844. A synopsis of the characters of the Carboniferous Limestone fossils of
Ireland. Dublin. 207 p.

McGhee, G.R., Sheehan, P.M., Bottjer, D.J., and Droser, M.L. 2012. Ecological ranking of Phanerozoic biodiversity crises: The Serpukhovian (early Carboniferous) crisis had a greater ecological impact than the end-Ordovician. Geology, 40(2): 147–150.

McKerrow, W.S., Mac Niocaill, C., and Dewey, J.F. 2000. The Caledonian orogeny redefined. Journal of the Geological Society, 157(6): 1149–1154.

Miller, K.G., Kominz, M.A., Browning, J.V., Wright, J.D., Mountain, G.S., Katz, M.E., Sugerman, P.J., Cramer, B.S., Christie-Blick, N., and Pekar, S.F. 2005. The Phanerozoic record of global sea-level change. Science, 310(5752): 1293–1298.

Moreau, C.S., and Bell, C.D. 2013. Testing the museum versus cradle tropical biological diversity hypothesis: phylogeny, diversification, and ancestral biogeographic range evolution of the ants. Evolution, 67: 2240–2257.

Modzalevskaya, T.L. and Popov, L.E. 1995: Earliest Silurian articulate brachiopods from central Kazakhstan. Acta Palaeontologica Polonica, 40: 399–426.

Munnecke, A., Samtleben, C., and Bickert, T. 2003. The Ireviken Event in the lower Silurian of Gotland, Sweden–relation to similar Palaeozoic and Proterozoic events. Palaeogeography, Palaeoclimatology, Palaeoecology, 195(1): 99–124.

Munnecke, A., Calner, M., Harper, D.A.T., and Servais, T. 2010. Ordovician and Silurian sea – water chemistry, sea level, and climate: a synopsis. Palaeogeography, Palaeoclimatology, Palaeocology, 296: 389–413.

Nikitina, O.I., Nikitin, I.F., Olenicheva, M.A., and Palets, L.M. 2015. Lower Silurian stratigraphy and brachiopods of the Chingiz range, eastern Kazakhstan. Stratigraphy and Geological Correlation, 23(3): 262–280.

Patzkowsky, M.E., Slupik, L.M., Arthur, M.A., Pancost, R.D., and Freeman, K.H. 1997. Late Middle Ordovician environmental change and extinction: Harbinger of the Late Ordovician or continuation of Cambrian patterns?. Geology, 25(10): 911–914.

Pianka, E.R. 1966. Latitudinal gradients in species diversity: a review of concepts. American Naturalist, 100: 33–46.

Powell, C.M., Li, Z.X., McElhinny, M.W., Meert, J.G., and Park, J.K. 1993. Paleomagnetic constraints on timing of the Neoproterozoic breakup of Rodinia and the Cambrian formation of Gondwana. Geology, 21(10), 889–892.

Raup, D.M., and Sepkoski Jr, J.J. 1982. Mass extinctions in the marine fossil record. Science, 215: 1501–1503.

Richardson, J.R. 2002. Ecology of Articulated Brachiopods. Treatise on Invertebrate Paleontology. Part H, Brachiopoda (revised), 1: H441–H462.

Rong, J., and Harper, D.A. 2002. The latest Ordovician Hirnantia Fauna (Brachiopoda) in time and space. Lethaia, 35(3): 231–249.

Rong, J., Zhan, R., and Jin, J. 2004. The Late Ordovician and Early Silurian pentameride brachiopod *Holorhynchus* Kiaer, 1902 from North China. Journal of Paleontology, 78(02): 287–299.

Rong, J., Jin, J., and Zhan, R. 2005. Two new genera of Early Silurian stricklandioid brachiopods from South China and their bearing on stricklandioid classification and paleobiogeography. Journal of Paleontology, 79(06): 1143–1156.

Rong, J., Boucot, A.J., Harper, D.A., Zhan, R.B., and Neuman, R.B. 2006. Global analyses of brachiopod faunas through the Ordovician and Silurian transition: reducing the role of the Lazarus effect. Canadian Journal of Earth Sciences, 43(1): 23–39.

Rong, J., Jin, J., and Zhan, R. 2007. Early Silurian *Sulcipentamerus* and related pentamerid brachiopods from South China. Palaeontology, 50(1): 245–266.

Rowland, S.M., and Gangloff, R.A. 1988. Structure and paleoecology of lower Cambrian reefs. Palaios, 3: 111–135.

Rudwick, M.J.S. 1970. Living and Fossil Brachiopods. Hutchinson University Library, London. 199 pp.

Rzhonsnitskaia, M.A. 1956. Systemization of Rhynchonellida. *In* Resumenes de Los Trabajos Presentados. International Geological Congress, Mexico, Report 20. *Edited by* Guzman, E. et al. p. 125–126.

Sanford, B.V. 1987. Paleozoic geology of the Hudson platform. *In* Sedimentary Basins and Basin Forming Mechanisms, Canadian Society of Petroleum Geologists Memoir 12. *Edited by* Beaumont, C., and Tankard, A.J. p. 483–505.

Sapelnikov, V.P. 1961. Venlokskie *Pentameroides* srednego Urala. Paleontologicheskii Zhurnal, 1: 102–107.

Sapelnikov, V.P. 1985. Sistema i stratigraficheskoe znachenie brakhiopod podotryada pentameridin. Akademiya Nauk SSSR, Uralskyi Nauchnyi Tsentr, Nauka, Moskva. 206 p.

Sapelnikov, V.P. and Rukavishnikova, T.B. 1975. The Upper Ordovician, Silurian, and
     Lower Devonian pentamerids of Kazakhstan. Akademia Nauk, Uralskyi Nauchnyi
     Tsentr, Institut Geologii i Geofiziki. Izdatel'stvo 'Nauka'. Sverdlovsk. 227, 43.

Sapelnikov, V.P., Bogoyavlenskaya, O.V., Mizesn, L.I., and Shuysky,
     V.P. 1999. Silurian and Early Devonian benthic communities of the Ural–Tien-
     Shan region, *In* Paleocommunities – A Case Study from the Silurian and Lower
     Devonian. Cambridge University Press. *Edited by* Boucot, A.J., and Lawson, J.D.
     Boucot, and J. D. p. 510–544.

Schubert, J.K., and Bottjer, D.J. 1995. Aftermath of the Permian–Triassic mass extinction
     event: Paleoecology of Lower Triassic carbonates in the western USA.
     Palaeogeography, Palaeoclimatology, Palaeoecology, 116(1): 1–39.

Schuchert, C., and Cooper, G.A. 1931. Synopsis of the brachiopod genera of the
     suborders Orthoidea and Pentameroidea, with notes on the Telotremata. American
     Journal of Science, 20: 241–251.

Schuchert C., and LeVene, C.M. 1929. Brachiopoda (Generum et Genotyporum Index et
     Bibliographia). Fossilium Catalogus I: Animalia, 42. W. Junk. Berlin.

Servais, T., Owen, A.W., Harper, D.A.T., Kroger, B., and Munnecke, A. 2010. The Great
     Ordovician Biodiversification Event (GOBE): the palaeoecological dimension,
     Palaeogeography, Palaeoclimatology, Palaeoecology, 294: 99–119.

Sepkoski Jr, J.J. 1984. A kinetic model of Phanerozoic taxonomic diversity. III. Post-
     Paleozoic families and mass extinctions. Paleobiology, 10(2): 246–267.

Sepkoski Jr, J.J., and Miller, A.I. 1985. Evolutionary faunas and the distribution of
     Paleozoic marine communities in space and time. *In* Phanerozoic Diversity

Patterns: Profiles in Macroevolution. Princeton University Press, Princeton, NJ. *Edited by* Valentine, J.W. p. 153–190.

Sheehan, P. M. 1975. Brachiopod synecology in a time of crisis (Late Ordovician–Early Silurian). Paleobiology, 1: 205–212.

Sheehan, P. 2001. The Late Ordovician mass extinction. Annual Review of Earth and Planetary Sciences, 29: 331–364.

Sheehan, P.M., and Coorough, P.J., 1990. Brachiopod zoogeography across the Ordovician–Silurian extinction event. Geological Society, London, Memoirs, 12(1): 181-187.

Shen, S.Z., Zhang, H., Li, W.Z., Mu, L., and Xie, J.F. 2006. Brachiopod diversity patterns from Carboniferous to Triassic in South China. Geological Journal, 41: 345–361.

Stott, C.A., and Jin, J. 2007. Rhynchonelliformean brachiopods from the Manitoulin Formation of Ontario, Canada: potential implications for the position of the Ordovician–Silurian boundary in cratonic North America. Acta Palaeontologica Sinica, 46: 449–459.

Suchy, D.R., and Stearn, C.W. 1993. Lower Silurian reefs and post-reef beds of the Attawapiskat Formation, Hudson Bay Platform, northern Ontario. Canadian Journal of Earth Sciences, 30: 575–590.

Torsvik, T.H., and Cocks, L.R.M. 2013. New global palaeogeographical reconstructions for the Early Palaeozoic and their generation. Geological Society, London, Memoirs, 38: 5–24.

Trotter, J.A., Williams, I.S., Barnes, C.R., Männik, P., and Simpson, A. 2016. New conodont δ 18 O records of Silurian climate change: Implications for environmental and biological events. Palaeogeography, Palaeoclimatology, Palaeoecology, 443: 34–48.

Ulrich, E.O., and Cooper, G.A. 1936. New genera and species of Ozarkian and Canadian brachiopods. Journal of Paleontology. 10(7): 616–631.

van Staal, C.R., Whalen, J.B., McNicoll, V.J., Pehrsson, S., Lissenberg, C.J., Zagorevski, A., van Breeman, O., and Jenner, G.A. 2007. The Notre Dame arc and the Taconic orogeny in Newfoundland. Geological Society of America Memoirs, 200: 511–552.

Wang, G., Li, Y., Kershaw, S., and Deng, X. 2014. Global reef recovery from the end-Ordovician extinction: evidence from late Aeronian coral–stromatoporoid reefs in South China. GFF, 136: 286–289.

Watkins, R. 1994. Evolution of Silurian pentamerid communities in Wisconsin. Palaios, 9: 488–499.

Watkins, R., 1998, Silurian reef-dwelling pentamerid brachiopods, Wisconsin and Illinois, USA. Palaontologische Zeitschrift, 72: 99–109.

Watkins, R. 2000. Silurian reef-dwelling brachiopods and their ecologic implications. Palaios, 15(2): 112–119.

Watkins, R., and Boucot, A.J. 1975. Evolution of Silurian brachiopod communities along the southeastern coast of Acadia. Geological Society of America Bulletin, 86(2): 243–254.

Williams, A. 1951. Llandovery brachiopods from Wales with special reference to the Llandovery District. Quarterly Journal of the Geological Society, London, 57: 85–136.

Zapalski, M.K., Hubert, B.L., Nicollin, J.P., Mistiaen, B., and Brice, D. 2007. The palaeobiodiversity of stromatoporoids, tabulates and brachiopods in the Devonian of the Ardennes–changes through time. Bulletin de la Société Géologique de France, 178(5): 383–390.

Ziegler, A.M. 1965. Silurian marine communities and their environmental significance. Nature, 207: 270–272.

Ziegler, A.M., Cocks, L.R.M., and Bambach, R.K. 1968. The composition and structure of lower Silurian marine communities. Lethaia, 1: 1–27.

Chapter 2 – Geological Settings

2.1 Tectonic Arrangement of Laurentia

During the Silurian, the majority of modern day North America, along with Greenland, Scotland, and Northern Ireland were combined as one continent known as Laurentia. This continent occupied largely tropical latitudes, extending from 30° south to 10° north, and was rotated ~80° clockwise in relation to North America with the modern east coast facing south. Directly to the east of Laurentia were Baltica and Avalonia, the former composed of modern north – central Europe and the latter composed of present-day England, Nova Scotia, and Newfoundland (Torsvik and Cocks 2013). These two landmasses had become sutured together by Llandovery time and were slowly moving towards Laurentia. Due to the relatively high sea levels that persisted throughout much of the Silurian, Laurentia and Baltica (as well as other tropic continents) were episodically inundated by shallow, intracratonic seas (Johnson 1987; Johnson et al. 1991). These tropical seas provided relatively stable environments for marine organisms to thrive following the end Ordovician mass extinction.

Much of northern Canada consists of exposed, highly deformed, Pre-Cambrian cratonic rock known as the Canadian Shield. In large areas of North America overlying Phanerozoic sediments overlie the basement rock in large platforms. Central and Eastern Canada are comprised of the Hudson Platform, which includes the regions of Hudson Bay, James Bay, and their surrounding lowlands, and the St. Lawrence Platform, extending from southern Ontario northeast to Newfoundland (Fig. 2.1; Stott and Aiken
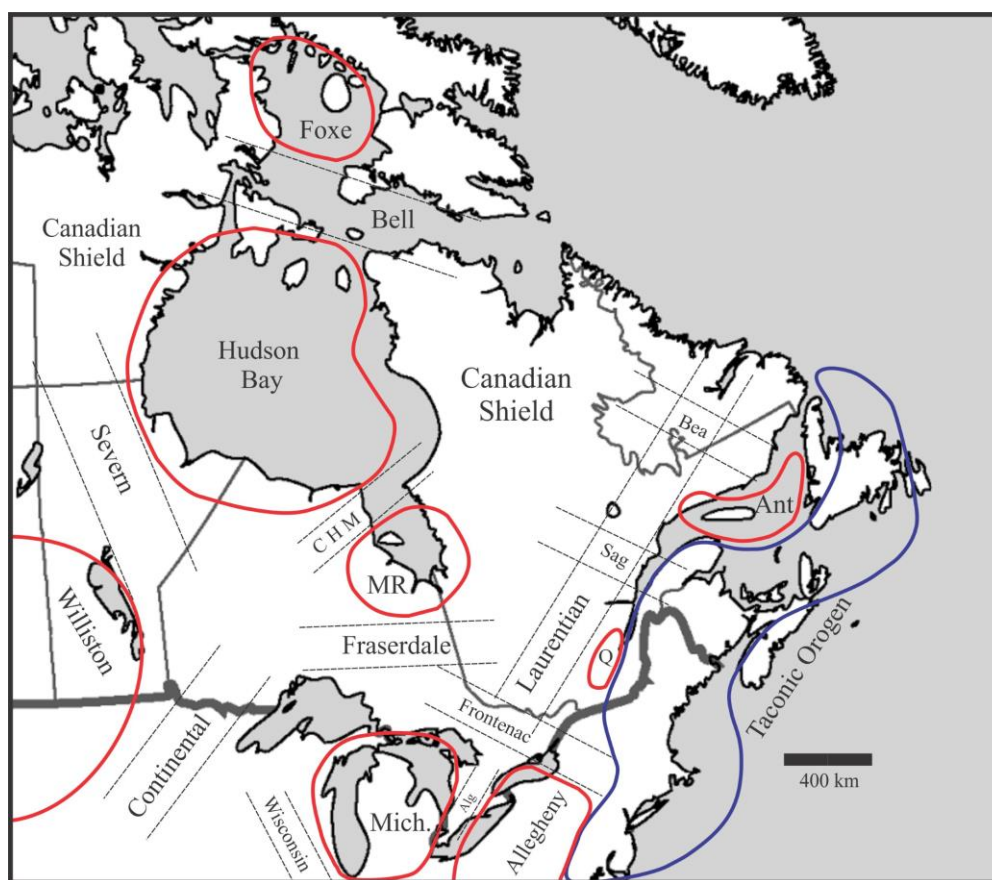
Figure 2.1: Map of principal geologic structures in central – eastern Canada and the northeastern United States. Basins are encircled in red, arches are enclosed by dotted lines, and the Taconic Orogen is shown in blue. Abbreviations are as follows: C M H- Cape Henrietta Maria Arch, Alg- Algonquin Arch, Sag- Saguenay Arch, Bea- Beaugé Arch, MR- Moose River Basin, Mich- Michigan Basin, Q- Quebec Basin, Ant- Anticosti Basin. Data from Sanford and Norris 1973 and Norris 1993.

1993). These platforms are divided into basins, areas of negative relief filled by Phanerozoic sediments, or arches, areas of positive relief, separating the basins.

The Hudson Platform consists of the large Hudson Bay Basin and smaller Moose River Basin, which are separated by the northeast trending Cape Henrietta Maria Arch (Norris 1993). To the north of the Hudson Platform, the Bell Arch separates the Hudson Bay Basin and the Foxe Basin in the Arctic. The Severn Arch separates the Hudson Bay Basin and the Williston Basin in the southwest and the Fraserdale Arch separates the Hudson Platform from St. Lawrence Platform to the south (Sanford and Norris 1973).

The St. Lawrence Platform extends over much of southeastern and eastern Canada ranging from the Michigan Basin and southern Ontario in the southwest to the Anticosti Basin in the northeast. The Taconic Orogen in the southeast and Canadian Shield in the northwest border the platform. The Michigan Basin is separated from the Allegheny Basin to its east by the Algonquin Arch which, in turn, runs northeast to the Laurentian Arch. Smaller southeast trending arches, which separate several foreland basins adjacent to the Taconic Orogen, transect the Laurentian Arch. The Allegheny (or Appalachian) Basin is separated from the small Quebec Basin by the Frontenac Arch which is, in turn, separated from the Anticosti Basin by the Saguenay Arch. The Beaugé Arch borders the Anticosti Basin to its northwest and is the final arch in the northeast trending St. Lawrence Platform (Sanford 1993).

2.2 Coral-stromatoporoid Reefs in the Llandovery

The relatively high sea level during the Llandovery, punctuated by glacio-eustatic falls, caused the continental interior of Laurentia to be flooded by shallow tropical seas ranging from 30–90 m in water depth (Johnson 1987, 2006, 2010). At their greatest areal extent, these seas covered greater than 65% of the Laurentian craton. It should be noted that during the Llandovery, the only emergent landmasses in eastern Laurentia were the Taconic Mountains and the Fraserdale Arch. As such, many of the watermasses that occupied the intracratonic and foreland basins were connected through shared seaways (Hudson and Moose River, Hudson and Foxe, Michigan and Allegheny; Johnson 1987).

Level-bottom carbonate environments with abundant marine invertebrate communities quickly became abundant throughout the flooded regions of the continent due to the connectivity and general stability of the basinal seas (Johnson and Colville 1982). By Telychian time, large coral-stromatoporoid reef complexes with abundant brachiopod-dominated benthic communities began to develop in these inland seas (Long and Copper 1987; Jin et al. 1993; Suchy and Stearn 1993; Brunton and Copper 1994; Watkins 1998, 2000; Jin and Copper 2000; Copper et al. 2013; Copper and Jin 2012, 2015). In this thesis, several such reef localities were selected to investigate the paleoecology of reef-dwelling brachiopods in Laurentia. Reef-hosting stratigraphic units studied herein include the Attawapiskat Formation, Hudson Platform; the Laframboise Member, Ellis Bay Formation, the East Point Member, Meniér Formation, and the Chicotte Formation of Anticosti Island; the Racine Formation, Wisconsin, Michigan Basin; and the Högklint Formation of Gotland, Sweden (Fig. 2.2; Fig. 2.3). The level-bottom pentamerid brachiopod communities of the Fossil Hill
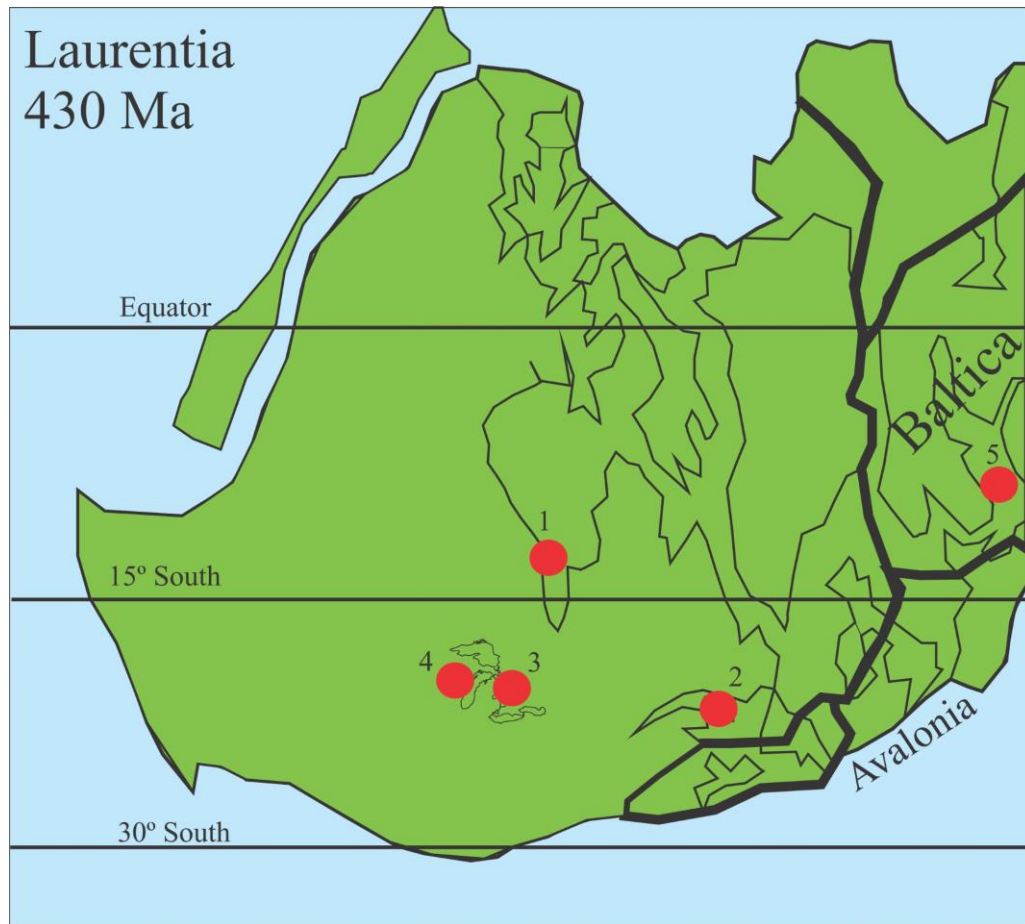
Figure 2.2: Study localities on schematic paleomap of Laurentia and Baltica. Thickened lines show boundaries between paleoplates. 1. Attawapiskat Formation, Akimiski Island, James Bay, Nunavut; 2. Anticosti Island, Quebec; 3. Fossil Hill Formation, Manitoulin Island, Ontario, 4. Racine Formation, Wisconsin; 5. Högklint Formation, Gotland, Sweden. Modified from Torsvik and Cocks 2013.
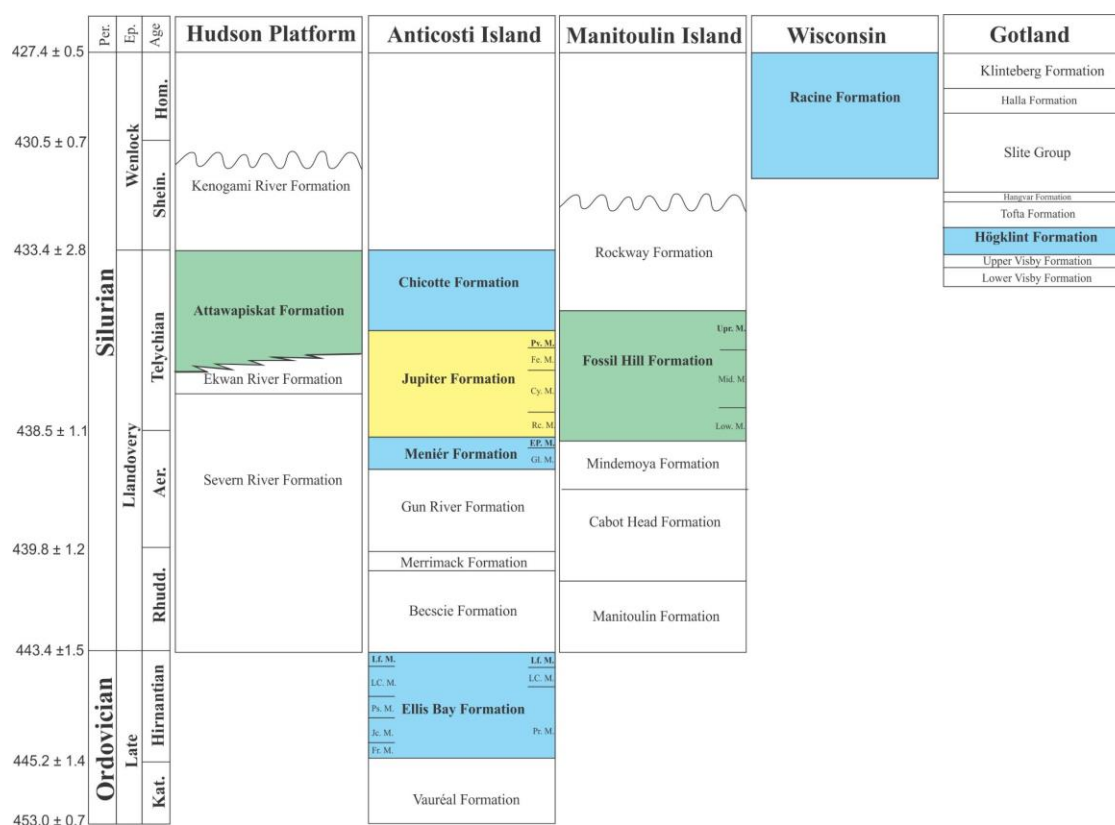
Figure 2.3: Stratigraphy of study locations. Yellow shows formations studied in Chapter 3, blue shows those studied in Chapter 4, Green shows those studied in both chapters 3 and 4. Members in bold signify collection sites. Member abbreviations are as follows: Pv. M.- Pavillon Member, Fe. M.- Ferrum Member, Cy. M.- Cybèle Member, Rc. M.- Richardson Member, EP. M.- East Point Member, Gl. M. Goéland Member, Lf. M.- Laframboise Member, LC. M.- Lousy Cove Member, Ps. M.- Parastro Member, Jc. M.- Juncliff Member, Fr. M.- Fraise Member, Pr. M.- Prinsta Member, Upr. M.- Upper Member, Mid. M.- Middle Member, Low. M. Lower Member. Dates are in million years. Data from Liberty 1968; Calner et al. 2004; Copper and Jin 2012, 2015; Eggie et al. 2014.

Formation of Manitoulin Island and the Pavillon Member of Jupiter Formation on Anticosti Island are included in this thesis as comparisons to the reefal communities. In the discussion below, the geological settings of several formations and study areas are provided in relation to the significance of brachiopod faunas, as well as a regional biostratigraphic correlation of the formations referred to throughout the thesis.

2.3 The Attawapiskat Formation, Hudson Platform

The Hudson Platform refers to a large region of the North American craton that was inundated several times in the Paleozoic by tropical epicontinental seas during episodes of sea-level high stands (Johnson 2006; Haq and Schutter 2008). The present-day Hudson Bay and James Bay basins together represent one of the few intracratonic seas on Earth (although unlike many of the epicontinental seas of the Paleozoic, this present-day example is located in a temperate climate). The Paleozoic strata of the Hudson Platform are predominantly Ordovician, Silurian, and Devonian carbonates, but also includes units of evaporites, and siliciclastics. This package of Paleozoic sediments unconformably overlies Precambrian basement bedrock (Sanford 1987). The carbonate-dominated Severn River, Ekwan River, and Attawapiskat formations collectively represent the Llandovery Series on the Hudson Platform, and are overlain by the Wenlock evaporite-dominated Kenogami River Formation (Norris 1986; Hahn and Armstrong 2013; Fig. 2.3). During the Telychian, the Hudson Platform spanned tropical latitudes from 3–15° south (Torsvik and Cocks 2013; Fig. 2.2).

The Severn River Formation is an early–middle Llandovery succession of sparsely fossiliferous calcareous mudstone–wackestones interbedded with evaporitic dolostones (Sanford 1987; Hahn and Armstrong 2013). Recent revision by Hahn and Armstrong (2013) has divided the Severn River Formation into three units: a lower fossiliferous limestone unit, a middle dolomudstone dominated member, and an upper member of alternating sub-tidal fossiliferous limestone and evaporitic dolosiltstones. The basal 52 m of the formation is characterized by *Virgiana*-rich brachiopod packstone and wackestone, indicating a late Rhuddanian age (Jin et al. 1993). Fossils common in the upper unit of the Severn River include trilobites, bryozoans, brachiopods, crinoids, stromatoporoids, molluscs, and ostracods (Johnson and Baarli 1987; Hahn and Armstrong 2013).

Unlike the Severn River Formation, which thickens towards the centres of the Hudson Bay and Moose River basins, the overlying Ekwan River and Attawapiskat formations form thick sections of highly fossiliferous limestones and dolostones on the margins of the basins (Sanford 1987). The Ekwan River Formation is a richly fossiliferous sequence of bioclastic wackestone and packstone although varying degrees of dolomitization occurs throughout the formation (Eggie et al. 2014). Common fossils of this formation include stromatoporoids, crinoids, brachiopods, bryozoans, molluscs, and trilobites (Jin et al. 1993; Hahn and Armstrong 2013). This formation underlies or locally interfingers with the reefal Attawapiskat Formation of middle–late Telychian age (Sanford 1987; Eggie et al. 2014).

The Attawapiskat Formation is characterized by highly fossiliferous limestones and dolostones containing large coral-stromatoporoid reefs and diverse communities of

benthic, shelly, marine organisms (Norford 1981; Norris 1986). The formation itself is areally expansive, occuring in both the Hudson Bay and Moose River basins, and cropping out on Akimiski Island in James Bay and along the Attawapiskat River in northern Ontario (Fig. 2.4; Sandford 1987). In subcrop, the formation continues beneath Hudson and James bays as well as throughout much of their surrounding lowlands in northern Ontario, northern Manitoba, and Nunavut (Ramdoyal et al. 2013; Eggie et al. 2014). Lithologically, the Attawapiskat reefs vary in composition with coral-stromatoporoid framestones and rudstones, skeletal mudstone–wackestone, and cement- and calcimicrobe-rich boundstones and inter-reef areas consisting of shallow-water limestones and dolostones (Eggie et al. 2014). Micritic cement is typically rare in the Attawapiskat Formation, possibly signifying relatively turbulent fairweather conditions. Blockly to coarse-mosaic calcite cement, however, is very common in the limestones of the Attawapiskat Formation and occurs in the porespaces between sediment grains or skeletal fragments and in the interiors of some brachiopod shells (Eggie et al. 2014). It has been estimated that the reefs reached 8–10 m of relief at the time of deposition (Norris 1986; Suchy and Stearn 1993).

The high abundance and diversity of the benthic fauna as well as the occurrence of the coral-stromatoporoid reefs indicates that the majority of the Attawapiskat Formation records well-oxygenated open marine conditions (Hahn and Armstrong 2013). Above this formation, thick laterally extensive beds of *Nuia*-dominated algal grainstone that are, in turn, overlain by the evaopites of the Kenogami River Formation (Suchy and Stearn 1993; Hahn and Armstrong 2013). This shallowing-upward succession (reefal limestones passing upward into supra- to intertidal grainstones and capped by evaporites)
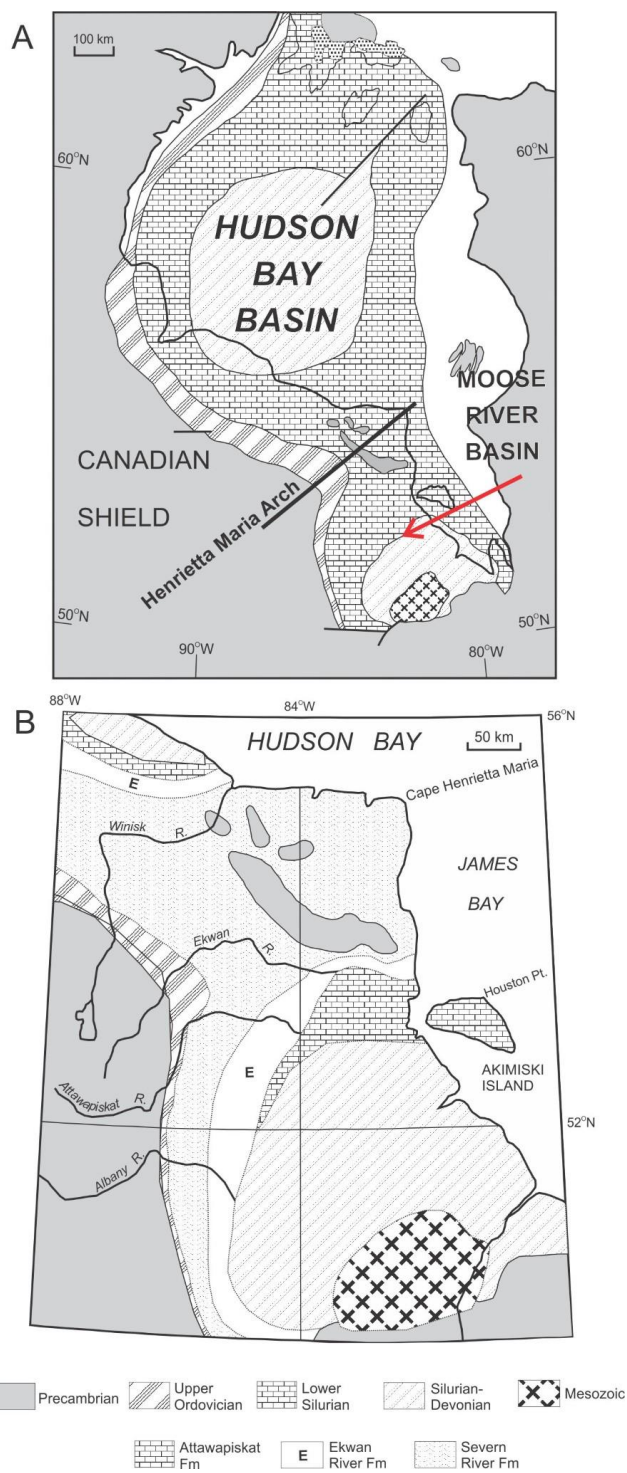
Figure 2.4: Simplified bedrock geology of the A) Hudson Platform and B) The James Bay lowlands of northern Ontario. Modified from Jin et al. 1993; Jin 2005.

suggest that sea level fell in this region during the latest Llandovery and earliest Wenlock. This event correlates with the late Telychian global regression (Haq and Schutter 2008) and was the cause of extinction for the Attawapiskat reefs (Sanford 1987).

The Attawapiskat Formation marks the full recovery of the reef ecosystem after the end Ordovician mass extinction and contains one of the earliest known examples of diverse brachiopod-dominated faunas within a reef environment (Chow and Stearn 1988). Besides the dominant brachiopods, the reef and inter-reef fauna include common gastropods, bivalves, trilobites, and ostracods (Norford 1981; Jin et al. 1993; Westrop and Rudkin 1999; Hahn and Armstrong 2013). In contrast to the level-bottom communities from elsewhere in North America, the early Silurian level-bottom brachiopod community zonation (Ziegler 1965, Ziegler et al. 1968) is not easily applicable to the reefal and inter-reefal settings of the Attawapiskat Formation. The *Eocoelia*, *Pentameroides* and *Clorinda* brachiopod associations are found in close proximity to one another within the reefs while *Stricklandia* is entirely absent (Jin 2003). This shows that this simple depth-dependant community structure cannot be applied to reefal settings, likely due to the high substrate heterogeneity, vertical tiering, or other complex ecological factors.

The brachiopod communities within this formation, however, have been divided into more complex community assemblages based on their dominant components by Jin (2002). These assemblages are the *Lissatrypa* Association, the *Septatrypa* Association, the *Septatrypa–Pentameroides* Association, the *Gypidula* Association, the *Gotatrypa* Association, the *Trimerella* Association, the *Eocoelia* Association, and the *Pentameroides* Association. The community structures of this formation will be further discussed in Chapter 4.

2.3.1 Materials

The brachiopod fauna of this formation are exceptional in both abundance and diversity. Over 50 brachiopod species and 9000 specimens collected from the Attawapiskat Formation of Akimiski Island, James Bay, Nunavut were examined in this thesis. Thrity-two collections were made by Dr. J. Jin and Mr. David Rudkin from the north shore of the island over several years of field work in the early 2000s. Detailed GPS UTM coordinates along with the number of species and specimens per locality can be found in Table 2.1. The location of each study site can be seen in Figure 2.5. Due to the close proximity of the individual collection localities only general localitions are represented in the figure. The preservation of the brachiopods is excellent as well. Shells are often found articulated and intact, with little to no deformation, and hollow (i.e. lacking sediment infill) with a lining of isopachous calcitic cement. The consistently high quality of preservation in such a great abundance of specimens has made this formation an excellent unit for paleoecologic studies. In this thesis, the large shelled *Pentameroides septentrionalis*, the second most common Attawapiskat brachiopod species, was selected as the primary species to examine the functional morphology of reef-dwelling brachiopods (see Chapter 3). This species was selected due to its high abundance, large size, easily measured outer morphological features, and its close relation to the nearby and contemporaneous level-bottom inhabiting species *Pentameroides subrectus*.

Table 2.1 Collection locality data from the Attawapiskat Formation, Akimiski Island, Nunavut.

Locality	UTM Coordinates	Number Species	Number Specimens
AK1a	17 E0502968, N5883572	19	988
AK1-01a	N/A	14	258
AK2a	17 E0502919, N5883641	19	752
AK2b	17 E0502915, N5883664	25	822
AK2c	17 E0502916, N5883663	22	1632
AK2-01a	17 E0502818, N5883943	17	365
AK3a	17 E0502897, N5883928	18	343
AK3b	N/A	11	76
AK3-01a	N/A	18	136
AK4a	17 E0492190, N5894890	2	3
AK4b	17 E0492180, N5894740	12	215
AK4c	17 E0492221, N5894749	10	54
AK5a	17 E0492166, N5894590	12	197
AK5b	17 E0492179, N5894538	1	619
AK5c	17 E0492171, N5894626	1	23
AK5d	17 E0492171, N5894626	15	243
AK5-01a	17 E0492170, N5894598	3	71
AK6-01a	17 E0491896, N5894682	14	207
AK6-01b	17 E0491863, N5894675	4	144
AK6-01c	17 E0491889, N5894656	4	384
AK7-01a	17 E0492704, N5893037	9	89
AK7-01b	17 E0492724, N5893028	13	113
AK7-01c	17 E0492712, N5893009	11	36
AK8-01a	17 E0492769, N5892837	11	171
AK8-01b	17 E0492776, N5892827	9	248
AK8-01c	17 E0492807, N5892733	12	172
AK8-01d	17 E0492757, N5892783	2	4
AK8-01e	17 E0492757, N5892783	8	156
AK9-01a	17 E0493104, N5892209	15	202
AK9-01b	N/A	17	92
HP01a	17 E0492121, N5895165	7	159
HP01b	17 E1492087, N5895268	2	58

N/A = Not available.
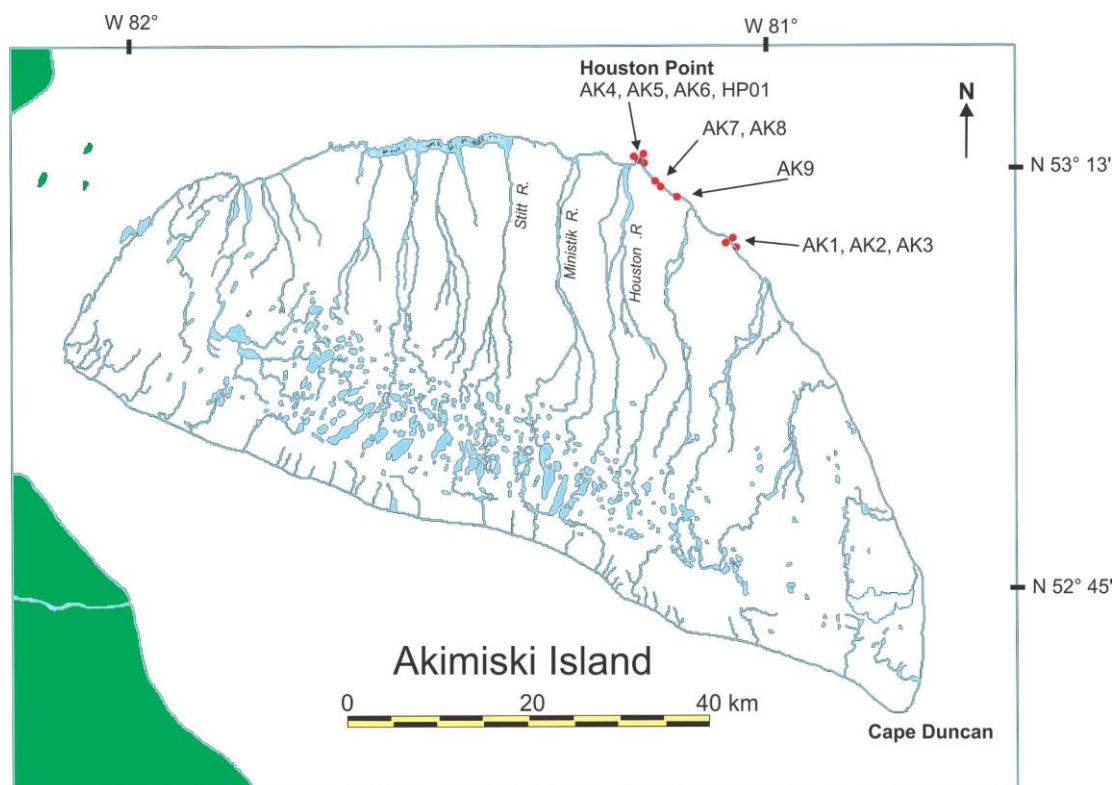
Figure 2.5: Collection localities from the Attawapiskat Formation of Akimiski Island, James Bay, Nunavut. GPS data provided by J. Jin.

2.4 Anticosti Island

Anticosti Island is approximately 222 km long, 56 km wide, and situated in the Gulf of Saint Lawrence. A continuous succession of Upper Ordovician–lower Silurian carbonate strata, ~1100 m thick, is exposed on the island, representing a remnant of the Ordovician–Silurian carbonate shelf of the Anticosti Basin (Long and Copper 1987; Copper and Long 1990; Long 2007; Desrochers et al. 2010). The succession is divided into eight formations; in ascending order, these are the Upper Ordovician Vauréal and Ellis Bay formations and the lower Silurian Becsie, Merrimack, Gun River, Meniér, Jupiter, and Chicotte formations (Copper and Long 1990; Copper et al. 2012, 2013; Copper and Jin 2015; Fig. 2.3). This succession is thought to have accumulated in the high paleotropic typhoon belt at ~25° south, as supported by evidence of storm activity in these strata (Desrochers et al. 2010; Torsvik and Cocks 2013; Fig. 2.2). Besides this storm deformation, the carbonate strata of Anticosti Island is largely pristine, despite its proximity to the Taconic Orogeny. Both tectonic disturbance and siliciclastic influence on the strata of the island is limited to absent in most outcropping successions (Long and Copper 1987; Long 2007). Remarkebly, peritidal deposits, such as ooids, have not been found in the successions of the island signifying the Anticosti Basin was entirely carbonate shelf during the Late Ordovician and the early Silurian. The pristinely preserved strata and fossil biotas of this island make Anticosti Island a valuable site for studying the paleoenvironmental change and mass extinction event across the Ordovician–Silurian boundary.

In this thesis, brachiopod faunas from specific study sites of four outcropping stratigraphic units (discussed below) were made from Anticosti Island. These units range

from Hirnantian to late Telychian in age and show reef communities during the Late
Ordovician glaciations and their recovery in the Llandovery. This large expanse of time
allows for the detailed study of the recovery of coral-stromatoporoid reef systems and
their brachiopod communities.

2.4.1 Laframboise Member, Ellis Bay Formation

The Ellis Bay Formation is a Hirnantian sequence of fossiliferous limestones and
shales capped by distinct coral-stromatoporoid reef buildup (Achab et al. 2013; Copper et
al. 2013; Fig. 2.2 herein). The stratigraphy of this formation is complex and is much
thicker on the western side of the island than on the eastern side. The western facies of
the Ellis Bay Formation are separated into five distinct units: the Fraise Member, the
Juncliff Member, the Parastro Member, the Lousy Cover Member, and the Laframboise
Member (Copper et al. 2013). The two uppermost members are relatively correlatable
across the island, but the bottom three units are equivalent to the Prinsta Member found
in the eastern outcrops (Long and Copper 1987). The fauna of this formation shows a
transition from typical Richmondian fauna at the base of the formation to a Hirnantian
fauna dominated by *Hindella.* Early Silurian brachiopod progenitors, such as *Mendacella*,
Parastrophinella, and *Eospiringia*, first appear in this formation as well. The uppermost
strata of this formation record the extinction of the Hirnantian fauna, with only 10% of
Ordovician genera surviving into the Llandovery (Copper et al. 2013).

The Fraise Member is composed of calcarenites and thin shales at its base but
becomes shale-dominated higher in the member. The Katian–Hirnantian boundary likely

occurs at the base of this member as there is a transition from typical Richmondian fauna to cooler water hold-over taxa such as *Herbertella maria*, *Plaesiomys anticostiensis*, and *Vellamo diversa* (Jin and Zhan 2008) as well as the first appearances of typical Hirnantian brachiopods *Hindella* and *Eospirigerina* (Copper et al. 2013). These two genera dominate the fauna of the top of the Fraise Member with *Hindella* being very abundant in coeval strata in the Prinsta Member across the island.

The Juncliff Member is easily recognizable at its contact with the Fraise Member as the shales of the lower unit pass upward to grey to white, evenly bedded micrites. The fauna of this member is less diverse and abundant than the underlying Fraise Member although new species of *Hindella* and *Eospirigerina* dominate the shelly fauna. A diagnostic species of the Juncliff Member is *Barbarorthis laurentina*, while *Pleasiomys*, *Mendacella*, *Ptychopleura*, and *Vinlandostrophia* are also common elements of the brachiopod fauna (Jin and Zhan 2008). The overlying Parastro Member, consisting of thinly bedded shales and soft, platy to nodular limestones, is exceptional within the Ellis Bay Formation due to the dominance of *Parastrophinella reversa* within it. This species occurs alongside a diverse fauna consisting of *Hindella*, *Vinlandostrophia*, *Mendecella*, *Herbertella*, and *Leptaena*. *Eospirigerina* is present but rare in this member (Jin and Copper 2008). The Lousy Cover Member has a similar lithology to the Juncliff member consisting of platy micrites and shales. Faunally, this member is dominated by *Hindella* but contains abundant large aulaceratid stromatoporoids and smaller coral and crinoid components (Long and Copper 1987).

The Laframboise Member is the most biologically diverse unit of the Ellis Bay Formation with coral-stromatoporoid patch reefs growing 5–15 m in thickness (Petryk

1981). Overlying a thin unit of *Girvenella* oncolite these reefs are capped by crinoidal grainstones containing a *Hirnantia sagittifera* dominated brachiopod fauna (Long and Copper 1987; Jin and Zhan 2008). Other common brachiopods found in this member are *Hindella*, *Mendecella*, and *Leptaena*. The top of this member marks the second pulse of the Late Ordovician mass extinctions and reefs do not appear to survive into the Rhuddanian Becscie Formation (Copper 2001; Copper et al. 2013). This member was selected for study due to its rich reef-dwelling brachiopod fauna during the latest Ordovician, a time of intense climatic and biologic stress. The brachiopod communities of the Laframboise reefs serve as a background and comparison for those of the recovering faunas in the early Silurian.

The overlying Becscie, Merrimack, and Gun River formations were not included in this thesis for two reasons: 1) as this study focused on reef-dwelling brachiopods, and these formations are not reef-bearing (Long and Copper 1987) their brachiopod faunas were unsuitable for the analyses, and 2) the genus *Pentameroides*, which was selected for study in Chapter 3 because of its occurrence in both level-bottom and reef habitats, is restricted to the Telychian and as such does not occur in the pentameride brachiopod faunas of these older Llandovery formations.

2.4.2 East Point Member, Meniér Formation

The East Point Member of the Meniér Formation is mid-Aeronian in age and characterized by coral-stromatoporoid reefs and crinoidal grainstones (Fig. 2.3). The Meniér Formation was established by Copper and Jin (2012, 2015) to comprise the

Goéland Member and East Point Member, previously considered the lower part of the Jupiter Formation (Copper and Long 1990). Patch reefs of the East Point Member were constructed mainly by tabulate corals, rugose corals, and stromatoporoids, and contain relatively common brachiopods, crinoids, and nautiloids. These reefs are relatively small, but show some of the earliest known symbiotic intergrowth between stromatoporoids and corals in the Llandovery (Copper and Jin 2012). A transgressive event occurs above the Meniér Formation, as indicated by the dominance of micritic mudstones and calcareous shale in the Richardson Member at the base of the Jupiter Formation, with stricklandiid and *Dicoelosia* brachiopod communities of an outer shelf (BA4 to BA5) depositional environment (Jin and Copper 1999; Jin 2008).

Brachiopods are locally common in the East Point Member, although not as abundant nor diverse as in later coral-stromatoporoid reef environments such as those from the Attawapiskat Formation. *Stergerhynchus* is the dominant brachiopod taxon, making up ~85% of the brachiopod fauna of the reefs. Less common taxa include the pentamerides *Clorinda* and *Pentamerus* and the orthide *Dolerorthis*. Importantly, the reefs show the initial association of the large-shelled *Pentamerus* in the early Silurian. In the underlying Gun River Formation pentameride faunas slowly replace the older Rhuddanian fauna, but they begin to become more dominant in the Meniér Formation. The brachiopod faunal turnover as well as the reef recovery may have both been initiated in association with favourable climatic conditions (Copper et al. 2012).

2.4.3 Pavillon Member, Jupiter Formation

The Jupiter Formation is ~170 m thick, late Aeronian–middle Telychian in age, consisting of calcareous mudstone, skeletal wackestone, packstone, and grainstone (Copper and Long 1990; Fig. 2.3). This formation, as revised by Copper and Jin (2015), is divided into four members: in ascending order, these are the Richardson Member, the Cybèle Member, the Ferrum Member, and the Pavillon Member. The entire formation represents one regressive cycle bounded by the East Point patch reefs of the Meniér Formation below (Copper and Jin 2012) and the reefal and crinoidal grainstones of the Chicotte Formation above (Brunton and Copper 1994). Clayer and Desrochers (2014) suggest that the regression of the Jupiter Formation is overprinted by several smaller scale transgressive-regressive cycles near the top of the formation and that the Jupiter–Chicotte boundary corresponds to a mid-Telychian glaciation event. Reefs do not occur in the Jupiter Formation except locally at Jupiter-Chicotte formational boundary. The level-bottom brachiopod communities are well preserved and used in this study for comparison with the reef dwelling communities to help understand the origin of reef-dwelling brachiopod communities in the early Silurian.

Pentameride brachiopods dominate the fauna of this formation, with well-developed *Stricklandia, Costistricklandia, Ehlersella*, and *Pentamerus* communities that were characteristic of the Llandovery (Jin and Copper 2000). Other important fossil groups in the formation include trilobites, crinoids, ostracods, bryozoans, molluscs, corals, stromatoporoids, and sponges (Copper and Long 1990). The Jupiter Formation, preserving abundant storm deposits, is interpreted to have accumulated in the higher tropics of the early Silurian, where the seafloor was frequently disturbed by storms

(Copper and Jin 2012, 2015). Even in the mid-shelf (BA 3) settings, brachiopod shells in the *Pentamerus* and stricklandiid shell beds show evidence of reworking, truncation, and disarticulation (Jin 2008). This is true also for *Pentameroides*, used as study specimens in Chapter 3, as its shells in the upper Pavillon Member range from well preserved in micritic mudstone to broken and disarticulated in shell packstones.

The Richardson Member records the deepest marine environment of this sucession and is composed of thinly bedded calcareous shales. The overlying Cybèle and Ferrum members are primarily composed of argillaceous limestones and cleaner limestones respectively represent a shallowing upward sequence culminating in the Pavillon Member (Copper and Long 1990). Pentameride brachiopod faunas of these members are dominated by stricklandiids suggesting a deep shelf (BA 4) environment (Jin 2008).

The Pavillon Member is composed of grey argillaceous micrite, wakestones, packstones, grainstones, blueish-green shale, and contains abundant shell beds (Petryk 1981). Brachiopods are very common in this member with abundant atrypides, athyrides, and pentamerides (Jin and Copper 2000). Due to the dominance of *Pentamerus* in this member, the depth has been interpreted as mid-shelf depth (BA3–BA4; see Jin 2008). The top few meters of the member record the transition from *Pentamerus oblongus* to *Pentameroides subrectus* in a cladogenesis event (Jin and Copper 2000; Glasser 2002). Small patch reefs appear the uppermost section of the Pavillon Member before being succeeded by the Chicotte Formation's crinoidal reefs.

2.4.4 Chicotte Formation

The overlying Chicotte Formation is late Telychian in age and the youngest of the strata of Anticosti Island. This ~75 m-thick formation occurs on the southwest outcrops of the island and is generally monolithic as ~95% of the formation consists of crinoid skeletal packstones and grainstones (Brunton and Copper 1994; Fig. 2.3). Coral-stromatoporoid boundstones and bryozoan-rich mudmounds also occur in this formation (Desrochers et al. 2007).

In terms of brachiopod fauna, *Stergerhynchus* and *Gotatrypa* are the most abundant brachiopod taxa in this formation, similar to the reefs of the East Point Member, with minor occurrences of other brachiopods, such as *Pentamerus*, *Costistricklandia*, *Clorinda*, and *Whitfieldella*. *Pentameroides* has not been found in the Chicotte Formation, despite its younger strata overlying the *Pentameroides*-bearing Pavillon Member of the Jupiter Formation (Jin and Copper, 2000). Other fossils present in the Chicotte Formation include trilobites, cephalopods, gastropods, and bryozoans (Brunton and Copper 1994).

2.5 Michigan Basin

The Michigan Basin is a nearly circular intracratonic basin in the Lower Peninsula of Michigan State, under lakes Michigan and Huron, in eastern Wisconsin, and on Bruce Peninsula and Manitoulin Island of Ontario. The Silurian strata of the Michigan Basin is composed of open marine and reefal limestones as well as evaporitic dolostones (Copper 1978; Watkins 1991; Brunton et al. 2009). In this thesis, two formations, the Fossil Hill

Formation of Manitoulin Island, Ontario, and the Racine Formation of Wisconsin, were investigated to compare their pentameride brachiopods with those of the Hudson Bay and Anticosti Island (Fig. 2.2). In the Fossil Hill Formation, abundant *Pentameroides subrectus* occurs as shell beds in a level-bottom carbonate setting, in contrast to the reef-dwelling brachiopod *Pentameroides septentrionalis* in the Hudson Bay region. The younger Racine Formation, however, contains a diverse and abundant brachiopod fauna in coral-stromatoporoid reef deposits.

2.5.1 Fossil Hill Formation, Manitoulin Island

The Fossil Hill Formation is middle Telychian in age, ~30–40 m thick (Copper 1978), and consists of grey, medium bedded, richly fossiliferous dolostones (Chiang 1971; Fig. 2.3). It overlies the thin, dolomitized, ripple-marked Mindemoya Formation, and is disconformably overlain by the grey-green, argillaceous dolomicrite to wackestone of the Rockway Formation from Manitoulin Island to Niagara Falls (Liberty 1968; Brunton et al. 2009). In mainland southern Ontario, the Fossil Hill Formation is partly correlative to the Merriton Formation which occurs from Bruce Peninsula to the Niagara Falls region of New York State (Brunton et al. 2009).

On Manitoulin Island, the Fossil Hill Formation is divided into three unnamed units. The lower unit contains shell beds of large-shelled *Pentamerus* that gives way to the less fossiliferous lime mudstone-wackestone middle unit (Stott and von Bitter 2000), with locally abundant favositid coral and stromatoporoid biostromes in the mudstone (Copper 1978, Johnson 1981). In the upper Fossil Hill member, *Pentameroides subrectus* becomes dominant constituting up to 97% of the community, with minor amounts of

Stegerynchus, *Callipentamerus*, and *Plickostricklandia*. These *Pentameroides* dominated level-bottom communities are used as a comparison with the reef-dwelling *Pentameroides septentrionalis* in Chapter 3 and to the reefal communities in Chapter 4.

The Fossil Hill Formation was most likely deposited in an open and well-oxygenated marine system due to the occurrences of abundant brachiopod and coral faunas, in the mid to high tropics (15–20°) south of the equator (Torsvik and Cocks 2013; Fig. 2.2). Being further from the equator, this shallow marine ecosystem would have been within the Silurian typhoon belt as shown by the thin lenses of pentameride coquina and the predominantly broken, disarticulated, and infilled shells found throughout the more fossiliferous units (Copper 1978; Brunton et al. 2009).

2.5.2 Racine Formation, Wisconsin

The Racine Formation represents a mid-Sheinwoodian to Homerian (Wenlock) succession of Silurian reef tract (Willman 1973; Fig. 2.3). The reefs of this formation were deposited on the modern southwestern margin of the Michigan Basin and existed at 15–20° south in a shallow, high-energy environment (Watkins 1998; Torsvik and Cocks 2013; Fig. 2.2). Lithologically, the formation is composed of coral-stromatoporoid bioherms overlying cross-stratified grainstone and thinly bedded inter-reef dolostones (Willman 1973). Further from the reef core, oncolite packstone and wackestone replace the coral-stromatoporoid-calcimicrobe boundstones. The reefs themselves are quite large with individual reefs reaching 90 m in thickness and over 2 km in diameter (Watkins 1998). Both reef builders and dwellers exhibit high diversity with the benthic fauna dominated the by the brachiopods *Antirhynchonella*, *Reserella*, and *Dicoelosia* (Watkins

1994). Other fossil groups within the Racine Formation are crinoids, gastropods, cephalopods, bryozoans, and trilobites (Watkins 1991, 1993). Unlike the Attawapiskat reefs, pentameride brachiopods only make up a small component of this reef-dwelling brachiopod fauna. Adjacent to the reefs however, the pentameride genera *Kirkidium* and *Apopentamerus* are the dominant brachiopod types (Watkins 1994, 1998).

2.6 Högklint Formation, Gotland, Sweden (Baltica)

The Baltic Basin is an intracratonic or pericratonic basin that lies south of the Fennoscandian Shield and west of the East European Platform (Porpawa et al. 1999; Fig. 2.6). Within this basin is the island of Gotland, Sweden that contains 500–700 m of early to middle Silurian carbonate strata (Calner et al. 2004). The Silurian succession of Gotland is interpreted as remnants of a larger Silurian carbonate basin which extends southward in subcrop to Ukraine (Samtleben et al. 1996). Gotland is very similar in many respects to Anticosti Island, as both contain large sections of relatively undisturbed and fossiliferous carbonates. The chief difference between the two localities is age. Whereas Anticosti extends from the Katian to Telychian, the strata of Gotland ranges from late Telychian to Ludfordian. The strata of Gotland was deposited ~10° south of the paleoequator, likely at the edge of the Silurian typhoon belt (Torsvik and Cocks 2013; Jin et al. 2013; Fig. 2.2). As such, the stratigraphy and fossils of Gotland are not as deformed by storm activity as those on Anticosti Island.

The Högklint Formation (Sheinwoodian) contains some of the best-developed patch reefs on Gotland. The entire formation consists of these reefs and inter-reef

Figure 2.6: Location of Gotland, Sweden within the Baltic Basin. Baltic Basin encircled in red. Shields are enclosed in dotted lines. Modified from Porpawa et al. 1999 and Calner et al. 2004.

limestones and is up to 35 m thick at its maximum exposure (Calner et al. 2004),

surrounded by well-sorted crinoidal boundstones and grainstones. The inter-reef

limestones alternate with marls and contain a rich marine benthic fauna abundant with

diverse stromatoporoids, corals, brachiopods, bryozoans, crinoids, and trilobites

(Samtleben et al. 1996; Watkins 2000). This formation has been divided into four units

(A–D) which grade from bioherm-dominated in A and lower B to biostromes in the upper

B and C unit. At the top of unit C exists an unconformity which is overlain by unit D

(Calner et al. 2004). In terms of reef structure, stromatoporoids are recognized as the

most abundant framework builders with lesser tabulate corals, calcareous algae, and

cyanobacteria. Higher in the formation algae becomes more dominant and shows areas

of exposure and desiccation, suggesting that the top of the Högklint Formation may have

formed in peritidal conditions (Sambtleben et al. 1996).

Dicoelosia is a locally abundant component of brachiopod fauna of this formation

with common *Pentlandina, Rhyncotreta*, and *Whitfieldella* locally (Watkins 2000). Rarer

genera found in the Högklint Formation include *Isorthis*, *Clorinda*, *Leptaena*,

Spinatrypina, and *Linoporella* (Watkins 2000). The common occurrence of *Clorinda* and

Dicoelosia in the Högklint Formation, which would indicate an outer shelf (BA 5)

depositional environment in level-bottom brachiopod community zonation (Boucot,

1975; Jin and Copper 1999) suggest that the level-bottom brachiopod community model

cannot be applied readily to reefal communities as suggested by Jin (2003) regarding the

Attawapiskat reefs.

2.7 Biostratigraphic Correlations

The Attawapiskat Formation, the Fossil Hill Formation, and the Pavillon Member of the Jupiter Formation have been dated as middle Telychian in age as based on their pentameride brachiopod faunal zones and conodont biozones (Norris 1986; Jin et al. 1993; Zhang and Barns 2002a, 2007; Fig. 2.3). The Attawapiskat Formation is characterized by the *Pentameroides septentrionalis–Lissatrypa variabilis* faunal zone. This zone correlates directly to the *Pentameroides subrectus–Plicostricklandia manitouensis* faunal zone of the Rockway and upper Fossil Hill formations of Manitoulin Island and the *Pentameroides subrectus–Costistricklandia gaspeensis* faunal zone of the Pavillon Member of the Jupiter Formation (Jin et al. 1993; Jin and Copper 2000). It is likely that the Jupiter and Fossil Hill formations are slightly older, most likely early–middle Telychian, than the Attawapiskat Formation that likely represents a middle–late Telychian age due to the first appearance datum (FAD) of *Pentameroides* found in the locations. Despite this, the three formations remain comparable especially considering the similarities of the brachiopod faunas found in all three locations, specifically the occurrence and dominance of *Pentameroides* as opposed to *Pentamerus*.

The brachiopod-based correlation is corroborated by conodont biozones, which have been used as index fossils in biostratigraphic studies for several decades. The original North American conodont biostratigraphic work was largely carried out during the 1970s and 80s (see Barnes and Fåhræus 1975; Le Fèvre et al. 1976; Barnes and Bergström 1988), but recent revisions of Upper Ordovician and lower Silurian conodont biozones on Anticosti Island and the Hudson Platform (Zhang and Barnes 2002a, 2002b, 2004, 2007) have allowed for detailed correlation between brachiopod and conodont

biozones within and across sedimentary basins. On Anticosti Island, the *Apsidognathus tuberculatus–Pterospathodus celloni–P. pennatus procerus–Carniodus carnulus–Ozarkodina policlinanta* conodont community (A.P.P.C.O.) occurs at the Jupiter–Chicotte boundary (Zhang and Barnes 2002a) alongside the first occurrence of *Pentameroides subrectus* (Glasser 2002). The occurrence of *Pterospathodus celloni* in this community suggests that the Jupiter–Chicotte contact is middle Telychian as this species globally correlates to that age (Männick 1998). This species occurs in the Hudson Platform as part of the *Pterospathodus celloni–P. eopennatus* biozone (Zhang and Barnes 2007) which has been found from the upper Severn River Formation to the lower Kenogami River Formation suggesting that the Attawapiskat Formation is middle Telychian in age. Due to the occurrence of the two *Pterospathodus celloni* conodont biozones and the three *Pentameroides* brachiopod biozones, the Pavillon Member of the Jupiter Formation, the upper unit of the Fossil Hill Formation and the Attawapiskat Formation are directly correlatable and middle Telychian in age.

References

Achab, A., Asselin, E., Desrochers, A., and Riva, J.F. 2013. The end-Ordovician chitinozoan zones of Anticosti Island, Québec: definition and stratigraphic position. Review of Palaeobotany and Palynology, 198: 92–109.

Barnes, C.R., and Fåhræus, L.E. 1975. Provinces, communities, and the proposed nektobenthic habit of Ordovician conodontophorids. Lethaia, 8(2): 133–149.

Barnes, C.R., and Bergström, S.M. 1988. Conodont biostratigraphy of the uppermost Ordovician and lowermost Silurian. *In* A Global Analysis of the Ordovician and lowermost Silurian, Bulletin of the British Museum Natural History Geology 43, *Edited by* Cocks, L.R.M., and Rickards, R.B. p. 325–343.

Boucot, A.J. 1975. Evolution and extinction rate controls. Elsevier, New York.

Brunton, F.R., and Copper, P. 1994. Paleoecologic, temporal, and spatial analysis of early Silurian reefs of the Chicotte Formation, Anticosti Island, Quebec, Canada. Facies, 31: 57–79.

Brunton, F.R., Turner, E., and Armstrong, D. 2009. A guide to the Paleozoic geology and fossils of Manitoulin Island and northern Bruce Peninsula, Ontario, Canada. Canadian Paleontology Conference Field Trip Guidebook, 14.

Calner, M., Jeppsson, L., and Munnecke, A. 2004. The Silurian of Gotland—Part I: Review of the stratigraphic framework, event stratigraphy, and stable carbon and oxygen isotope development. Erlanger geologische Abhandlungen, Sonderband, 5: 113–131.

Chiang, K.K. 1971. Silurian pentameracean brachiopods of the Fossil Hill Formation, Ontario. Journal of Paleontology, 45: 849–861.

Chow, A.M., and Stearn, C.W. 1988. Attawapiskat patch reefs, Lower Silurian, Hudson Bay Lowlands, Ontario. Canadian Society of Petroleum Geologists Memoir, 13: 273–270.

Clayer, F., and Desrochers, A. 2014. The stratigraphic imprint of a mid-Telychian (Llandovery, Early Silurian) glaciation on far-field shallow-water carbonates, Anticosti Island, Eastern Canada. Estonian Journal of Earth Sciences, 63(4): 207–213.

Copper, P. 1978. Paleoenvironments and paleocommunities in the Ordovician-Silurian sequence of Manitoulin Island. Michigan Basin Geological Society Special Papers, 3: 47–61.

Copper, P. 2001. Reefs during multiple crises towards the Ordovician-Silurian boundary: Anticosti Island, eastern Canada, and worldwide. Canadian Journal of Earth Sciences, 38: 153–171.

Copper, P., and Long, D.G.F. 1990. Stratigraphic revision of the Jupiter Formation, Anticosti Island, Canada: a major reference section above the Ordovician-Silurian boundary. Newsletters on Stratigraphy, 23: 11–36.

Copper, P., and Jin, J. 2012. Early Silurian (Aeronian) East Point coral patch reefs of Anticosti Island, Eastern Canada: first reef recovery from the Ordovician/Silurian mass extinction in eastern Laurentia. Geosciences, 2: 64–89.

Copper, P. and Jin, J. 2015. Tracking the early Silurian post-extinction faunal recovery in the Jupiter Formation of Anticosti Island, eastern Canada: A stratigraphic revision. Newsletters on Stratigraphy, 48(2): 221–240.

Copper, P., Long, D.G., and Jin, J. 2012. The Early Silurian Gun River Formation of Anticosti Island, eastern Canada: A key section for the mid-Llandovery of North America. Newsletters on Stratigraphy, 45(3): 263-280.

Copper, P., Jin, J., and Desrochers, A. 2013. The Ordovician–Silurian boundary (late Katian-Hirnantian) of western Anticosti Island: revised stratigraphy and benthic megafaunal correlations. Stratigraphy, 10(4): 213–227.

Desrochers, A., Bourque, P.A., and Neuweiler, F. 2007. Diagenetic versus biotic accretionary mechanisms of bryozoan–sponge buildups (Lower Silurian, Anticosti Island, Canada). Journal of Sedimentary Research, 77(7): 564–571.

Desrochers, A., Farley, C., Achab, A., Asselin, E., and Riva, J.F. 2010. A far-field record of the end Ordovician glaciation: the Ellis Bay Formation, Anticosti Island, Eastern Canada. Palaeogeography, Palaeoclimatology, Palaeoecology, 296(3): 248–263.

Eggie, L.A., Pietrus, E., Ramdoyal, A. and Chow, N. 2014. Diagenesis of the Lower Silurian Ekwan River and Attawapiskat formations, Hudson Bay Lowland, northern Manitoba (parts of NTS 54B, F, G); *in* Report of Activities 2014, Manitoba Mineral Resources, Manitoba Geological Survey: 161–171.

Glasser, P.M. 2002. Mode of evolution in the early Silurian *Pentamerus–Pentameroides* lineage, Anticosti Island, Quebec. M.Sc. thesis, Department of Earth Sciences, The University of Western Ontario, London, Ontario.

Hahn, K.E., and Armstrong, D.K. 2013. Project Unit 10-028. Petrographic Analysis of Paleozoic Strata in the Hudson Platform, Northern Ontario. Summary of Field Work and Other Activities 2013, Ontario Geological Survey, Open File Report 6290. p 35-1 to 35-12.

Haq, B.U., and Schutter, S.R. 2008 A chronology of Paleozoic sea level changes. Science, 322: 64–68.

Jin, J. 2002. Niche partitioning of reef-dwelling brachiopod communities in the Lower Silurian Attawapiskat Formation, Hudson Bay Basin, Canada. IPC 2002, Geological Society of Australia, Abstracts No. 68, 83–84.

Jin. J. 2003. The Early Silurian Brachiopod *Eocoelia* from the Hudson Bay Basin, Canada. Palaeontology, 46: 885–902.

Jin, J. 2005. Reef-dwelling gypiduloid brachiopods in the Lower Silurian Attawapiskat Formation, Hudson Bay region. Journal of Paleontology, 79(1): 48–62.

Jin, J. 2008. Environmental control on temporal and spatial differentiation of Early Silurian pentameride brachiopod communities, Anticosti Island, eastern Canada. Canadian Journal of Earth Sciences, 45: 159–187.

Jin, J., and Copper, P. 1999. The deep-water brachiopod *Dicoelosia* King, 1850, from the Early Silurian tropical carbonate shelf of Anticosti Island, eastern Canada. Journal of Paleontology, 73(6): 1042–1055.

Jin, J., and Copper, P. 2000. Late Ordovician and Early Silurian pentamerid brachiopods from Anticosti Island, Québec, Canada. Palaeontographica Canadiana, 18: 1–140.

Jin, J., and Copper, 2008. Response of brachiopod communities to environmental change during the Late Ordovician mass extinction interval, Anticosti Island, eastern Canada. Fossils and Strata, 54: 41–51.

Jin, J., and Zhan, R. 2008. Late Ordovician Orthide and Billingsellide brachiopods from Anticosti Island, Eastern Canada: diversity change through mass extinction. NCR Research Press, Ottawa, Ontario, Canada, 159 pp.

Jin, J., Caldwell, W.G.E., and Norford, B.S. 1993. Early Silurian brachiopods and biostratigraphy of the Hudson Bay lowlands, Manitoba, Ontario, and Quebec. Geological Survey of Canada Bulletin, 457.

Jin, J., Harper, D.A.T., Cocks, L.R.M., McCausland, P.J.A., Rasmussen, C.M.Ø., and Sheehan, P.M. 2013. Precisely locating the Ordovician equator in Laurentia. Geology, 41: 107–110.

Johnson, M.E. 1981. Correlation of Lower Silurian strata from the Michigan Upper Peninsula to Manitoulin Island. Canadian Journal of Earth Sciences, 18(5): 869–883.

Johnson, M.E. 1987. Extent and bathymetry of North American platform seas in the early Silurian. Paleoceanography, 2: 185–211.

Johnson, M.E. 2006. Relationship of Silurian sea-level fluctuations to oceanic episodes and events. GFF, 128(2): 115–121.

Johnson, M.E. 2010. Tracking Silurian eustasy: Alignment of empirical evidence or pursuit of deductive reasoning?. Palaeogeography, Palaeoclimatology, Palaeoecology, 296(3): 276–284.

Johnson, M.E. and Colville, V.R., 1982. Regional integration of evidence for evolution in the Silurian *Pentamerus–Pentameroides* lineage. Lethaia, 15: 41–54.

Johnson, M. E., and Baarli, B.G. 1987. Encrusting corals on a latest Ordovician to earliest Silurian rocky shore, southwest Hudson Bay, Manitoba, Canada. Geology, 15(1): 15–17.

Johnson, M.E., Baarli, B.G., Nestor, H., Rubel, M., and Worsley, D. 1991. Eustatic sea-level patterns from the Lower Silurian (Llandovery Series) of southern Norway and Estonia. Geological Society of America Bulletin, 103(3): 315–335.

Le Fèvre, J., Barnes, C.R., and Tixier, M. 1976. Paleoecology of Late Ordovician and Early Silurian conodontophorids, Hudson Bay Basin. Geological Association of Canada, Special Paper, 15: 69–89.

Liberty, B.A. 1968. Ordovician and Silurian stratigraphy of Manitoulin Island, Ontario. Michigan Basin Geological Society, Field Trip Guidebook, pp. 25–37.

Long, D.G.F. 2007. Tempestite frequency curves: a key to Late Ordovician and Early Silurian subsidence, sea-level change, and orbital forcing in the Anticosti foreland basin, Quebec, Canada. Canadian Journal of Earth Sciences, 44(3): 413–431.

Long, D.G.F., and Copper, P. 1987. Stratigraphy of the Upper Ordovician upper Vaureal and Ellis Bay formations, eastern Anticosti Island, Quebec. Canadian Journal of Earth Sciences, 24(9): 1807–1820.

Männick, P. 1998. Evolution and taxonomy of the Silurian conodont *Pterospathouds*.
Palaeontology, 41(5): 1001–1050.

Norford, B.S. 1981. The trilobite fauna of the Silurian Attawapiskat Formation, northern
Ontario and northern Manitoba. Geological Survey of Canada Bulletin, 327.

Norris, A. W. 1986. Review of Hudson Platform Paleozoic stratigraphy and
biostratigraphy. *In* Canadian Inland Seas. *Edited by* Martini I.P., p. 17–42.

Norris, A.W. 1993. Hudson Platform – Geology. Chapter 8 *In* Sedimentary Cover of the
Craton in Canada, Geological Survey of Canada, Geology of Canada, No, 5.
Edited by Stott, D.F., and Aiken, J.D. p. 653–700.

Petryk, A.A. 1981. Stratigraphy, sedimentology and paleogeography of the upper
Ordovician–lower Silurian of Anticosti Island, Quebec. *In* Field Meeting,
Anticosti-Gaspé, Québec, 1981, Volume 2: Stratigraphy and Paleontology. Edited
by Lespérance P.J. p. 11–40.

Poprawa, P., Šliaupa, S., Stephenson, R., and Lazauskien, J. 1999. Late Vendian–Early
Palaeozoic tectonic evolution of the Baltic Basin: regional tectonic implications
from subsidence analysis. Tectonophysics, 314(1): 219–239.

Ramdoyal, A., Nicolas, M.P.B. and Chow, N. 2013: Lithofacies analysis of the Silurian
Attawapiskat Formation in the Hudson Bay Lowland, northeastern Manitoba; *in*
Report of Activities 2013, Manitoba Mineral Resources, Manitoba Geological
Survey, p. 144–155.

Samtleben, C., Munnecke, A., Bickert, T., and Pätzold, J. 1996. The Silurian of Gotland (Sweden): facies interpretation based on stable isotopes in brachiopod shells. Geologische Rundschau, 85(2): 278–292.

Sanford, B.V. 1987. Paleozoic geology of the Hudson platform. *In* Sedimentary Basins and Basin Forming Mechanisms, Canadian Society of Petroleum Geologists Memoir 12. *Edited by* Beaumont, C., and Tankard, A.J. p. 483–505.

Sanford, B.V. 1993. St. Lawrence Platform – Geology. Chapter 11 *In* Sedimentary Cover of the Craton in Canada, Geological Survey of Canada, Geology of Canada, No, 5. *Edited by* Stott, D.F., and Aiken, J.D. p. 723–786.

Sanford, B.V. and Norris, A.W. 1973. The Hudson Platform. *In* The Future Petroleum Provinces of Canada, their Geology and Potential. Canadian Society of Petroleum Geologists Memoir 1. *Edited by* MeCrossan R.G. p. 387–409.

Stott, D.F., and Aiken, J.D. 1993. Introduction. Chapter 1 *In* Sedimentary Cover of the Craton in Canada, Geological Survey of Canada, Geology of Canada, No, 5. *Edited by* Stott, D.F., and Aiken, J.D. p. 1–7.

Stott, C.A., and von Bitter, P.H. 2000. Lithofacies and age variation in the Fossil Hill Formation (Lower Silurian), southern Georgian Bay region, Ontario. Canadian Journal of Earth Sciences, 36(10): 1743–1762.

Suchy, D.R., and Stearn, C.W. 1993. Lower Silurian reefs and post-reef beds of the Attawapiskat Formation, Hudson Bay Platform, northern Ontario. Canadian Journal of Earth Sciences, 30: 575–590.

Torsvik, T.H., and Cocks, L.R.M. 2013. New global paleogeographical reconstructions for the early Paleozoic and their generation. Geological Society London Memoirs, 38: 5–24.

Watkins, R. 1991. Guild structure and tiering in a high-diversity Silurian community, Milwaukee County, Wisconsin. Palaios, 6: 465–478.

Watkins, R. 1993. The Silurian (Wenlockian) reef fauna of southeastern Wisconsin. Palaios, 8(4): 325–338.

Watkins, R. 1994. Evolution of Silurian pentamerid communities in Wisconsin. Palaios, 9: 488–499.

Watkins, R. 1998. Silurian reef-dwelling pentamerid brachiopods, Wisconsin and Illinois, USA. Palaontologische Zeitschrift, 72: 99–109.

Watkins, R. 2000. Silurian reef-dwelling brachiopods and their ecologic implications. Palaios, 15(2): 112–119.

Westrop, S.R., and Rudkin, D.M. 1999. Trilobite taphonomy of a Silurian reef: Attawapiskat Formation, northern Ontario. Palaios, 14: 389–397.

Willman, H.B. 1973. Rock stratigraphy of the Silurian System in northeastern and northwestern Illinois. Circular 479, Illinois Geological Survey, Urbana, Illinois. 55 pp.

Zhang, S., and Barnes, C.R. 2002. Late Ordovician–early Silurian (Ashgillian–Llandovery) sea level curve derived from conodont community analysis, Anticosti Island, Québec. Palaeogeography, Palaeoclimatology, Palaeoecology, 180(1): 5–32.

Zhang, S., and Barnes, C.R. 2002. Paleoecology of Llandovery conodonts, Anticosti Island, Quebec. Palaeogeography, Palaeoclimatology, Palaeoecology, 180(1): 33–55.

Zhang, S. and Barnes, C.R. 2004. Conodont bio-events, cladistics, and response to glacio-eustasy, Ordovician–Silurian boundary through Llandovery, Anticosti Basin, Québec. *In* The Palynology and Micropalaeontology of Boundaries. Geological Society, London, Special Publications, 230. *Edited by* Beaudin, A.B. and Head, M.J. p. 73–104.

Zhang, S., and Barnes, C.R. 2007. Late Ordovician–early Silurian conodont biostratigraphy and thermal maturity, Hudson Bay Basin. Bulletin of Canadian Petroleum Geology, 55(3): 179–216.

Ziegler, A.M. 1965. Silurian marine communities and their environmental significance. Nature, 207: 270–272.

Ziegler, A.M., Cocks, L.R.M., and Bambach, R.K. 1968. The composition and structure of lower Silurian marine communities. Lethaia, 1: 1–27.

Chapter 3 – The Paleolatitudinal morpho-gradient of *Pentameroides* in Telychian Laurentia[1]

3.1 Introduction

The Order Pentamerida Schuchert and Cooper, 1931 is divided into two suborders, the Syntrophiidina Ulrich and Cooper, 1936 which was common in the Early Ordovician and the Pentameridina Schuchert and Cooper, 1931 which originated in the Late Ordovician, but diversified rapidly following the end Ordovician mass extinction and became important brachiopod components during the Silurian (Harper et al. 2013). This suborder is separated into four superfamilies (Carlson et al. 2002), the Stricklandioidea Schuchert and Cooper, 1931, Gypiduloidea Schuchert and LeVene, 1929, Clorindoidea Rzhonsnitskaia, 1956, and Pentameroidea M'Coy, 1844. Within the Superfamily Pentameroidea, the Family Pentameridae M'Coy, 1844 is most characteristic, represented by several diverse genera commonly found in middle–late Llandovery carbonate deposits throughout Laurentia, Baltica, and South China (Basset and Cocks 1974; Boucot and Johnson 1979; Jin et al. 1993; Jin and Copper 2000; Rong et al. 2006). Some examples of common early Silurian pentamerid genera include *Pentamerus* Sowerby, 1813, *Sulcipenatmerus* Zeng, 1987, *Harpidium* Kirk, 1925, and

---

[1] A version of this chapter has been published online as: Gushulak, C.A.C., Jin, J., and Rudkin, D. 2016. Paleolatitudinal morpho-gradient of the early Silurian brachiopod *Pentameroides* in Laurentia. Canadian Journal of Earth Sciences, 53(7): 680–694.

Pentameroides Schuchert and Cooper, 1931, the last of which being the focus of this study.

Pentameroides is a large-shelled pentameride brachiopod that is commonly found in the Telychian carbonate facies of Laurentia and Baltica. In modern North America, well-preserved shells of *Pentameroides* are abundant in the Attawapiskat Formation in the Hudson Platform lowlands of northern Ontario, Manitoba, and Nunavut (Jin et al. 1993), the Hopkinton Dolomite of Iowa (Johnson 1979), the Merriton Formation of southern Ontario and New York (Kilgour 1963), the Fossil Hill Formation of Manitoulin Island, Ontario (Chiang 1971; Copper 1978), the Pavillon Member of the Jupiter Formation on Anticosti Island, Quebec (Jin and Copper 2000), and the Samuelsen Høj and Hauge Bjerge formations of North Greenland (Rasmussen 2009; Fig. 3.1). The occurrence of *Pentameroides* in deep-water basinal facies is known from the upper Whittaker Formation (uppermost Telychian–basal Sheinwoodian) of the Mackenzie Mountains, although such specimens may be allochthonous faunal components that were transported from shallower carbonate shelf settings via debris flows (Jin and Chatterton 1997).

Pentameroides evolved from *Pentamerus oblongus* Sowerby, 1839 during the early–middle Telychian. Previous work on the origin and evolution of *Pentameroides* was primarily done by Johnson (1979; see also Johnson and Colville 1982) on the *Pentameroides* of the Hopkinton Dolomite in Iowa, who proposed a *Pentamerus–Pentameroides* lineage. These authors suggested that the evolution was typical of Darwinian phyletic gradualism due to the apparent gradual convergence and eventual fusion of the inner hinge plates (= outer plates of older usage) of the dorsal valves to form
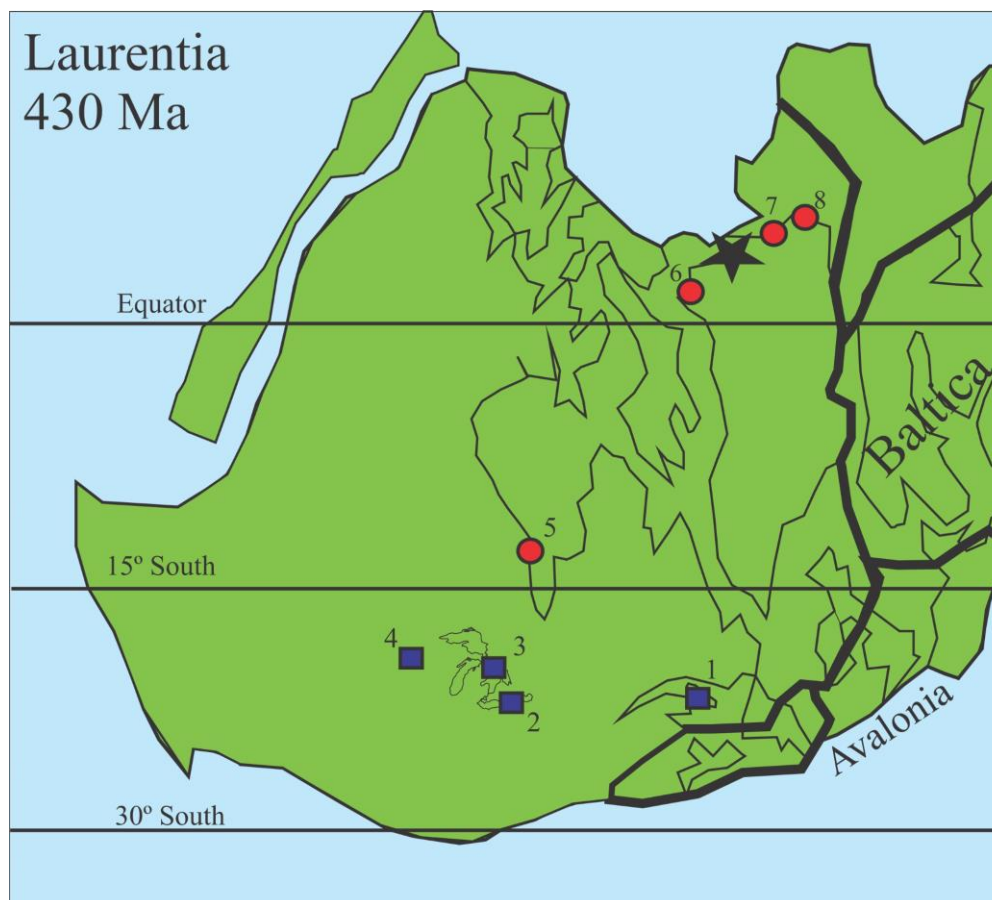
Figure 3.1: Map of Laurentia, Baltica, and Avalonia in the late Telychian (430 Ma). Thickened lines indicate boundaries of the paleoplates. Squares denote collection locations of *Pentameroides subrectus*: 1. Jupiter Formation, Anticosti Island, Quebec; 2. Merriton Formation, Southern Ontario and New York; 3. Fossil Hill Formation, Manitoulin Island, Ontario; 4. Hopkinton Dolomite, Iowa. Circles indicate locations of *Pentameroides septentrionalis*; 5. Attawapiskat Formation, Hudson Bay and Moose River basins; 6, 7, 8. Samuelsen Høj and Hauge Bjerge formations, North Greenland. Star denotes location of *Harpidium* and *Sulcipentamerus* Washington Land Group, North Greenland. Based on Torsvik and Cock's (2013) paleogeography.

the cruralium, which is expressed in external morphology as a junction of the long median septum with the valve floor. The mode of this speciation event has been debated, however, with more recent research suggesting a pattern of punctuated equilibrium because the abundant *Pentamerus oblongus* populations from Anticosti Island, Quebec, do not show a clear trend of converging inner hinge plates during the *Pentamerus–Pentameroides* transition interval (Glasser 2002). In any case, *Pentameroides* existed alongside *Pentamerus* during the middle–late Telychian, showing that the origin of *Pentameroides* was indeed a case of cladogenesis (Glasser 2002). From the southern margin of Laurentia *Pentameroides* spread northwards to occupy subequatorial intracratonic basins by the late Llandovery, with the genus comprising of at least three species: *Pentameroides subrectus* Hall and Clarke, 1893, *Pentameroides costellata* Chiang, 1971, and *Pentameroides septentrionalis* Whiteaves, 1904.

This study is based on two species of *Pentameroides*, *Pentameroides subrectus* found throughout the higher paleo-tropical latitude setting in the American mid-continent (Johnson 1979), Michigan Basin (Chiang 1971), and Anticosti Island (Jin and Copper 2000), and *Pentameroides septentrionalis* (see Jin and Copper 1986) in the sub-equatorial region of the Hudson Bay and Moose River basins (Jin et al. 1993). In addition to living at different latitudes, the two species inhabited different shallow marine environments. *P. subrectus* is found in storm-dominated, level-bottom environments (Copper 1978), whereas *P. septentrionalis* inhabited relatively low-turbulence coral-stromatoporoid reefal settings minimally affected by frequent severe storms (Jin et al. 1993; Jin 2002; Jin et al. 2013). *P. costellata* is not included in this study because it is a rare species and very few well-preserved shells are available for biometric study. In relation to Ziegler's (1965)

classic level-bottom brachiopod community zones (see also Ziegler et al. 1968; Boucot 1975), *Pentameroides* is thought to be equivalent to *Pentamerus* (Chiang 1971; Johnson 1979); inhabiting a mid-shelf environment (benthic assemblage (BA) 3) between the *Eocoelia* and *Stricklandia* community zones. This zoned community structure, however, cannot be applied directly to reefal settings due to high substrate heterogeneity and more complex paleoecological and paleocommunity structures (Jin 2003).

Gradients along paleolatitudes and depositional environments appear to manifest in differing morphological and taphonomic characters between localities and species of *Pentameroides*. *P. septentrionalis* exhibits excellent preservation, with large, complete, and very thin-walled hollow (non-infilled) shells (their anterior parts being as thin as an egg shell) found commonly in apparently shallow-water, coral-stromatoporoid reefs. This is in contrast to the micrite-infilled and broken shells of *P. subrectus* from higher latitude environments. In this chapter, specimens of *P. septentrionalis* from Akimiski Island, Nunavut, and *P. subrectus* from Manitoulin Island, Ontario, and Anticosti Island, Quebec were biometrically measured and statistically analyzed in order to identify any significant morphological differences between the species and to determine what environmental factors, if any, affected the evolution of the genus.

3.2 Materials and Methods

For biometric analysis, well-preserved specimens of *P. septentrionalis* (Fig. 3.2; Collections at Western University, to be deposited in the Invertebrate Palaeontology
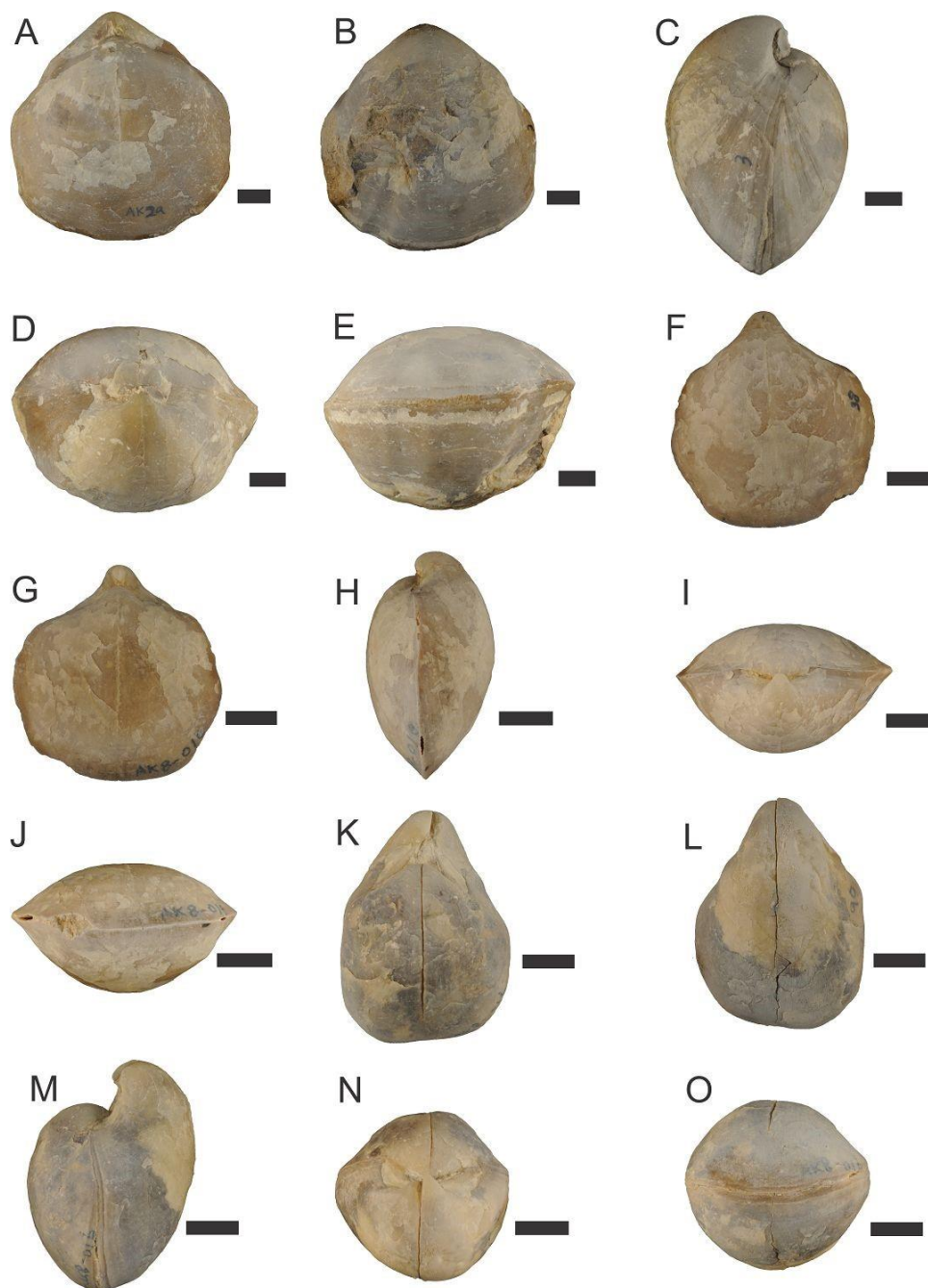
Figure 3.2: *Pentameroides septentrionalis*, Attawapiskat Formation, Akimiski Island, Nunavut. A–E: Specimen ROM 63693 late ontogeny, dorsal, ventral, lateral, posterior, and anterior views. F–J: Specimen ROM 63694 early ontogeny, dorsal, ventral, lateral, posterior, and anterior views. K–O: Specimen ROM 63695 transitioning morphology, dorsal, ventral, lateral, posterior, and anterior views. Scale bars are 1 cm.

collection, Royal Ontario, Museum, Toronto, Ontario), were selected from five localities (samples AK2, AK4, AK5, AK6, and AK8) of the Attawapiskat Formation along the north shore of Akimiski Island, Nunavut. Each of the five samples contributed 59, 53, 52, 53, and 105 specimens respectively, making up a total of 322 specimens. Specimens used for analysis were selected on the basis of their high degree of preservation as well as easily identifiable and measurable outer morphological characteristics.

These shells are often found in life (ventral umbo-down) position, associated with large framework-building tabulate corals and stromatoporoids of the reef. Disarticulation is relatively rare and most shells are found intact and often hollow with only a thin layer of isopachous calcitic cement lining the interior (Fig. 3.3: A, B). Well-preserved shells representing a complete ontogenetic sequence of this species can be observed, from very small (<10 mm) juvenile to very large (>65 mm) adult growth forms. The large mature shells from this formation often show asymmetrical and distorted shapes as a consequence of growing in tightly crowded clusters, but these specimens were not included in biometric analysis. These clusters generally occur in depressions within the reef between the large favositid tabulate corals where young shells could grow before being compressed and deformed by other surrounding shells (Jin 2002).

Specimens of *P. subrectus*, collected by P. Copper from the Fossil Hill Formation of Manitoulin Island, Ontario (Fig. 3.4), were also selected for measurement in this study. Although the samples are dominated by disarticulated and broken shells, well-preserved, articulated whole shells from two collections (M25 and M26) were selected for analysis. These two subsets consisted of 39 and 36 specimens respectively, amounting to a total of 75 specimens. One small collection containing 6 specimens of *P. subrectus* from the
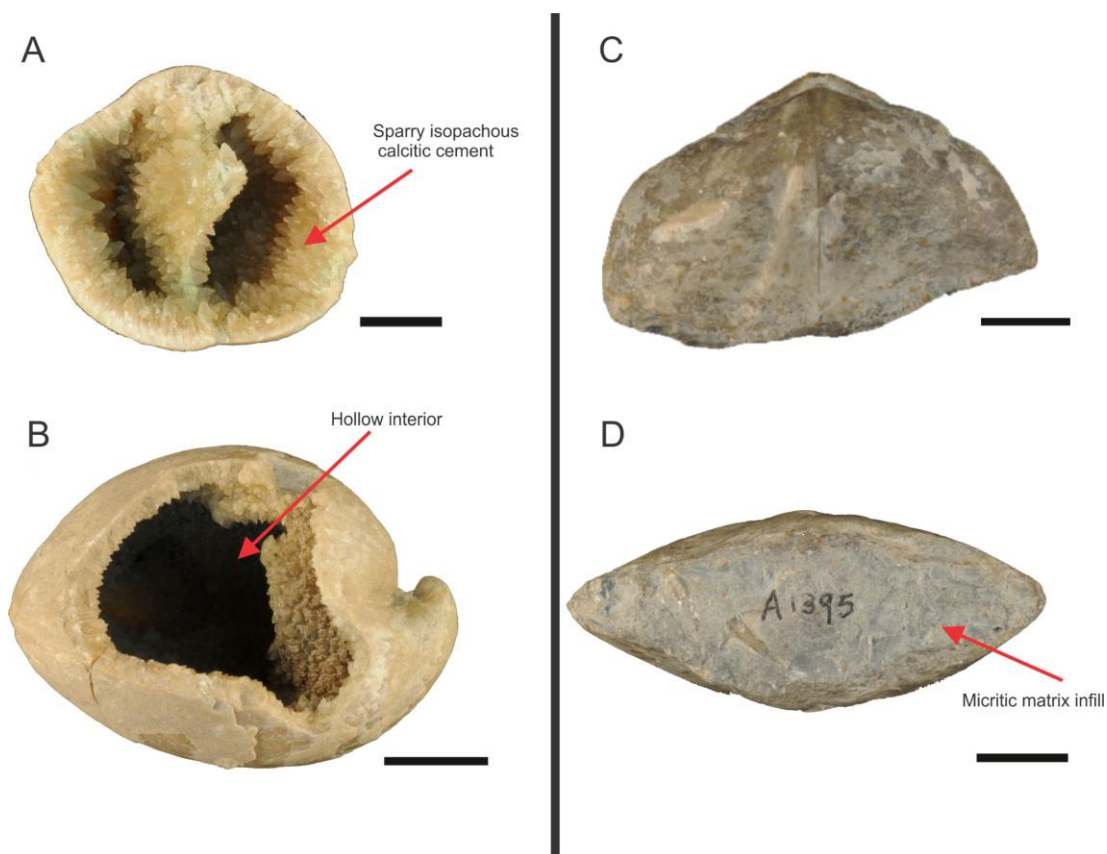
Figure 3.3: Differing preservation of *P. septentrionalis* (A/B) and *P. subrectus* (C/D). Note the egg-thin shell and isopachous cement filling in A/B and the broken and infilled shell of C/D. Scale bars are 1 cm. Specimen A: ROM 63696, Specimen B: ROM 63697, Specimen C/D: A1395.
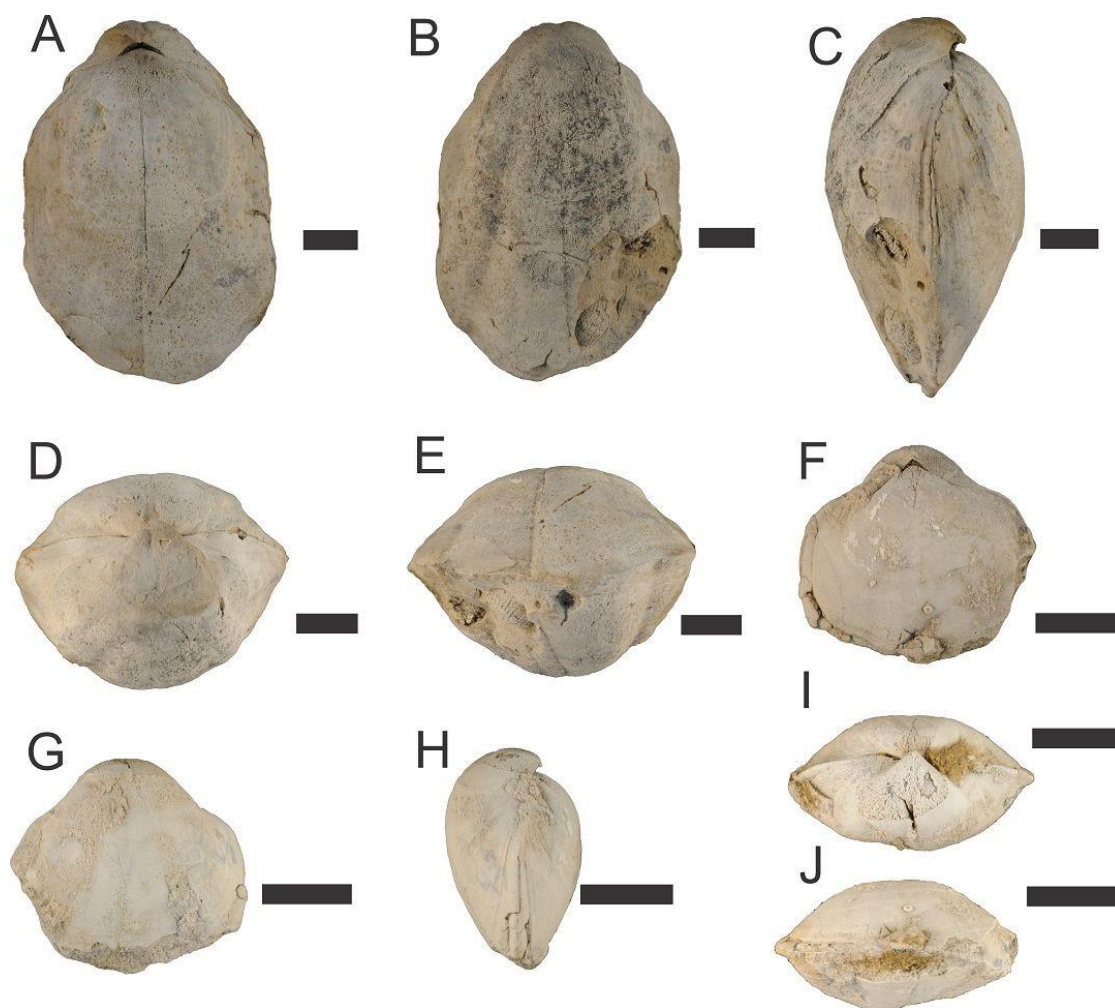
Figure 3.4: *Pentameroides subrectus*, Fossil Hill Formation, Manitoulin Island, Ontario. A–E: Specimen M25-2 dorsal, ventral, lateral, posterior, and anterior views. F–J: Specimen M25-43 dorsal, ventral, lateral, posterior, and anterior views. Scale bars are 1 cm.

Jupiter Formation of Anticosti Island, Quebec (reported in Jin and Copper, 2000) was also used for this study.

A total of 403 specimens were measured using a pair of 0.1 mm precise digital The shells from these localities are more poorly preserved than those from Akimiski Island and are often broken, deformed (particularly in the transverse plane), and filled by a fine grained micritic matrix (Fig. 3.3: C, D). This poorer preservation results in the relatively small size of the Manitoulin and Anticosti collections compared to the Akimiski Island collection.

A total of 403 specimens were measured using a pair of 0.1 mm precise digital calipers for the following characteristics (Fig. 3.5):

total shell length (L): linear measurement from anterior to posterior of the shell;

ventral umbonal height (U): linear measurement from the hinge line of the shell to the maximum distance of the ventral umbo;

length from the dorsal apex to the ventral umbo (A-B): linear measurement from the peak of the dorsal umbo to the beak of the ventral umbo;

total shell width (W): linear measurement of the shell at its widest point;

total shell thickness (T): linear measurement of the shell at its thickest/deepest point;

thickness of the ventral valve (Tv): linear measurement from the deepest/thickest point of the ventral valve to the commissural plane:

thickness of the dorsal valve (Td): linear measurement from the deepest/thickest point of the dorsal valve to the commissural plane.
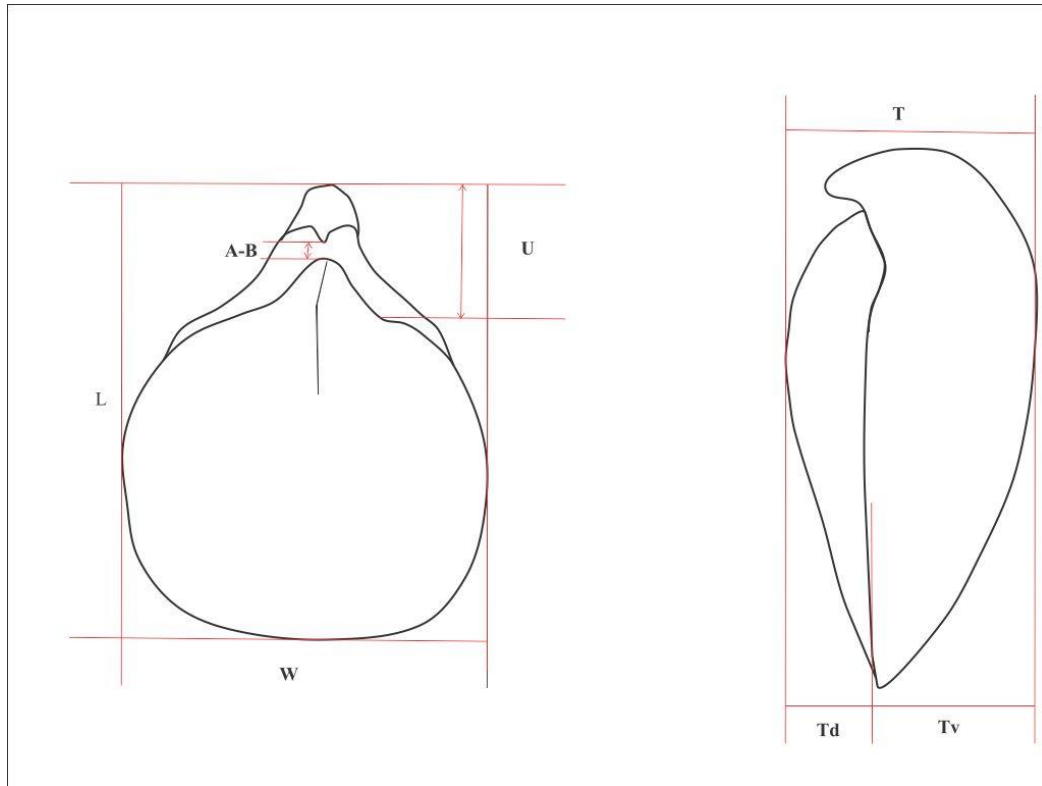
Figure 3.5: External morphological characters measured in this study. L: total shell length, U: ventral umbonal height, A-B: dorsal apex to ventral beak length, W: total shell width, T: total shell thickness, Td: dorsal valve thickness, Tv: ventral valve thickness.

In addition to these seven measurements, three morphology indices were developed and utilized in the statistical comparison between the two species. The indices are as follows:

T/W: **Thickness/width,** proxy for globosity — a higher value means a more globose shell;

U/L: **Ventral umbonal height/ length**, proxy for the size of the ventral umbo compared to the total shell — higher values indicate a large umbo and larger umbonal shell proportion;

Td/Tv: **Dorsal valve thickness/Ventral valve thickness**, proxy for biconvexity — higher values indicate a more convex shell.

The dataset derived from the measurements (Appendix 1) was analyzed statistically using the PAST Software Package v 3.08 (Hammer et al. 2001; Hammer and Harper 2006) in several linear regression comparisons between the different collections and species. This statistical software was selected for use as it is specifically designed to be utilized in the analysis of paleontological data sets. Principal components analysis (PCA) was also performed to create a scatter plot to detect possible ordination or trends of morphological changes. PCA is a quantitative analytical method which groups the multiple variables of a data set into a smaller (typically 2) and more manageable number, which is then plotted into a 2-dimensional graph (Hammer and Harper 2006). The principal components generated by the analysis represent the maximum amount of variance within the variables of the data set. Simplified, this means that PCA condenses complex multivariate data sets into a manageable bivariate plot. The practical use of this is to create plots that compare the original multivariate data points directly and group them into clouds of related points. The plot PCA produces is overlain by a series of

biplots which signify the relatedness of the variables being compared. The length of the biplot line, however, does not define the variable as more or less weighted as any other variable. The apparent difference in lengths of the biplots is due to the compression of the data points and biplot trajectories from multidimensional to 2-dimensional space.

3.3 Results

Statistical analyses of the biometric measurements revealed several morphological trends among the collections of *P. septentrionalis* and *P. subrectus*. All slopes from linear regressions of the discovered trends as well as their associated standard errors are shown together in Table 3.1A. Based on these values, t-tests were performed on the slopes for each comparison to determine if the results are statistically significant. It was found that the differences in slopes represent statistically different results at a 95% confidence interval in all cases (Table 3.1B).

Table 3.1. **A)** Slope and standard error values for each of the morphological character linear regression comparisons. **B)** Statistical t-Tests for each comparison.

A)

Morphology Comparison	Slopes		Standard Errors	
	P. septentrionalis	*P. subrectus*	*P. septentrionalis*	*P. subrectus*
Shell Thickness: Shell Width	0.58348	0.41369	0.023744	0.047881
Umbonal Height: Shell Length	0.24953	0.14285	0.012661	0.014602
Dorsal Thickness: Ventral Thickness	0.67324	0.51835	0.026515	0.065183

Table 3.1. **A)** Slope and standard error values for each of the morphological character

linear regression comparisons. **B)** Statistical t-Tests for each comparison

(continued).

B)				
t-Test (0.95 confidence)	**t- value**	**d.f.**	**p- value**	**Conclusion**
Shell Thickness: Shell Width	3.17691103	399	0.00160433	Statistically different
Umbonal Height: Shell Length	5.51983974	399	6.00E-08	Statistically different
Dorsal Thickness: Ventral Thickness	2.20109516	399	0.02830133	Statistically different

Note: d.f. = degrees of freedom

3.3.1 Shell Size and Globosity

The shells of *P. septentrionalis* tend to be much larger and more globose (total

shell width compared to total shell thickness) than those of *P. subrectus* (Table 3.2).

Maximum widths and thicknesses of the three groups clearly show the size differences

between *P. septentrionalis* (maximum width = 68.1 mm, thickness = 46.8 mm), *P.*

subrectus of Manitoulin Island (max. width = 45.0 mm; thickness = 33.8 mm), and *P.*

subrectus of Anticosti Island (max. width = 48.0 mm; thickness = 20.7 mm). The two

species also show a clear difference in the linear regression comparison of these features

(slope of *P. septentrionalis*= 0.58 ± 0.02; slope of *P. subrectus*= 0.41 ± 0.05; Fig. 3.6).
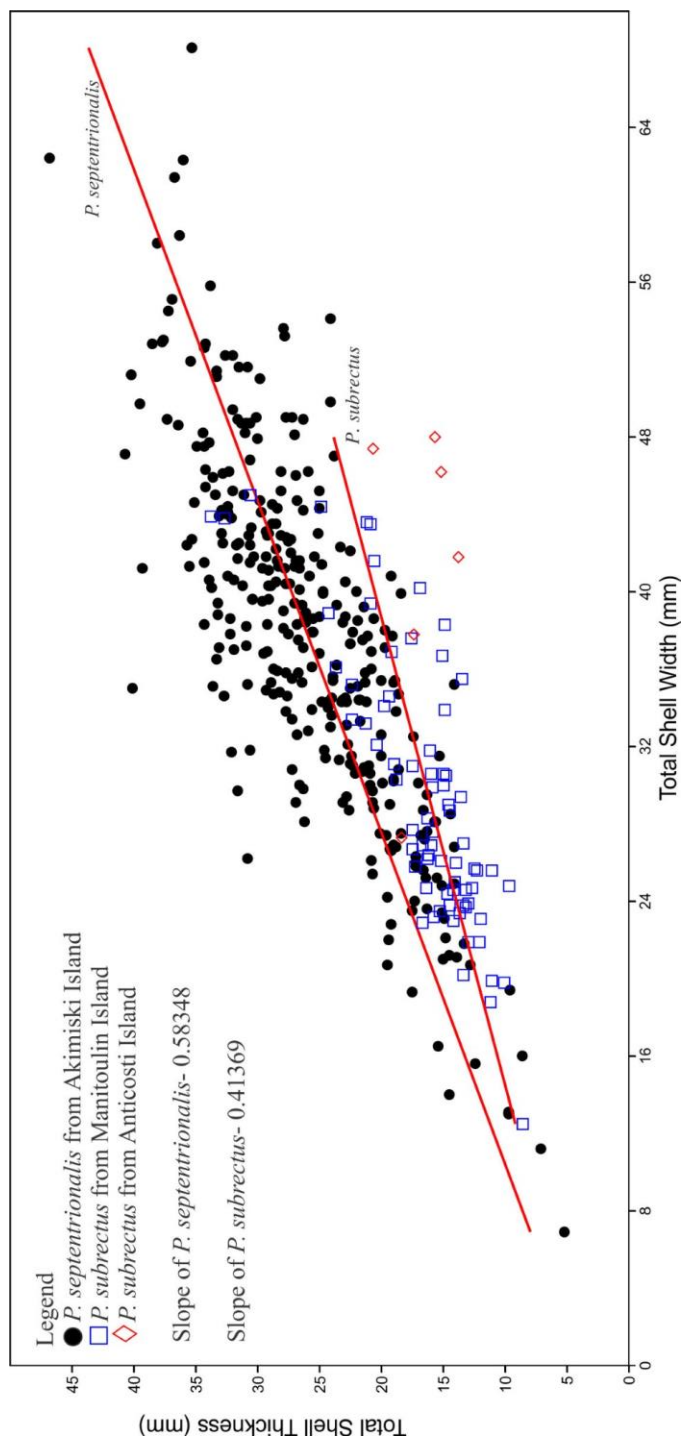
Figure 3.6: Plot comparing globosity (total shell width to total shell thickness) of *P. septentrionalis* and *P. subrectus*.

Table 3.2. Maximum and minimum values (mm) of total shell length, total shell width, and total shell thickness for the three collections.

	Number of Specimens	**Max Length**	**Min Length**	**Max Width**	**Min Width**	**Maxi Thickness**	**Min Thickness**
P. septentrionalis	322	66.4	7.7	68.1	6.9	46.8	5.2
P. subrectus- Manitoulin Island	75	64.5	13.6	45.0	12.5	33.8	8.6
P. subrectus- Anticosti Island	6	N/A (broken shell)	27.1	48.0	27.3	20.7	13.8

Note: N/A = not available

3.3.2 Ventral Umbonal Height vs. Total Shell Length

The ventral umbones of *P. septentrionalis* are generally high, with an average umbonal height of 7.6 mm (max = 20.0 mm). This character contrasts with the smaller umbones of *P. subrectus* from Manitoulin Island (average = 6.0 mm, max. = 11.4 mm) and Anticosti Island (average = 4.6 mm, max. = 6.6 mm). When compared to the total shell length, the ventral umbones of *P. septentrionalis* take up a larger proportion of the shell than the umbones of *P. subrectus* (Table 3.3). This trend is shown graphically in Figure 3.7 with *P. septentrionalis* having a slope of 0.25 ± 0.01 and *P. subrectus* having a slope of 0.14 ± 0.01.
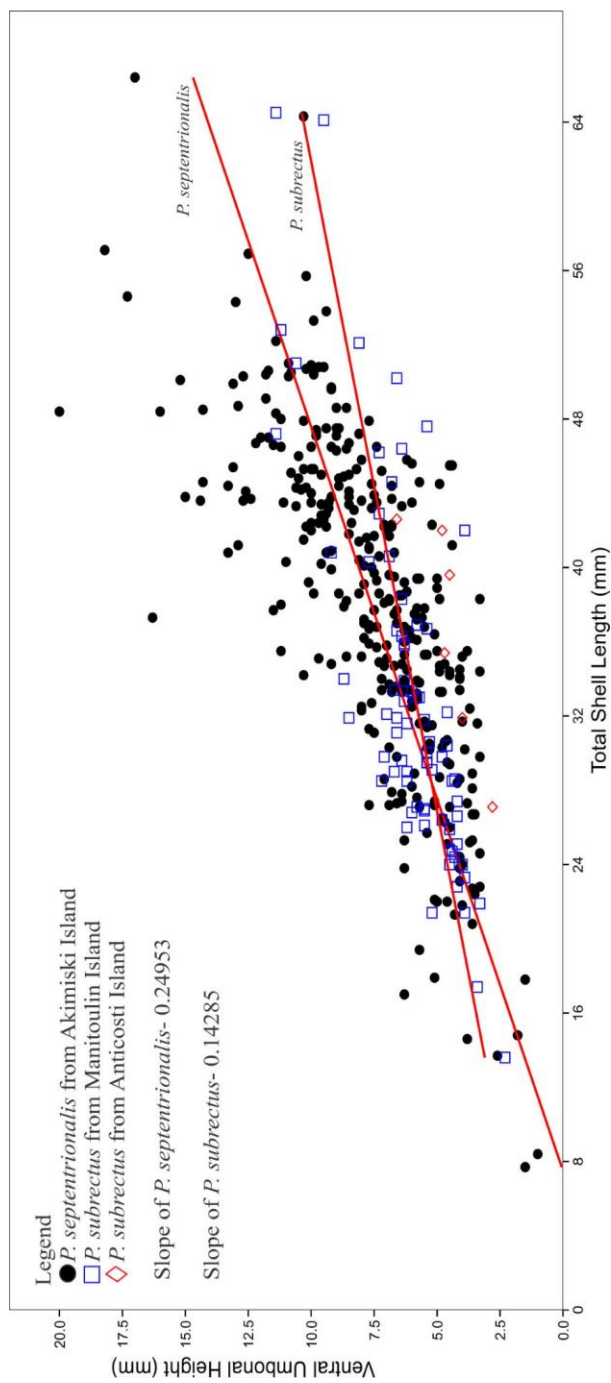
Figure 3.7: Plot comparing ventral umbonal length to total shell length of *P. septentrionalis* and *P. subrectus*.

Table 3.3. Maximum, minimum, and average ventral umbo lengths (mm) and average proportion (%) of ventral umbo to total shell length for the three collections.

	Maximum Ventral Umbo Length	Minimum Ventral Umbo Length	Average Ventral Umbo Length	Average Proportion of Total Shell Length
P. septentrionalis	20.0	1.0	7.6	19.8
P. subrectus- Manitoulin Island	11.4	2.3	6.0	18.4
P. subrectus- Anticosti Island	6.6	2.8	4.6	12.4

3.3.3 Dorsal Valve Thickness vs. Ventral Valve Thickness (depth)

A third morphological difference lies in the ratio between the thicknesses (depth) of the two valves between the species. The average dorsal to ventral valve depth ratio is 0.76 for *P. septentrionalis*, compared to 0.68 for *P. subrectus*. This difference is less pronounced than the other relationships but is still significantly different (Table 3.1B) in the linear regressions (Fig. 3.8). The slope of the regression of *P. septentrionalis* is 0.67 ± 0.03 while the slope of *P. subrectus* is 0.52 ± 0.07.

3.3.4 Principal Components Analysis (PCA)

Principal components analysis yielded a distinct grouping pattern based on 403 specimens and seven biometric variables (see 3.2: Materials and Methods). Due to the
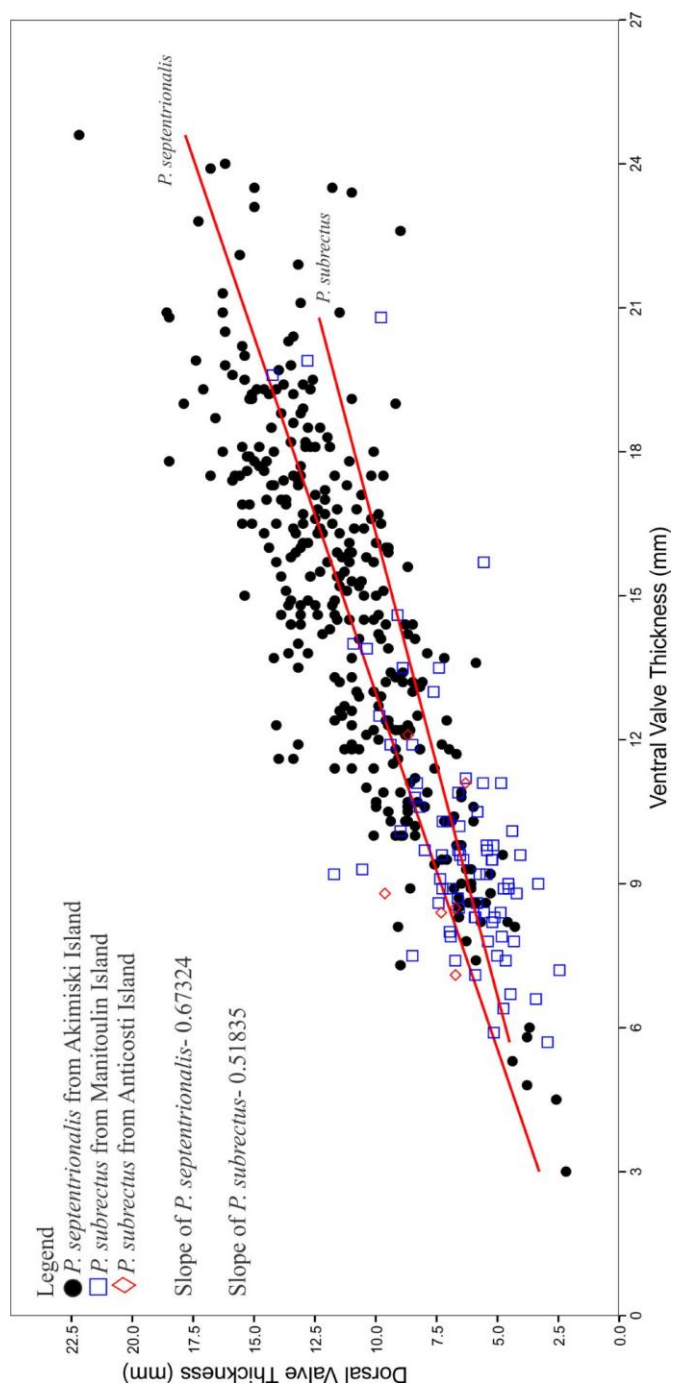
Figure 3.8: Plot comparing biconvexity (dorsal valve thickness to ventral valve thickness) of *P. septentrionalis* and *P. subrectus*.

large number of well-preserved *P. septentrionalis* samples, including juvenile shells, the ontogenetic variation of *P. septentrionalis* can be seen in its widespread data points. In this analysis Component 1 accounted for ~77% of the variance with Component 2 accounting for ~11% of the total variance within the sample. This suggests that the PCA yielded distinct principal components, which are statistically representative of the variation observed between the two *Pentameroides* species. Three groups were identifiable in the PCA plot (Fig. 3.9); Group A represents very small juvenile shells of *P. septentrionalis* as well as an outlying small specimen of *P. subrectus* from Manitoulin Island, Group B contains the majority of *P. subrectus* from both localities and the mid-sized specimens of *P. septentrionalis*, and Group C consists of the large to giant sized specimens of *P. septentrionalis* and large outlying specimens of *P. subrectus*.

3.4 Discussion

Autecology, the study of functional morphology, can provide insight into an extinct organism's feeding habits, mobility, or reproductive function. Fixosessile organisms such as brachiopods provide an opportunity to examine a particular variety of autecology: adaptation to a permanent environment. Unlike mobile animals, which are free to move around their environment in times of stress, brachiopods cannot move once their larval stage settles to the seafloor resulting in an adult animal which must be perfectly adapted to its environment. This has resulted in the evolution of a wide variety of brachiopod shell shapes corresponding to substrate type, water energy level, or depth (Richards 1972; Fursich and Hurst 1981; Bordeaux and Brett 1990). The following discussion sections examine the evolutionary and ecological implications of the shell
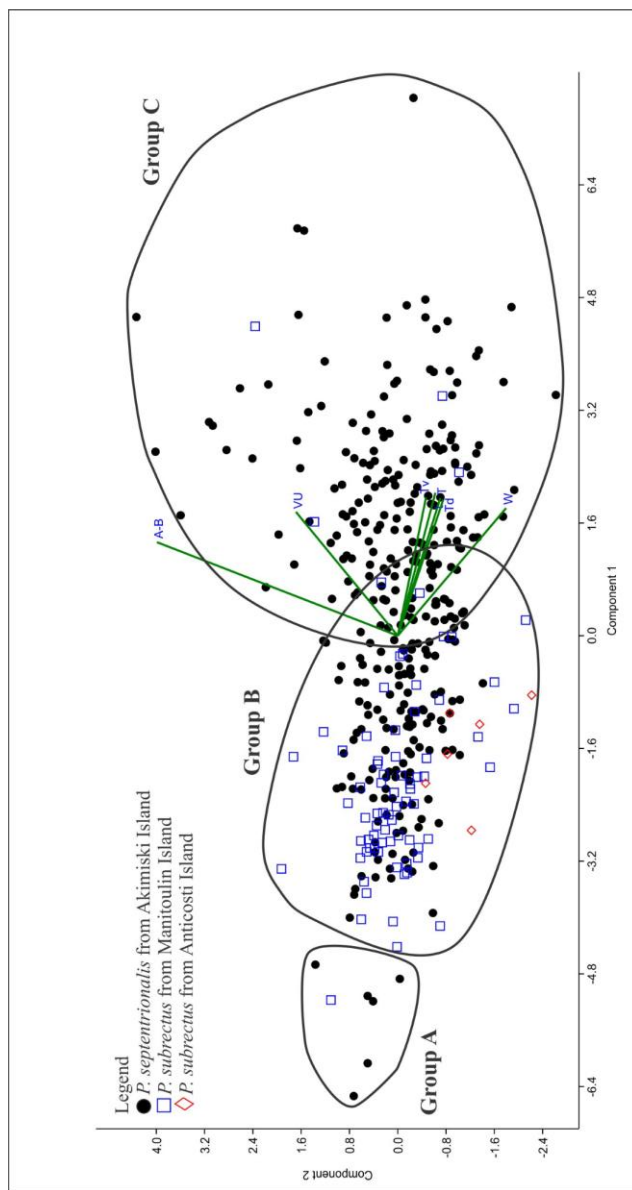
Figure 3.9: PCA plot showing distribution of the three collections. Group A: juvenile *P. septentrionalis* and outlying small *P. subrectus* from Manitoulin Island; Group B: mid-sized *P. septentrionalis* and adult *P. subrectus*; Group C: large sized *P. septentrionalis* and outlying large *P. subrectus* from Manitoulin Island. Biplot labels are as follows: A-B: dorsal apex to ventral beak length, VU: ventral umbonal height, Tv: ventral valve thickness, T: total shell thickness, L: total shell length, Td: dorsal valve thickness, W: total width shell.

morphology of the reef-dwelling *Pentameroides septentrionalis*. In addition, a more

detailed description of the Attawapiskat reefal environment is discussed based on the

autecology of *P. septentrionalis*.

3.4.1 Morphology and Implications for Paleoecology and Evolution

The large samples of well-preserved *P. septentrionalis* shells made it possible to

examine a fairly complete ontogenetic sequence using multivariate analysis. In the PCA

plot (Fig. 3.9), Groups A and B show that juvenile specimens of this species cluster

closely with the majority of the adult specimens of *P. subrectus* before diverging into

their derived adult morphology in Group C. It appears that *P. subrectus* maintains its

lenticular morphology, only increasing in size, throughout ontogeny (Fig. 3.4), whereas

P. septentrionalis diverges into its more globular and biconvex adult morphology in late

ontogeny (Figs. 3.6, 3.7, 3.8). The ontogenetic transformation of *P. septentrionalis* shell

morphology is so drastic that the equibiconvex shells in early ontogeny were originally

classified in a separate genus and species, *Meristina expansa* Whiteaves, 1904 before

being revised (see Jin and Copper 1986). The similarities in early ontogeny between *P.

subrectus* and *P. septentrionalis*, combined with the first appearance datum (FAD) (*P.

subrectus* in the middle Telychian; *P. septentrionalis* in the late Telychian) strongly

suggest that *P. septentrionalis* evolved from *P. subrectus* during the middle–late

Telychian as the genus migrated from high and mid-tropics to equatorial settings.

The adult of morphology of *P. septentrionalis* (Fig. 3.2 A–E) likely evolved as a

mechanism to improve energy efficiency in the shallow water reefal environment it

inhabited. The globular shell shape and increased convexity would allow for the organism to house larger lophophores and therefore improve feeding and respiratory efficiency. The large ventral umbones of the adult specimens reflect a change in life position throughout ontogeny. Like most pentamerides, *Pentameroides* did not have a functioning pedicle to anchor itself to the substrate. They instead maintained their posterior-down life position by crowding and thickening the shell walls of their posteriors (Ziegler et al. 1966). The large reef-dwelling *P. septentrionalis* expanded on this life strategy by enlarging their ventral valves and umbones and changed from an erect or sub-erect life position in early ontogeny to a recumbent orientation in late ontogeny. This enabled the growth of a deeper and largely immobile ventral valve to accommodate larger lophophores (projected from a relatively small dorsal valve, to which the lophophores are attached) to improve feeding and respiratory efficiency. It would also reduce metabolic energy output, requiring only the small and thin dorsal valve to be mobilized for opening and closing the shell.

This type of life position and morphology also occurs in the level-bottom-dwelling *Sulcipentamerus* and *Harpidium* of the paleoequatorial lower Silurian Washington Land Group of North Greenland (Fig. 3.1; Jin et al. 2009). In these taxa the morphology is more extreme than in *P. septentrionalis* as the ventral valve has deepened into a horn like structure with the dorsal valve sitting atop as a 'lid' (Fig. 3.10). It is important to note that these taxa inhabited a level-bottom environment while *P. septentrionalis* inhabited a reefal environment, indicating that this morphology was independent of ecological guild types. It should also be noted that the North Greenland pentamerides evolved into this derived morphology in the level-bottom ecosystem, but *P*
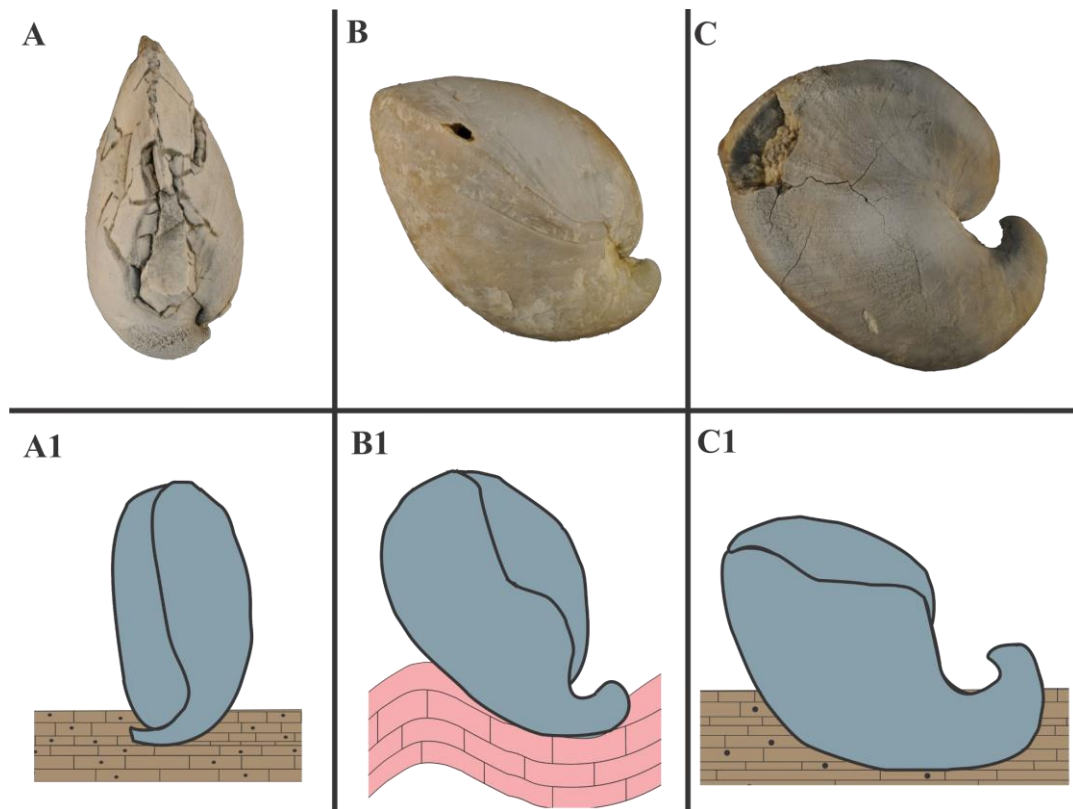
Figure 3.10: The interpreted life positions of: *P. subrectus* in high tropical level-bottom environments (A/A1), *P. septentrionalis* in low tropical reefal environments (B/B1), and *Harpidium* and *Sulcipentamerus* in equatorial level-bottom environments (C/C1). Note the transition in life position from vertical (*P. subrectus*) to recumbent (*P. septentrionalis* and *Harpidium/Sulcipentamerus*) as latitude decreases. A1 and C1 represent level-bottom carbonate environments while B1 represents coral-stromatoporoid reef facies.

. *subrectus*, which also inhabited level-bottom environments, retained its vertical life position like *Pentamerus* (Jin 2008). As shown in the PCA plot (Fig. 3.9), *P. subrectus* maintains a lenticular, nearly equibiconvex shell shape throughout ontogeny while *P. septentrionalis* become globular and more ventribiconvex in gerontic forms.

A possible explanation is that high frequency of severe storms in the mid–high paleotropics (such as the Michigan and Anticosti basins) prevented *P. subrectus* from evolving a recumbent life position because a relatively deep, immobile ventral valve in such a position would be susceptible to smothering by mud during storms. A shell vertically oriented on the substrate would be much more efficient for shedding storm-deposited mud when the two valves are open. A high energy environment would provide sufficient oxygenation and nutrient supply so that the selection pressure for larger lophophores would be much reduced for *P. subrectus* compared to *P. septentrionalis*.

3.4.2 Taphonomy and Paleoenvironmental Interpretations

The differences in morphology and taphonomy between the two species of *Pentameroides* are closely related to relative storm frequency in the environments that they inhabited. It has been shown by Jin et al. (2013) that in the Ordovician and Silurian Laurentia featured a hurricane-free zone approximately 10° north and south of the equator, similar to that of the modern near-equatorial tropics. Paleogeographically, the Michigan and Anticosti Basins were 15–25° south while the Hudson Bay region was within 10° of the equator (Fig. 3.1; Torsvik and Cocks 2013). This suggests that the Attawapiskat coral-stromatoporoid reefal environments experienced very few severe

storms which allowed *P. septentrionalis* to evolve a larger, globular shell, with a proportionally larger and deeper recumbent ventral valve, resulting in a recumbent living position in gerontic forms (Fig. 3.9 Group C).

This interpretation finds support in the taphonomic characters of *P. septentrionalis* in the Attawapiskat Formation, especially the common preservation of larger, thin-walled, hollow shells in a shallow water reefal setting (Fig. 3.3: A, B). This type of preservation could not have occurred in an environment subjected to frequent, hurricane-grade storms. The shells of *P. subrectus* from the higher tropics, however, do signify a storm-dominated environment as they are often broken, disarticulated, deformed, and infilled with micritic matrix (Fig. 3.3: C, D). These taphonomic features are even more significant when depth of water is taken into account. The level-bottom *P. subrectus* dominated communities likely inhabited a mid to outer shelf (BA 3/BA 4) depth and were subjected to powerful storms while the much shallower Attawapiskat reefal settings experienced insignificant storm damage (Fig. 3.11). These taphonomic differences indicate that storm frequency and therefore paleolatitudinal position were major factors influencing the derivation of *P. septentrionalis* from *P. subrectus*.

3.5 Conclusions

Based on the biometric analyses of 322 specimens of *Pentameroides septentrionalis* from the Attawapiskat Formation and 81 specimens of *Pentameroides subrectus* from the Fossil Hill and the Jupiter formations, ranging from sub-paleoequatorial to higher paleotropical latitudes, the following conclusions can be drawn from the morphological
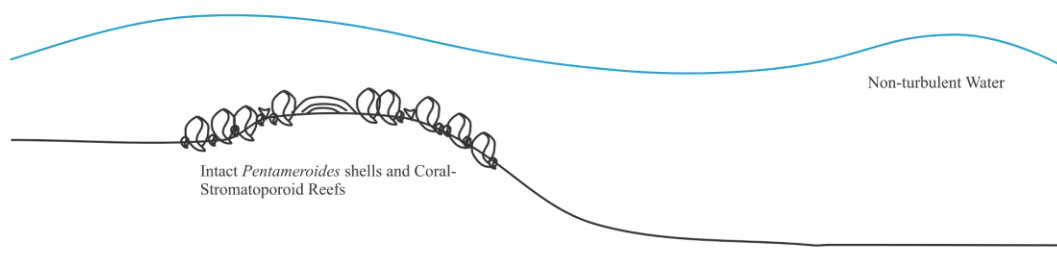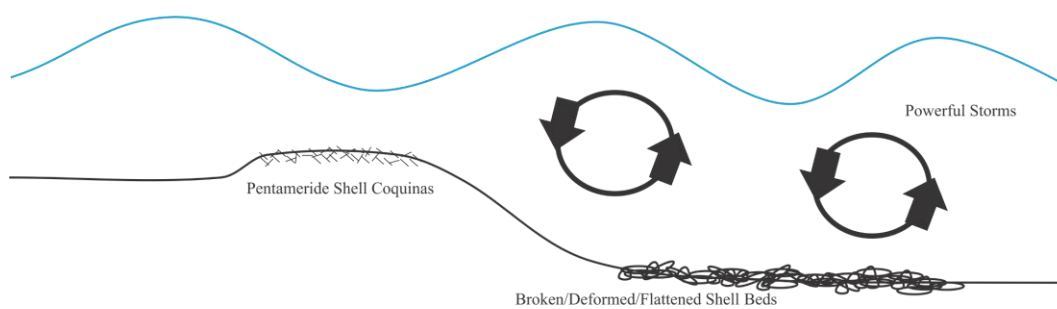
Figure 3.11: Comparison between environments of A) low tropical reef environment and B) high tropical storm-dominated level-bottom communities. Differences in water depth habitation and taphonomy are shown in the reconstructed shell beds.

data and the evolutionary, paleoecological, and paleoenvironmental interpretations discussed above.

1. Principal component analysis shows that *P. septentrionalis* resembles *P. subrectus* at early growth stage but diverges in morphology during late ontogeny, indicating that *P. septentrionalis* evolved from *P. subrectus*.

2. Morphological characteristics of *P. septentrionalis* (increased globosity and convexity, larger ventral valve and umbo) are adaptations to increase energy efficiency living in a hurricane-free, but nutrient-stressed environment. This change in morphology is maximized in the *Harpidium* and *Sulcipentamerus* shells of paleoequatorial North Greenland.

3. A change from vertical (*P. subrectus*) to recumbent (*P. septentrionalis*) life position was related to reduced need for mud-shedding in a depositional setting that lacked hurricane grade storms.

4. Excellent preservation of large, egg-thin shells of *P. septentrionalis* in the shallow-water reefal facies of the Attawapiskat Formation indicates a hurricane free near-equatorial paleoenvironment, whereas poorly preserved shell of *P. subrectus* from Manitoulin and Anticosti islands suggest high tropical storm-dominated environments.

References

Basset, M.G., and Cocks, R.L.M. 1974. A review of Silurian brachiopods from Gotland. Fossils and Strata, 3: 56 p.

Bordeaux, Y.L., and Brett, C.E. 1990. Substrate specific associations of epebionts on Middle Devonian brachiopods: implications for paleoecology. Historical Biology, 4: 203–220.

Boucot, A.J. 1975. Evolution and extinction rate controls. Elsevier, New York.

Boucot, A.J., and Johnson, M.E. 1979. Pentamerinae (Silurian Brachiopoda). Paleontographica A, 163: 87–129.

Carlson, S.J., Boucot, A.J., Rong, J., and Blodgett, R.B. 2002. Pentamerida. Treatise on Invertebrate Paleontology. Part H, Brachiopoda, 4, H921–H1026.

Chiang, K.K. 1971. Silurian pentameracean brachiopods of the Fossil Hill Formation, Ontario. Journal of Paleontology, 45: 849–861.

Copper, P. 1978. Paleoenvironments and paleocommunities in the Ordovician–Silurian sequence of Manitoulin Island. Michigan Basin Geological Society Special Papers, 3: 47–61.

Fursich, F.T., and Hurst, J.M. 1981. Autecology of the Silurian brachiopod *Sphaerirhynchia wilsoni* (J. Sowerby, 1816). Journal of Paleontology, 55(4): 805–809.

Hall, J., and Clarke, J.M. 1892–1894. An introduction to the study of the genera of Palaeozoic Brachiopoda. New York State Geological Survey, Palaeontology of New York, 8: 1–317.

Hammer, Ø., Harper, D.A.T. 2006. Paleontological Data Analysis. Blackwell Publishing, Malden, Massachusetts.

Hammer, Ø., Harper, D.A.T., Ryan, P. 2001. PAST: Paleontological statistics software package for education and data analysis. Palaeontologia Electronica 4(1).

Harper, D.A., Rasmussen, C.M.Ø, Liljeroth, M., Blodgett, R.B., Candela, Y., Jin, J., Percival, I.G., Rong, J., Villas, E., and Zhan, R.B. 2013. Biodiversity, biogeography and phylogeography of Ordovician rhynchonelliform brachiopods. Geological Society, London, Memoirs, 38(1): 127–144.

Glasser, P.M. 2002. Mode of evolution in the early Silurian *Pentamerus–Pentameroides* lineage, Anticosti Island, Quebec. M.Sc. thesis, Department of Earth Sciences, The University of Western Ontario, London, Ontario.

Jin, J. 2002. Niche partitioning of reef-dwelling brachiopod communities in the Lower Silurian Attawapiskat Formation, Hudson Bay Basin, Canada. IPC 2002, Geological Society of Australia, Abstracts No. 68: 83–84.

Jin. J. 2003. The Early Silurian Brachiopod *Eocoelia* from the Hudson Bay Basin, Canada. Palaeontology, 46: 885-902.

Jin, J. 2008. Environmental control on temporal and spatial differentiation of Early Silurian pentameride brachiopod communities, Anticosti Island, eastern Canada. Canadian Journal of Earth Sciences, 45: 159–187.

Jin, J., and Copper, P. 1986. The Early Silurian Brachiopod *Pentameroides* from the Hudson Bay Lowlands, Ontario. Canadian Journal of Earth Sciences, 23: 1309–1317.

Jin, J., and Chatterton, B.D.E. 1997. Latest Ordovician-Silurian articulate brachiopods and biostratigraphy of the Avalanche Lake area, southwestern District of Mackenzie. Palaeontographica Canadiana, 13: 1–167.

Jin, J., and Copper, P. 2000. Late Ordovician and Early Silurian pentamerid brachiopods from Anticosti Island, Québec, Canada. Palaeontographica Canadiana, 18: 1–140.

Jin, J., Caldwell, W.G.E., and Norford, B.S. 1993. Early Silurian brachiopods and biostratigraphy of the Hudson Bay lowlands, Manitoba, Ontario, and Quebec. Geological Survey of Canada Bulletin, 457: 1–219.

Jin, J., Harper, D.A., and Rasmussen, C.M.Ø. 2009. *Sulcipentamerus* (Pentamerida, Brachiopoda) from the Lower Silurian Washington Land Group, North Greenland. Palaeontology, 52: 385–399.

Jin, J., Harper, D.A.T., Cocks, L.R.M., McCausland, P.J.A., Rasmussen, C.M.Ø., and Sheehan, P.M. 2013. Precisely locating the Ordovician equator in Laurentia. Geology, 41: 107–110.

Johnson, M.E. 1979. Evolutionary brachiopod lineages from the Llandovery series of eastern Iowa. Paleontology, 22: 549–567.

Johnson, M.E., and Colville, V.R. 1982. Regional integration of evidence for evolution in the Silurian *Pentamerus–Pentameroides* lineage. Lethaia, 15: 41–54.

Kilgour, W.J. 1963. Lower Clinton (Silurian) relationships in western New York and Ontario. Geological Society of America Bulletin, 74: 1127–1142.

Kirk, E. 1925. *Harpidium*, a new pentameroid brachiopod genus from southeastern Alaska. Proceedings of the United States National Museum, 66(32): 1–7.

M'Coy, F. 1844. A synopsis of the characters of the Carboniferous Limestone fossils of
Ireland. Dublin. 207 p.

Rassmussen, C.M.Ø. 2009. A paleoecological and biogeographical investigation of the
Ordovician–Silurian boundary based on brachiopods. Ph. D. Thesis, Department
of Geosciences and Natural Resource Management, University of Copenhagen,
Copenhagen, Denmark.

Richards, R.P. 1972. Autecology of Richmondian brachiopods (late Ordovician of
Indiana and Ohio). Journal of Paleontology, 46(3): 386–405.

Rong, J., Jin, J., and Zhan, R. 2006. Early Silurian *Sulcipentamerus* and related
pentamerid brachiopods from South China. Paleontology, 50(1): 245–266.

Rzhonsnitskaia, M.A. 1956. Systemization of Rhynchonellida. *In* Resumenes de Los
Trabajos Presentados. International Geological Congress, Mexico, Report 20.
Edited by Guzman, E. et al. p. 125–126.

Schuchert, C., and Cooper, G.A. 1931. Synopsis of the brachiopod genera of the
suborders Orthoidea and Pentameroidea, with notes on the Telotremata. American
Journal of Science, 20: 241–251.

Schuchert C., and LeVene, C.M. 1929. Brachiopoda (Generum et Genotyporum Index et
Bibliographia). Fossilium Catalogus I: Animalia, 42. W. Junk. Berlin.

Sowerby, J. de C. 1812–1822. The mineral conchology of Great Britain; or coloured
figures and descriptions of those remains of testaceous animals or shells, which
have been preserved at various times and depths in the earth, v. 1–4, Pl. 1–383.

Sowerby, J. de C. 1839. Organic remains. *In* The Silurian System. *Edited by* R.I
Murchison. John Murray, London, pp. 579–765.

Torsvik, T.H., and Cocks, L.R.M. 2013. New global paleogeographical reconstructions for the early Paleozoic and their generation. Geological Society London Memoirs, 38: 5–24.

Ulrich, E.O., and Cooper, G.A. 1936. New genera and species of Ozarkian and Canadian brachiopods. Journal of Paleontology. 10(7): 616–631.

Whiteaves, J.F. 1904. Preliminary list of fossils from the Silurian (Upper Silurian) rocks of the Ekwan River and Sutton Mill Lakes, Keewatin, collected by D.B. Dowling in 1901 with descriptions of such species as appear to be new. Geological Survey of Canada, Annual Report, 14: 38–59.

Zeng Q. 1987. Brachiopoda. *In* Yichang Institute of Geology and Mineral Resources, Biostratigraphy of the Yangtze Gorge area, Early Palaeozoic Era. Geological Publishing House, Beijing, p. 209–245.

Ziegler, A.M. 1965. Silurian marine communities and their environmental significance. Nature, 207: 270–272.

Ziegler, A.M., Boucot, A.J., and Sheldon, R.P. 1966. Silurian pentamerid brachiopods preserved in position of growth. Journal of Paleontology, 40: 1032–1036.

Ziegler, A.M., Cocks, L.R.M., and Bambach, R.K. 1968. The composition and structure of lower Silurian marine communities. Lethaia, 1: 1–27.

Chapter 4 – Biodiversity and Community Organization of Reef-Dwelling Brachiopods from the Late Ordovician–early Silurian

4.1 Introduction

In modern ecological studies, the community structures and relationships between different organisms can be observed directly. In paleoecological studies, however, the lack of most direct behavioural and physiological data makes the interpretation of these relationships a challenge. Despite these problems, paleoecologists have recognized the importance of examining long-term (e.g. million-year scale) ecosystem changes based on the fossil record, and have made significant progress over the past five decades in describing various ecological aspects of fossil species. For example, the study of the community organization of brachiopod dominated faunas from the early Silurian has been well studied by several key workers over this time. Ziegler (1965) and Ziegler et al. (1968) first organized the brachiopod fauna of the Llandovery Welsh Borderlands into five distinct community zones based on dominant type. These community zones, the *Lingula*, *Eocoelia*, *Pentamerus*, *Stricklandia*, and *Clorinda* zones, are interpreted as being related to water depth, beginning in the intertidal zone (*Lingula*) to the deep shelf below storm wave base (*Clorinda*). Boucot (1975) expanded Ziegler's community zones into the now well-known Benthic Assemblages (BAs) which are also based on water depth with BA 1 equivalent to the *Lingula* community and BA 5 being equivalent to the *Clorinda* community. Such paleoecological studies culminated in a large compendium of

papers on the Silurian–Devonian fossil communities and paleoenvironments worldwide (Boucot and Lawson 1999).

One of the most challenging aspects of the early Silurian paleoecology has been assigning absolute depths to the faunal organizations and BAs. Differing lines of evidence drawn from studies in sedimentology, geochemistry, and paleobiology, have been used to estimate the depths of BA 2–BA 5 with varied results (Brett et al. 1993). Estimates for the maximum extent of BA 5, for example, have ranged from 150 m (Cocks and McKerrow 1984) to 1500 m (Hancock et al. 1974), although the majority of published data on this subject suggests an absolute maximum depth of approximately 200 m (Boucot 1975; Rong et al. 1984; Brett et al. 1993). The occurrence of photosynthetic organisms (corals, algae) have been used to interpret absolute depth. Brett et al. (1993) have shown that the photic zone likely extended to the BA 4–BA 5 boundary, or into the upper reaches of the BA 5 zone, due to the occurrence of photosynthetic organisms and arthropods with well-developed eyes. In addition, the authors have used the occurrences of hummocky cross-stratification, gutter casts, and coquinas to show that BA 3 and BA 4 experienced a turbulent, storm-influenced environment, while BA 5 was a quiet environment existing below normal storm wave base.

One strength of the BA system is that dominant pentameride brachiopods, are widespread and usually abundant in the early Silurian across several major tectonic plates, such as in North America (Johnson and Colville 1982; Johnson 1987, 1997; Jin and Chatterton 1997; Jin and Copper 2000; Watkins et al. 2000; Jin 2008; Jin et al. 2009), Europe (Baarli and Harper 1986; Baarli 1988; Johnson 1989, 2006; Johnson et al. 1991), Russia (Sapelnikov 1961, 1985; Sapelnikov et al. 1999), and China (Rong et al. 2004,

2005, 2007), which facilitates regional or global comparison and correlation. The wide paleogeographic range of these brachiopods in the Llandovery was part of the biotic recovery following the end Ordovician mass extinction. The level-bottom carbonate shelves and ramps of the vacant early Silurian intracratonic seas were quickly invaded by surviving and newly evolved organisms (Rong and Harper 1999; Rong and Zhan 2006; Cocks and Rong 2007), resulting in widespread cosmopolitanism across the early Silurian tropical continents (Sheehän 1975; Sheehan and Corough 1990; Jin et al. 2007; Rong and Cocks 2014).

Despite the plethora of previous work on early Silurian brachiopod faunal recovery and community organization in level-bottom habitats, similar work on reefal settings has proven to be more difficult. The reasons for this difficulty are the generally limited extent of well-developed reef systems during the Llandovery and that community definitions, such as Ziegler's community zones or Boucot's BA system, cannot be applied directly to reefal settings (Jin 2003, 2005). In the middle–late Telychian reefs of the Attawapiskat Formation in the Hudson Bay and Moose River basins, for example, *Eocoelia-*, *Pentameroides-,* and *Clorinda*-dominated brachiopod assemblages occur within close proximity to one another, whereas *Stricklandia* is absent.

Coral-stromatoporoid reefs first appeared in the Late Ordovician, but declined during the end Ordovician mass extinction and would not recover as a widespread reef ecosystem until the mid-Aeronian, several million years later. Except for a few isolated Rhuddanian, or putatively Rhuddanian and likely latest Hirnantian, occurrences (Copper and Brunton 1991; Bergström et al. 2011), coral-stromatoporoid reefs were largely absent during the earliest Llandovery. Early Silurian coral-stromatoporoid patch reefs first

appeared on the high tropical southern margin of Laurentia (Copper and Jin 2012) and spread throughout the lower tropics, increasing in diversity and paleogeographic extent in Laurentia (Watkins 1991, 1998; Suchy and Stearn 1993; Jin et al. 1993; Brunton and Copper 1994; Copper and Jin 2012), Baltica (Nield 1982; Kershaw 1993; Sambleten et al. 1996; Watkins 2000; Tuuling and Flodén 2013; Ernst et al. 2015), Siberia (Soja and Antoshkina 1997; Antoshkina 1998; Soja et al. 2000; Antoshkina and Soja 2006) and China (Yue et al. 2002; Yue and Kershaw 2003; Li 2004; Wang et al. 2014) by the end of the Llandovery. These recovered reefs would reach their Silurian peak in terms of species diversity and spatial distribution during the mid-Wenlock before going into decline (Copper 1994, 2002). As in level-bottom communities, brachiopods became the dominant benthic shelly components in the early Silurian reef system (Jin et al. 1993; Watkins 2000; Jin 2003, 2005), but not until the Telychian, (Chow and Stearn 1988), much later than their level-bottom relatives.

The reef-bearing Attawapiskat Formation of the Hudson Bay and Moose River basins provides an excellent opportunity for studying both reefal brachiopod recovery and community organization during the early Silurian as it not only contains abundant, diverse, and well-preserved brachiopods and other shelly organisms, but is the earliest known reef system in life history to show complex community interactions between brachiopods and reef building organisms (Chow and Stearn 1988). In addition, both reef and inter-reef facies are preserved and exposed, allowing for a more detailed study of brachiopod community organization within these areas. Built on the preliminary investigations of the reef-dwelling brachiopod associations of the Attawapiskat Formation (Jin 2002a, 2003, 2005), this project aims for a more comprehensive

delineation of the brachiopod communities and interpretation of their paleoecological significance.

In order to examine the recovery of reef-dwelling brachiopods on a broader scale, specimens from several other reefal formations from the Late Ordovician–early Silurian have been selected and incorporated in this study on the basis of their well-documented and abundant reef-dwelling brachiopod faunas. These additional formations are the Hirnantian Ellis Bay Formation, the Aeronian Meniér Formation, and the Telychian Chicotte Formation of Anticosti Island, Quebec; the Sheinwoodian Högklint Formation of Gotland, Sweden; and the Homerian Racine Formation of Wisconsin. The level-bottom brachiopod fauna of the Telychian Fossil Hill Formation, Manitoulin Island, Ontario are also included in this study to act as a comparison to contemporaneous reef environments.

This chapter has the following objectives: 1) to determine the diversity levels of the brachiopod faunas in reefal locations during the early Silurian recovery period in order to examine the brachiopod community recovery process after the Late Ordovician mass extinction, and 2) to assess the invasion of the reef ecosystem and subsequent community organization of the rich brachiopod fauna in the Attawapiskat Formation, and provide a comparison with the early Silurian level-bottom brachiopod communities.

4.2 Materials and Methods

For this study, reef-dwelling brachiopod faunal data were compiled from the following stratigraphic units and collection localities: the Hirnantian Ellis Bay, the

Aeronian Meniér, and the Telychian Chicotte formations, Anticosti Island, Quebec; the

Telychian Attawapiskat Formation, Akimiski Island, James Bay, Nunavut; the

Sheinwoodian Högklint Formation, Gotland, Sweden; and the Homerian Racine

Formation, Wisconsin. In addition, the diversity values of the level-bottom brachiopod

fauna from the Telychian Fossil Hill Formation, Manitoulin Island, Ontario were also

measured for comparative purposes in this study. Taxonomic and abundance data from

Akimiski, Anticosti, and Manitoulin islands were obtained first hand from specimens

previously collected and made available by J. Jin and P. Copper, currently stored at the

University of Western Ontario. Abundance and taxonomic data for the Racine Formation

was extracted from Watkins (1991) who published full species lists along with abundance

data on four reefal localities. The publication of Watkins (2000) was used to gather

diversity data of reef-dwelling brachiopods from three reef localities in the Högklint

Formation. Unfortunately, comprehensive species lists and abundance data were not

available in this publication, with only the Shannon diversity indices included in this

study. The formations have been separated into collection localities in which Shannon

and Simpson diversity indices were calculated for each locality. Average and total

diversity indices for each formation were calculated by averaging and combining locality

data respectively. The 32 fossil samples from the Attawapiskat Formation of Akimiski

Island were made in close proximity to each other (see Chapter 2.3.1; Fig. 2.5) at 10

general collection localities by J. Jin to reflect the high degree of substrate heterogeneity

of the reefal environment for the benthic shelly organisms (Appendix 2).

The Shannon diversity index (Shannon and Weaver 1949) is used commonly in

both ecological and paleoecological studies as it incorporates abundance data with

species richness to create a robust and standardized indicator of diversity. Results of the Shannon index are presented as a number with 0 indicating no diversity and larger numbers indicating higher levels of diversity. As only brachiopods were analyzed in this study, a Shannon index value less than 1.0 is considered low diversity, a value from 1.0–1.9 is considered moderate diversity and a value 2.0 or greater is considered high diversity. Brachiopods were the only taxonomic group considered in this study because so far taxonomic identifications and abundance data (number of specimens per species and per locality) are available only for this fossil group, whereas those for other fossil groups (such as bivalves, gastropods, nautiloids, and trilobites) have not been completed for the Attawapiskat Formation. The Shannon index is calculated by finding the negative sum of the proportion of each species compared to the total number of individuals multiplied by the natural log of themselves where p_i is the proportion of the individuals belonging to the *ith* species in the total collection, R is the total number of species in the collection, and ln is the natural log (Eq. 4.1).

$$\text{Shannon index } H \; = \; -\sum_{i=1}^{R} p_i \; \ln p_i \qquad \qquad \text{(Equation 4.1)}$$

Along with the Shannon index, the Simpson index of diversity (Simpson 1949) was used to measure the degree of evenness of the species in the brachiopod communities. The measure of diversity in the Simpson index is represented by a number ranging between 0 and 1, with a smaller value denoting a lower level of domination and therefore and higher degree of evenness in a locality. The Simpson evenness index is

defined in this study as follows: a value from 0.0–0.25 is considered highly even, 0.26–

0.74 is considered moderately even, and 0.75–1.0 is considered to be highly uneven. The

Simpson index is calculated by finding the sum of the squared proportions of the

individuals of one species compared to the total number of individuals in which p_i and R

are again the proportion of individuals belonging to the *ith* species and the total number

of species in the collection respectively (Eq. 4.2).

$$\text{Simpson index } S \ = \ \sum_{i=1}^{R} p_i^2 \hspace{4cm} \text{(Equation 4.2)}$$

In order to examine the community organization of the Attawapiskat samples at a

multivariate level, the relative abundance data of each species in each collection was

analyzed in cluster and principal components analyses (PCA), using the PAST 3 v. 3.08

statistical software package (Hammer et al. 2001; Hammer and Harper 2006). The

absolute abundance data was normalized to relative (percentage) data in order to

minimize the effect of variable sample sizes on the cluster analysis (Appendix 3).

Squared Euclidean distance was selected for cluster analysis as it is the best index of

dissimilarity when dealing with datasets with many species which have relative

abundance taxa (Hammer and Harper 2006) and to maintain order with the similar

multivariate studies of Jin (2008) and Jin and Copper (2008) who used this method to

determine the community organization of the brachiopods of the Jupiter and Ellis Bay

formations of Anticosti Island.

Squared Euclidean distance measures the dissimilarity of the samples using Equation 4.3 (Krebs 1989) in which *Xi* and *Xj* represent the relative abundance of a species in samples *i* and *j* respectively. A larger sum of the square of $X_i - X_j$ indicates a greater degree of faunal dissimilarity. Hence, Euclidean cluster analysis groups samples with the most similar faunal makeup together and reveals how dissimilar samples are from one another simultaneously.

$$\text{Squared Euclidean distance} = \sum (X_i - X_j)^2 \qquad \text{(Equation 4.3)}$$

Principal components analysis was used as a complementary method to graphically cluster the samples from the Attawapiskat Formation. This method condenses complex multivariate data into a simple bivariate plot. The biplot axes created by the PCA show the direction in which certain variables trend, but due to the multivariable nature of the data the length of the biplots are not representative of their contribution to the variance of the data (Hammer and Harper 2006).

In addition to diversity and multivariate analysis, living space requirements were estimated for the brachiopods of the Attawapiskat Formation. Due to the large number (9009) of specimens considered in this study, it was considered inefficient to measure each specimen. Therefore specimens representing an average range of shell sizes were selected for each species to estimate the shell volume as a proxy for space requirement. The shell length, shell width, and shell thickness of each specimen was measured to a precision of 0.1 mm using a pair of electronic calipers. These measurements were used to

determine the approximate volume of the shells using Equation 4.4 where L is shell length, W is shell width, and T is shell thickness.

$$\text{Shell volume proxy } V = L * W * T * \left(\frac{1}{3}\right) \quad\quad\quad\quad \text{(Equation 4.4)}$$

These volume measurements were then averaged for each species and multiplied to the abundance of that species in each sample from the Attawapiskat Formation to show the total volume occupied by that species. Using this value the proportion of the total living space used by each species was approximated (Appendix 4). Due to the overall good preservation of the shells of this formation, most species have average shell volume measurements. Exceptions are those species where the majority of specimens are contained within a solid block of rock which prevents accurate biometric measurements from being performed. The only common or abundant species in which this is an issue are *Eocoelia akimiskii*, *Cyphomenoidea parvula*, and *Leptaena* sp. The collections that contain species without volume measurements were excluded from analysis if more than 5% of the total number of specimens were without volume measurements. If a collection has 95% or higher of their specimens represented with volume estimates the missing elements were removed from the analysis, but the collection was included.

In previous paleoecological studies the terms fossil assemblage, association, and paleocommunity were often used interchangeably. This study follows the concepts proposed by Brenchley and Harper (1998) that an assemblage refers to a group of fossils collected from a single bed (or a set of genetically related beds) without information on

its taphonomic properties (in situ or transported) or its temporal-spatial stability. An association, however, reflects a collection made from a single bed (or a set of genetically related beds) in which there was limited or no transport of the material. If a fossil association is found to be stable in time and space, such as by occurring over a large geographic region and recurring multiple times through a stratigraphic section, it can be classified as a paleocommunity (Zhan et al. 2006; Jin 2008). By these definitions the brachiopod fauna of the Attawapiskat Formation in this study are classified as associations as the excellent preservation of small shells and large, egg-thin shells suggests limited transport, but these associations have not been proven to have a wide geographic or stratigraphic range and therefore cannot be defined as paleocommunities.

4.3 Results

4.3.1 Reef-dwelling Brachiopod Diversity during the Silurian Reef Recovery Phase

Shannon and Simpson diversity indices were calculated for each of the localities of the Ellis Bay, Meniér, Chicotte, Fossil Hill, Attawapiskat, Högklint, and Racine formations. These values were averaged, if possible, and combined to show average and total diversity of the formations (Table 4.1). Figure 4.1 shows the Shannon indices of the individual localities plotted in order from older to younger stratigraphic units. There is a sharp drop in diversity at the end of the Ordovician, a long recovery period with no reef activity until the Aeronian, before increasing significantly in the Telychian and into the Wenlock. It must be noted that the low diversity of the Fossil Hill Formation does not represent a reefal environment, but serves as a level-bottom comparison to the
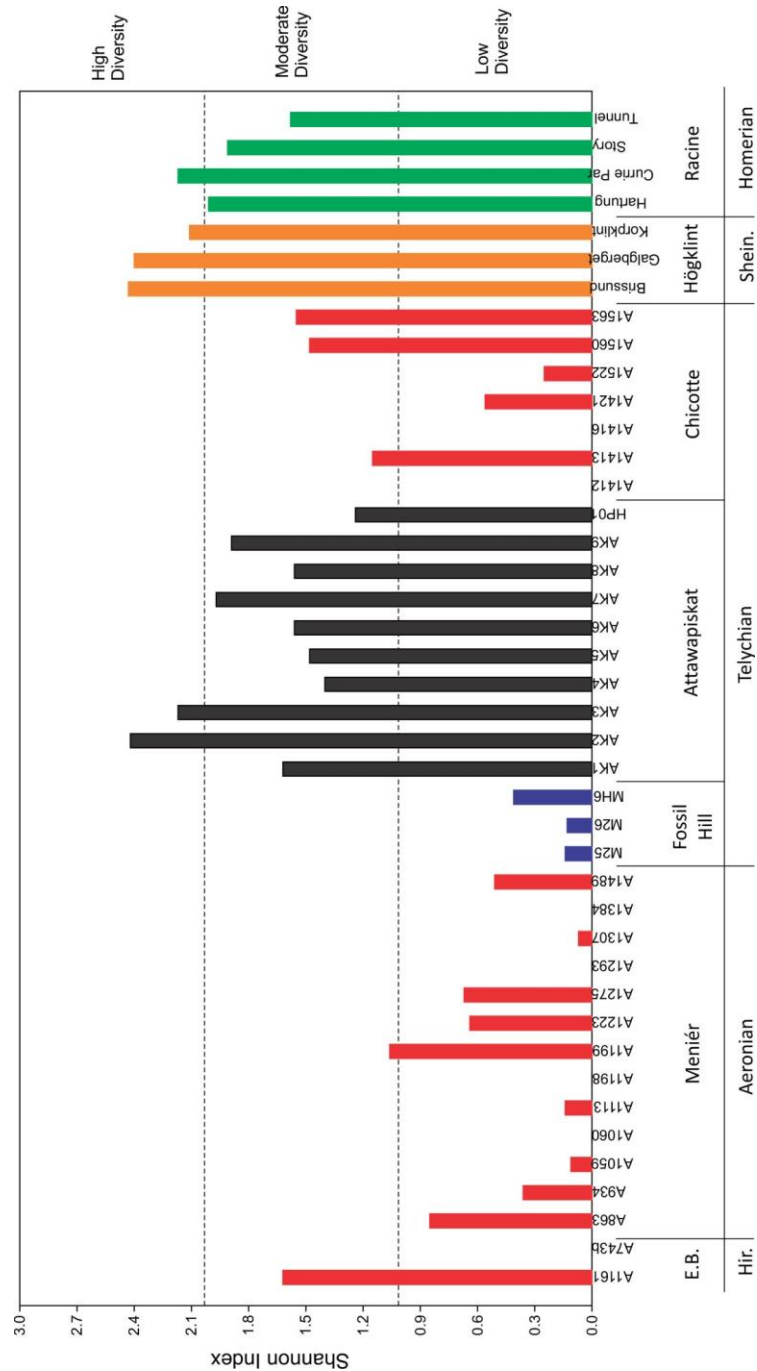
Figure 4.1: Shannon diversity indices of reef-dwelling brachiopods across space and time. Red bars from Anticosti Island, Quebec; blue bars from Manitoulin Island, Ontario; black bars from Akimiski Island, James Bay, Nunavut; orange bars from Gotland, Sweden; and green bars from Wisconsin. E.B: Ellis Bay Formation, Hir.: Hirnantian, Shein.: Sheinwoodian.

contemporaneous, reef bearing Attawapiskat Formation. It can be clearly seen that the nearly monotypic Fossil Hill Formation has much lower diversity than the reefal localities.

Table 4.1. Average and total Shannon (H) and Simpson (S) diversities for each study location.

Formation	Localities	Species	Specimens	AH	AS	TH	TS
Ellis Bay	2	6	80	0.81	0.61	1.61	0.23
Meniér	13	19	1213	0.37	0.82	0.69	0.76
Fossil Hill	3	7	2813	0.22	0.89	0.14	0.95
Attawapiskat	10	53	9009	1.73	0.28	2.51	0.12
Chicotte	7	15	226	0.71	0.65	1.45	0.43
Högklint	3	N/A	1921	2.3	N/A	N/A	N/A
Racine	4	33	1855	1.92	0.23	2.14	0.2

Note: AH = Average Shannon diversity, AS = Average Simpson diversity, TH = Total Shannon diversity, TS = Total Shannon diversity, N/A = not available

4.3.2 Brachiopod Associations in the Attawapiskat Formation

Cluster and principal component analyses recognized 10 distinct brachiopod community associations among the 32 collections from the Attawapiskat reefs on Akimiski Island (Fig. 4.2, Fig. 4.3). These associations are defined primarily by their dominant taxa along with their associated common and lesser taxa. Statistically, groups of collections which were separated from others by a Euclidean distance value of 42 or higher were named as associations. The only exception to this are collections AK1 and
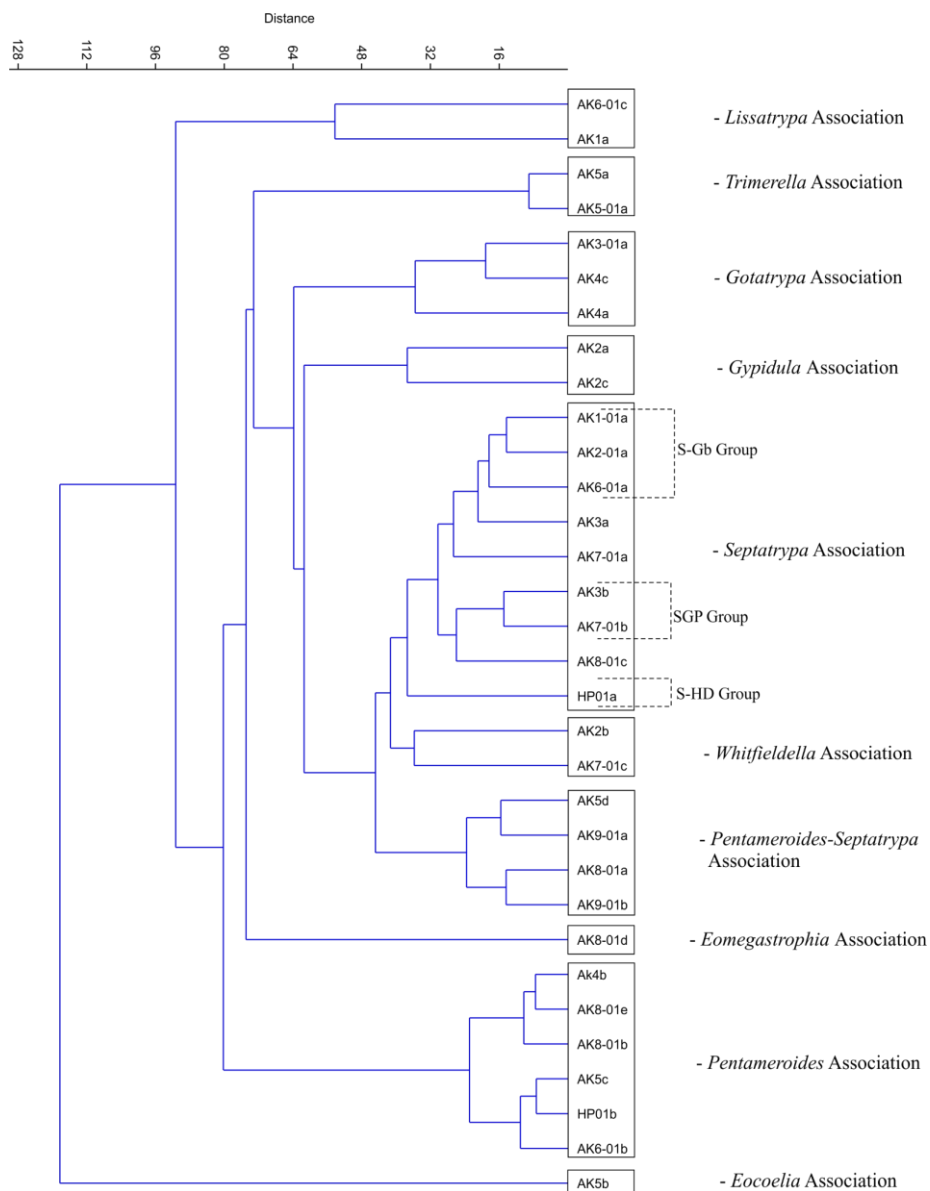
Figure 4.2: cluster analysis of the reef-dwelling brachiopods from the Attawapiskat Formation. Boxes show defined community associations. *Septatrypa* Association, *Gotatrypa*-bearing group: S-Gb group; *Septatrypa* Association, *Septatrypa–Gotatrypa–Pentameroides* group: SGP group; *Septatrypa* Association, high dominance group: S-HD group.
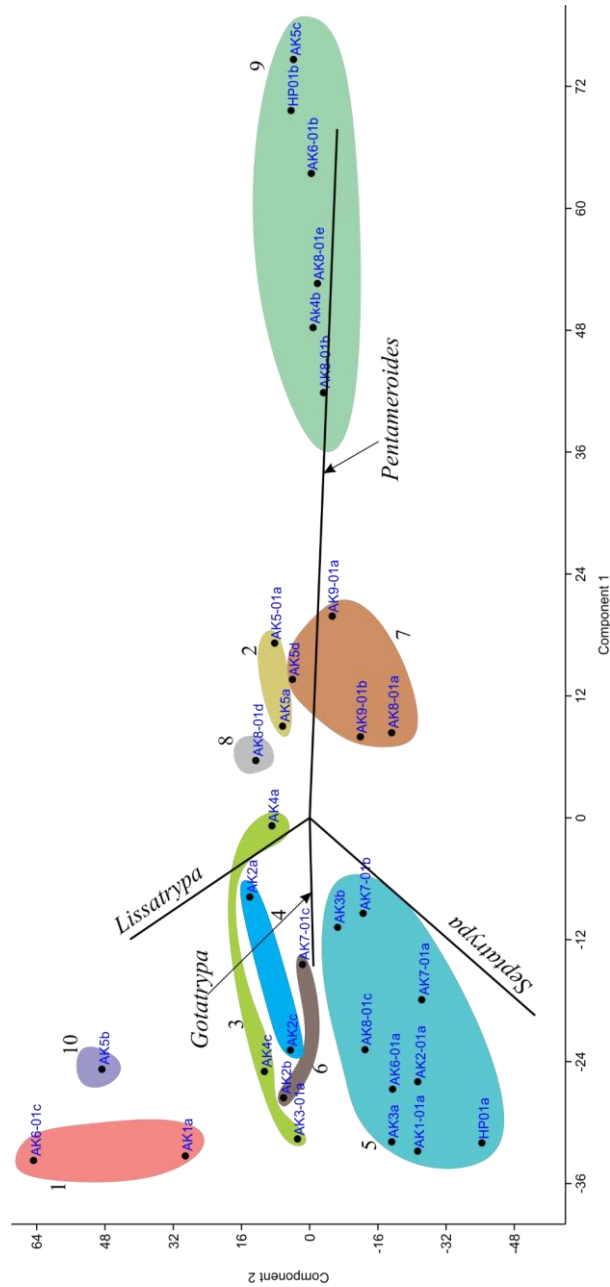
Figure 4.3: Principal components analysis and scatter plot of the Attawapiskat community associations. Axis bars show increasing dominance of most abundant species. 1. *Lissatrypa* Association, 2. *Trimerella* Association, 3. *Gotatrypa* Association, 4. *Gypidula* Association, 5. *Septatrypa* Association, 6. *Whitfieldella* Association, 7. *Pentameroides–Septatrypa* Association, 8. *Eomegastrophia* Association, 9. *Pentameroides* Association, 10. *Eocoelia* Association.

AK6-01a which are grouped as one association but are separated from each other by a distance of 54. These collections are grouped together because they are the only two collections in one branch of the scatter plot which separates from the main group of collections at a Euclidean distance of 93 and are both dominated by the species *Lissatrypa variabilis* (Fig. 4.2). In addition, the PCA scatterplot places these two collections more closely to each other than to other groups of collections suggesting the grouping of these two collections as one association is valid (Fig. 4.3).

In the following sections, each of these associations will be discussed in terms of their taxonomic composition, relative abundances of species, diversity, shell volumes, and relative living space requirements. The average Shannon diversity indices, Simpson diversity indices, and shell volumes of the associations are shown in Table 4.2. The relative abundances of brachiopod taxa are defined as follows: a dominant taxon signifies that this taxon is the most common brachiopod type in the specific collection or association; likewise secondary and tertiary taxa reflect the second and third most common taxa in the collection or association; a common taxon is one that is not dominant but commonly present (>2% relative abundance) within the collection or occurs across the collections of an association; a minor or lesser taxon occurs at low (<2%) abundances within the collection or in only some of the collections of the association.

Table 4.2. Average Shannon (H) diversity, Simpson (S) diversity, and shell volume of the Attawapiskat reefal brachiopod associations.

Association	Average H	Average S	Average Shell Volume (mm³)
Lissatrypa	0.87	0.61	199
Trimerella	1.05	0.43	11695
Gotatrypa	1.36	0.4	1299
Gypidula	1.77	0.32	1420
Septatrypa	1.72	0.27	1447
Whitfieldella	2.29	0.16	912
Pentameroides–Septatrypa	1.74	0.27	3298
Eomegastrophia	0.69	0.31	2704
Pentameroides	0.57	0.75	6569
Eocoelia	0	1	N/A

Note: H = Shannon diversity index, S = Simpson diversity index, N/A = not available

4.3.2.1 *Lissatrypa* Association

This association is characterized by the dominance of the small, smooth, and biconvex shells of *Lissatrypa variabilis* (Fig. 4.4) which makes up ~48% of the brachiopod specimens in collection AK1a, and ~95% in AK6-01c. Common but non-dominant components of this association are *Gotatrypa hedei* and *Septatrypa varians*, with collection AK1a also containing common *Gypidula akimiskiformis* and minor *Pentameroides septentrionalis*, *Eoplectodonta* sp., and *Erilevigatella euthylomata* (Fig. 4.5 A). Owing to the high dominance of *Lissatrypa* in AK6-01c, this association has a low average Shannon index (H = 0.87) and a moderate Simpson index (S = 0.61). Despite the numerical specimen richness, the average shell volume of this association is very low

Figure 4.4: Dominant and common species of the Attawapiskat brachiopod associations.

A–E: W2982, *Lissatrypa variablis*, dorsal, ventral, lateral, posterior, and anterior views. Note the small size of the shell compared to *Trimerella*. Collection AK1a, Attawapiskat Formation, Akimiski Island. Scale bar is 2.5 mm.

F–J: W2983, *Trimerella ekwanensis*, dorsal, ventral, lateral, posterior, and anterior views showing the large weakly biconvex shell with highly pointed triangular ventral umbo. Collection AK5a, Attawapiskat Formation, Akimiski Island. Scale is 1 cm.
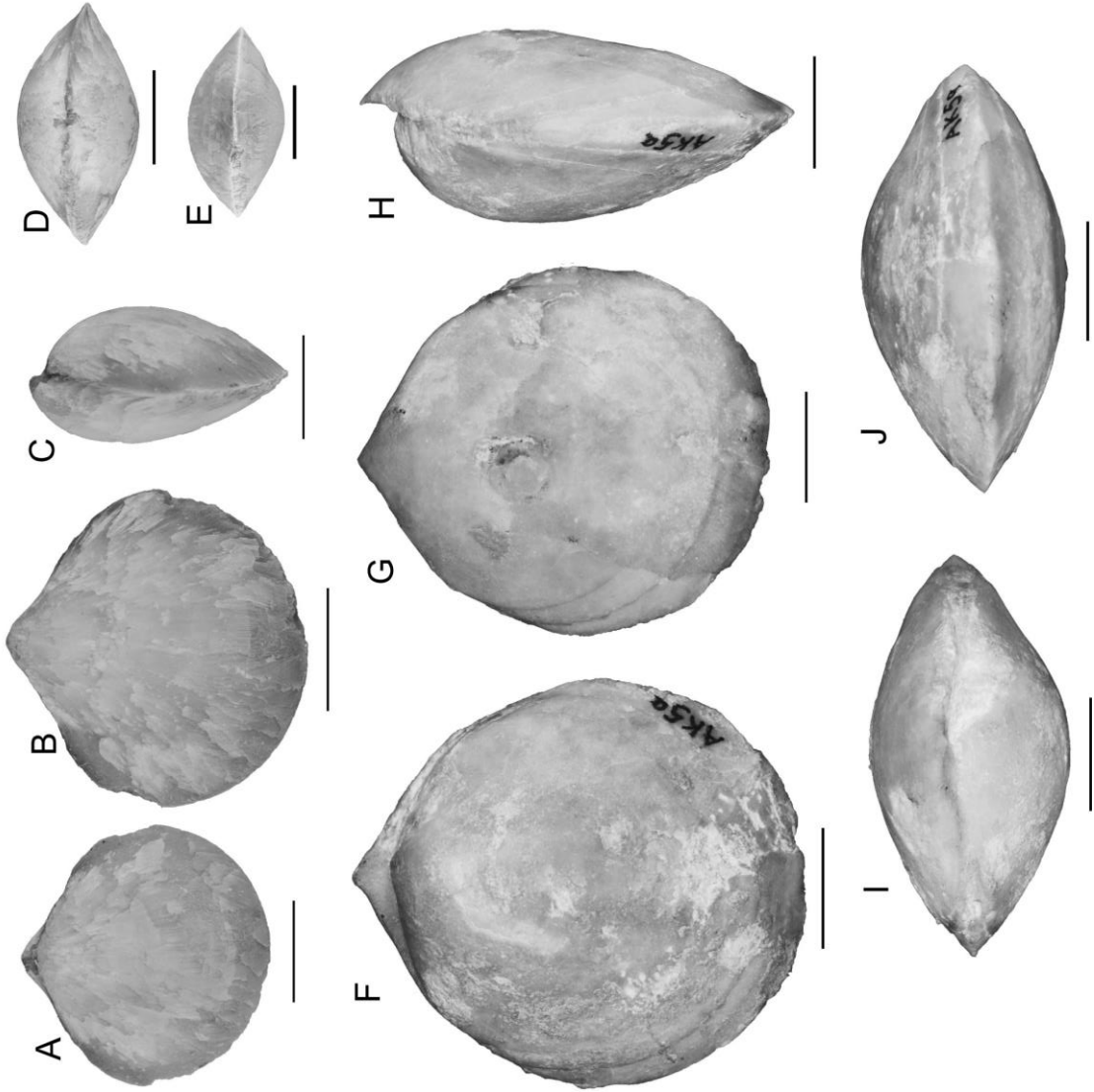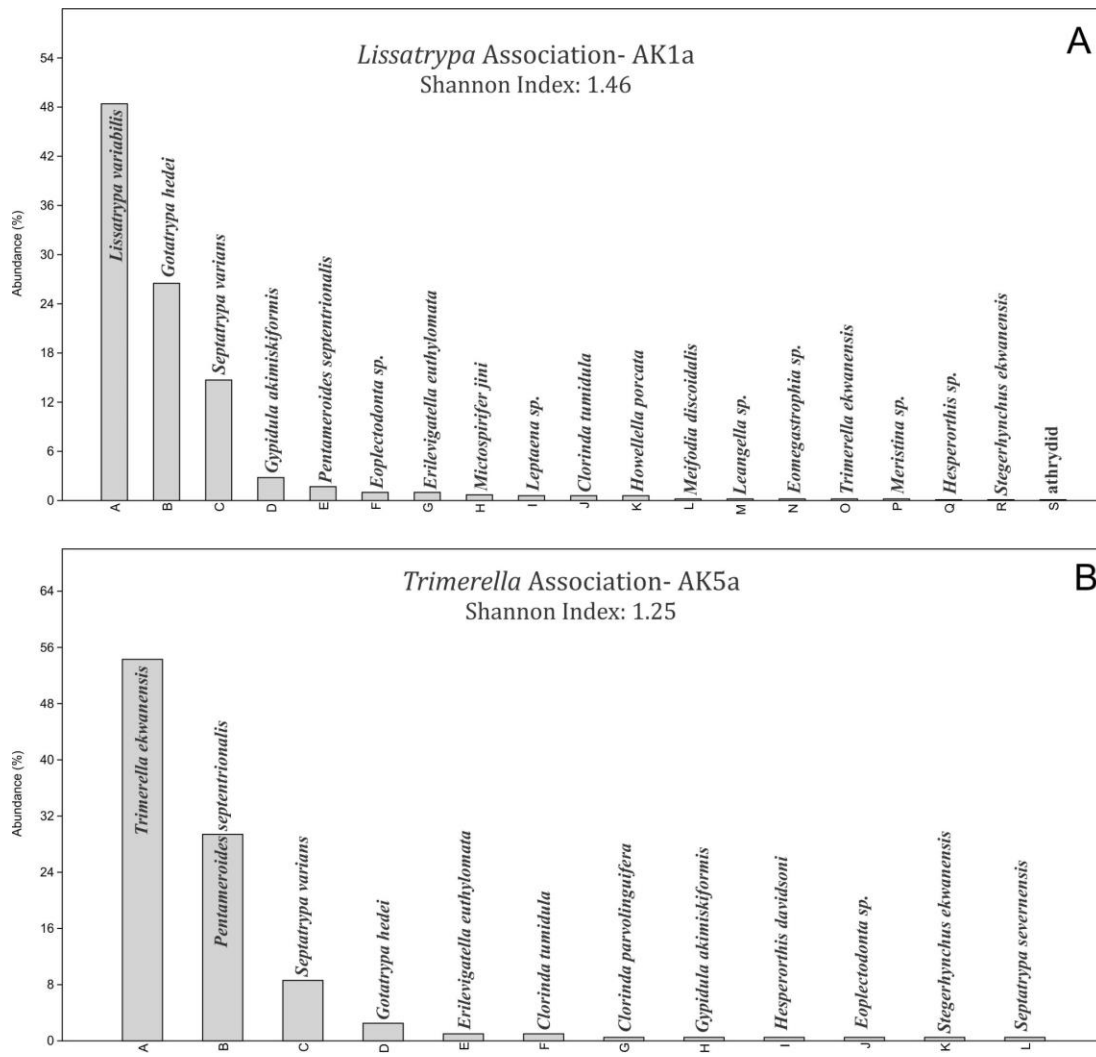
Figure 4.5: Constituent species and relative abundances of representative collections of the Attawapiskat associations. A) *Lissatrypa* Association, collection AK1a; B) *Trimerella* Association, collection AK5a.

(199 mm^3) due to the abundance of small-shelled *Lissatrypa* and *Gotatrypa* as well as an overall lack or paucity of large-shelled *Pentameroides*. There is, however, a major contrast between the relative abundance of *Lissatrypa* and its required living space and the relative abundance and living space requirement of *Pentameroides*. In AK1a, where both species are present, *Lissatrypa* comprised ~48% relative abundance at this collecting locality, while only taking up ~6% of the living space. In comparison, *Pentameroides* only comprises <2% relative abundance but utilizes ~38% of the living space.

4.3.2.2 *Trimerella* Association

Trimerella ekwanensis (Fig. 4.4) dominates this association, comprising an average of ~55% relative abundance between the two collections grouped within the association, which also contain such non-dominant common taxa as *Pentameroides septentrionalis*, *Septatrypa varians*, and *Gotatrypa hedei*, with minor taxa such as *Clorinda tumidula* and *Erilevigatella euthylomata* (Fig. 4.5 B). This species is notable due to its large and triangular ventral umbo, relatively low degree of biconvexity (compared to other Attawapiskat dominant species), and its partially aragonitic composition. Shannon diversity is low to moderate (H = 1.05) while evenness is moderate (S = 0.43) in this association. Due to the abundance of large sized *Trimerella* and *Pentameroides* specimens this association has the largest average shell volume among the associations recognized in the Attawapiskat Formation (11 695 mm^3). As a result, the relative abundance is positively related to the required living space in this association, in contrast to some other associations, such as the *Lissatrypa* Association. In

collection AK5a, for example, *Trimerella* has a ~54% relative abundance and occupies ~79% of the living space.

As noted above, living *Trimerella* originally had aragonitic shells, which remained well-preserved after diagenetic inversion to calcite and even with some aragonitic micro-layers preserved today (Balsathar et al. 2011). This is the only aragonitic-shelled brachiopod species in the Attawapiskat Formation. There is a general lack of small or juvenile shells of *Trimerella*, suggesting a preservation bias favouring large shells of this species in contrast to the other brachiopods of these reefs, in which small shells, such as *Lissatrypa variabilis* and *Gotatrypa hedei*, are found in abundance and good preservation.

4.3.2.3 *Gotatrypa* Association

The *Gotatrypa* Association is dominated by the spire-bearer *Gotatrypa hedei* (Fig. 4.6) which on average comprises ~60% of the relative abundance of this association, although the actual relative abundance of this species in the constituent collections ranges from 52% to 67%. Unlike the other dominant brachiopods of the Attawapiskat associations which have smooth shells, *Gotatrypa hedei* has fine ribbing and prominent concentric frills (see Jin et al. 1993). Secondary taxa vary across the collections for this association, represented by *Pentameroides septentrionalis* in AK4a, *Gypidula akimiskiformis* in AK4c, and *Septatrypa varians* in AK3-01a. The differences in secondary components are likely contributing factors for the elongated shape of this association in the PCA scatter plot (Fig. 4.3). Other common taxa include *Clorinda*

Figure 4.6: Dominant and common species of the Attawapiskat brachiopod associations.

A–E: W2984, *Gotatrypa hedei*, dorsal, ventral, lateral, posterior, and anterior views. Note the prominent concentric frills and ribbing along the margin of the shell. Collection AK3-01a, Attawapiskat Formation, Akimiski Island. Scale bar is 5 mm.

F–J: W2985, *Gypidula akimiskiformis*, dorsal, ventral, lateral, posterior, and anterior views showing the deep plicosulcate anterior commissure and highly ventribiconvex shell. Collection AK2a, Attawapiskat Formation, Akimiski Island. Scale bar is 5 mm.
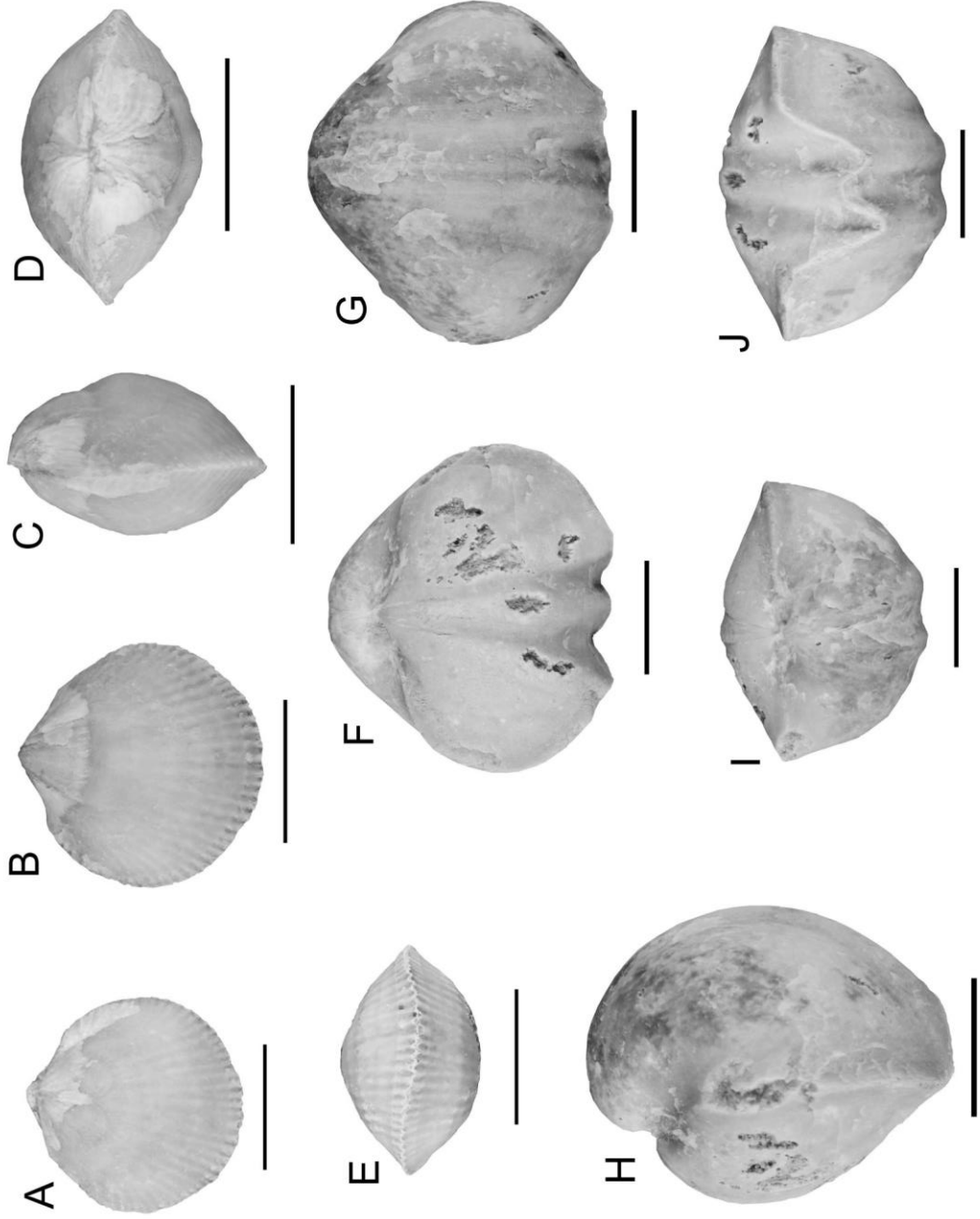
parvolinguifera, and *Lissatrypa variabilis* (Fig. 4.7 A). Overall the diversity of this association is moderate (H = 1.36), but this is due to the low diversity of collection AK4a (H = 0.64) contrasting the other two collections which have much higher Shannon indices (AK3-01a: H = 1.83; AK4c: H = 1.61). The Simpson evenness is more conservative between the collections, with a moderate average of 0.4 and a range of 0.30–0.56. The average shell volume is small to moderate (1299 mm^3) due to the abundance of small-shelled *Gotatrypa*. The average shell size is larger than the *Lissatrypa* Association, however, due to the relatively common occurrence of moderately sized *Septatrypa* and large-shelled *Pentameroides* in this association. As in the *Lissatrypa* Association, the dominant brachiopod type in terms of relative abundance does not dominate the living space. In collection AK4c, for example, *Gotatrypa hedei* comprises ~56% relative abundance, but only ~13% of the living space, whereas *Pentameroides septentrionalis* comprises ~7% relative abundance and ~69% of the living space.

4.3.2.4 *Gypidula* Association

Gypidula akimiskiformis (Fig. 4.6), which is the oldest known *Gypidula* known so far (Jin 2005), dominates the *Gypidula* Association. The most obvious feature of this species is the large plicosulcate anterior and the strong ribbing which occurs in the medial portion of both valves. The flank areas of the shell is smooth. Interestingly, shell shape shows some degree of homeomorphy with that of the large *Pentameroides septentrionalis*, with a highly ventribiconvex shell and deepened ventral umbo compared to its dorsal valve. The secondary taxa of the *Gypidula* Association are *Pentameroides septentrionalis* in AK2a and *Septatrypa varians* in AK2c. This difference in secondary
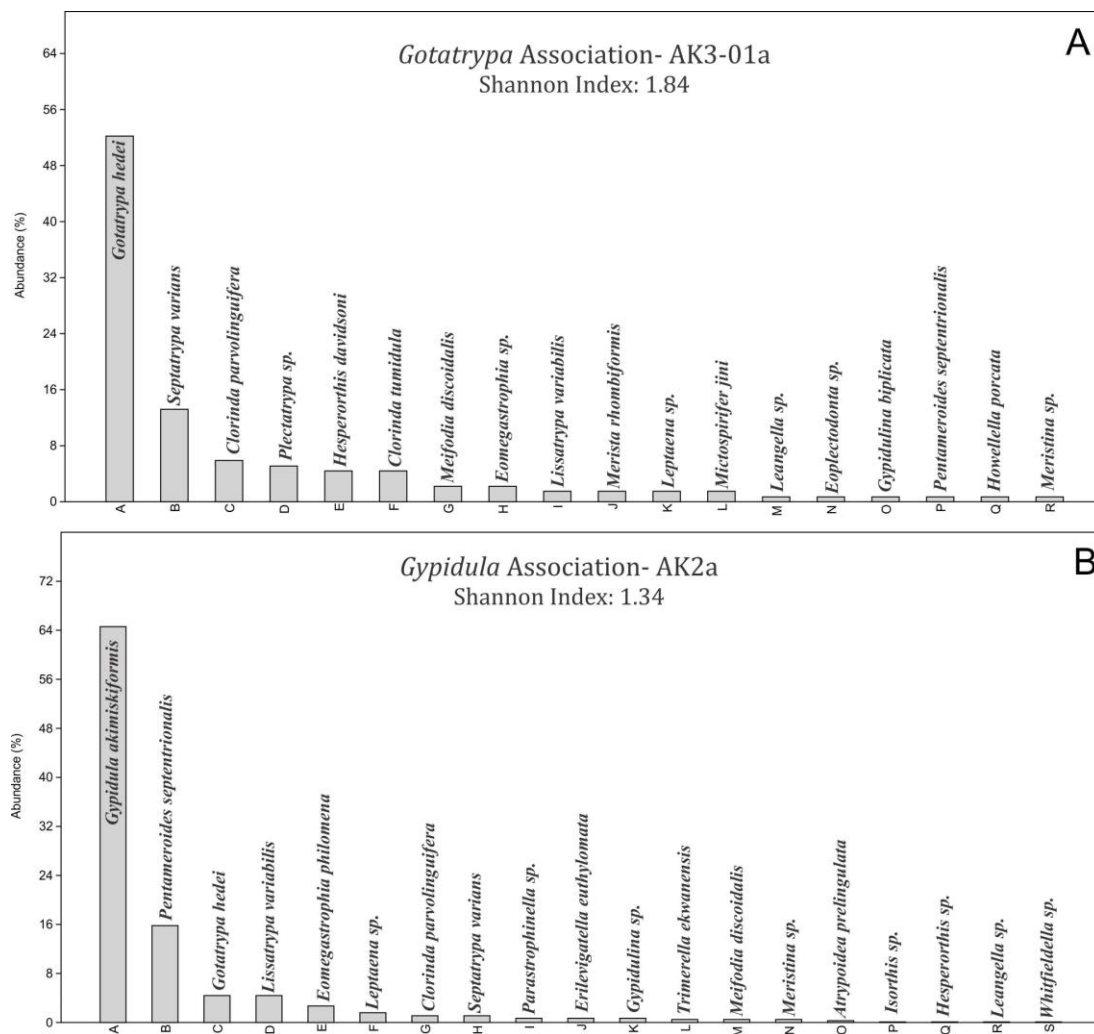
Figure 4.7: Constituent species and relative abundances of representative collections of the Attawapiskat associations. A) *Gotatrypa* Association, collection AK3-01a; B) *Gypidula* Association, collection AK2a.

 taxa likely contributes to the irregular shape of the *Gypidula* association in the PCA

scatter plot, similar to that of the *Gotatrypa* Association (Fig. 4.3). Common shared taxa

of this association include *Pentameroides septentrionalis*, *Septatrypa varians*, *Gotatrypa*

hedei, *Lissatrypa variabilis*, and *Eomegastrophia philomena* (Fig. 4.7 B).

The dominance indices of *Gypidula* in individual collections of this association

vary from ~35% in AK2c to ~65% in AK2a, and results in differing diversity estimates

for each collection. The Shannon diversity and Simpson evenness are moderate in AK2a

(H = 1.34; S = 0.45), but high in AK2c (H = 2.19; S = 0.18). These values give the

Gypidula Association moderate average diversity and evenness levels (H = 1.77, S =

0.32). The average shell volume is moderate (1420 mm^3) due to a mixture of small-

shelled *Gypidula*, *Lissatrypa*, and *Gotatrypa* and larger *Septatrypa* and *Pentameroides*

shells. Like other small shelled dominant associations examined in this study, the

dominant *Gypidula akimiskiformis* takes up a small average relative proportion (50% of

relative abundance, 16% living space) of the living space, whereas the larger

Pentameroides occupies a larger average proportion (10% relative abundance, 49%

living space).

4.3.2.5 *Septatrypa* Association

While most of the Attawapiskat associations consist of fewer than five

collections, the *Septatrypa* Association comprises nine, suggesting its common

occurrences in the reefal facies. This association is dominated by the relatively large,

smooth shells of *Septatrypa varians* (Fig. 4.8). This species, previously classified as

Figure 4.8: Dominant and common species of the Attawapiskat brachiopod associations.

A–E: W2986, *Septatrypa varians*, dorsal, ventral, lateral, posterior, and anterior views showing the uniplicate anterior commissure. Collection AK2-01a, Attawapiskat Formation, Akimiski Island. Scale bar is 5 mm.

F–J: W2987, *Whitfieldella sulcatina*, dorsal, ventral, lateral, posterior, and anterior views. Note the extreme small size, but high biconvexity of the shell. Collection AK2b, Attawapiskat Formation, Akimiski Island. Scale bar is 2.5 mm.
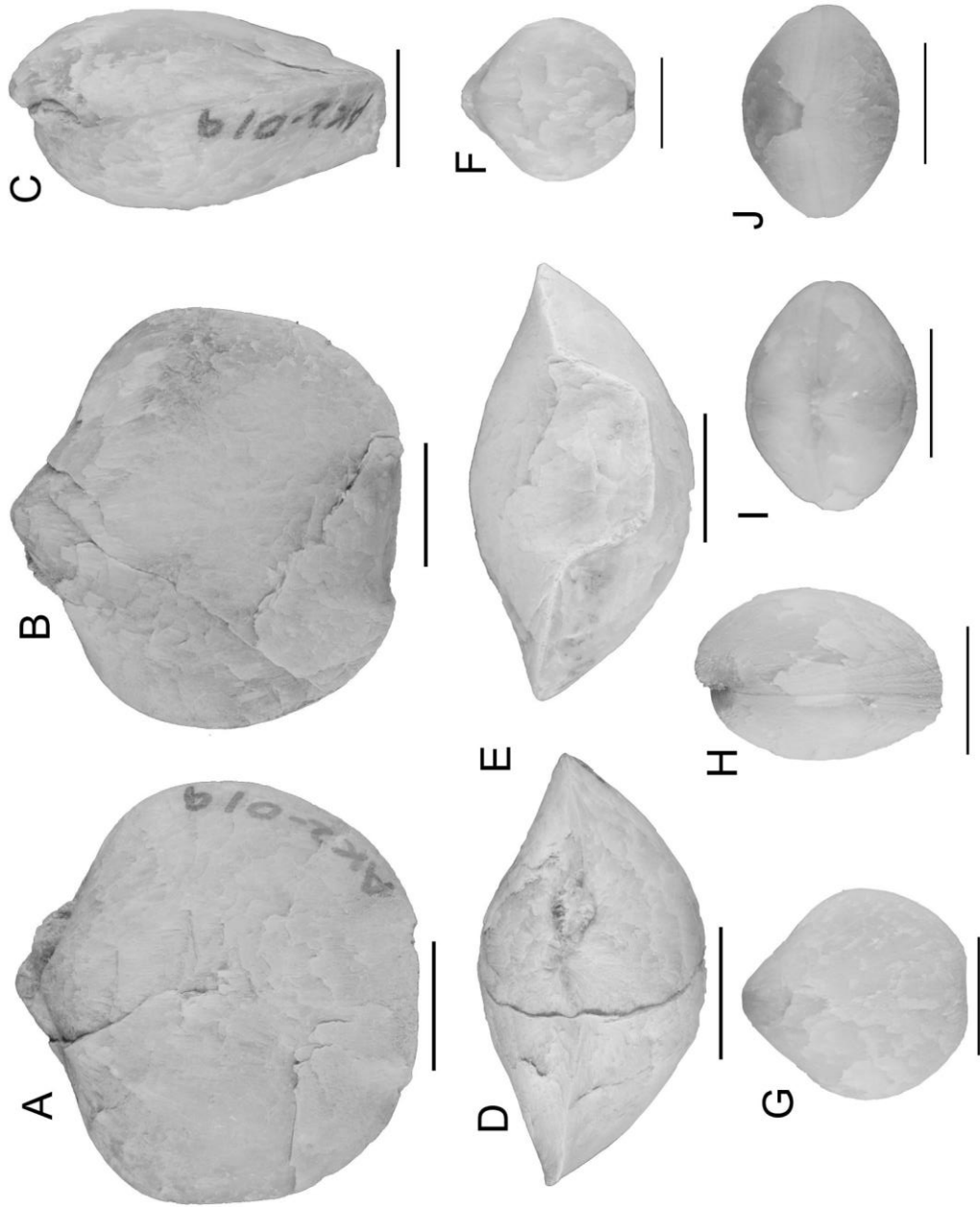
Atrypopsis varians, is easily identifiable by its subangularly uniplicate anterior commissure. The dominance of *Septatrypa* in this association varies from highly dominant in collection HP01 (~72% relative abundance) to subordinate in AK3b where it is the secondary taxa (~22% relative abundance). The heterogeneous taxonomic compositions and variable levels of dominance of *Septatrypa* allow the *Septatrypa* Association to be subdivided into smaller groups (Fig. 4.2). The *Gotatrypa*-bearing group is characterized by *Gotatrypa hedei* as the secondary species. Other common taxa in this group are *Gypidula akimiskiformis*, *Pentameroides septentrionalis*, *Clorinda tumidula*, and *Erilevigatella euthylomata* (Fig. 4.9 A). The *Septatrypa–Gotatrypa–Pentameroides* group is characterized by having these three brachiopod types as their dominant, secondary, and tertiary taxa at comparable relative abundances (Fig. 4.9 B). Common taxa besides these three species include *Erilevigatella euthylomata*, *Meifodia discoidalis*, and *Whitfieldella sulcatina*. The group with the most dominant *Septatrypa* is typified by collection HP01a, in which ~72% of specimens are *Septatrypa varians*. *Pentameroides septentrionalis*, *Gotatrypa hedei*, and *Erilevigatella euthylomata* are the next most common taxa within this group (Fig. 4.10 A). The remaining collections of the *Septatrypa* Association do not fall into any specific grouping, but the secondary taxa include *Clorinda tumidula*, *Meifodia discoidalis*, and *Cyphomenoidea parvula* for AK7-01a, AK8-01c, and AK3a respectively. *Gypidula akimiskiformis* and *Pentameroides septentrionalis* are less common but still relatively abundant components of these collections (Fig. 4.10 B).

Due to the large number of collections in the *Septatrypa* Association, the Shannon and Simpson indices are quite varied. Shannon diversity ranges from low-moderate in

Figure 4.9: Species composition and relative abundance of representative collections within the Attawapiskat associations. A) *Septatrypa* Association–*Gotatrypa* bearing group, collection AK2-01a; B) *Septatrypa* Association, *Septatrypa–Gotatrypa–Pentameroides* group, collection AK7-01b.

Figure 4.10: Species constituents and relative abundance of representative collections within the Attawapiskat associations. A) *Septatrypa* Association–High dominance group, collection HP01a; B) *Septatrypa* Association, collection AK3a.

HP01a (H = 1.05) to high in AK8-01c (H = 2.04). Similarly the Simpson evenness of these collections has a range from moderate to high values (S = 0.54–0.07). The wide ranges in both diversity estimates result in moderate average values for the *Septatrypa* Association (average H = 1.72; average S = 0.27). Like the moderate average diversity level, the average shell volume of this association is also moderate (1447 mm^3) due to the high abundance of moderately sized *Septatrypa*. This average value reflects the mixing of numerous, relatively small shells such as *Gotatrypa* and *Gypidula* with larger *Pentameroides* shells in the nine collections of this association. In terms of living space requirement, the dominant *Septatrypa* utilizes a relatively large proportion of the living space (average 20%) but, as is most other Attawapiskat brachiopod associations, the large *Pentameroides* shells take up a larger proportion (average 53%) of the living space.

4.3.2.6 *Whitfieldella* Association

Unlike the other associations, the *Whitfieldella* Association is not defined by its dominant component. It is, however, characterized by its relatively high abundance (6–14% relative abundance) of *Whitfieldella sulcatina* (Fig. 4.8). This species has the smallest shell size among the major Attawapiskat species described in this study, and is also smooth and strongly biconvex like many of the larger dominant species in the reefs. In the other collections, this species is typically very minor (<2% relative abundance) or absent, with the exception of collection AK3b, in which ~7% of the specimens are *Whitfieldella sulcatina*. The dominant, and common taxa in this locality are not shared among the constituent samples, with *Septatrypa varians* and *Lissatrypa variabilis* being the primary and secondary taxa in AK2b and *Gotatrypa hedei* and *Clorinda tumidula*

being the primary and secondary taxa for AK7-01c. *Gotatrypa hedei* is in fact common (~13% relative abundance) in AK2b, but these collections cannot be attributed to the *Gotatrypa* Association, despite their location in the PCA scatter (Fig. 4.3), due to the complete absence of *Whitfieldella sulcatina* in the *Gotatrypa* Association. *Gypidula akimiskiformis*, *Merista rhombiformis*, and *Eoplectodonta* sp. are some of the shared common components of the *Whitfieldella* Association (Fig. 4.11 A).

The Shannon diversity and Simpson evenness are both high in this association (H = 2.29; S = 0.16), due to the high Shannon diversity of AK2b (H = 2.51) and AK7-01c (H = 2.07). In both of these collections the Simpson index is high with a value of S = 0.16. The average shell volume of this association is small (912 mm^3) due to the predominance of small-shelled *Whitfieldella*, *Lissatrypa*, and *Gotatrypa*. Despite *Whitfieldella* being the smallest major species in this study, the *Lissatrypa* Association has a lower average shell volume. This is due to the relatively low abundance of *Whitfieldella* in its own association compared to the very high abundance of *Lissatrypa* in its association. In addition, the dominant *Septatrypa* component of AK2b and the relative high abundance of *Pentameroides* in AK7-01c (~14% relative abundance) greatly increases the average shell volume. Accordingly, the small *Whitfieldella*, *Lissatrypa*, and *Gotatrypa* shells take up a very minor proportion of the living space in this association. The numerically dominant (~28% relative abundance) *Gotatrypa* in AK7-01c only occupies ~3% of the living space, the common *Whitfieldella* in AK2b (~14% relative abundance) only makes up ~0.5% the living space, and in AK2b *Lissatrypa* only utilized ~2% of the living space despite making up ~14% (relative abundance) of the collection. *Septatrypa* and *Pentameroides* occupy a larger proportion of the living space than their relative
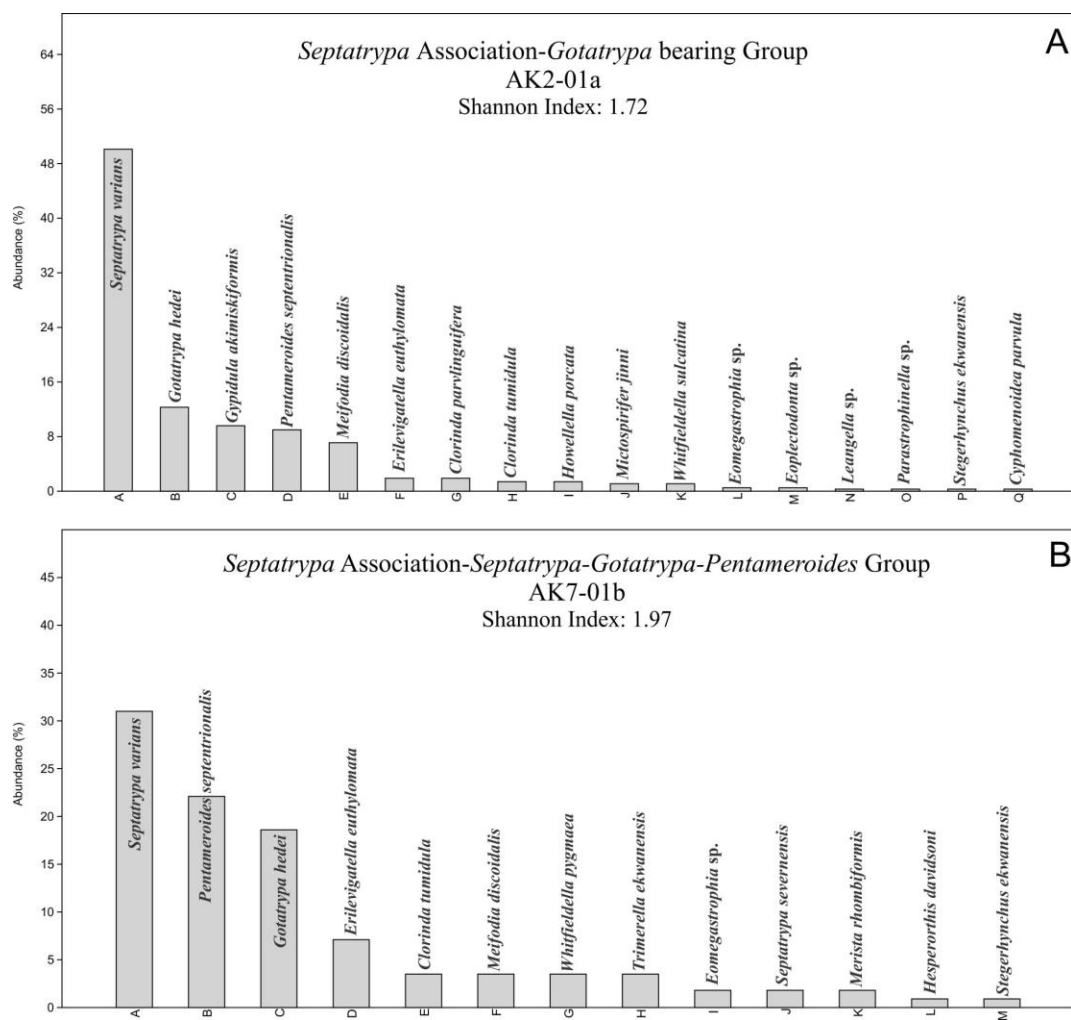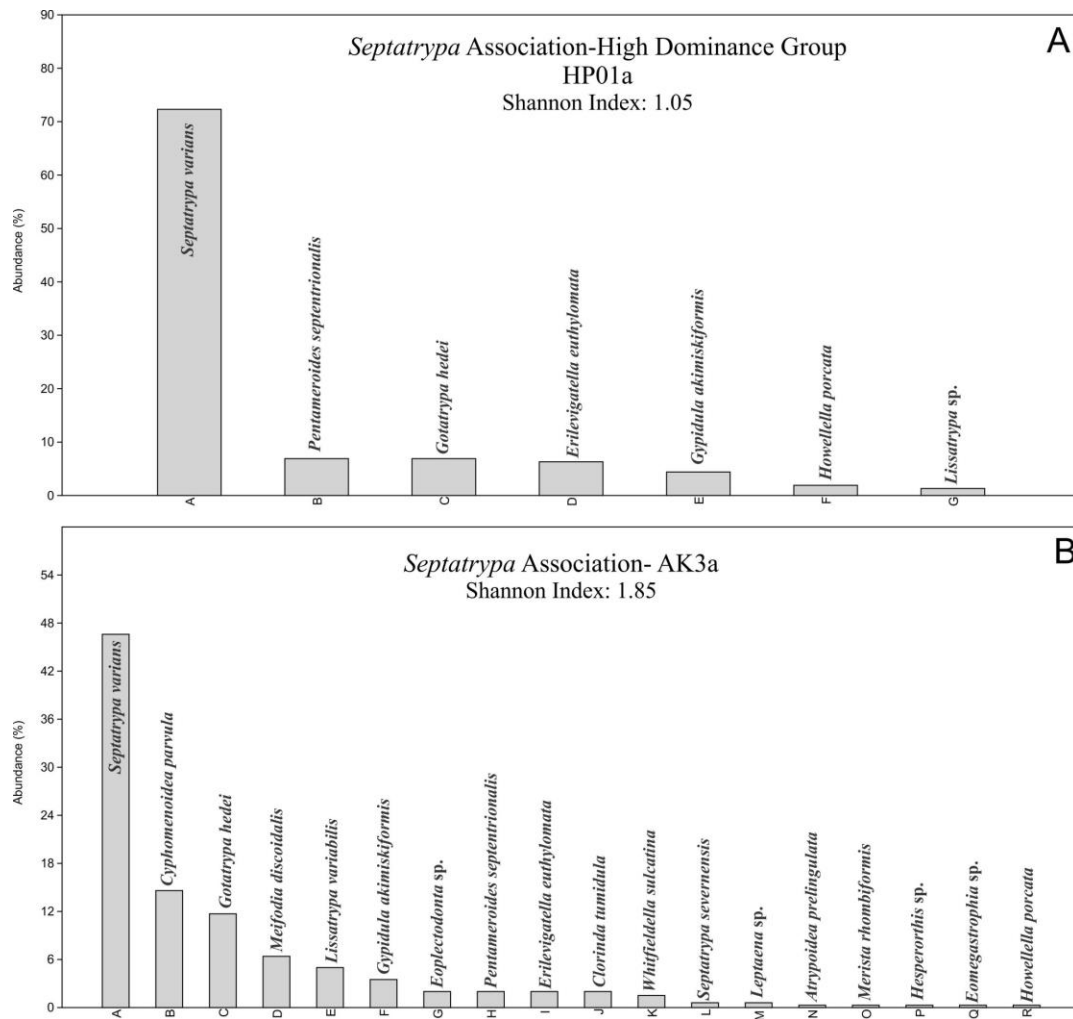
Figure 4.11: Species constituents and relative abundance of representative collections within the Attawapiskat associations. A) *Whitfieldella* Association, collection AK2b; B) *Pentameroides–Septatrypa* Association, collection AK9-01b.

abundance values would suggest with *Septatrypa* utilizing ~24% and *Pentameroides*

occupying ~48% of the association's total living space.

4.3.2.7 *Pentameroides–Septatrypa* Association

This association is unusual in that it is defined by the co-dominance of

Pentameroides septentrionalis and *Septatrypa varians*. Collections AK5d, AK8-01a, and

AK9-01b are dominated by *Pentameroides* with secondary *Septatrypa* while AK9-01a is

dominated by *Septatrypa* with secondary *Pentameroides*. The level of dominance varies

in each collection from a rather low relative abundance value of ~37% *Pentameroides* in

AK9-01b, and a higher ~48% relative abundance of *Septatrypa* in AK9-01a. These low

abundances of *Pentameroides* are likely the reason these collections are grouped together

instead of within the *Pentameroides* association. As is discussed below, the

Pentameroides Association is characterized by extremely high levels of dominance of

this species. The wide separation of these two associations in the PCA plot (Fig. 4.3)

shows this difference of dominance between the two associations. The common taxa

shared among the collections of this association include *Clorinda tumidula*, *Gotatrypa*

hedei, and *Gypidula akimiskiformis* (Fig. 4.11 B).

The Shannon diversity ranges from moderate (H = 1.47) to near high (H = 1.93)

with an average of H = 1.74). The Simpson evenness is also moderate with an average of

S = 0.27 and a constrained range from 0.32–0.24. Diversity levels in this association are

moderate due to the low dominance of the co-dominant *Pentameroides* and *Septatrypa* in

this association as high levels of dominance by one species results in lower diversity

levels (see Materials and Methods). The shell volume is greater than the majority of the

Attawapiskat associations with an average value of 3298 mm^3, being outdone by the

Trimerella and *Pentameroides* associations. The large volume is due to the high

abundances of the co-dominant *Septatrypa* and *Pentameroides* as well as the common

occurrences of moderately sized *Clorinda* shells. Small shells such as *Gotatrypa* and

Lissatrypa are found in this association but are of such minor relative abundances that

they have little effect on overall shell size. On average, *Pentameroides septentrionalis*

occupies ~79% of the living space in this association with *Septatrypa varians* taking up

~7% of the living space. In AK9-01a, *Septatrypa* only occupies ~14% of the living space

while *Pentameroides* occupies ~77%. Despite *Septatrypa* being much more abundant

than *Pentameroides* (48% relative abundance *Septatrypa* compared to 18% relative

abundance *Pentameroides*), the co-dominance of *Pentameroides* greatly increased the

utilization of living space in the brachiopod associations of the Attawapiskat Formation.

4.3.2.8 *Eomegastrophia* Association

This association is represented by a single sample from locality AK8-01d, which

is comprised of only 3 species; *Eomegastrophia* sp., *Eoplectodonta hudsonensis*, and

Pentameroides septentrionalis (Fig. 4.12 A), resulting in a low diversity (H = 0.69), but a

moderate evenness (S = 0.31) due to the low number of species in which none are

overwhelmingly dominant. The average shell volume is large (2704 mm^3) as all

specimens in this association have moderately to large sized shells with *Pentameroides*

occupying ~70% of the living space despite its low (25%) relative abundance value. This
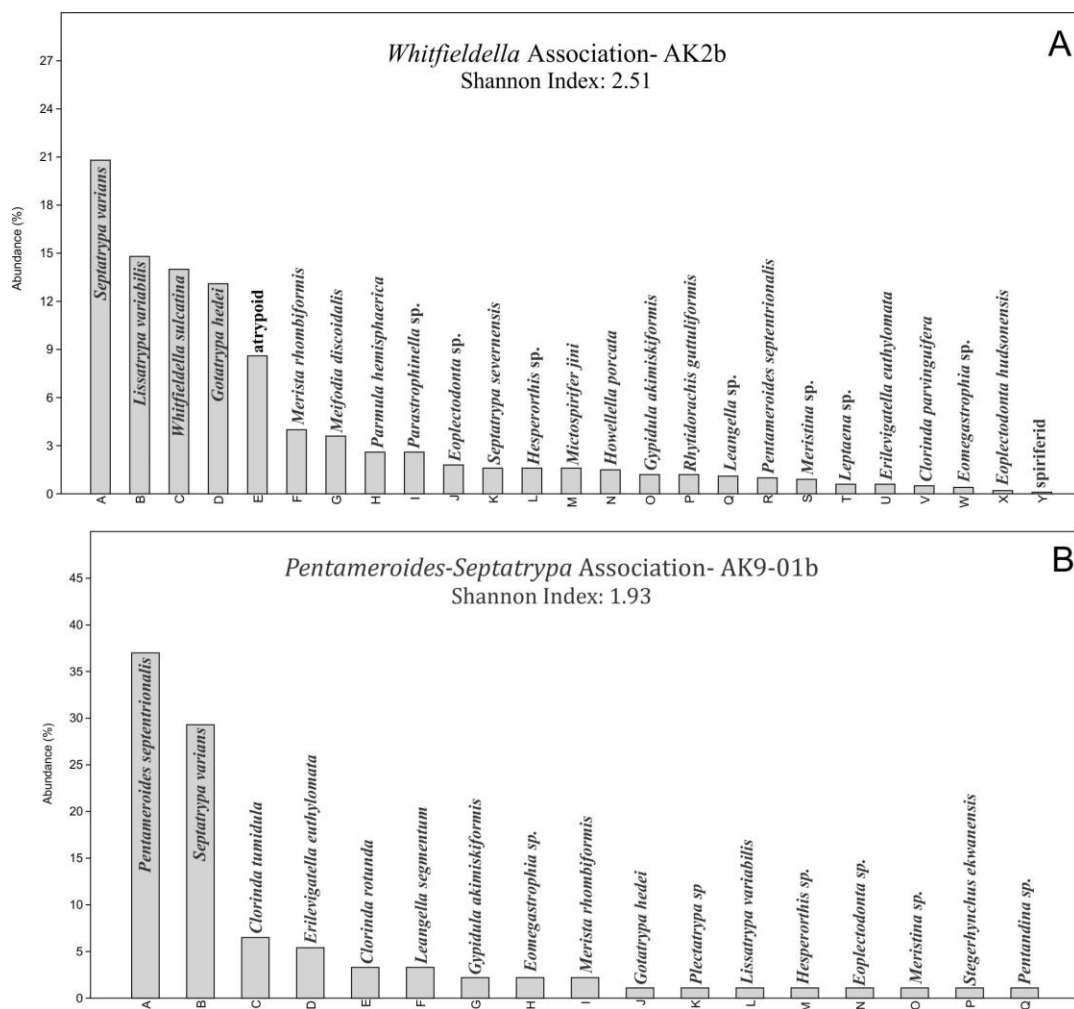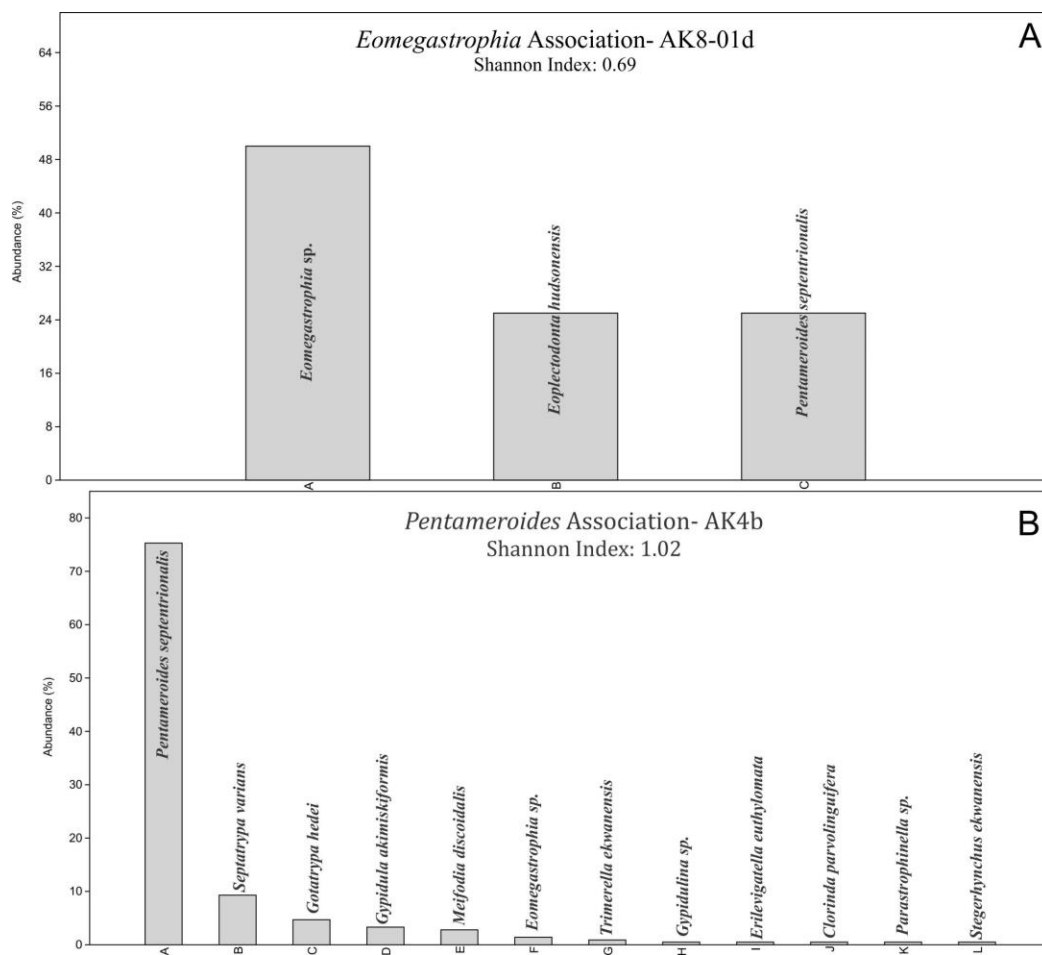
Figure 4.12: Species constituents and relative abundance of representative collections within the Attawapiskat associations. A) *Eomegastrophia* Association, collection AK8-01d; B) *Pentameroides* Association, collection AK4b.

association is likely an outlier, as the flattened, concavo-convex, strophomenide shells of *Eomegastrophia* are not abundant in any other Attawapiskat collections.

4.3.2.9 *Pentameroides* Association

The high dominance of the large strongly ventribiconvex *Pentameroides septentrionalis* (Fig. 4.13), which varies from 71%–100% relative abundance defines this association. As noted above, the high level of dominance of *Pentameroides* in this association is likely what separates this association from the *Pentameroides–Septatrypa* Association and can be seen graphically in the PCA scatter plot (Fig. 4.3). *Septatrypa varians* is the most common non-dominant taxon in this association, with *Gypidula akimiskiformis* as the secondary component in collection HP01b, but this is a small collection consisting of only *Pentameroides* and *Gypidula*. Common taxa in this association include *Gotatrypa hedei*, *Gypidula akimiskiformis*, and *Clorinda tumidula* (Fig. 4.12 B). Due to the overwhelming dominance of *Pentameroides* in all collections of this association diversity levels are some of the lowest in this study. The Shannon diversity ranges from 0–1.02 averaging to a value of H = 0.57. The Simpson evenness is more moderate with an average value of S = 0.75 and a range of 1.0–0.53. The abundance of large and giant-sized *Pentameroides* shells contributes to the large average shell size (6569 mm^3) of this association. The average is lower than the *Trimerella* association due the relatively high abundances of moderately sized *Septatrypa*. In addition, very small juvenile specimens of *Pentameroides* are present in these collections which lower the overall shell volume of the species compared to the average volume of *Trimerella* which is larger due to the absence of juvenile *Trimerella* specimens in the

Figure 4.13: Dominant and common species of the Attawapiskat brachiopod associations

 A–E: W2988, *Pentameroides septentrionalis*, Dorsal, ventral, lateral, posterior, and anterior views showing the highly biconvex shell with strongly convex ventral umbones. Collection AK8-01b, Attawapiskat Formation, Akimiski Island. Scale is 1 cm.

F: GS 117887, block of *Eocoelia akimiskii*, Note the coarse, simple costae along the lengths of the shells. Collection AK5b, Attawapiskat Formation, Akimiski Island. Scale is 1 cm.
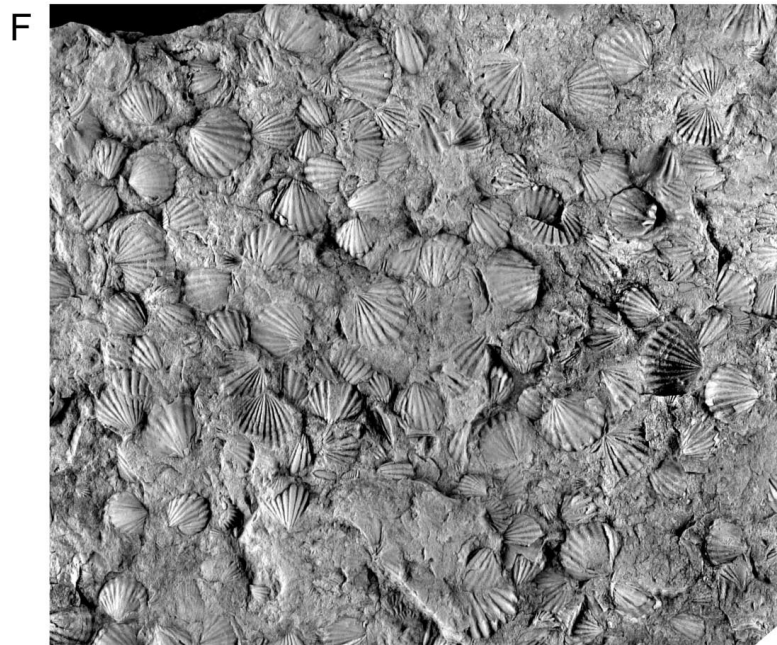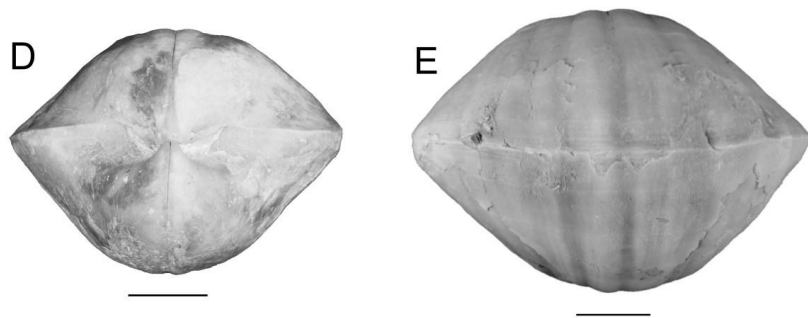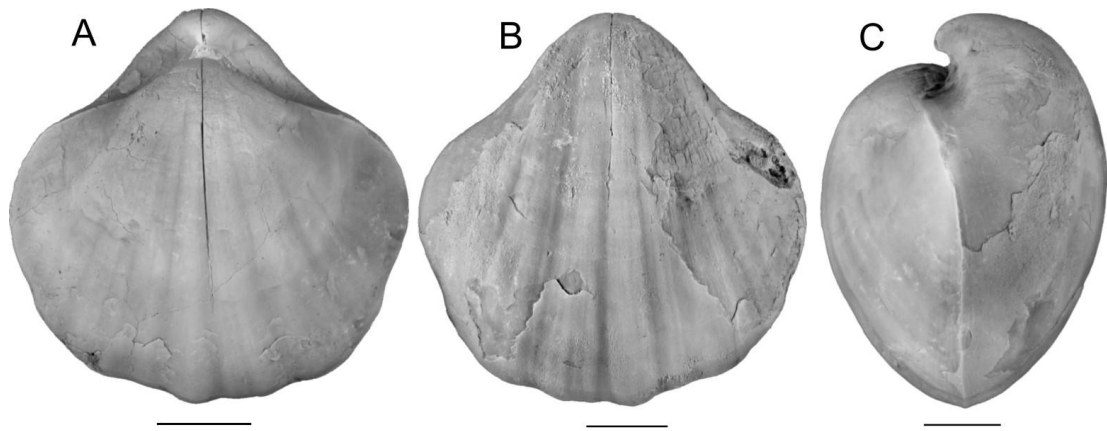
collections. As expected, *Pentameroides* completely dominates the living space of this association occupying an average of ~99%.

4.3.2.10 *Eocoelia* Association

The *Eocoelia* Association is the most unique among all the associations recognized in this study (Fig. 4.2). It is represented by a single monotypic collection of the small and ribbed species *Eocoelia akimiskii* (Fig. 4.13) from locality AK5b. This species does not appear in any other Attawapiskat collections. Due to its monospecificity, the diversity and evenness ($H = 0$, $S = 1$) cannot be meaningfully measured. Unfortunately, the shells collected from this collection are contained within a slab of limestone (see Jin 2003) and as such, accurate shell volume measurements could not be made.

4.4 Discussion

Synecology, or the study of ecology at a community level, examines biodiversity at the community or faunal levels, intra- and inter-species interactions, and the relationship between organisms and their living environments. Long-term processes such as faunal evolution and migration are included in paleoecological studies, despite the general lack of genetic, physiological, and behavioural data available to modern ecologists (Sheehan 1975). The only exceptions in paleoecological investigations are: 1) trace fossils which tend to be common and well-preserved and can shed some light on ancient behaviours, and 2) exceptional soft tissue preservation, which can yield

information on the physiology of fossil organisms. Recent advances in the field of marine paleoecology have contributed greatly to our understanding of ancient ecosystems due to abundant shelly fossils, particularly brachiopods, found worldwide and spanning a long geological history, with Silurian paleoecological study as a good example (e.g. Ziegler 1965; Ziegler et al. 1968; Sheehan 1973, 1985; Cocks and McKerrow 1984; Brett et al. 1993; Watkins 2000; Jin 2008). In the following sections, the recovery phase of early Silurian reef-dwelling brachiopods is discussed alongside the paleoecological interpretations of the brachiopod community associations in the Attawapiskat Formation. The environmental and ecological factors that controlled the organization and distribution of these brachiopod communities will also be explored.

4.4.1 Silurian Reef Recovery Phase

As shown in Figure 4.1, reef-dwelling brachiopod diversity declined dramatically at the end of the Ordovician and did not begin to recover until Aeronian time. During the Telychian, reef diversity increased rapidly and reached a post-extinction peak in the Wenlock. This may have been related, at least partly, to the unstable marine environments (fluctuating sea level and climatic conditions) in the earliest Silurian which improved over the Llandovery (Harper et al. 2014). Interestingly, there were both paleolatitudinal and temporal differences in reefal diversity patterns. Reef-dwelling brachiopods first appeared on the southern margin of Laurentia in the high tropical zone of Anticosti Island during the Aeronian but only achieved modest diversity levels. When reefs reached the paleoequatorially located Hudson Bay Basin (Attawapiskat Formation), there was an increase in the reef-dwelling brachiopod diversity, whereas the

contemporaneous Chicotte Formation on Anticosti Island had a notably lower brachiopod diversity level. By the Wenlock, however, high diversity reefal communities extended beyond the equatorial zone to the mid tropical zone as seen in the Racine Formation of the Michigan Basin of Laurentia, and the Högklint, Slite, and Klinteberg formations of Gotland, Baltica (Samtleben et al. 1996).

Several researchers have shown that many of the early Silurian brachiopods found in Laurentia are immigrants from Baltica (Sheehan 1973; Cocks and McKerrow 1973; McKerrow and Cocks 1976; Jin 2002b). During the latest Ordovician and early Silurian, the Iapetus Ocean separating Laurentia from Baltica was quickly closing. This seaway, which had at one time provided an ample barrier between marine faunas, was now narrow enough to allow the pelagic larvae of benthic organisms to invade across continents (McKerrow and Cocks 1976). The lack of exposed land separating the intracratonic basins of Laurentia would have allowed for the invading organisms from Baltica to quickly spread throughout Laurentia, creating the large-scale zoogeographical provinces described by Sheehan (1975). Furthermore, Watkins et al. (2000), based on the work of Brett and Baird (1995), have shown that the sudden appearance of new communities was more likely a result of inter-basinal invasion than the evolution of an entirely new community.

Following the extinction of the highly endemic Laurentian Ordovician faunas, the early Silurian epicontinental seas over Laurentia would have largely been an ecological vacuum and facilitated invasion from the Baltican level-bottom faunas. During the Aeronian, climatic amelioration and recovery of the corals-stromatoporoid reefs provided new habitats or niches for level-bottom brachiopod faunas to invade. Watkins (1998)

suggested that even by Wenlock times the reef-dwelling brachiopods had not fully integrated into the reef setting and retained distinct level-bottom characteristics. This serves as an evolutionary clue that these earliest reef-dwelling forms invaded the reefs from level-bottom environments. Once reefs and their associated brachiopod faunas had reached the equatorial zone in the Hudson Bay and Moose River basins in the middle–late Telychian they quickly diversified, likely due to the generally stable environment of the equatorial zone (Jin et al. 2013), before radiating into the mid- and higher tropics during the Wenlock.

4.4.2 Paleoecological Implications of the Brachiopod Associations

Jin (2002a) originally used ClustanGraphics, a clustering software produced in 1997, to organize the Attawapiskat Formation brachiopods into eight community associations: the *Lissatrypa* Association, the *Septatrypa* Association, the *Septatrypa–Pentameroides* Association, the *Gypidula* Association, the *Gotatrypa* Association, the *Trimerella* Association, the *Eocoelia* Association, and the *Pentameroides* Association. These associations correlate directly to the majority of the associations described in this study, with the exceptions of the *Eomegastrophia* and *Whitfieldella* associations which are only recognized in this study.

Collection AK9-01a, which is shown to belong to the *Pentameroides–Septatrypa* association in this study, was grouped in the *Septatrypa* Association in Jin (2002a). In addition, collections AK2b and AK7-01c of the *Whitfieldella* Association were assigned to the *Septatrypa–Pentameroides* Association, and AK7-01b and AK8-01c of the

Septatrypa Association in this study were in the *Septatrypa–Pentameroides* Association

of Jin (2002a). The *Eomegastrophia* Association is represented by a single collection,

AK8-01d, which was not included in the study of Jin (2002a) because it is an outlier and

likely does not reflect an actual community assemblage. The occurrence of the

Whitfieldella Association, which does not occur in Jin's (2002a) study is likely due to the

improved clustering resolution of the PAST software package. In addition, collections

AK3b, AK4a, and AK8-01d were not included in the 2002 study and their inclusion in

this work likely altered of grouping of other collections.

In terms of their composition and diversity levels, the 10 Attawapiskat Formation

associations recognized in this study can be divided into two major types, the level-

bottom type and the cryptic type. The level-bottom type associations are dominated by

large-sized shells and typically low diversity levels, represented by the *Pentameroides*,

Pentameroides–Septatrypa, *Eocoelia*, and *Trimerella* associations. The collections for

these associations are mostly from reef flank and inter-reef areas in the Attawapiskat

Formation, where open or relatively flat spaces allowed these shells to grow into fairly

densely packed shell pavement (Fig. 4.14). Perhaps the most characteristic species of this

ecological grouping is *Pentameroides septentrionalis*, which is common or dominant in

the constituent associations (except for the monotypic *Eocoelia* association) and

dominates the living space within each of these associations. *Pentameroides*

septentrionalis was capable of forming dense patches of shells on the open substrate

within a reef (Fig. 4.14 C), scattered shells living among the corals and stromatoporoids

(Fig. 4.14 A), or crowded shell beds in relative flat, inter-reef substrate.
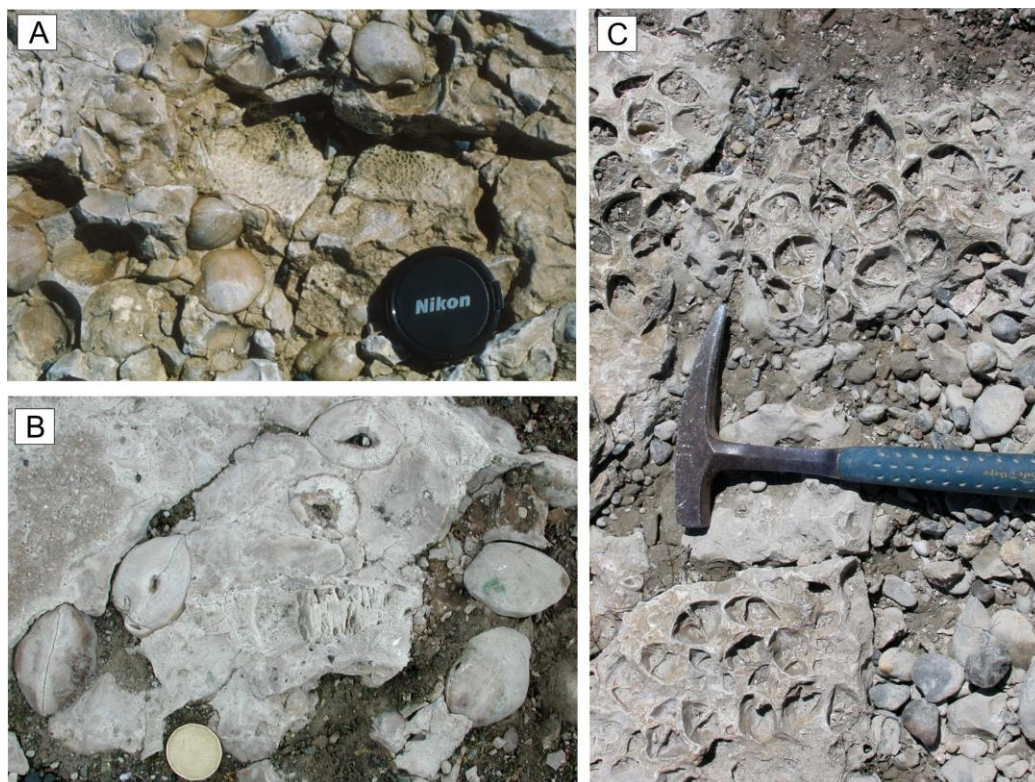
Figure 4.14: Occcurrences of level-bottom type brachiopod associations in the Attawapiskat Formation. A) *Pentameroides* living among corals, locality AK4; B) Free-lying *Pentameroides*, locality AK8. C) *Pentameroides* shell patch, along the Severn River, northern Ontario. Lens cap is 6.5 cm in diameter, coin is 2.5 cm in diameter, hammer blade length is 18 cm.

The cryptic-type brachiopod associations are characterized by the dominance of small-shelled species with typically higher diversity levels, such as the *Lissatrypa*, *Gotatrypa*, *Gypidula*, and *Whitfieldella* associations. Collections of these associations were usually made from small "pockets" among corals, stromatoporoids, and demosponges within a reef. The term 'cryptic' is used here to refer to small cavities or depressions in the reef framework, where the small shells would have lived in a protected environment (Fig. 4.15). Alternatively, it is possible that these depressions and cavities within the reefs acted as accumulation spots for dead shells as a result of gentle wave and current action because the delicate shells are usually very well preserved. The *Septatrypa* Association shows some transitional characteristics between the level-bottom and the cryptic types, since it shows a high level of abundance and diversity, but common occurrence of both large 'level-bottom-type' and small 'cryptic' species.

It is important to note that the dominant species of the level-bottom type associations did not have a functioning pedicle in later ontogeny to attach the shells to the substrate and needed to live on relatively flat substrates to maintain an umbo-down life position through tight crowding to support one another (Ziegler et al. 1966), as is typical of *Pentameroides* and other large pentameride shells (Jin 2008). The small shells of the cryptic associations, however, mostly have an open delthyrium for the pedicle muscle and would have been able to attach to the walls or ceilings of these cavities. Despite this, large shelled brachiopods were able to invade these cavities, although only in small numbers. The interpretation of cryptic associations is corroborated by the striking contrast between a high abundance value and a small living space required by the dominant species of these associations, as discussed above under shell volume
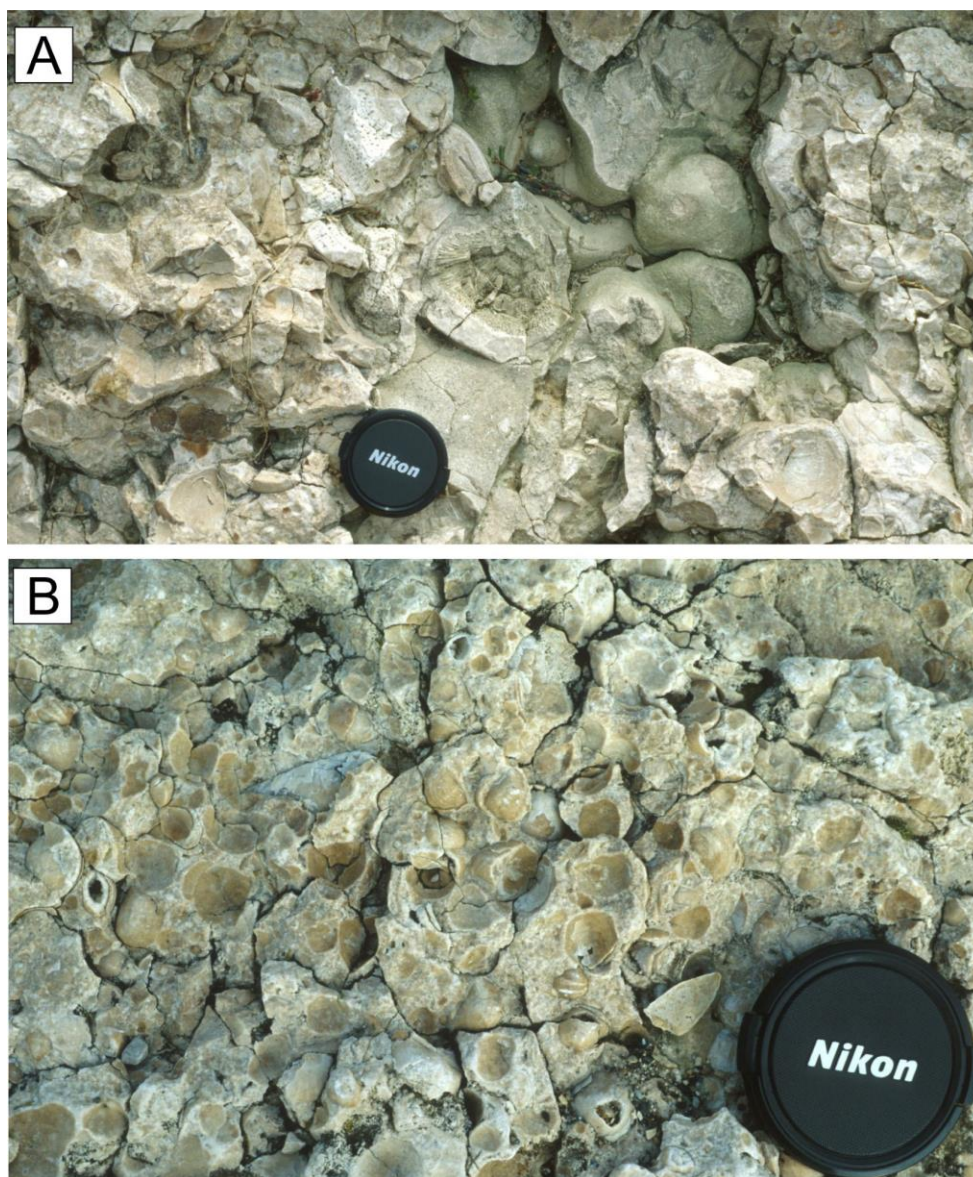
Figure 4.15: Examples from the cryptic type. A) Example of a reef cavity, locality AK2; B) *Gypidula* shells and shell impressions, locality AK2. Lens cap is 6.5 cm in diameter.

estimation. These associations also tend to lack, or have rare, large-sized shells more typical of the 'level-bottom' like associations such as *Pentameroides septentrionalis*. This clearly shows the importance of large, smooth-shelled pentameride brachiopods over smaller, ribbed, or spine bearing brachiopods in the reef environment of this time. In general, the cryptic brachiopod associations are dominated by smooth shells, with strongly costate shells being either absent or rare.

4.4.3 Spatial Distribution of Brachiopod Benthic Assemblages (BAs) in the Attawapiskat Reefs

As shown in this study and by Jin (2003, 2005), the dominant components of BA 2 (*Eocoelia*), BA 3 (*Pentameroides*), and BA 5 (*Clorinda* and *Gypidula*) are found in close proximity to one another while the dominant BA 4 component (*Stricklandia*) is entirely absent in the Attawapiskat Formation. This irregular spatial distribution pattern differs significantly from the approximately parallel zones of brachiopod communities in level-bottom environments (Ziegler 1965; Boucot 1975). The controlling factors for the different shell community or BA distributions remain a subject of continued study. Reasons for the mixing of key taxa from adjacent benthic assemblages is likely a combination of water temperature and storm severity. In their description of the early Silurian benthic community zones of the Welsh borderlands, Ziegler et al. (1968) already noted some degree of mixing of typical taxa between adjacent brachiopod community zones, but they were still able to delineate broad community zonation parallel to the early Silurian shoreline. The *Eocoelia* and *Pentameroides* communities usually occur adjacent to each other in level-bottom environments and, therefore, their presence in close

proximity to each other in the Attawapiskat reefal settings bears some similarity to their level-bottom counterparts. However, the occurrence of abundant *Clorinda* and *Gypidula* shells in the apparently shallow-water Attawapiskat reefal settings cannot be explained readily by classic brachiopod community or BA models.

In typical level-bottom environments, the BA 5 community is diverse with many species of small-shelled brachiopods dominated by *Clorinda* or *Gypidula* (depending on the stratigraphic levels) with common *Leptaena*, *Dicoelosia*, *Coolinia*, and others with a low population density in a quiet outer shelf setting (Cocks and McKerrow 1984; Brett et al. 1993; Watkins et al. 2000). The BA 3 and BA 4 communities, however, are composed of lower diversity, large-shelled pentameride and strophomenide brachiopods in storm-dominated depositional environments. Jin (2008) has shown that *Pentamerus* from BA 3 will invade the deeper waters of BA 4 when the dominant stricklandiids periodically become absent in the carbonate level-bottom Jupiter Formation of Anticosti Island. Based on the stratigraphic successions of pentameride communities in the Meniér and Jupiter formations (mid Aeronian to mid Telychian), Jin (2008) suggested that the *Pentamerus* community could replace the *Stricklandia* community during periods of oceanic warming, or vice versa during episodes of cooling. Global oxygen isotopic data from Azmy et al. (2006) confirms this hypothesis as periods of *Pentamerus* dominance coincide with warming periods while cooler climates correspond to stricklandiid dominance in the BA3–4 depths of Anticosti Island. The lack of *Stricklandia* in the Attawapiskat Formation, therefore, could be due to the warmer water mass in the paleoequatorial epicontinental seas. Rong et al. (2005) have shown that stricklandiids were rare in the paleoequatorial region during the Llandovery, which agrees with the

absence of *Stricklandia* from the Attawapiskat Formation. Therefore, it seems reasonable to interpret that the cool-water *Stricklandia* did not succeed in invading the paleoequtorial warmer waters of the Hudson Bay and Moose River basins.

The warm water environment of the Attawapiskat reef environment is further supported by the abundant and large, well-preserved aragonitic brachiopod shells of *Trimerella*. Aragonitic shells are chemically less stable than calcitic shells and tend to go through recrystallization and dissolution during diagenesis in relatively cool-water carbonate depositional environments. In the paleoequatorial setting, the water temperature is both stable and high, and remains supersaturated with respect to $CaCO_3$ precipitation. Thus the shells were much less likely to go through recrystallization or dissolution, resulting in the unusual excellent preservation of shell composition and texture, including some residual aragonite shell layers in the *Trimerella* shells. *Trimerella* from the Attawapiskat Formation has the oldest record of preserved aragonite after more than 400 million years of burial (Balthasar et al. 2011).

Clorinda and *Gypidula*, however, typically inhabit an even deeper and colder level-bottom environment than *Stricklandia*, but are found in abundance in the warm shallow water of the Attawapiskat reefs. Compared to the large adult shells of *Pentamerus*, *Pentameroides,* and *Stricklandia*, the shells of *Clorinda* and *Gypidula* are much smaller, although they are still generally larger than other biconvex brachiopod shells of the Attawapiskat Formation. It was likely that the small shell size that constrained these species to the deep shelf environments of the BA 5 zone as the small shells would be smothered by mud deposits during storm events. The large sizes of *Pentamerus*, *Pentameroides,* and *Stricklandia*, however, allowed these species to inhabit

the storm zone without being smothered in the storm dominated BA 3 and BA 4 zones (Cocks and McKerrow 1984). It has been shown that, similar to the equatorial regions today, the paleoequatorial zone did not experience hurricane-grade storms during the Ordovician and Silurian (Jin et al. 2013) and therefore would allow the small shells of the BA 5 community to inhabit the shallow waters of this region without being smothered by muddy sediments mobilized by frequent and severe storms. This interpretation also explains why *Pentamerus*, and not *Clorinda*, moves into the BA 4 zone during periods of oceanic warming in the storm-dominated, higher tropical depositional environments. Therefore, successful invasion of the *Clorinda* and *Gypidula* associations into the Attawapiskat reefal environment from their deep water origin has been closely related to the lack of hurricane-grade storms in the early Silurian equatorial zone. In addition, the protections of skeletal reefs provided further low-energy substrates that would be similar to the quiet water deep shelf environments originally occupied by these groups.

4.5 Conclusions

In this study, diversity and community analyses were carried out based on 14,304 reef-dwelling brachiopod shells from the Ellis Bay, Meniér, and Chicotte formations of Anticosti Island, Quebec; the Attawapiskat Formation, Akimiski Island, James Bay, Nunavut; the Högklint Formation, Gotland, Sweden; and the Racine Formation, Wisconsin, as well as 2813 level-bottom-dwelling brachiopods from the Fossil Hill Formation, Manitoulin Island, Ontario. The following conclusions can be drawn from their paleoenvironmental and paleoecological investigations.

1. Early Silurian reef-dwelling brachiopods were likely to have descended from level-bottom dwellers that invaded Laurentian intracratonic seas from Baltica in the earliest Silurian by crossing the narrow Iapetus seaway.

2. In Laurentia, Silurian-type reefs first recovered in the high tropical region during the mid-Aeronian before dispersing into the equatorial zone in the Telychian. By this time the equatorial reefs had increased dramatically in brachiopod diversity due to a stable equatorial environment. Reef-dwelling brachiopods radiated in diversity and expanded paleogeographically from the equator during the Wenlock.

3. The reef-dwelling brachiopods from 32 collections in the Attawapiskat Formation can be divided into 10 community associations, which can be further grouped into the level-bottom type or the cryptic type depending on their dominant brachiopod species, average shell size, and diversity levels. The level-bottom-type associations are dominated by large-shelled species with low diversity in inter-reef and reef flank facies, whereas the cryptic associations have a high species diversity, dominated by small-shelled brachiopods that lived in cavities or depressions within the reef.

4. In terms of living space requirement, the large-shelled *Pentameroides septentrionalis* dominated in the level-bottom type associations due to its typically high abundance and strongly biconvex shell shape. The successful invasion of the *Pentameroides* Association into the reef environment was also reflected in its ability to live as dense shell patches in open spaces within the reef, in tight spaces among the reef frame-building corals and stromatoporoids, and on flat substrate in inter-reef areas.

5. The close spatial relationships among the *Eocoelia, Pentameroides*, and *Clorinda*/*Gypidula* associations in the Attawapiskat Formation were controlled by the lack of hurricane-grade storms in the paleoequatorially positioned Hudson Bay Basin. This enabled the large but delicately thin shells of *Pentameroides* to live in the shallow-water reef environment, and small-shelled *Clorinda* and *Gypidula*, which originated in the deep shelf (BA5) settings, to find their favoured quiet water substrate without the hazard of mud smothering. The excellent preservation of the *Trimerella* Association dominated by large aragonitic shells, and the absence of the cool-water *Stricklandia* community, are interpreted as the result of the predominance of warm water mass in the paleoequatorially located Hudson Bay Basin.

References

Antoshkina, A.I. 1998. Organic buildups and reefs on the Palaeozoic carbonate platform

    margin, Pechora Urals, Russia. *Sedimentary Geology*, 118(1): 187–211.

Antoshkina, A.I., and Soja, C.M. 2006. Late Silurian reconstruction indicated by

    migration of reef biota between Alaska, Baltica (Urals), and Siberia

    (Salair). GFF, 128(2): 75–78.

Azmy, K., Veizer, J., Jin, J., Copper, P., and Brand, U. 2006. Paleobathymetry of a

    Silurian shelf based on brachiopod assemblages: an oxygen isotope test. Canadian

    Journal of Earth Sciences, 43(3): 281–293.

Baarli, B.G. 1988. Bathymetric co-ordination of proximality trends and level-bottom

    communities: A case study from the Lower Silurian of Norway. Palaios, 3(6): 577–

    587.

Baarli, B.G. and Harper, D.A.T. 1986: Relict Ordovician brachiopod faunas in the Lower

    Silurian of Asker, Oslo Region, Norway. Norsk Geologisk Tidsskrift, 66: 87–98.

Balthasar, U., Cusack, M., Faryma, L., Chung, P., Holmer, L.E., Jin, J., Percival, I.G. and

    Popov, L.E. 2011. Relic aragonite from Ordovician–Silurian Brachiopods –

    implications for the evolution of calcification. Geology, 39: 967–970.

Bergström, S.M., Kleffner, M., Schmitz, B., and Cramer, B.D. 2011. Revision of the

    position of the Ordovician–Silurian boundary in southern Ontario: regional

    chronostratigraphic implications of δ13C chemostratigraphy of the Manitoulin

    Formation and associated strata. Canadian Journal of Earth Sciences, 48(11):

    1447–1470.

Boucot, A.J. 1975. Evolution and extinction rate controls. Elsevier, New York.

Boucot, A.J., and Lawson, J.D. 1999. Paleocommunities: a case study from the Silurian
and Lower Devonian. Cambridge University Press, London. 895 pp.

Brenchley, P.J., and Harper, D.A.T 1998. Palaeoecology: Ecosystems, environments and
evolution. Chapman and Hall, London, UK.

Brett, C.E., and Baird, G.C. 1995. Coordinated stasis and evolutionary ecology of
Silurian to Middle Devonian faunas in the Appalachian Basin. *In* New approaches
to speciation in the fossil record. Columbia University Press, New York. Edited by
Erwin, D.H., and Antsey, R.L. p. 285–315.

Brett, C.E., Boucot, A.J., and Jones, B. 1993. Absolute depths of Silurian benthic
assemblages. Lethaia, 26(1): 25–40.

Brunton, F.R., and Copper, P. 1994. Paleoecologic, temporal, and spatial analysis of early
Silurian reefs of the Chicotte Formation, Anticosti Island, Quebec,
Canada. Facies, 31: 57–79.

Chow, A.M., and Stearn, C.W. 1988. Attawapiskat patch reefs, Lower Silurian, Hudson
Bay Lowlands, Ontario. Canadian Society of Petroleum Geologists Memoir, 13:
273–270.

Cocks, L.R.M., and McKerrow, W.S. 1973. Brachiopod distributions and faunal
provinces in the Silurian and Lower Devonian. Organisms and continents through
time. Special Paper in Palaeontology, 12: 201–304.

Cocks, L.R.M., and McKerrow, W.S. 1984. Review of the distribution of the commoner
animals in Lower Silurian marine benthic communities. Palaeontology, 27(4):
663–670.

Cocks, L.R.M., and Rong, J. 2007. Earliest Silurian faunal survival and recovery after the end Ordovician glaciation: evidence from the brachiopods. Earth and Environmental Science Transactions of the Royal Society of Edinburgh, 98: 291–301.

Copper, P. 1994. Ancient reef ecosystem expansion and collapse. Coral reefs, 13: 3–11.

Copper, P. 2002. Silurian and Devonian reefs: 80 million years of global greenhouse between two ice ages. *In* Phanerozoic Reef Patterns, SEPM Special Publication No. 72. *Edited by* Kiessling, W., Flugel, E., and Golonka, J. p. 181–238.

Copper, P., and Brunton, F.R. 1991. A global review of Silurian reefs. Special Papers in Palaeontology, 44: 225–259.

Copper, P., and Jin, J. 2012. Early Silurian (Aeronian) East Point coral patch reefs of Anticosti Island, Eastern Canada: first reef recovery from the Ordovician/Silurian mass extinction in eastern Laurentia. Geosciences, 2: 64–89.

Ernst, A., Munnecke, A., and Oswald, I. 2015. Exceptional bryozoan assemblage of a microbial-dominated reef from the early Wenlock of Gotland, Sweden. GFF, 137(2): 102–125.

Hammer, Ø., and Harper, D.A.T. 2006. Paleontological Data Analysis. Blackwell Publishing, Malden, Massachusetts.

Hammer, Ø., Harper, D.A.T., Ryan, P. 2001. PAST: Paleontological statistics software package for education and data analysis. Palaeontologia Electronica 4(1).

Hancock, N.J., Hurst, J.M., and Fürsich, F.T. 1974. The depths inhabited by Silurian brachiopod communities. Journal of the Geological Society, 130(2): 151–156.

Harper, D.A., Hammarlund, E.U., and Rasmussen, C.M.Ø. 2014. End Ordovician extinctions: a coincidence of causes. Gondwana Research, 25: 1294–1307.

Jin, J. 2002a. Niche partitioning of reef-dwelling brachiopod communities in the Lower Silurian Attawapiskat Formation, Hudson Bay Basin, Canada. IPC 2002, Geological Society of Australia, Abstracts No. 68: 83–84.

Jin, J. 2002b. The Early Silurian pentamerid brachiopod *Costistricklandia canadensis* (Billings, 1859) and its biostratigraphic and paleobiogeographic significance. Journal of Paleontology, 76(4): 638–647.

Jin. J. 2003. The Early Silurian Brachiopod *Eocoelia* from the Hudson Bay Basin, Canada. Palaeontology, 46: 885–902.

Jin, J. 2005. Reef-dwelling gypiduloid brachiopods in the Lower Silurian Attawapiskat Formation, Hudson Bay region. Journal of Paleontology, 79(1): 48–62.

Jin, J. 2008. Environmental control on temporal and spatial differentiation of Early Silurian pentameride brachiopod communities, Anticosti Island, eastern Canada. Canadian Journal of Earth Sciences, 45: 159–187.

Jin, J., and Chatterton, B.D.E. 1997. Latest Ordovician-Silurian articulate brachiopods and biostratigraphy of the Avalanche Lake area, southwestern District of Mackenzie. Palaeontographica Canadiana, 13: 1–167.

Jin, J., and Copper, P. 2000. Late Ordovician and Early Silurian pentamerid brachiopods from Anticosti Island, Québec, Canada. Palaeontographica Canadiana, 18: 1–140.

Jin, J., and Copper, P. 2008. Response of brachiopod communities to environmental change during the Late Ordovician mass extinction interval, Anticosti Island, eastern Canada. Fossils and Strata, 54: 41–51.

Jin, J., Caldwell, W.G.E., and Norford, B.S. 1993. Early Silurian brachiopods and biostratigraphy of the Hudson Bay lowlands, Manitoba, Ontario, and Quebec. Geological Survey of Canada, 457.

Jin, J., Copper, P., and Renbin, Z. 2007. Species-level response of tropical brachiopods to environmental crises during the Late Ordovician mass extinction. Acta Palaeontologica Sinica, 46: 194–200.

Jin, J., Harper, D.A., and Rasmussen, C.M.Ø. 2009. *Sulcipentamerus* (Pentamerida, Brachiopoda) from the Lower Silurian Washington Land Group, North Greenland. Palaeontology, 52: 385–399.

Jin, J., Harper, D.A.T., Cocks, L.R.M., McCausland, P.J.A., Rasmussen, C.M.Ø., and Sheehan, P.M. 2013. Precisely locating the Ordovician equator in Laurentia. Geology, 41: 107–110.

Johnson, M.E. 1987. Extent and bathymetry of North American platform seas in the Early Silurian. Paleoceanography, 2: 185–211.

Johnson, M.E. 1989. Tempestites recorded as variable *Pentamerus* layers in the Lower Silurian of southern Norway. Journal of Paleontology, 63: 195–205.

Johnson, M.E. 1997. Silurian event horizons related to the evolution and ecology of pentamerid brachiopods. *In* Paleontological events, stratigraphic, ecological, and evolutionary implications. *Edited by* Brett, C.E., and Baird, G.C. p. 162–180.

Johnson, M.E. 2006. Relationship of Silurian sea-level fluctuations to oceanic episodes and events. GFF, 128: 115–121.

Johnson, M.E. and Colville, V.R. 1982. Regional integration of evidence for evolution in the Silurian *Pentamerus–Pentameroides* lineage. Lethaia, 15: 41–54.

Johnson, M.E., Baarli, B.G., Nestor, H., Rubel, M., and Worsley, D. 1991. Eustatic sea-level patterns from the Lower Silurian (Llandovery Series) of southern Norway and Estonia. Geological Society of America Bulletin, 103(3): 315–335.

Kershaw, S. 1993. Sedimentation control on growth of stromatoporoid reefs in the Silurian of Gotland, Sweden. Journal of the Geological Society, 150(1): 197–205.

Krebs, C.J. 1989. Ecological Methadology. Harper & Row, New York.

Li, Y. 2004. Late Ordovician to Early Silurian reef evolution in south China. In Mass Extinction and Recovery-Evidences from the Palaeozoic and Triassic of South China. *Edited by* Rong, J., and Fang, Z. p. 97–126.

McKerrow, W.S., and Cocks, L.R.M. 1976. Progressive faunal migration across the Iapetus Ocean. Nature, 263: 304–306.

Nield, E.W. 1982. The earliest Gotland reefs: two bioherms from the Lower Visby Beds (upper Llandovery). Palaeogeography, Palaeoclimatology, Palaeoecology, 39: 149–164.

Rong, J., and Harper, D.A. 1999. Brachiopod survival and recovery from the latest Ordovician mass extinctions in South China. Geological Journal, 34(4): 321–348.

Rong, J., and Zhan, R. 2006. Surviving the end-Ordovician extinctions: evidence from the earliest Silurian brachiopods of northeastern Jiangxi and western Zhejiang provinces, east China. Lethaia, 39(1): 39–48.

Rong, J., and Cocks, L.R.M. 2014. Global diversity and endemism in Early Silurian (Aeronian) brachiopods. Lethaia, 47(1): 77–106.

Rong, J., Johnson, M.E., and Yang, X. 1984. Early Silurian (Llandovery) sea-level changes in the Upper Yangtze region of central and southwestern China. Acta Palaeontologica Sinica, 23: 687–697.

Rong, J., Zhan, R., and Jin, J. 2004. The Late Ordovician and Early Silurian pentameride brachiopod *Holorhynchus* Kiaer, 1902 from North China. Journal of Paleontology, 78(02): 287–299.

Rong, J., Jin, J., and Zhan, R. 2005. Two new genera of early Silurian stricklandioid brachiopods from South China and their bearing on stricklandioid classification and paleobiogeography. Journal of Paleontology, 79(6): 1143–1156.

Rong, J., Jin, J., and Zhan, R. 2007. Early Silurian *Sulcipentamerus* and related pentamerid brachiopods from South China. Palaeontology, 50(1): 245–266.

Samtleben, C., Munnecke, A., Bickert, T., and Pätzold, J. 1996. The Silurian of Gotland (Sweden): facies interpretation based on stable isotopes in brachiopod shells. Geologische Rundschau, 85(2): 278–292.

Sapelnikov, V.P. 1961. Venlokskie *Pentameroides* srednego Urala. Paleontologicheskii
Zhurnal, 1: 102–107.

Sapelnikov, V.P. 1985. Sistema i stratigraficheskoe znachenie brakhiopod podotryada
pentameridin. Akademiya Nauk SSSR, Uralskyi Nauchnyi Tsentr, Nauka,
Moskva. 206 p.

Sapelnikov, V.P., Bogoyavlenskaya, O.V., Mizesn, L.I., and Shuysky,
V.P. 1999. Silurian and Early Dvonian benthic communities of the Ural–Tien-
Shan region, *In* Paleocommunities – A Case Study from the Silurian and Lower
Devonian. Cambridge University Press. *Edited by* Boucot, A.J., and Lawson, J.D.
Boucot, and J. D. p. 510–544.

Shannon, C.E., and Weaver, W. 1949. The Mathematical Theory of Communication.
University of Illinois Press, Urbana, IL.

Sheehan, P.M. 1973. The relation of Late Ordovician glaciation to the Ordovician–
Silurian changeover in North American brachiopod faunas. Lethaia, 6(2): 147–154.

Sheehan, P.M. 1975. Brachiopod synecology in a time of crisis (Late Ordovician-Early
Silurian). Paleobiology, 1: 205–212.

Sheehan, P.M. 1985. Reefs are not so different—they follow the evolutionary pattern of
level-bottom communities. Geology, 13(1): 46–49.

Sheehan, P.M., and Coorough, P.J. 1990. Brachiopod zoogeography across the
Ordovician-Silurian extinction event. Geological Society, London, Memoirs, 12(1):
181–187.

Simpson, E.H. 1949. Measurement of diversity. Nature, 163: 688.

Soja, C.M., and Antoshkina, A.I. 1997. Coeval development of Silurian stromatolite reefs
    in Alaska and the Ural Mountains: Implications for paleogeography of the
    Alexander terrane. Geology, 25(6): 539–542.

Soja, C.M., White, B., Antoshkina, A., Joyce, S., Mayhew, L., Flynn, B., and Gleason, A.
    2000. Development and decline of a Silurian stromatolite reef complex, Glacier
    Bay National Park, Alaska. Palaios, 15(4): 273–292.

Suchy, D.R., and Stearn, C.W. 1993. Lower Silurian reefs and post-reef beds of the
    Attawapiskat Formation, Hudson Bay Platform, northern Ontario. Canadian
    Journal of Earth Sciences, 30: 575-590.

Tuuling, I., and Flodén, T. 2013. Silurian reefs off Saaremaa and their extension towards
    Gotland, central Baltic Sea. Geological Magazine, 150(05): 923–936.

Wang, G., Li, Y., Kershaw, S., and Deng, X. 2014. Global reef recovery from the end-
    Ordovician extinction: evidence from late Aeronian coral–stromatoporoid reefs in
    South China. GFF, 136: 286–289.

Watkins, R. 1991. Guild structure and tiering in a high-diversity Silurian community,
    Milwaukee County, Wisconsin. Palaios, 6: 465-478.

Watkins, R., 1998. Silurian reef-dwelling pentamerid brachiopods, Wisconsin and
    Illinois, USA. Palaontologische Zeitschrift, 72: 99–109.

Watkins, R. 2000. Silurian reef-dwelling brachiopods and their ecologic implications.
    Palaios, 15(2): 112-119.

Watkins, R., Coorough, P.J., and Mayer, P.S. 2000. The Silurian *Dicoelosia* communities: temporal stability within an ecologic evolutionary unit. Palaeogeography, Palaeoclimatology, Palaeoecology, 162(3): 225–237.

Yue, L., and Kershaw, S. 2003. Reef reconstruction after extinction events of the latest Ordovician in the Yangtze platform, South China. Facies, 48(1): 269–284.

Yue, L., Kershaw, S., and Xu, C. 2002. Biotic structure and morphology of patch reefs from South China (Ningqiang Formation, Telychian, Llandovery, Silurian). Facies, 46(1): 133–148.

Zhan, R., Jin, J., and Rong, J. 2006. β-diversity fluctuations in Early–Mid Ordovician brachiopod communities of South China. Geological Journal, 41: 271–288.

Ziegler, A.M. 1965. Silurian marine communities and their environmental significance. Nature, 207: 270–272.

Ziegler, A.M., Boucot, A.J., and Sheldon, R.P. 1966. Silurian pentamerid brachiopods preserved in position of growth. Journal of Paleontology, 40: 1032–1036.

Ziegler, A.M., Cocks, L.R.M., and Bambach, R.K. 1968. The composition and structure of lower Silurian marine communities. Lethaia, 1: 1–27.

Chapter 5 – Summary and Conclusions

5.1 Summary

This thesis examined various aspects of the paleoecology of reef-dwelling brachiopods and their communities during the early Silurian in Laurentia. The study was conducted in five steps: 1) a review of early Silurian paleogeography, climate, oceanic conditions, and marine faunas with an emphasis on pentameride brachiopods; 2) description of the coral-stromatoporoid reef and brachiopod-bearing formations related to this thesis; 3) biometric analysis of the reef-dwelling brachiopod *Pentameroides septentrionalis* from the Attawapiskat Formation, with comparisons to its contemporaneous level-bottom relative *Pentameroides subrectus*; 4) calculation of Shannon index diversity levels of reef-dwelling brachiopod faunas ranging from Hirnantian–Homerian of Laurentia and Baltica; and 5) multivariate analyses of the reef-dwelling brachiopod fauna from the Attawapiskat Formation, based on 9009 specimens from 32 collections, to determine community organization.

Following the Late Ordovician mass extinctions, the earliest Llandovery experienced fluctuating sea-levels and ocean temperatures, and increasing levels of faunal cosmopolitanism (Sheehan and Coorough 1990; Sheehan 2001; Haq and Schutter 2008; Finnegan et al. 2011; Harper et al. 2014). During this recovery phase, pentameride brachiopods became the dominant components of level-bottom carbonate and some siliciclastic depositional environments in Laurentia, Baltica, Avalonia, Siberia, and China (Sapelnikov 1961, 1985; Ziegler 1965; Ziegler et al. 1968; Baarli 1988; Jin et al. 1993;

Johnson 1997; Watkins 1998; 2000; Jin and Copper 2000; Rong et al. 2005, 2007; Jin 2008). Throughout the Llandovery, climatic and oceanic conditions ameliorated and by the mid-Aeronian coral-stromatoporoid patch reefs began appearing in the high tropical zones of Laurentia and China (Copper 2002; Copper and Jin 2012, 2015; Wang et al. 2014). By late Telychian time, these reefs had spread to the equatorial region, formed large barrier and fringing reef complexes, and were invaded by highly abundant and diverse pentameride brachiopod dominated faunas for the first time in Earth history.

Six coral-stromatoporoid reef-bearing formations and two level-bottom carbonate formations containing abundant brachiopod faunas were investigated in this thesis. The primary study site is the middle–late Telychian Attawapiskat Formation of the Hudson Bay and Moose River basins. This formation contains the earliest known occurrence of rich and diverse brachiopod-dominated faunas invading a coral-stromatoporoid reef environment (Chow and Stearn 1988; Jin et al. 1993). Additional reef-bearing formations in this thesis are the Hirnantian Ellis Bay, Aeronian Meniér, and Telychian Chicotte formations, Anticosti Island, Quebec; the Sheinwoodian Högklint Formation, Gotland, Sweden; and the Homerian Racine Formation, Wisconsin. The level-bottom Telychian Fossil Hill Formation, Manitoulin Island, Ontario and Telychian Jupiter Formation, Anticosti Island, Quebec were included to serve as comparisons with contemporaneous reef-dwelling brachiopods and communities.

Paleolatitude is an important factor in the evolution and community organization of the reef-dwelling brachiopods considered in this study. The Anticosti Basin was located in the high tropical zone ~25° south of the early Silurian equator and was subjected to frequently hurricane-grade storm activity (Long 2007; Torsvik and Cocks

2013). The Fossil Hill and Racine formations were situated in the mid-tropics, approximately 15–20° south, but still within the hurricane belt. The Attawapiskat and Högklint formations, however, were located from 0–10° south and did not experience frequent hurricane-grade storms (Jin et al. 2013; Torsvik and Cocks 2013).

The reef-dwelling *Pentameroides septentrionalis* is ideal for biometric analysis as several hundred well-preserved specimens, comprising a full ontogenetic morphological series, have been collected from the Attawapiskat Formation, Akimiski Island, James Bay, Nunavut. Well-preserved specimens were analyzed for several outer morphological characteristics and compared to the contemporaneous level-bottom-dwelling *Pentameroides subrectus* from the Fossil Hill and Jupiter formations. Biometric comparisons found that *P. septentrionalis* has larger ventral umbones, is more globose, and is more biconvex than *P. subrectus*, likely due to different latitudes and environments these species inhabited.

The highly ventribiconvex and globose shell of *P. septentrionalis* evolved to contain large lophophores which increased respiratory and feeding efficiency in the low-energy paleoequatorial reef environment where nutrient and oxygen were more stressed than in the storm-dominated higher tropics. In addition, the enlarged ventral umbo caused a transition from a vertical life position seen in *P. subrectus* to the recumbent life position in *P. septentrionalis*. This transition in life position also reflects differing storm intensities in the equatorial and high tropical regions as the vertical orientation of *P. subrectus* was required to shed mud deposited during storm events from the interior of the shell. This trait was lost in *P. septentrionalis* due to the absence or paucity of hurricane-grade storms in the paleoequatorial Hudson Bay and Moose River basins. The

lack of hurricane-grade storms in this region is also shown in the well-preserved juvenile and adult specimens of *P. septentrionalis* while *P. subrectus* often displays deformation, breakage, and infill by storm activity. Due to the similarities between adult specimens of *P. subrectus* and juvenile specimens of *P. septentrionalis* it is likely that the latter evolved from the former as the genus migrated from high tropical level-bottom environments into equatorial reef settings.

Coral-stromatoporoid reef recovery during the early Silurian can be measured by the diversity of their benthic faunas. In this thesis brachiopod faunas from the six reef-bearing formations mentioned above and the level-bottom fauna of the Fossil Hill Formation were analyzed for Shannon diversity indices. The first Silurian-type patch reefs appear in the Aeronian on the high tropical southern continental margin of Laurentia (Copper and Jin 2012) where immigrants from Baltica were invading the impoverished pericratonic and intracratonic seas (Sheehan 1975; McKerrow and Cocks 1976; Jin et al. 2007). Reefs then dispersed from the high tropics and into the equatorial region and became much more diverse than contemporaneous higher tropical reefs by the late Telychian. It was not until the Wenlock that diverse reef systems expanded past the equatorial zone back into higher latitudes.

Cluster and principal components analyses based squared Euclidean distances recognized 10 distinct the reef-dwelling brachiopod associations in the Attawapiskat Formation. These associations; the *Lissatrypa*, *Trimerella*, *Gotatrypa*, *Gypidula*, *Septatrypa*, *Whitfieldella*, *Pentameroides–Septatrypa*, *Eomegastrophia*, *Pentameroides*, and *Eocoelia* associations, are primarily defined by their dominant brachiopod taxa. These associations can be grouped into two larger types based on their living

environment, common taxonomic components, diversity levels, and average shell size.
The level-bottom type is dominated by large, smooth-shelled brachiopods such as
Pentameroides and *Trimerella* which formed densely packed shell patches or beds in the
relatively flat inter-reef and reef flanking areas. These lower-diversity associations are
dominated volumetrically by the large shells of *Pentameroides septentrionalis*, which did
not have a pedicle but relied on an enlarged and thickened ventral umbo to assume a
crowding life strategy and required relatively large space with even substrate. The cryptic
type consists of higher-diversity associations dominated by small shelled brachiopods.
Found within reef cavities and depressions, the small shells of these associations
achieved high abundances, but did not dominate the living space of these environments.
Large-shelled species, particularly *Pentameroides septentrionalis*, which was able to live
both among the reef-building corals and sponges and in tightly packed inter-reef colonies,
utilized a much larger proportion of the living space than the abundant small-shelled
species. This shows the importance of large-shelled brachiopods that expanded from
level-bottom environments to reefal settings by the late Telychian.

The occurrence of *Eocoelia*, *Pentameroides* and *Clorinda*/*Gypidula* in close
proximity with an absence of *Stricklandia* in the Attawapiskat brachiopod fauna shows
that Ziegler's community zones and the Benthic Assemblages (BAs) cannot be applied
directly to this reefal setting (Jin 2003, 2005). It has been suggested that *Stricklandia* was
a cool-water dependent species, which is very rare in the early Silurian equatorial zone
(Rong et al. 2005; Jin 2008). This, coupled with the occurrence of partially aragonitic
Trimerella shells from the Attawapiskat Formation (Balthasar et al. 2011), suggests that
the Hudson Bay and Moose River basins had a water mass too warm for the cool-adapted

Stricklandia lineage. This absence of stricklandiids and the lack of hurricane-grade storms in the equatorial zone allowed the small sized *Clorinda* and *Gypidula* to move into the shallow water reefal setting. These brachiopods are typically restricted to deep shelf environments below storm wave base due to their smother-prone small shells but, as discussed above, this hazard was much reduced in the paleoequatorial zone and provided an opportunity for these small-shelled brachiopods to live in protected areas in the shallower-water reef environments.

5.2 Conclusions

The importance of latitude on the ecology and evolution on Silurian benthic marine organisms has been emphasized in this study as well as in previous work (e.g. Cocks and Fortey 1990; Jin et al. 2014). This study focused on the importance of the presence or absence of hurricane-grade storm events in tropical environments. Based on the autecology and synecology of the brachiopods examined in this study it appears that the early Silurian tropics can be divided into a high tropical hurricane zone and an equatorial hurricane-free zone. The biometric analysis of *Pentameroides* in Chapter 3 has clearly shown the importance of storm frequency on the evolution of benthic marine organisms.

The higher levels of brachiopod diversity in the Attawapiskat reefs compared to contemporaneous higher latitude reefs suggests that the stable environment of the equatorial basins allowed for rapid diversification following the brachiopod invasion of this region. In addition, the abundance and dominance of level-bottom type brachiopods

such as *Pentameroides septentrionalis* in the Attawapiskat Formation shows both the importance of these organisms in the reefal environment and that invasion from higher latitude level-bottom environments contributed greatly to the high brachiopod biodiversity of this region. Furthermore, the lack of hurricane-grade storms in the equatorial belt allowed for the invasion and proliferation of numerous brachiopod species from level-bottom communities, such as the small-shelled *Clorinda* and *Gypidula* from deep outer-shelf environment, and the large, egg-thin shells of *Pentameroides* from mid-shelf setting. These lines of evidence give validity to the Museum hypothesis of tropical biodiversity (Moreau and Bell 2013). It must be noted, however, that the diversity-depleted early Silurian intracratonic seas after the Late Ordovician mass extinction may have had a strong ecological vacuum effect and facilitated invasion and proliferation of organisms from level-bottom pericratonic environments (Sheehan and Coorough 1990; Jin et al. 2014). Therefore it is difficult to make a direct or simplistic comparison between the species richness in the paleoequatorial Attawapiskat reefs with that of other geological periods because the geological settings and evolutionary background vary with regions and geological time. In the case of the early Silurian, it appears that invasion from higher latitudes was the primary contributing factor for the high biodiversity and specimen abundance reef-dwelling benthic shelly organisms in the equatorial Attawapiskat reefs.

References

Baarli, B.G. 1988. Bathymetric co-ordination of proximality trends and level-bottom communities: A case study from the Lower Silurian of Norway. Palaios, 3(6): 577–587.

Balthasar, U., Cusack, M., Faryma, L., Chung, P., Holmer, L.E., Jin, J., Percival, I.G. and Popov, L.E. 2011. Relic aragonite from Ordovician–Silurian Brachiopods – implications for the evolution of calcification. Geology, 39: 967–970.

Chow, A.M., and Stearn, C.W. 1988. Attawapiskat patch reefs, Lower Silurian, Hudson Bay Lowlands, Ontario. Canadian Society of Petroleum Geologists Memoir, 13: 273–270.

Cocks, L.R.M., and Fortey, R.A. 1990. Biogeography of Ordovician and Silurian faunas. Geological Society, London, Memoirs, 12(1): 97–104.

Copper, P. 2002. Silurian and Devonian reefs: 80 million years of global greenhouse between two ice ages. *In* Phanerozoic Reef Patterns, SEPM Special Publication No. 72. *Edited by* Kiessling, W., Flugel, E., and Golonka, J. p. 181–238.

Copper, P., and Jin, J. 2012. Early Silurian (Aeronian) East Point coral patch reefs of Anticosti Island, Eastern Canada: first reef recovery from the Ordovician/Silurian mass extinction in eastern Laurentia. Geosciences, 2: 64–89.

Copper, P. and Jin, J. 2015. Tracking the early Silurian post-extinction faunal recovery in the Jupiter Formation of Anticosti Island, eastern Canada: A stratigraphic revision. Newsletters on Stratigraphy, 48(2): 221–240.

Finnegan, S., Bergmann, K., Eiler, J.M., Jones, D.S., Fike, D.A., Eisenman, I., Hughes, N.C., Tripati, A.K., and Fischer, W.W. 2011. The magnitude and duration of Late Ordovician–Early Silurian glaciation. Science, 331: 903–906.

Haq, B.U., and Schutter, S.R. 2008 A chronology of Paleozoic sea level changes. Science, 322: 64–68.

Harper, D.A., Hammarlund, E.U., and Rasmussen, C.M.Ø. 2014. End Ordovician extinctions: a coincidence of causes. Gondwana Research, 25: 1294–1307.

Jin. J. 2003. The Early Silurian Brachiopod *Eocoelia* from the Hudson Bay Basin, Canada. Palaeontology, 46: 885–902.

Jin, J. 2005. Reef-dwelling gypiduloid brachiopods in the Lower Silurian Attawapiskat Formation, Hudson Bay region. Journal of Paleontology, 79(01): 48–62.

Jin, J. 2008. Environmental control on temporal and spatial differentiation of Early Silurian pentameride brachiopod communities, Anticosti Island, eastern Canada. Canadian Journal of Earth Sciences, 45: 159–187.

Jin, J., and Copper, P. 2000. Late Ordovician and Early Silurian pentamerid brachiopods from Anticosti Island, Québec, Canada. Palaeontographica Canadiana, 18: 1–140.

Jin, J., Caldwell, W.G.E., and Norford, B.S. 1993. Early Silurian brachiopods and biostratigraphy of the Hudson Bay lowlands, Manitoba, Ontario, and Quebec. Geological Survey of Canada, 457.

Jin, J., Copper, P., and Renbin, Z. 2007. Species-level response of tropical brachiopods to environmental crises during the Late Ordovician mass extinction. Acta Palaeontologica Sinica, 46: 194–200.

Jin, J., Harper, D.A.T., Cocks, L.R.M., McCausland, P.J.A., Rasmussen, C.M.Ø., and
Sheehan, P.M., 2013. Precisely locating the Ordovician equator in Laurentia.
Geology, 41: 107–110.

Jin, J., Sohrabi, A., and Sproat, C. 2014. Late Ordovician brachiopod endemism and
faunal gradient along palaeotropical latitudes in Laurentia during a major sea
level rise. GFF, 136(1): 125–129.

Johnson, M.E. 1997. Silurian event horizons related to the evolution and ecology of
pentamerid brachiopods. *In* Paleontological events: stratigraphic, ecological, and
evolutionary implications. *Edited by* Brett, C.E., and Baird, G.C. Columbia
University Press, New York. p. 162–180.

Long, D.G.F. 2007. Tempestite frequency curves: a key to Late Ordovician and Early
Silurian subsidence, sea-level change, and orbital forcing in the Anticosti foreland
basin, Quebec, Canada. Canadian Journal of Earth Sciences, 44(3): 413–431.

McKerrow, W.S., and Cocks, L.R.M. 1976. Progressive faunal migration across the
Iapetus Ocean. Nature, 263: 304–306.

Moreau, C.S., and Bell, C.D. 2013. Testing the museum versus cradle tropical biological
diversity hypothesis: phylogeny, diversification, and ancestral biogeographic
range evolution of the ants. Evolution, 67: 2240–2257.

Rong, J., Jin, J., and Zhan, R. 2005. Two new genera of early Silurian stricklandioid
brachiopods from South China and their bearing on stricklandioid classification
and paleobiogeography. Journal of Paleontology, 79(6): 1143–1156.

Rong, J., Jin, J., and Zhan, R. 2007. Early Silurian *Sulcipentamerus* and related pentamerid brachiopods from South China. Palaeontology, 50(1): 245–266.

Sapelnikov, V.P. 1961. Venlokskie *Pentameroides* srednego Urala. Paleontologicheskii Zhurnal, 1: 102–107.

Sapelnikov, V.P. 1985. Sistema i stratigraficheskoe znachenie brakhiopod podotryada pentameridin. Akademiya Nauk SSSR, Uralskyi Nauchnyi Tsentr, Nauka, Moskva. 206 p.

Sheehan, P.M. 1975. Brachiopod synecology in a time of crisis (Late Ordovician-Early Silurian). Paleobiology, 1: 205–212.

Sheehan, P. 2001. The Late Ordovician mass extinction. Annual Review of Earth and Planetary Sciences, 29: 331–364.

Sheehan, P.M., and Coorough, P.J., 1990. Brachiopod zoogeography across the Ordovician–Silurian extinction event. Geological Society, London, Memoirs, 12(1): 181-187.

Torsvik, T.H., and Cocks, L.R.M. 2013. New global palaeogeographical for the early Palaeozoic and their generation. Geological Society, London, Memoirs, 38: 5–24.

Wang, G., Li, Y., Kershaw, S., and Deng, X. 2014. Global reef recovery from the end-Ordovician extinction: evidence from late Aeronian coral–stromatoporoid reefs in South China. GFF, 136: 286–289.

Watkins, R., 1998, Silurian reef-dwelling pentamerid brachiopods, Wisconsin and Illinois, USA. Palaontologische Zeitschrift, 72: 99–109.

Watkins, R. 2000. Silurian reef-dwelling brachiopods and their ecologic implications. Palaios, 15(2): 112–119.

Ziegler, A.M. 1965. Silurian marine communities and their environmental significance. Nature, 207: 270–272.

Ziegler, A.M., Cocks, L.R.M., and Bambach, R.K. 1968. The composition and structure of lower Silurian marine communities. Lethaia, 1: 1–27.

Appendix 1: Measured *Pentameroides* Specimens

Appendix 1 contains the measurements of all specimens used in Chapter 3. Abbreviations are the same as used in Chapter 3.

Table 1: Collection AK2, Akimiski Island, Nunavut – *Pentameroides septentrionalis*

Table 2: Collection AK4, Akimiski Island, Nunavut – *Pentameroides septentrionalis*

Table 3: Collection AK5, Akimiski Island, Nunavut – *Pentameroides septentrionalis*

Table 4: Collection AK6, Akimiski Island, Nunavut – *Pentameroides septentrionalis*

Table 5: Collection AK8, Akimiski Island, Nunavut – *Pentameroides septentrionalis*

Table 6: Collection M25, Manitoulin Island, Nunavut – *Pentameroides subrectus*

Table 7: Collection M26, Manitoulin Island, Nunavut – *Pentameroides subrectus*

Table 8: Anticosti Island, Quebec – *Pentameroides subrectus*

Table 1: Collection AK2, Attawapiskat Formation, Akimiski Island, Nunavut – *Pentameroides septentrionalis*

Specimen Number	L (mm)	U (mm)	A (mm)	W (mm)	T (mm)	Tv (mm)	Td (mm)
1	46.52	10.01	1.64	45.89	33.55	19.19	14.36
2	56.88	12.47	2.61	62.26	36.01	19.79	16.22
3	66.42	16.99	2.99	62.36	46.81	24.64	22.17
4	55.69	10.15	3.20	61.43	36.67	20.45	16.22
5	49.68	9.23	2.54	42.93	29.21	15.94	13.27
6	46.67	8.53	2.29	54.09	24.13	12.41	11.72
7	42.23	9.42	1.47	40.63	31.92	18.79	13.13
8	42.57	9.46	1.15	43.30	30.48	17.30	13.18
9	43.18	7.63	1.27	44.73	26.75	15.45	11.30
10	44.47	7.56	3.11	47.93	30.01	18.11	11.90
11	45.47	4.51	1.75	48.87	26.73	14.64	12.09
12	41.69	7.49	6.58	45.97	26.94	15.42	11.52
13	40.01	7.63	2.19	40.06	26.57	14.82	11.75
14	37.32	5.62	1.77	36.22	23.55	12.63	10.92
15	34.19	4.53	1.02	34.33	21.18	12.23	8.95
16	29.84	3.32	0.96	31.46	15.31	8.68	6.63
17	27.75	6.36	1.78	28.68	22.61	12.74	9.87
18	34.74	7.10	1.96	31.84	24.6	14.53	10.07
19	27.23	7.74	0.62	27.47	18.37	9.97	8.40
20	37.87	8.69	1.59	34.46	24.02	14.40	9.62
21	23.83	6.32	1.25	20.71	19.46	13.64	5.82
22	23.10	4.13	0.98	24.76	15.13	8.99	6.14
23	27.34	3.77	1.07	30.05	17.01	9.35	7.66
24	27.3	6.55	1.03	24.21	19.54	12.38	7.16
25	34.52	4.12	1.37	34.43	21.69	13.18	8.51
26	34.08	4.12	1.31	34.42	23.08	11.83	11.25
27	34.69	4.91	1.46	35.29	19.04	10.31	8.73
28	40.21	9.59	2.07	35.81	26.66	13.49	13.17
29	25.27	3.57	0.87	26.75	14.14	8.80	5.34
30	29.76	6.55	1.72	25.36	20.7	10.69	10.01
31	22.04	4.58	0.76	21.00	15.04	8.88	6.16
32	43.20	9.31	2.98	38.22	30.91	16.30	14.61
33	50.28	10.86	3.81	47.48	34.86	19.47	15.39
34	46.49	7.37	2.68	41.74	31.61	17.32	14.29
35	36.87	7.69	1.91	38.32	26.76	15.67	11.09
36	36.24	6.03	1.06	37.90	25.60	14.50	11.10
37	42.93	9.35	3.33	34.32	24.26	13.32	10.94
38	36.84	5.46	1.27	33.78	18.81	11.77	7.04

Table 1: Collection AK2, Attawapiskat Formation, Akimiski Island, Nunavut – *Pentameroides septentrionalis* (continued)

Specimen Number	L (mm)	U (mm)	A (mm)	W (mm)	T (mm)	Tv (mm)	Td (mm)
39	33.26	6.38	1.75	30.09	19.86	10.85	9.01
40	34.37	3.34	1.66	36.92	20.79	11.47	9.32
41	31.48	5.17	1.51	31.45	22.43	11.37	11.06
42	29.48	4.63	1.33	30.33	18.96	10.74	8.22
43	30.45	5.30	0.81	28.79	20.60	10.90	9.70
44	26.69	3.51	1.47	29.01	19.31	10.55	8.76
45	26.33	4.65	1.86	26.29	17.23	8.06	9.17
46	24.00	3.97	0.65	25.15	15.48	8.96	6.52
47	27.86	6.84	1.02	25.79	17.19	10.42	6.77
48	21.78	4.03	1.16	19.28	17.52	10.31	7.21
49	22.04	5.03	1.03	22.11	14.84	8.62	6.22
50	23.81	4.07	0.68	24.90	14.14	7.83	6.31
51	20.80	3.55	0.07	21.76	13.25	7.40	5.85
52	19.41	5.68	0.68	16.45	15.39	9.28	6.11
53	17.91	5.10	0.98	15.58	12.36	8.12	4.24
54	17.03	6.26	0.81	13.96	14.48	9.22	5.26
55	14.83	1.81	0.79	16.01	8.58	4.83	3.75
56	14.55	3.79	1.45	13.04	9.72	5.31	4.41
57	13.69	2.56	0.72	13.08	9.69	6.03	3.66
58	8.38	1.01	0.59	11.24	7.07	4.54	2.53
59	7.67	1.45	0.46	6.93	5.24	3.03	2.21

Table 2: Collection AK4, Attawapiskat Formation, Akimiski Island, Nunavut – *Pentameroides septentrionalis*

Specimen Number	L (mm)	U (mm)	A (mm)	W (mm)	T (mm)	Tv (mm)	Td (mm)
1	42.04	6.98	2.21	48.95	27.24	17.50	9.74
2	37.72	11.49	1.82	38.68	24.99	14.95	10.04
3	50.25	12.73	1.85	51.90	35.37	20.04	15.33
4	38.22	6.92	1.38	49.79	24.12	14.21	9.91
5	48.59	9.03	2.22	48.66	30.63	18.07	12.56
6	43.52	6.00	1.51	53.61	27.91	14.82	13.09
7	41.50	10.26	2.39	42.62	27.45	15.93	11.52
8	48.43	16.02	3.74	42.86	30.74	17.02	13.72
9	44.41	13.34	3.22	42.75	27.74	17.52	10.22
10	48.00	11.24	2.71	44.96	33.39	19.25	14.14
11	43.4	9.55	2.90	42.67	27.32	16.35	10.97
12	37.31	16.34	3.57	29.71	31.57	22.56	9.01
13	49.87	13.10	4.89	40.4	27.42	13.82	13.60
14	41.79	8.47	2.93	34.8	28.24	19.02	9.22
15	44.61	14.34	4.16	35.07	33.61	18.06	15.55
16	45.29	10.32	1.83	41.42	24.76	15.07	9.69
17	35.47	11.20	2.05	30.72	21.48	12.96	8.52
18	27.18	6.91	1.61	26.03	17.22	10.34	6.88
19	27.05	5.70	1.50	26.84	18.78	10.85	7.93
20	32.49	8.04	2.23	30.98	22.32	13.44	8.88
21	35.10	9.69	1.13	34.26	23.22	14.44	8.78
22	22.11	5.13	1.14	23.14	14.93	8.31	6.62
23	28.15	5.95	1.89	28.07	15.59	9.27	6.32
24	33.32	4.89	1.29	40.80	19.20	10.04	9.16
25	43.64	8.02	1.69	44.50	28.77	15.10	13.67
26	33.74	6.91	1.58	37.34	22.50	14.09	8.41
27	46.27	9.00	2.60	39.54	29.55	16.29	13.26
28	43.78	8.52	1.14	45.20	28.14	17.99	10.15
29	50.55	11.66	1.48	48.61	36.41	19.31	17.10
30	39.11	7.86	1.65	38.54	21.90	11.98	9.92
31	44.14	12.62	2.11	44.21	32.90	17.64	15.26
32	44.35	8.89	1.70	46.06	32.82	18.45	14.37
33	40.76	9.41	1.96	41.77	25.44	15.86	9.58
34	43.47	11.09	2.85	42.5	31.53	17.34	14.19
35	57.12	18.18	3.81	55.10	36.94	19.02	17.92
36	43.59	14.41	1.34	41.20	39.33	20.76	18.57
37	44.95	9.60	2.21	48.99	27.65	15.73	11.92
38	48.69	12.86	2.24	42.72	35.27	23.54	11.73

Table 2: Collection AK4, Attawapiskat Formation, Akimiski Island, Nunavut – *Pentameroides septentrionalis* (continued)

Specimen Number	L (mm)	U (mm)	A (mm)	W (mm)	T (mm)	Tv (mm)	Td (mm)
39	42.36	8.39	1.36	40.42	27.67	17.06	10.61
40	43.54	9.99	1.76	42.95	29.13	15.96	13.17
41	35.09	7.04	2.12	37.47	26.65	15.17	11.48
42	42.33	5.17	1.77	41.11	29.05	16.99	12.06
43	44.32	10.24	2.00	40.15	33.65	19.73	13.92
44	38.66	6.22	0.85	38.89	26.05	14.47	11.58
45	46.51	9.16	2.77	46.84	30.62	17.53	13.09
46	34.19	10.34	2.10	36.84	25.03	11.64	13.39
47	43.68	12.38	0.82	38.28	34.33	17.51	16.82
48	38.63	8.91	1.27	37.73	19.13	10.31	8.82
49	45.37	13.06	2.12	42.46	32.80	17.78	15.02
50	33.88	6.33	1.41	35.80	21.32	13.21	8.11
51	41.97	10.01	2.86	43.03	25.05	11.89	13.16
52	45.76	6.22	1.32	48.2	30.96	18.05	12.91
53	27.59	5.83	1.42	27.51	20.05	9.96	10.09

Table 3: Collection AK5, Attawapiskat Formation, Akimiski Island, Nunavut – *Pentameroides septentrionalis*

Specimen Number	L (mm)	U (mm)	A (mm)	W (mm)	T (mm)	Tv (mm)	Td (mm)
1	44.62	5.73	1.64	53.23	27.81	15.48	12.33
2	43.31	6.39	1.02	51.35	33.27	17.52	15.75
3	37.66	6.61	1.71	43.49	28.48	17.29	11.19
4	45.53	4.36	1.25	49.37	31.99	18.58	13.41
5	50.78	9.70	1.21	54.52	37.24	20.91	16.33
6	43.53	7.38	1.59	47.53	34.30	18.01	16.29
7	46.38	8.63	1.97	48.65	30.91	16.96	13.95
8	64.26	10.27	1.71	68.07	35.33	18.71	16.62
9	54.26	12.95	2.04	58.41	36.25	17.78	18.47
10	50.89	10.00	1.59	49.66	39.54	20.93	18.61
11	53.27	9.85	1.87	52.63	34.32	19.13	15.19
12	45.79	8.03	1.81	49.01	30.08	19.06	11.02
13	43.86	7.46	1.27	44.74	29.82	15.72	14.10
14	44.44	6.78	1.41	46.20	28.11	15.35	12.76
15	47.53	9.44	1.47	45.40	34.18	19.31	14.87
16	43.67	6.84	2.07	43.82	32.08	16.89	15.19
17	44.49	4.94	1.39	47.04	23.81	13.04	10.77
18	37.21	5.79	1.06	41.28	26.99	15.85	11.14
19	43.46	7.41	1.36	40.27	31.22	17.44	13.78
20	39.19	10.09	0.87	43.05	29.34	15.83	13.51
21	37.03	6.55	1.44	39.40	27.03	15.40	11.63
22	42.15	7.14	1.75	42.34	23.34	12.26	11.08
23	38.09	7.12	1.61	40.54	28.47	14.63	13.84
24	35.53	3.75	1.01	37.9	22.33	12.22	10.11
25	45.19	7.18	1.65	42.88	28.12	15.36	12.76
26	34.75	4.65	1.03	39.24	21.41	12.16	9.25
27	33.42	4.06	0.93	35.36	18.86	10.01	8.85
28	33.97	4.05	1.12	37.95	19.69	11.13	8.56
29	31.60	3.39	0.89	35.38	19.96	10.53	9.43
30	35.24	4.01	1.05	38.57	20.61	10.63	9.98
31	33.59	6.25	1.83	34.27	22.84	11.77	11.07
32	41.02	7.72	1.61	39.59	29.09	16.07	13.02
33	33.37	7.17	1.12	36.91	29.21	16.79	12.42
34	32.49	5.98	1.36	37.79	27.51	14.37	13.14
35	32.82	5.98	1.61	33.92	25.56	11.64	13.92
36	30.72	4.60	1.57	31.08	22.53	12.11	10.42
37	35.27	5.53	1.16	35.91	28.36	14.84	13.52
38	34.35	4.48	1.32	39.34	26.42	14.2	12.22

Table 3: Collection AK5, Attawapiskat Formation, Akimiski Island, Nunavut – *Pentameroides septentrionalis* (continued)

Specimen Number	L (mm)	U (mm)	A (mm)	W (mm)	T (mm)	Tv (mm)	Td (mm)
39	35.22	7.99	3.68	28.1	26.19	14.25	11.94
40	30.29	4.8	1.37	32.51	17.42	10.85	6.57
41	31.43	5.44	1.10	34.73	18.64	10.63	8.01
42	28.42	4.21	1.09	26.74	19.31	10.57	8.74
43	28.86	3.57	1.36	30.81	18.63	10.19	8.44
44	31.14	7.49	1.54	29.68	20.69	10.65	10.04
45	26.70	3.60	0.82	26.55	19.23	10.46	8.77
46	27.36	6.39	1.48	29.45	16.27	7.34	8.93
47	26.49	4.81	1.39	26.93	19.03	10.01	9.02
48	22.77	3.28	0.70	23.44	15.10	8.46	6.64
49	24.39	4.13	1.39	25.62	16.59	9.45	7.14
50	22.37	3.48	1.44	21.09	13.93	8.19	5.74
51	22.69	3.58	0.86	21.19	14.47	8.55	5.92
52	17.81	1.50	0.59	19.44	9.61	5.79	3.82

Table 4: Collection AK6, Attawapiskat Formation, Akimiski Island, Nunavut – *Pentameroides septentrionalis*

Specimen Number	L (mm)	U (mm)	A (mm)	W (mm)	T (mm)	Tv (mm)	Td (mm)
1	48.53	14.31	2.56	52.98	37.56	21.33	16.23
2	47.05	8.95	1.34	48.92	31.56	16.51	15.05
3	49.57	9.21	2.62	52.22	32.63	19.18	13.45
4	47.44	9.77	3.08	51.64	30.80	17.73	13.07
5	46.68	12.18	1.40	46.33	34.17	19.06	15.11
6	51.03	10.92	1.84	48.91	37.29	19.94	17.35
7	46.54	11.22	1.73	46.23	32.34	17.76	14.58
8	45.64	5.98	1.53	51.03	29.83	16.42	13.41
9	46.97	11.70	2.08	44.08	29.71	16.72	12.99
10	45.34	9.95	1.82	42.38	35.71	20.24	15.47
11	50.78	9.46	1.33	51.58	31.47	16.99	14.48
12	48.38	19.95	2.89	44.62	35.09	21.87	13.22
13	47.45	8.97	1.39	41.50	34.32	19.21	15.11
14	44.11	8.48	2.89	43.87	33.11	17.86	15.25
15	50.11	15.15	6.16	40.83	32.42	16.93	15.49
16	43.79	14.99	1.83	35.03	40.08	22.81	17.27
17	44.19	10.35	2.50	40.33	28.93	17.76	11.17
18	40.09	7.86	1.49	39.25	23.58	12.87	10.71
19	39.19	6.32	1.38	41.58	26.58	14.87	11.71
20	40.37	8.11	1.31	39.58	30.43	14.97	15.46
21	38.31	3.31	0.92	42.14	22.48	11.81	10.67
22	40.91	9.21	2.61	39.03	27.91	13.73	14.18
23	38.17	8.60	1.82	35.25	28.86	16.07	12.79
24	38.58	9.92	2.35	33.84	27.68	14.88	12.80
25	39.90	9.23	3.26	35.96	28.74	16.34	12.40
26	40.83	13.28	3.86	38.30	29.16	17.46	11.70
27	38.62	7.29	2.14	34.61	27.58	16.81	10.77
28	39.66	7.48	1.41	39.99	21.98	12.37	9.61
29	40.31	11.00	0.95	31.77	30.62	16.88	13.74
30	38.55	8.13	2.27	34.92	29.32	15.38	13.94
31	35.71	7.44	1.59	35.83	27.66	14.61	13.05
32	38.01	11.24	2.06	33.35	27.22	13.97	13.25
33	37.84	5.80	2.48	35.38	23.89	14.11	9.78
34	36.04	6.29	1.54	37.52	21.50	11.39	10.11
35	36.24	7.89	2.27	34.56	32.72	18.78	13.94
36	38.28	4.92	1.50	40.45	22.93	11.94	10.99
37	37.72	7.54	2.74	35.25	26.44	12.30	14.14
38	35.32	6.32	1.49	34.26	24.83	14.13	10.7

Table 4: Collection AK6, Attawapiskat Formation, Akimiski Island, Nunavut – *Pentameroides septentrionalis* (continued)

Specimen Number	L (mm)	U (mm)	A (mm)	W (mm)	T (mm)	Tv (mm)	Td (mm)
39	36.38	5.05	1.43	33.63	23.99	12.74	11.25
40	32.29	8.02	1.88	32.14	22.67	12.87	9.80
41	39.44	5.84	1.95	39.91	24.72	13.16	11.56
42	35.93	7.71	2.72	34.42	21.83	12.25	9.58
43	36.6	6.34	1.47	41.18	26.58	13.76	12.82
44	33.39	6.09	1.57	35.08	21.89	12.40	9.49
45	33.89	5.84	1.50	32.96	24.13	12.63	11.5
46	35.15	8.57	2.51	29.06	26.93	15.9	11.03
47	34.81	9.17	2.12	30.81	27.21	15.83	11.38
48	33.18	5.75	1.39	37.05	19.68	10.27	9.41
49	30.22	3.94	0.65	35.19	14.05	8.61	5.44
50	34.74	6.72	2.42	30.99	20.99	11.82	9.17
51	28.63	4.08	1.36	32.59	20.01	11.84	8.17
52	28.66	4.89	1.22	27.36	16.77	9.45	7.32
53	25.66	5.42	0.70	23.56	16.34	9.75	6.59

Table 5: Collection AK8, Attawapiskat Formation, Akimiski Island, Nunavut – *Pentameroides septentrionalis*

Specimen Number	L (mm)	U (mm)	A (mm)	W (mm)	T (mm)	Tv (mm)	Td (mm)
1	50.65	10.15	2.79	52.77	34.21	21.05	13.16
2	48.58	8.62	1.85	51.14	33.26	17.41	15.85
3	47.14	9.84	1.56	47.73	33.93	19.27	14.66
4	50.42	11.83	2.27	51.15	40.21	24.02	16.19
5	44.75	8.89	1.94	48.15	34.39	23.40	10.99
6	48.32	11.36	3.51	43.96	32.45	17.71	14.74
7	44.92	8.68	2.57	45.16	25.02	13.31	11.71
8	43.46	9.32	1.88	41.45	30.59	16.48	14.11
9	42.29	7.07	1.87	41.95	27.31	14.76	12.55
10	42.84	9.56	2.29	44.96	31.14	18.21	12.93
11	47.26	9.78	1.75	42.36	30.64	17.41	13.23
12	44.77	10.48	1.05	45.17	32.03	19.28	12.75
13	44.03	10.02	2.52	37.14	33.12	17.50	15.62
14	43.78	9.21	2.07	41.79	30.26	18.32	11.94
15	47.90	10.32	2.52	42.98	32.91	18.13	14.78
16	40.76	6.73	2.06	44.22	26.26	15.25	11.01
17	42.43	10.03	1.26	37.80	32.21	17.63	14.58
18	45.09	10.79	1.91	38.55	32.23	17.95	14.28
19	42.15	10.22	2.63	38.77	33.24	19.44	13.80
20	42.16	6.78	2.02	43.53	28.84	16.65	12.19
21	47.19	8.05	1.98	48.68	31.25	18.48	12.77
22	45.33	8.15	2.35	48.07	26.99	14.57	12.42
23	41.38	8.08	1.98	39.38	33.23	17.91	15.32
24	43.30	10.62	2.79	42.38	31.73	18.21	13.52
25	42.29	6.81	2.14	41.55	28.44	16.78	11.66
26	36.77	7.37	1.74	35.16	30.75	18.09	12.66
27	39.55	6.92	1.36	34.71	28.74	16.41	12.33
28	41.66	6.91	1.71	46.16	25.86	15.16	10.70
29	43.41	8.54	3.94	38.55	25.52	16.03	9.49
30	38.47	6.42	2.21	38.08	27.94	14.41	13.53
31	41.58	7.77	2.52	40.27	29.12	16.62	12.5
32	39.42	5.01	1.66	41.59	26.87	16.39	10.48
33	37.01	7.93	2.08	36.99	31.92	18.94	12.98
34	37.52	6.69	2.20	38.42	26.1	16.06	10.04
35	37.45	5.89	1.51	35.52	27.16	16.12	11.04
36	42.35	9.69	2.01	36.47	33.29	19.79	13.5
37	41.21	12.91	4.71	31.43	24.49	14.58	9.91
38	40.61	7.33	1.16	38.71	22.88	14.42	8.46

Table 5: Collection AK8, Attawapiskat Formation, Akimiski Island, Nunavut –
Pentameroides septentrionalis (continued)

Specimen Number	L (mm)	U (mm)	A (mm)	W (mm)	T (mm)	Tv (mm)	Td (mm)
39	34.35	4.86	1.25	35.96	20.79	12.53	8.26
40	36.65	7.71	2.24	37.85	25.53	14.95	10.58
41	35.79	7.04	1.66	36.07	25.60	15.97	9.63
42	37.75	5.48	1.82	37.68	21.07	12.22	8.85
43	36.05	5.77	1.59	35.01	22.47	13.27	9.20
44	34.46	6.21	1.86	31.27	23.44	13.87	9.57
45	32.35	3.74	0.84	39.85	18.37	11.67	6.70
46	35.52	4.98	2.22	30.56	20.86	13.72	7.14
47	33.76	5.74	1.65	33.28	21.66	13.76	7.90
48	33.33	6.78	2.21	34.48	22.94	14.19	8.75
49	34.88	7.31	1.92	32.76	25.91	15.29	10.62
50	33.29	4.83	1.56	31.54	20.04	11.77	8.27
51	31.59	5.66	1.98	30.24	19.01	11.37	7.64
52	30.23	5.31	1.62	29.97	20.88	12.10	8.78
53	31.7	3.99	1.28	35.29	21.27	13.10	8.17
54	31.71	5.52	1.34	30.93	21.40	11.04	10.36
55	30.64	4.71	1.18	29.92	20.97	12.28	8.69
56	30.26	6.88	1.92	29.14	23.05	11.38	11.67
57	32.86	5.81	1.64	29.12	20.71	11.55	9.16
58	29.38	4.50	1.33	29.37	22.80	13.41	9.39
59	28.86	5.91	0.89	26.11	20.83	12.23	8.60
60	25.98	4.47	0.69	27.59	16.28	10.29	5.99
61	28.09	3.61	1.16	27.16	16.45	9.84	6.61
62	30.31	5.37	1.97	27.37	19.59	11.24	8.35
63	27.43	5.07	1.34	28.74	16.58	10.64	5.94
64	27.09	4.48	1.27	28.12	15.65	8.94	6.71
65	24.56	3.32	0.54	28.53	14.36	9.61	4.75
66	25.25	6.26	1.22	23.54	17.48	8.91	8.57
67	21.33	4.31	1.27	20.68	12.83	8.24	4.59
68	28.59	7.12	1.71	22.01	19.44	10.70	8.74
69	25.24	3.68	1.08	25.22	16.35	9.78	6.57
70	25.11	4.55	0.93	22.75	19.15	11.94	7.21
71	27.17	5.14	2.01	23.99	17.32	10.75	6.57
72	31.32	7.71	1.93	30.59	22.11	13.22	8.89
73	32.69	7.57	0.89	29.82	26.29	15.06	11.23
74	33.63	6.61	1.87	33.96	24.27	15.58	8.69
75	35.28	5.44	1.65	35.62	23.85	12.47	11.38
76	33.95	7.15	0.98	30.01	26.55	16.71	9.84

Table 5: Collection AK8, Attawapiskat Formation, Akimiski Island, Nunavut – *Pentameroides septentrionalis* (continued)

Specimen Number	L (mm)	U (mm)	A (mm)	W (mm)	T (mm)	Tv (mm)	Td (mm)
77	34.78	6.37	0.78	33.09	22.77	13.24	9.53
78	38.32	6.87	1.83	32.64	26.75	16.60	10.15
79	36.76	6.31	1.67	37.13	26.27	16.50	9.77
80	36.62	6.14	1.10	40.81	25.75	15.67	10.08
81	38.46	6.52	1.59	38.43	23.14	13.02	10.12
82	41.24	4.39	1.51	44.34	24.98	14.49	10.49
83	39.39	5.65	1.25	38.58	26.21	15.76	10.45
84	38.89	5.01	1.16	39.98	24.71	13.74	10.97
85	42.82	9.58	2.75	41.22	27.84	16.32	11.52
86	37.19	7.91	2.79	37.24	30.91	17.45	13.46
87	41.09	7.73	1.71	36.79	29.46	16.54	12.92
88	39.32	7.39	2.57	26.23	30.84	18.48	12.36
89	39.54	6.71	1.75	41.75	29.26	17.20	12.06
90	43.56	12.73	4.56	31.69	32.05	19.51	12.54
91	44.99	8.52	2.86	41.33	28.33	16.49	11.84
92	43.11	8.30	2.42	41.21	29.61	17.10	12.51
93	47.53	8.89	1.84	44.35	32.41	20.93	11.48
94	44.33	10.57	2.25	39.59	30.43	16.04	14.39
95	46.56	11.51	0.72	41.32	35.51	19.63	15.88
96	45.98	10.54	3.72	40.62	33.91	20.29	13.62
97	49.08	11.83	3.69	44.28	28.39	14.91	13.48
98	45.28	9.85	3.07	42.18	28.51	16.32	12.19
99	47.85	7.65	2.22	52.16	31.99	16.45	15.54
100	46.95	12.04	2.77	44.07	32.36	19.35	13.01
101	52.24	11.35	1.42	52.75	38.46	23.51	14.95
102	50.52	10.84	2.37	57.95	38.06	23.11	14.95
103	50.38	9.89	2.94	55.79	33.83	20.36	13.47
104	53.75	9.42	0.31	52.90	37.68	22.05	15.63
105	54.58	17.28	3.81	47.09	40.71	23.93	16.78

Table 6: Collection M25, Fossil Hill Formation, Manitoulin Island, Ontario – *Pentameroides subrectus*

Specimen Number	L (mm)	U (mm)	A (mm)	W (mm)	T (mm)	Tv (mm)	Td (mm)
1	64.49	11.42	4.88	43.81	32.65	19.86	12.79
2	64.13	9.52	1.92	43.91	33.84	19.62	14.22
3	44.55	6.79	0.00	44.44	24.94	14.03	10.91
4	46.41	6.44	1.24	43.51	20.85	9.15	11.70
5	40.82	9.22	1.21	33.24	21.28	11.90	9.38
6	40.29	7.74	1.41	33.35	22.37	12.53	9.84
7	46.18	7.30	1.32	40.22	16.89	9.62	7.27
8	27.4	4.16	0.76	26.09	15.20	9.77	5.43
9	21.41	5.23	1.07	26.42	16.19	8.94	7.25
10	35.81	6.31	0.68	31.02	17.51	10.91	6.60
11	36.71	5.35	1.36	36.92	19.19	10.81	8.38
12	29.45	5.44	1.14	30.04	14.95	8.00	6.95
13	30.39	4.58	0.88	24.41	14.73	9.53	5.20
14	32.21	4.63	0.00	34.63	19.36	11.07	8.29
15	28.52	6.24	0.77	29.94	15.91	11.07	4.84
16	33.86	6.32	1.19	26.86	16.71	11.13	5.58
17	28.48	4.41	1.17	24.72	16.41	9.07	7.34
18	31.87	6.63	0.70	28.27	16.29	10.48	5.81
19	26.55	4.19	0.73	23.89	12.98	7.08	5.90
20	26.94	5.48	0.92	25.04	14.13	7.41	6.72
21	33.28	6.04	1.09	24.58	13.21	7.83	5.38
22	26.36	4.83	0.93	31.10	19.04	10.07	8.97
23	26.13	5.54	0.97	24.55	14.23	8.31	5.92
24	28.60	4.31	0.64	26.97	13.42	8.89	4.53
25	24.79	4.48	0.51	26.87	16.01	8.60	7.41
26	29.01	6.65	0.96	23.48	15.28	8.66	6.62
27	30.61	5.28	1.36	24.36	14.73	9.51	5.22
28	25.86	4.50	0.57	23.75	13.36	8.16	5.20
29	23.99	4.46	0.74	25.98	13.96	8.42	5.54
30	27.13	5.82	1.04	23.41	13.67	9.62	4.05
31	26.95	5.54	1.24	21.87	12.98	8.78	4.20
32	21.85	3.26	0.00	23.14	12.02	7.37	4.65
33	24.74	4.39	1.25	23.18	15.80	8.88	6.92
34	24.39	4.26	0.84	23.04	14.21	8.32	5.89
35	23.31	3.91	1.22	21.94	12.07	7.76	4.31
36	26.02	6.15	1.11	24.68	12.68	7.87	4.81
37	22.83	4.23	1.16	20.19	13.42	8.31	5.11
38	21.43	3.92	1.13	18.84	11.16	6.42	4.74

Table 6: Collection M25, Fossil Hill Formation, Manitoulin Island, Ontario – *Pentameroides subrectus* (continued)

Specimen Number	L (mm)	U (mm)	A (mm)	W (mm)	T (mm)	Tv (mm)	Td (mm)
39	13.62	2.28	1.26	12.54	8.61	5.68	2.93

Table 7: Collection M26, Fossil Hill Formation, Manitoulin Island, Ontario – *Pentameroides subrectus*

Specimen Number	L (mm)	U (mm)	A (mm)	W (mm)	T (mm)	Tv (mm)	Td (mm)
1	42.94	7.26	0.00	39.38	20.87	13.48	7.39
2	47.19	11.36	1.68	43.58	21.24	15.69	5.55
3	50.22	6.62	1.21	41.55	20.59	12.98	7.61
4	52.81	11.21	1.02	45.04	30.55	20.78	9.77
5	52.06	8.10	1.43	36.11	23.67	14.58	9.09
6	36.92	5.81	1.41	30.29	18.78	10.59	8.19
7	32.99	5.65	0.99	36.72	15.14	9.73	5.41
8	38.25	6.41	1.78	34.14	19.82	9.28	10.54
9	41.98	3.89	0.00	35.18	22.36	13.48	8.88
10	35.93	6.29	0.00	32.09	20.36	11.88	8.48
11	31.91	8.47	1.18	33.86	14.94	9.22	5.72
12	36.28	6.43	1.14	27.67	17.45	11.16	6.29
13	36.61	6.63	1.86	38.31	14.94	9.78	5.16
14	50.99	10.62	3.11	38.94	24.25	13.90	10.35
15	47.61	5.41	1.07	37.61	17.64	9.67	7.97
16	40.63	6.85	2.45	35.47	13.53	8.99	4.54
17	33.98	8.66	1.07	30.51	14.79	7.88	6.91
18	31.83	5.50	1.00	31.82	16.08	9.56	6.52
19	28.49	7.22	2.71	30.60	15.04	8.47	6.57
20	29.77	4.84	0.75	25.79	17.32	10.33	6.99
21	31.64	6.19	0.96	27.57	15.85	9.46	6.39
22	29.05	5.17	1.07	28.67	14.47	8.64	5.83
23	32.83	6.29	1.16	26.22	16.34	9.74	6.60
24	32.14	6.95	2.04	30.62	15.99	7.51	8.48
25	33.39	6.70	0.91	23.83	14.48	10.10	4.38
26	33.03	5.84	0.97	26.73	17.53	10.29	7.24
27	29.81	7.07	1.26	22.88	16.71	10.16	6.55
28	25.07	4.17	0.65	29.01	14.62	9.18	5.44
29	29.59	6.41	1.69	29.38	13.64	8.91	4.73
30	28.97	6.16	1.06	23.73	13.22	8.36	4.86
31	31.14	6.62	0.93	25.62	11.06	5.92	5.14
32	29.53	5.43	1.44	25.66	12.54	7.54	5.00
33	29.95	5.39	1.21	25.55	12.29	8.98	3.31
34	26.75	5.95	2.25	19.82	10.05	6.64	3.41
35	24.03	3.95	0.73	24.79	9.68	7.24	2.44
36	17.43	3.40	0.49	19.87	11.11	6.66	4.45

Table 8: Anticosti Island, Jupiter Formation, Quebec – *Pentameroides subrectus*

Specimen Number	L (mm)	U (mm)	A (mm)	W (mm)	T (mm)	Tv (mm)	Td (mm)
1	41.99	4.81	0.71	47.98	15.65	8.35	7.30
2	42.64	6.57	0.92	46.23	15.18	8.47	6.71
3	27.11	2.79	0.51	41.77	13.78	7.07	6.71
4	31.87	3.99	0.86	27.34	18.37	8.76	9.61
5	39.58	4.49	0.00	47.38	20.72	12.06	8.66
6	35.41	4.71	0.79	37.78	17.37	11.07	6.00

Appendix 2: Shannon and Simpson Diversity Indices

Appendix 2 contains raw and relative abundance data as well as the values of the variables used in the Shannon and Simpson diversity indices calculations. All variables are defined in Chapter 4. Tables are organized by formation in order of time for oldest to youngest.

Tables 1–2: Laframboise Member, Ellis Bay Formation, Anticosti Island, Quebec.

Tables 3–15: East Point Member, Meniér Formation, Anticosti Island, Quebec.

Tables 16–18: Fossil Hill Formation, Manitoulin Island, Ontario.

Tables 19–50: Attawapiskat Formation, Akimiski Island, James Bay, Nunavut.

Tables 51–57: Chicotte Formation, Anticosti Island, Quebec.

Tables 58–61: Racine Formation, Wisconsin.

Table 1: Locality A1161, Laframboise Member, Ellis Bay Formation

Genus / species	N	p_i	$\ln(p_i)$	$p_i*\ln(p_i)$	$(p_i)^2$
Hirnantia segittifera	25	0.37879	-0.9708	-0.36772	0.14348
Leptaena sp.	11	0.16667	-1.7918	-0.29863	0.02778
Hindella sp.	10	0.15152	-1.8871	-0.28592	0.02296
Mendecella uberis	9	0.13636	-1.9924	-0.2717	0.0186
Platystrophia regularis	8	0.12121	-2.1102	-0.25578	0.01469
Eospiringia sp.	3	0.04545	-3.091	-0.1405	0.00207
				H = -1.62	**S = 0.23**

Table 2: Locality A743b, Laframboise Member, Ellis Bay Formation

Genus / species	N	p_i	$\ln(p_i)$	$p_i*\ln(p_i)$	$(p_i)^2$
Mendecella uberis	14	1	0	0	1
				H = 0	**S = 1**

Table 3: Locality A863, East Point Member, Meniér Formation

Genus / species	N	p_i	$\ln(p_i)$	$p_i*\ln(p_i)$	$(p_i)^2$
Stegerhynchus deltolingulatus	186	0.79828	-0.2253	-0.1798	0.63726
Clorinda sp.	20	0.08584	-2.4553	-0.2108	0.00737
Mendacella sp.	8	0.03433	-3.3716	-0.1158	0.00118
Levenea sp.	6	0.02575	-3.6593	-0.0942	0.00066
Anastrophia sp.	4	0.01717	-4.0647	-0.0698	0.00029
Platytrochalos sp.	4	0.01717	-4.0647	-0.0698	0.00029
Doleorthis sp.	2	0.00858	-4.7579	-0.0408	7.4E-05
Smooth athyridid	2	0.00858	-4.7579	-0.0408	7.4E-05
Ptychopleurella sp.	1	0.00429	-5.451	-0.0234	1.8E-05
				H = -0.85	**S = 0.65**

Table 4: Locality A934, East Point Member, Meniér Formation

Genus / species	N	p_i	$\ln(p_i)$	$p_i*\ln(p_i)$	$(p_i)^2$
Stegerhynchus deltolingulatus	107	0.92241	-0.0808	-0.0745	0.85085
Zygatrypa sp.	5	0.0431	-3.1442	-0.1355	0.00186
Eocoelia sp.	2	0.01724	-4.0604	-0.07	0.0003
Platytrochalos crudicostatus	1	0.00862	-4.7536	-0.041	7.4E-05
Gotatrypa sp.	1	0.00862	-4.7536	-0.041	7.4E-05
				H = -0.36	**S = 0.85**

Table 5: Locality A1059, East Point Member, Meniér Formation

Genus / species	N	p_i	$\ln(p_i)$	$p_i*\ln(p_i)$	$(p_i)^2$
Stegerhynchus deltolingulatus	95	0.97938	-0.0208	-0.0204	0.95919
Pentamerus sp.	1	0.01031	-4.5747	-0.0472	0.00011
Levenea sp.	1	0.01031	-4.5747	-0.0472	0.00011
				H = -0.11	**S = 0.96**

Table 6: Locality A1060, East Point Member, Meniér Formation

Genus / species	N	p_i	$\ln(p_i)$	$p_i*\ln(p_i)$	$(p_i)^2$
Stegerhynchus deltolingulatus	46	1	0	0	1
				H = 0	**S = 1**

Table 7: Locality A1113, East Point Member, Meniér Formation

Genus / species	N	p_i	$\ln(p_i)$	$p_i*\ln(p_i)$	$(p_i)^2$
Stegerhynchus deltolingulatus	402	0.96867	-0.0318	-0.0308	0.93833
Pentamerus oblongus	13	0.03133	-3.4633	-0.1085	0.00098
				H = -0.14	**S = 0.94**

Table 8: Locality A1198, East Point Member, Meniér Formation

Genus / species	N	p_i	$\ln(p_i)$	$p_i*\ln(p_i)$	$(p_i)^2$
Stegerhynchus deltolingulatus	6	1	0	0	1
				H = 0	**S = 1**

Table 9: Locality A1199, East Point Member, Meniér Formation

Genus / species	N	p_i	ln(p_i)	p_i*ln(p_i)	(p_i)^2
Stegerhynchus deltolingulatus	100	0.73529	-0.3075	-0.2261	0.54066
Dolerorthis sp.	9	0.06618	-2.7154	-0.1797	0.00438
Clorinda sp.	8	0.05882	-2.8332	-0.1667	0.00346
spirigerinids	8	0.05882	-2.8332	-0.1667	0.00346
Glyptorthis marilara	3	0.02206	-3.814	-0.0841	0.00049
Septatrypa sp.	3	0.02206	-3.814	-0.0841	0.00049
Gotatrypa sp.	1	0.00735	-4.9127	-0.0361	5.4E-05
Mendacella sp.	1	0.00735	-4.9127	-0.0361	5.4E-05
'Thebesia' sp.	3	0.02206	-3.814	-0.0841	0.00049
				H = -1.06	**S = 0.55**

Table 10: Locality A1223, East Point Member, Meniér Formation

Genus / species	N	p_i	ln(p_i)	p_i*ln(p_i)	(p_i)^2
Pentamerus oblongus	2	0.66667	-0.4055	-0.2703	0.44444
Whitfieldella sp.	1	0.33333	-1.0986	-0.3662	0.11111
				H = -0.64	**H =0.56**

Table 11: Locality A1275, East Point Member, Meniér Formation

Genus / species	N	p_i	ln(p_i)	p_i*ln(p_i)	(p_i)^2
smooth athyridids	3	0.6	-0.5108	-0.3065	0.36
Clorinda sp.	2	0.4	-0.9163	-0.3665	0.16
				H = -0.67	**S = 0.52**

Table 12: Locality A1293, East Point Member, Meniér Formation

Genus / species	N	p_i	ln(p_i)	p_i*ln(p_i)	(p_i)^2
Pentamerus oblongus	3	1	0	0	1
				H = 0	**S = 1**

Table 13: Locality A1307, East Point Member, Meniér Formation

Genus / species	N	p$_i$	ln(p$_i$)	p$_i$*ln(p$_i$)	(p$_i$)^2
Stegerhynchus deltolingulatus	417	0.98815	-0.0119	-0.0118	0.97644
Dolerorthis sp.	4	0.00948	-4.6587	-0.0442	9E-05
Gotatrypa sp.	1	0.00237	-6.045	-0.0143	5.6E-06
				H = -0.07	**S = 0.98**

Table 14: Locality A1384, East Point Member, Meniér Formation

Genus / species	N	p$_i$	ln(p$_i$)	p$_i$*ln(p$_i$)	(p$_i$)^2
Stegerhynchus deltolingulatus	95	1	0	0	1
				H = 0	**S = 1**

Table 15: Locality A1489, East Point Member, Meniér Formation

Genus / species	N	p$_i$	ln(p$_i$)	p$_i$*ln(p$_i$)	(p$_i$)^2
Pentamerus sp.	33	0.86842	-0.1411	-0.1225	0.75416
Gotatrypa sp.	3	0.07895	-2.539	-0.2004	0.00623
Stegerhynchus sp.	1	0.02632	-3.6376	-0.0957	0.00069
Didymothyris sp.	1	0.02632	-3.6376	-0.0957	0.00069
				H = -0.51	**S = 0.76**

Table 16: Locality M25, Fossil Hill Formation

Genus / species	N	p$_i$	ln(p$_i$)	p$_i$*ln(p$_i$)	(p$_i$)^2
Pentameroides subrectus	505	0.97868	-0.0215	-0.0211	0.95782
Plickostricklandia sp.	4	0.00775	-4.8598	-0.0377	6E-05
Dalejina sp.	2	0.00388	-5.553	-0.0215	1.5E-05
Eospirifier sp.	2	0.00388	-5.553	-0.0215	1.5E-05
Stegerhyncus? sp.	1	0.00194	-6.2461	-0.0121	3.8E-06
Calllipentamerus sp.	1	0.00194	-6.2461	-0.0121	3.8E-06
Gypidula? sp.	1	0.00194	-6.2461	-0.0121	3.8E-06
				H = -0.14	**S = 0.96**

Table 17: Locality M26, Fossil Hill Formation

Genus / species	N	p_i	$\ln(p_i)$	$p_i*\ln(p_i)$	$(p_i)^2$
Pentameroides subrectus	2222	0.97627	-0.024	-0.0234	0.95311
Stegerhyncus? sp.	46	0.02021	-3.9015	-0.0789	0.00041
Plickostricklandia sp.	5	0.0022	-6.1207	-0.0134	4.8E-06
Callipentamerus sp.	3	0.00132	-6.6316	-0.0087	1.7E-06
				H =-0.12	**S =0.95**

Table 18: Locality M-H6, Fossil Hill Formation

Genus / species	N	p_i	$\ln(p_i)$	$p_i*\ln(p_i)$	$(p_i)^2$
Penatmeroides subrectus	18	0.85714	-0.1542	-0.1321	0.73469
Plickostricklandia sp.	3	0.14286	-1.9459	-0.278	0.02041
				H = -0.41	**S = 0.76**

Table 19: Locality AK1A, Attawapiskat Formation

Genus / species	N	p_i	$\ln(p_i)$	$p_i*\ln(p_i)$	$(p_i)^2$
Lissatrypa variabilis	478	0.48381	-0.7261	-0.3513	0.23407
Gotatrypa hedei	262	0.26518	-1.3273	-0.352	0.07032
Septatrypa varians	145	0.14676	-1.9189	-0.2816	0.02154
Gypidula akimiskiformis	28	0.02834	-3.5635	-0.101	0.0008
Pentameroides septentrionalis	17	0.01721	-4.0625	-0.0699	0.0003
Eoplectodonta sp.	10	0.01012	-4.5931	-0.0465	0.0001
Erilevigatella euthylomata	10	0.01012	-4.5931	-0.0465	0.0001
Mictospirifer jini	7	0.00709	-4.9498	-0.0351	5E-05
Leptaena sp.	6	0.00607	-5.1039	-0.031	3.7E-05
Clorinda tumidula	6	0.00607	-5.1039	-0.031	3.7E-05
Howellella porcata	6	0.00607	-5.1039	-0.031	3.7E-05
Meifodia discoidalis	2	0.00202	-6.2025	-0.0126	4.1E-06
Leangella sp.	2	0.00202	-6.2025	-0.0126	4.1E-06
Eomegastrophia sp.	2	0.00202	-6.2025	-0.0126	4.1E-06
Trimerella ekwanensis	2	0.00202	-6.2025	-0.0126	4.1E-06
Meristina sp.	2	0.00202	-6.2025	-0.0126	4.1E-06

Table 19: Locality AK1A, Attawapiskat Formation (continued)

Genus / species	N	p_i	$\ln(p_i)$	$p_i*\ln(p_i)$	$(p_i)^2$
Hesperorthis sp.	1	0.00101	-6.8957	-0.007	1E-06
Stegerhynchus ekwanensis	1	0.00101	-6.8957	-0.007	1E-06
athyridid (minute)	1	0.00101	-6.8957	-0.007	1E-06
				H = -1.46	**S = 0.33**

Table 20: Locality AK1-01A, Attawapiskat Formation

Genus / species	N	p_i	$\ln(p_i)$	$p_i*\ln(p_i)$	$(p_i)^2$
Septatrypa varians	134	0.51938	-0.6551	-0.3403	0.26976
Gotatrypa hedei	58	0.22481	-1.4925	-0.3355	0.05054
Gypidula akimiskiformis	22	0.08527	-2.4619	-0.2099	0.00727
Eoplectodonta sp.	13	0.05039	-2.988	-0.1506	0.00254
Pentameroides septentrionalis	10	0.03876	-3.2504	-0.126	0.0015
Erilevigatella euthylomata	9	0.03488	-3.3557	-0.1171	0.00122
Clorinda tumidula	3	0.01163	-4.4543	-0.0518	0.00014
Meifodia discoidalis	2	0.00775	-4.8598	-0.0377	6E-05
Trimerella ekwanensis	2	0.00775	-4.8598	-0.0377	6E-05
Lissatrypa variabilis	1	0.00388	-5.553	-0.0215	1.5E-05
Dictyonella sp.	1	0.00388	-5.553	-0.0215	1.5E-05
Dalejina striata	1	0.00388	-5.553	-0.0215	1.5E-05
Meristina sp.	1	0.00388	-5.553	-0.0215	1.5E-05
Mictospirifer jini	1	0.00388	-5.553	-0.0215	1.5E-05
				H = -1.51	**S = 0.33**

Table 21: Locality AK2A, Attawapiskat Formation

Genus / species	N	p_i	$\ln(p_i)$	$p_i*\ln(p_i)$	$(p_i)^2$
Gypidula akimiskiformis	486	0.64628	-0.4365	-0.2821	0.41767
Pentameroides septentrionalis	119	0.15824	-1.8436	-0.2917	0.02504
Gotatrypa hedei	33	0.04388	-3.1262	-0.1372	0.00193
Lissatrypa variabilis	33	0.04388	-3.1262	-0.1372	0.00193
Eomegastrophia philomena	20	0.0266	-3.627	-0.0965	0.00071

Table 21: Locality AK2A, Attawapiskat Formation (continued)

Genus / species	N	p_i	$\ln(p_i)$	$p_i*\ln(p_i)$	$(p_i)^2$
Leptaena sp.	12	0.01596	-4.1378	-0.066	0.00025
Clorinda parvolinguifera	8	0.01064	-4.5433	-0.0483	0.00011
Septatrypa varians	8	0.01064	-4.5433	-0.0483	0.00011
Parastrophinella sp.	5	0.00665	-5.0133	-0.0333	4.4E-05
Erilevigatella euthylomata	5	0.00665	-5.0133	-0.0333	4.4E-05
Gypidulina sp.	5	0.00665	-5.0133	-0.0333	4.4E-05
Trimerella ekwanensis	4	0.00532	-5.2364	-0.0279	2.8E-05
Meifodia discoidalis	4	0.00532	-5.2364	-0.0279	2.8E-05
Meristina sp.	4	0.00532	-5.2364	-0.0279	2.8E-05
Atrypoidea prelingulata	2	0.00266	-5.9296	-0.0158	7.1E-06
Isorthis sp.	1	0.00133	-6.6227	-0.0088	1.8E-06
Hesperorthis sp.	1	0.00133	-6.6227	-0.0088	1.8E-06
Leangella sp.	1	0.00133	-6.6227	-0.0088	1.8E-06
Whitfieldella sp.	1	0.00133	-6.6227	-0.0088	1.8E-06
				H = -1.34	**S = 0.45**

Table 22: Locality AK2B, Attawapiskat Formation

Genus / species	N	p_i	$\ln(p_i)$	$p_i*\ln(p_i)$	$(p_i)^2$
Septatrypa varians	171	0.20803	-1.5701	-0.3266	0.04328
Lissatrypa variabilis	122	0.14842	-1.9077	-0.2831	0.02203
Whitfieldella sulcatina	115	0.1399	-1.9668	-0.2752	0.01957
Gotatrypa hedei	108	0.13139	-2.0296	-0.2667	0.01726
smooth atrypoids	71	0.08637	-2.4491	-0.2115	0.00746
Merista rhombiformis	33	0.04015	-3.2152	-0.1291	0.00161
Meifodia discoidalis	30	0.0365	-3.3105	-0.1208	0.00133
Parmula hemisphaerica	21	0.02555	-3.6672	-0.0937	0.00065
Parastrophinella sp.	21	0.02555	-3.6672	-0.0937	0.00065
Eoplectodonta sp.	15	0.01825	-4.0037	-0.0731	0.00033
Septatrypa severnensis	13	0.01582	-4.1468	-0.0656	0.00025
Hesperorthis sp.	13	0.01582	-4.1468	-0.0656	0.00025
Mictospirifer jini	13	0.01582	-4.1468	-0.0656	0.00025

Table 22: Locality AK2B, Attawapiskat Formation (continued)

Genus / species	N	p_i	$\ln(p_i)$	$p_i*\ln(p_i)$	$(p_i)^2$
Howellella porcata	12	0.0146	-4.2268	-0.0617	0.00021
Gypidula akimiskiformis	10	0.01217	-4.4092	-0.0536	0.00015
Rhytidorhachis guttuliformis	10	0.01217	-4.4092	-0.0536	0.00015
Leangella sp.	9	0.01095	-4.5145	-0.0494	0.00012
Pentameroides septentrionalis	8	0.00973	-4.6323	-0.0451	9.5E-05
Meristina sp.	7	0.00852	-4.7658	-0.0406	7.3E-05
Leptaena sp.	5	0.00608	-5.1023	-0.031	3.7E-05
Erilevigatella euthylomata	5	0.00608	-5.1023	-0.031	3.7E-05
Clorinda parvlinguifera	4	0.00487	-5.3254	-0.0259	2.4E-05
Eomegastrophia sp.	3	0.00365	-5.6131	-0.0205	1.3E-05
Eoplectodonta hudsonensis	2	0.00243	-6.0186	-0.0146	5.9E-06
spiriferid indet	1	0.00122	-6.7117	-0.0082	1.5E-06
				H = -2.51	**S = 0.16**

Table 23: Locality AK2C, Attawapiskat Formation

Genus / species	N	p_i	$\ln(p_i)$	$p_i*\ln(p_i)$	$(p_i)^2$
Gypidula akimiskiformis	572	0.35049	-1.0484	-0.3675	0.12284
Septatrypa varians	290	0.1777	-1.7277	-0.307	0.03158
Lissatrypa variabilis	134	0.08211	-2.4997	-0.2052	0.00674
Meifodia discoidalis	113	0.06924	-2.6702	-0.1849	0.00479
Eomegastrophia philomena	110	0.0674	-2.6971	-0.1818	0.00454
Gotatrypa hedei	93	0.05699	-2.865	-0.1633	0.00325
Pentameroides septentrionalis	64	0.03922	-3.2387	-0.127	0.00154
Eomegastrophia sp. A	60	0.03676	-3.3032	-0.1214	0.00135
Trimerella ekwanensis	50	0.03064	-3.4855	-0.1068	0.00094
Meristina sp.	26	0.01593	-4.1395	-0.0659	0.00025
Parastrophinella sp.	21	0.01287	-4.353	-0.056	0.00017
Erilevigatella euthylomata	15	0.00919	-4.6895	-0.0431	8.4E-05

Table 23: Locality AK2C, Attawapiskat Formation (continued)

Genus / species	N	p_i	$\ln(p_i)$	$p_i*\ln(p_i)$	$(p_i)^2$
Eoplectodonta hudsonensis	15	0.00919	-4.6895	-0.0431	8.4E-05
Howellela porcata	15	0.00919	-4.6895	-0.0431	8.4E-05
Mictospirifer jini	13	0.00797	-4.8326	-0.0385	6.3E-05
Clorinda parvolinguifera	11	0.00674	-4.9997	-0.0337	4.5E-05
Stegerhynchus ekwanensis	9	0.00551	-5.2003	-0.0287	3E-05
Hesperorthis sp.	7	0.00429	-5.4517	-0.0234	1.8E-05
Whitfieldella sulcatina	6	0.00368	-5.6058	-0.0206	1.4E-05
Coolinia sp.	4	0.00245	-6.0113	-0.0147	6E-06
Leangella sp.	2	0.00123	-6.7044	-0.0082	1.5E-06
Leptaena sp.	2	0.00123	-6.7044	-0.0082	1.5E-06
				H = -2.19	**S = 0.18**

Table 24: Locality AK2-01A, Attawapiskat Formation

Genus / species	N	p_i	$\ln(p_i)$	$p_i*\ln(p_i)$	$(p_i)^2$
Septatrypa varians	186	0.50959	-0.6742	-0.3435	0.25968
Gotatrypa hedei	45	0.12329	-2.0932	-0.2581	0.0152
Gypidula akimiskiformis	35	0.09589	-2.3445	-0.2248	0.00919
Pentameroides septentrionalis	33	0.09041	-2.4034	-0.2173	0.00817
Meifodia discoidalis	26	0.07123	-2.6418	-0.1882	0.00507
Erilevigatella euthylomata	7	0.01918	-3.954	-0.0758	0.00037
Clorinda parvlinguifera	5	0.0137	-4.2905	-0.0588	0.00019
Clorinda tumidula	4	0.01096	-4.5136	-0.0495	0.00012
Howellella porcata	5	0.0137	-4.2905	-0.0588	0.00019
Mictospirifer jini	4	0.01096	-4.5136	-0.0495	0.00012
Whitfieldella sulcatina	1	0.00274	-5.8999	-0.0162	7.5E-06
Eomegastrophia sp.	7	0.01918	-3.954	-0.0758	0.00037
Eoplectodonta sp.	2	0.00548	-5.2068	-0.0285	3E-05
Leangella sp.	1	0.00274	-5.8999	-0.0162	7.5E-06
Parastrophinella sp.	2	0.00548	-5.2068	-0.0285	3E-05

Table 24: Locality AK2-01A, Attawapiskat Formation (continued)

Genus / species	N	p_i	$\ln(p_i)$	$p_i*\ln(p_i)$	$(p_i)^2$
Stegerhynchus ekwanensis	1	0.00274	-5.8999	-0.0162	7.5E-06
Cyphonenoidea parvula	1	0.00274	-5.8999	-0.0162	7.5E-06
				H = -1.72	S = 0.3

Table 25: Locality AK3A, Attawapiskat Formation

Genus sp.	N	p_i	$\ln(p_i)$	$p_i*\ln(p_i)$	$(p_i)^2$
Septatrypa varians	160	0.46647	-0.7626	-0.3557	0.2176
Cyphomenoidea parvula	50	0.14577	-1.9257	-0.2807	0.02125
Gotatrypa hedei	40	0.11662	-2.1489	-0.2506	0.0136
Meifodia discoidalis	22	0.06414	-2.7467	-0.1762	0.00411
Lissatrypa variabilis	17	0.04956	-3.0045	-0.1489	0.00246
Gypidula akimiskiformis	12	0.03499	-3.3528	-0.1173	0.00122
Eoplectodonta sp.	7	0.02041	-3.8918	-0.0794	0.00042
Pentameroides septentrionalis	7	0.02041	-3.8918	-0.0794	0.00042
Erilevigatella euthylomata	7	0.02041	-3.8918	-0.0794	0.00042
Clorinda tumidula	7	0.02041	-3.8918	-0.0794	0.00042
Whitfieldella sulcatina	5	0.01458	-4.2283	-0.0616	0.00021
Septatrypa severnensis	2	0.00583	-5.1446	-0.03	3.4E-05
Leptaena sp.	2	0.00583	-5.1446	-0.03	3.4E-05
Atrypoidea prelingulata	1	0.00292	-5.8377	-0.017	8.5E-06
Merista rhombiformis	1	0.00292	-5.8377	-0.017	8.5E-06
Hesperorthis sp.	1	0.00292	-5.8377	-0.017	8.5E-06
Eomegastrophia sp.	1	0.00292	-5.8377	-0.017	8.5E-06
Howellella porcata	1	0.00292	-5.8377	-0.017	8.5E-06
				H = -1.85	S = 0.26

Table 26: Locality AK3B, Attawapiskat Formation

Genus / species	N	p_i	$\ln(p_i)$	$p_i*\ln(p_i)$	$(p_i)^2$
Gotatrypa hedei	18	0.23684	-1.4404	-0.3411	0.05609
Septatrypa varians	17	0.22368	-1.4975	-0.335	0.05003
Pentameroides septentrionalis	15	0.19737	-1.6227	-0.3203	0.03895
Meifodia discoidalis	7	0.09211	-2.3848	-0.2197	0.00848
Whitfieldella sulcatina	5	0.06579	-2.7213	-0.179	0.00433
Erilevigetalla euthylomata	4	0.05263	-2.9444	-0.155	0.00277
Clorinda tumidula	4	0.05263	-2.9444	-0.155	0.00277
Eomegastrophia sp.	3	0.03947	-3.2321	-0.1276	0.00156
Katastrophomena sp.	1	0.01316	-4.3307	-0.057	0.00017
Gypidula rudiplicativa	1	0.01316	-4.3307	-0.057	0.00017
Trimerella ekwanensis	1	0.01316	-4.3307	-0.057	0.00017
				H = -2.00	**S = 0.17**

Table 27: Locality AK3-01A, Attawapiskat Formation

Genus / species	N	p_i	$\ln(p_i)$	$p_i*\ln(p_i)$	$(p_i)^2$
Gotatrypa hedei	71	0.52206	-0.65	-0.3393	0.27255
Septatrypa varians	18	0.13235	-2.0223	-0.2677	0.01752
Clorinda parvolinguifera	8	0.05882	-2.8332	-0.1667	0.00346
Plectatrypa sp.	7	0.05147	-2.9667	-0.1527	0.00265
Hesperorthis davidsoni	6	0.04412	-3.1209	-0.1377	0.00195
Clorinda tumidula	6	0.04412	-3.1209	-0.1377	0.00195
Meifodia discoidalis	3	0.02206	-3.814	-0.0841	0.00049
Eomegastrophia sp.	3	0.02206	-3.814	-0.0841	0.00049
Lissatrypa variabilis	2	0.01471	-4.2195	-0.0621	0.00022
Merista rhombiformis	2	0.01471	-4.2195	-0.0621	0.00022
Leptaena sp.	2	0.01471	-4.2195	-0.0621	0.00022
Mictospirifer jini	2	0.01471	-4.2195	-0.0621	0.00022
Leangella sp.	1	0.00735	-4.9127	-0.0361	5.4E-05
Eoplectodonta sp.	1	0.00735	-4.9127	-0.0361	5.4E-05
Gypidulina biplicata	1	0.00735	-4.9127	-0.0361	5.4E-05
Pentameroides septentrionalis	1	0.00735	-4.9127	-0.0361	5.4E-05
Howellella porcata	1	0.00735	-4.9127	-0.0361	5.4E-05
Meristina sp.	1	0.00735	-4.9127	-0.0361	5.4E-05
				H = -1.83	**S = 0.30**

Table 28: Locality AK4A, Attawapiskat Formation

Genus / species	N	p_i	$\ln(p_i)$	$p_i*\ln(p_i)$	$(p_i)^2$
Gotatrypa hedei	2	0.66667	-0.4055	-0.2703	0.44444
Pentameroides septentrionalis	1	0.33333	-1.0986	-0.3662	0.11111
				H = -0.64	**S = 0.56**

Table 29: Locality AK4B, Attawapiskat Formation

Genus / species	N	p_i	$\ln(p_i)$	$p_i*\ln(p_i)$	$(p_i)^2$
Pentameroides septentrionalis	162	0.75349	-0.283	-0.2133	0.56774
Septatrypa varians	20	0.09302	-2.3749	-0.2209	0.00865
Gotatrypa hedei	10	0.04651	-3.0681	-0.1427	0.00216
Gypidula akimiskiformis	7	0.03256	-3.4247	-0.1115	0.00106
Meifodia discoidalis	6	0.02791	-3.5789	-0.0999	0.00078
Eomegastrophia sp.	3	0.01395	-4.272	-0.0596	0.00019
Trimerella ekwanensis	2	0.0093	-4.6775	-0.0435	8.7E-05
Gypidulina sp.	1	0.00465	-5.3706	-0.025	2.2E-05
Erilevigatella euthylomata	1	0.00465	-5.3706	-0.025	2.2E-05
Clorinda parvolinguifera	1	0.00465	-5.3706	-0.025	2.2E-05
Parastrophinella sp.	1	0.00465	-5.3706	-0.025	2.2E-05
Stegerhynchus ekwanensis	1	0.00465	-5.3706	-0.025	2.2E-05
				H = -1.02	**S = 0.59**

Table 30: Locality AK4C, Attawapiskat Formation

Genus / species	N	p_i	$\ln(p_i)$	$p_i*\ln(p_i)$	$(p_i)^2$
Gotatrypa hedei	30	0.55556	-0.5878	-0.3265	0.30864
Gypidula akimiskiformis	5	0.09259	-2.3795	-0.2203	0.00857
Pentameroides septentrionalis	4	0.07407	-2.6027	-0.1928	0.00549
Lissatrypa variabilis	3	0.05556	-2.8904	-0.1606	0.00309
Septatrypa varians	3	0.05556	-2.8904	-0.1606	0.00309
Leangella sp.	3	0.05556	-2.8904	-0.1606	0.00309
Mictospirifer jini	2	0.03704	-3.2958	-0.1221	0.00137
Eomegastrophia sp.	2	0.03704	-3.2958	-0.1221	0.00137

Table 30: Locality AK4C, Attawapiskat Formation (continued)

Genus / species	N	p_i	$\ln(p_i)$	$p_i*\ln(p_i)$	$(p_i)^2$
Erilevigatella euthylomata	1	0.01852	-3.989	-0.0739	0.00034
Stegerhynchus ekwanensis	1	0.01852	-3.989	-0.0739	0.00034
				H = -1.61	**S = 0.34**

Table 31: Locality AK5A, Attawapiskat Formation

Genus / species	N	p_i	$\ln(p_i)$	$p_i*\ln(p_i)$	$(p_i)^2$
Trimerella ekwanensis	107	0.54315	-0.6104	-0.3315	0.29501
Pentameroides septentrionalis	58	0.29442	-1.2228	-0.36	0.08668
Septatrypa varians	17	0.08629	-2.45	-0.2114	0.00745
Gotatrypa hedei	5	0.02538	-3.6738	-0.0932	0.00064
Erilevigatella euthylomata	2	0.01015	-4.5901	-0.0466	0.0001
Clorinda tumidula	2	0.01015	-4.5901	-0.0466	0.0001
Clorinda parvolinguifera	1	0.00508	-5.2832	-0.0268	2.6E-05
Gypidula akimiskiformis	1	0.00508	-5.2832	-0.0268	2.6E-05
Hesperorthis davidsoni	1	0.00508	-5.2832	-0.0268	2.6E-05
Eoplectodonta sp.	1	0.00508	-5.2832	-0.0268	2.6E-05
Stegerhynchus ekwanensis	1	0.00508	-5.2832	-0.0268	2.6E-05
Septatrypa severnensis	1	0.00508	-5.2832	-0.0268	2.6E-05
				H = -1.25	**S = 0.39**

Table 32: Locality AK5B, Attawapiskat Formation

Genus / species	N	p_i	$\ln(p_i)$	$p_i*\ln(p_i)$	$(p_i)^2$
Eocoelia akimiskii	619	1	0	0	1
				H = 0	**S = 1**

Table 33: Locality AK5C, Attawapiskat Formation

Genus / species	N	p_i	ln(p_i)	p_i*ln(p_i)	(p_i)^2
Pentameroides septentrionalis	23	1	0	0	1
				H = 0	**S = 1**

Table 34: Locality AK5D, Attawapiskat Formation

Genus / species	N	p_i	ln(p_i)	p_i*ln(p_i)	(p_i)^2
Pentameroides septentrionalis	103	0.42387	-0.8583	-0.3638	0.17966
Septatrypa varians	40	0.16461	-1.8042	-0.297	0.0271
Lissatrypa variabilis	30	0.12346	-2.0919	-0.2583	0.01524
Gypidula akimiskiformis	22	0.09053	-2.402	-0.2175	0.0082
Gotatrypa hedei	14	0.05761	-2.854	-0.1644	0.00332
Trimerella ekwanensis	11	0.04527	-3.0952	-0.1401	0.00205
Meifodia discoidalis	9	0.03704	-3.2958	-0.1221	0.00137
Clorinda tumidula	4	0.01646	-4.1068	-0.0676	0.00027
Lissatrypa sp.	3	0.01235	-4.3944	-0.0543	0.00015
Eoplectodonta sp.	2	0.00823	-4.7999	-0.0395	6.8E-05
Atrypoidea lentiformis	1	0.00412	-5.4931	-0.0226	1.7E-05
Clorinda n. sp.	1	0.00412	-5.4931	-0.0226	1.7E-05
Hesperorthis sp.	1	0.00412	-5.4931	-0.0226	1.7E-05
Leptaena sp.	1	0.00412	-5.4931	-0.0226	1.7E-05
Eomegastrophia sp.	1	0.00412	-5.4931	-0.0226	1.7E-05
				H = -1.84	**S = 0.24**

Table 35: Locality AK5E, Attawapiskat Formation

Genus / species	N	p_i	ln(p_i)	p_i*ln(p_i)	(p_i)^2
Trimerella ekwanensis	41	0.57746	-0.5491	-0.3171	0.33347
Pentameroides septentrionalis	26	0.3662	-1.0046	-0.3679	0.1341
Septatrypa varians	4	0.05634	-2.8764	-0.162	0.00317
				H = -0.85	**S = 0.47**

Table 36: Locality AK6-01A, Attawapiskat Formation

Genus / species	N	p$_i$	ln(p$_i$)	p$_i$*ln(p$_i$)	(p$_i$)^2
Septatrypa varians	87	0.42029	-0.8668	-0.3643	0.17664
Gotatrypa hedei	42	0.2029	-1.595	-0.3236	0.04117
Clorinda tumidula	24	0.11594	-2.1547	-0.2498	0.01344
Pentameroides septentrionalis	15	0.07246	-2.6247	-0.1902	0.00525
Erilevigatella euthylomata	7	0.03382	-3.3868	-0.1145	0.00114
Gypidula akimiskiformis	6	0.02899	-3.541	-0.1026	0.00084
Trimerella ekwanensis	4	0.01932	-3.9464	-0.0763	0.00037
Hesperorthis sp.	4	0.01932	-3.9464	-0.0763	0.00037
Eoplectodonta hudsonensis	4	0.01932	-3.9464	-0.0763	0.00037
Meristina sp.	4	0.01932	-3.9464	-0.0763	0.00037
Merista rhombiformis	3	0.01449	-4.2341	-0.0614	0.00021
Whitfieldella sulcatina	3	0.01449	-4.2341	-0.0614	0.00021
Howellella porcata	3	0.01449	-4.2341	-0.0614	0.00021
Mictospirifer jini	1	0.00483	-5.3327	-0.0258	2.3E-05
				H = -1.86	**S = 0.24**

Table 37: Locality AK6-01B, Attawapiskat Formation

Genus / species	N	p$_i$	ln(p$_i$)	p$_i$*ln(p$_i$)	(p$_i$)^2
Pentameroides septentrionalis	130	0.90278	-0.1023	-0.0923	0.81501
Septatrypa varians	10	0.06944	-2.6672	-0.1852	0.00482
Gotatrypa hedei	3	0.02083	-3.8712	-0.0807	0.00043
Clorinda tumidula	1	0.00694	-4.9698	-0.0345	4.8E-05
				H = -0.39	**S = 0.82**

Table 38: Locality AK6-01C, Attawapiskat Formation

Genus / species	N	p$_i$	ln(p$_i$)	p$_i$*ln(p$_i$)	(p$_i$)^2
Lissatrypa variabilis	363	0.94531	-0.0562	-0.0532	0.89362
Septatrypa varians	10	0.02604	-3.6481	-0.095	0.00068
Lissatrypa discoidalis	7	0.01823	-4.0047	-0.073	0.00033
Gotatrypa hedei	4	0.01042	-4.5643	-0.0475	0.00011
				H = -0.27	**S = 0.89**

Table 39: Locality AK7-01A, Attawapiskat Formation

Genus / species	N	p$_i$	ln(p$_i$)	p$_i$*ln(p$_i$)	(p$_i$)^2
Septatrypa varians	44	0.49438	-0.7044	-0.3483	0.24441
Clorinda tumidula	18	0.20225	-1.5983	-0.3232	0.0409
Pentameroides septentrionalis	14	0.1573	-1.8496	-0.2909	0.02474
Gotatrypa hedei	4	0.04494	-3.1023	-0.1394	0.00202
Erilevigatella euthylomata	4	0.04494	-3.1023	-0.1394	0.00202
Meifodia discoidalis	2	0.02247	-3.7955	-0.0853	0.0005
Gypidulina biplicata	1	0.01124	-4.4886	-0.0504	0.00013
Meristina sp.	1	0.01124	-4.4886	-0.0504	0.00013
Eomegastrophia sp.	1	0.01124	-4.4886	-0.0504	0.00013
				H = -1.48	**S = 0.31**

Table 40: Locality AK7-01B, Attawapiskat Formation

Genus / species	N	p$_i$	ln(p$_i$)	p$_i$*ln(p$_i$)	(p$_i$)^2
Septatrypa varians	35	0.30973	-1.172	-0.363	0.09594
Pentameroides septentrionalis	25	0.22124	-1.5085	-0.3337	0.04895
Gotatrypa hedei	21	0.18584	-1.6829	-0.3127	0.03454
Erilevigatella euthylomata	8	0.0708	-2.6479	-0.1875	0.00501
Clorinda tumidula	4	0.0354	-3.3411	-0.1183	0.00125
Meifodia discoidalis	4	0.0354	-3.3411	-0.1183	0.00125
Whitfieldella pygmaea	4	0.0354	-3.3411	-0.1183	0.00125
Trimerella ekwanensis	4	0.0354	-3.3411	-0.1183	0.00125
Eomegastrophia sp.	2	0.0177	-4.0342	-0.0714	0.00031
Septatrypa severnensis	2	0.0177	-4.0342	-0.0714	0.00031
Merista rhombiformis	2	0.0177	-4.0342	-0.0714	0.00031
Hesperorthis davidsoni	1	0.00885	-4.7274	-0.0418	7.8E-05
Stegerhynchus ekwanensis	1	0.00885	-4.7274	-0.0418	7.8E-05
				H = -1.97	**S = 0.19**

Table 41: Locality AK7-01C, Attawapiskat Formation

Genus / species	N	p$_i$	ln(p$_i$)	p$_i$*ln(p$_i$)	(p$_i$)^2
Gotatrypa hedei	10	0.27778	-1.2809	-0.3558	0.07716
Clorinda tumidula	7	0.19444	-1.6376	-0.3184	0.03781
Pentameroides septentrionalis	5	0.13889	-1.9741	-0.2742	0.01929
Septatrypa varians	4	0.11111	-2.1972	-0.2441	0.01235
Gypidula akimiskiformis	2	0.05556	-2.8904	-0.1606	0.00309
Whitfieldella sulcatina	2	0.05556	-2.8904	-0.1606	0.00309
Merista rhombiformis	2	0.05556	-2.8904	-0.1606	0.00309
Septatrypa severnensis	1	0.02778	-3.5835	-0.0995	0.00077
Didymothyris sp.	1	0.02778	-3.5835	-0.0995	0.00077
Eoplectodonta sp.	1	0.02778	-3.5835	-0.0995	0.00077
Eomegastrophia sp.	1	0.02778	-3.5835	-0.0995	0.00077
				H = -2.07	**S = 0.16**

Table 42: Locality AK8-01A, Attawapiskat Formation

Genus / species	N	p$_i$	ln(p$_i$)	p$_i$*ln(p$_i$)	(p$_i$)^2
Pentameroides septentrionalis	69	0.40351	-0.9076	-0.3662	0.16282
Septatrypa varians	67	0.39181	-0.937	-0.3671	0.15352
Trimerella ekwanensis	7	0.04094	-3.1958	-0.1308	0.00168
Gotatrypa hedei	7	0.04094	-3.1958	-0.1308	0.00168
Gypidula akimiskiformis	6	0.03509	-3.3499	-0.1175	0.00123
Erilevigatella euthylomata	4	0.02339	-3.7554	-0.0878	0.00055
Clorinda tumidula	3	0.01754	-4.0431	-0.0709	0.00031
Meifodia discoidalis	3	0.01754	-4.0431	-0.0709	0.00031
Eomegastrophia sp.	3	0.01754	-4.0431	-0.0709	0.00031
Mictospirifer jini	1	0.00585	-5.1417	-0.0301	3.4E-05
Meristina sp.	1	0.00585	-5.1417	-0.0301	3.4E-05
				H = -1.47	**S = 0.32**

Table 43: Locality AK8-01B, Attawapiskat Formation

Genus / species	N	p$_i$	ln(p$_i$)	p$_i$*ln(p$_i$)	(p$_i$)^2
Pentameroides septentrionalis	175	0.70565	-0.3486	-0.246	0.49794
Septatrypa varians	37	0.14919	-1.9025	-0.2838	0.02226
Gotatrypa hedei	15	0.06048	-2.8054	-0.1697	0.00366
Gypidula akimiskiformis	11	0.04435	-3.1155	-0.1382	0.00197
Lissatrypa variabilis	5	0.02016	-3.904	-0.0787	0.00041
Erilevigatella euthylomata	2	0.00806	-4.8203	-0.0389	6.5E-05
Clorinda tumidula	1	0.00403	-5.5134	-0.0222	1.6E-05
Trimerella ekwanensis	1	0.00403	-5.5134	-0.0222	1.6E-05
Whitfieldella sulcatina	1	0.00403	-5.5134	-0.0222	1.6E-05
				H = -1.02	**S = 0.53**

Table 44: Locality AK8-01C, Attawapiskat Formation

Genus / species	N	p$_i$	ln(p$_i$)	p$_i$*ln(p$_i$)	(p$_i$)^2
Septatrypa varians	56	0.32558	-1.1221	-0.3653	0.106
Meifodia discoidalis	32	0.18605	-1.6818	-0.3129	0.03461
Gotatrypa hedei	20	0.11628	-2.1518	-0.2502	0.01352
Gypidula akimiskiformis	17	0.09884	-2.3143	-0.2287	0.00977
Pentameroides septentrionalis	13	0.07558	-2.5825	-0.1952	0.00571
Clorinda tumidula	8	0.04651	-3.0681	-0.1427	0.00216
Mictospirifer jini	7	0.0407	-3.2016	-0.1303	0.00166
Eoplectodonta sp.	6	0.03488	-3.3557	-0.1171	0.00122
Erilevigatella euthylomata	5	0.02907	-3.5381	-0.1029	0.00085
Eomegastrophia sp.	3	0.01744	-4.0489	-0.0706	0.0003
Stegerhynchus ekwanensis	3	0.01744	-4.0489	-0.0706	0.0003
Meristina sp.	2	0.01163	-4.4543	-0.0518	0.00014
				H = -2.04	**S = 0.07**

Table 45: Locality AK8-01D, Attawapiskat Formation

Genus / species	N	pᵢ	ln(pᵢ)	pᵢ*ln(pᵢ)	(pᵢ)²
Eomegastrophia sp.	2	0.5	-0.6931	-0.3466	0.25
Eoplectodonta hudsonensis	1	0.25	-1.3863	-0.3466	0.0625
Pentameroides septentrionalis	1	0.25	-1.3863	-0.0347	0.0625
				H = -0.72	**S = 0.38**

Table 46: Locality AK8-01E, Attawapiskat Formation

Genus / species	N	pᵢ	ln(pᵢ)	pᵢ*ln(pᵢ)	(pᵢ)²
Pentameroides septentrionalis	124	0.79487	-0.2296	-0.1825	0.63182
Septatrypa varians	16	0.10256	-2.2773	-0.2336	0.01052
Eoplectodonta sp.	6	0.03846	-3.2581	-0.1253	0.00148
Gypidula akimiskiformis	5	0.03205	-3.4404	-0.1103	0.00103
Gotatrypa hedei	2	0.01282	-4.3567	-0.0559	0.00016
Parastrophinella sp.	1	0.00641	-5.0499	-0.0324	4.1E-05
Mictospirifer jini	1	0.00641	-5.0499	-0.0324	4.1E-05
Meristina sp.	1	0.00641	-5.0499	-0.0324	4.1E-05
				H = -0.81	**S = 0.65**

Table 47: Locality AK9-01A, Attawapiskat Formation

Genus / species	N	pᵢ	ln(pᵢ)	pᵢ*ln(pᵢ)	(pᵢ)²
Septatrypa varians	97	0.4802	-0.7336	-0.3523	0.23059
Pentameroides septentrionalis	38	0.18812	-1.6707	-0.3143	0.03539
Gypidula akimiskiformis	24	0.11881	-2.1302	-0.2531	0.01412
Gotatrypa hedei	12	0.05941	-2.8234	-0.1677	0.00353
Meristina sp.	8	0.0396	-3.2288	-0.1279	0.00157
Meifodia discoidalis	4	0.0198	-3.922	-0.0777	0.00039
Clorinda tumidula	3	0.01485	-4.2097	-0.0625	0.00022
Clorinda rotunda	3	0.01485	-4.2097	-0.0625	0.00022
Eomegastrophia sp.	3	0.01485	-4.2097	-0.0625	0.00022
Erilevigatella euthylomata	2	0.0099	-4.6151	-0.0457	9.8E-05
Eoplectodonta sp.	2	0.0099	-4.6151	-0.0457	9.8E-05

Table 47: Locality AK9-01A, Attawapiskat Formation (continued)

Genus / species	N	p_i	$\ln(p_i)$	$p_i*\ln(p_i)$	$(p_i)^2$
Howellella porcata	2	0.0099	-4.6151	-0.0457	9.8E-05
Mictospirifer jini	2	0.0099	-4.6151	-0.0457	9.8E-05
Merista rhombiformis	1	0.00495	-5.3083	-0.0263	2.5E-05
Atrypoidea lentiformis	1	0.00495	-5.3083	-0.0263	2.5E-05
				-1.7158	**0.28669**

Table 48: Locality AK9-01B, Attawapiskat Formation

Genus / species	N	p_i	$\ln(p_i)$	$p_i*\ln(p_i)$	$(p_i)^2$
Pentameroides septentrionalis	34	0.36957	-0.9954	-0.3679	0.13658
Septatrypa varians	27	0.29348	-1.226	-0.3598	0.08613
Clorinda tumidula	6	0.06522	-2.73	-0.178	0.00425
Erilevigatella euthylomata	5	0.05435	-2.9124	-0.1583	0.00295
Clorinda rotunda	3	0.03261	-3.4232	-0.1116	0.00106
Leangella segmentum	3	0.03261	-3.4232	-0.1116	0.00106
Gypidula akimiskiformis	2	0.02174	-3.8286	-0.0832	0.00047
Eomegastrophia sp.	2	0.02174	-3.8286	-0.0832	0.00047
Merista rhombiformis	2	0.02174	-3.8286	-0.0832	0.00047
Gotatrypa hedei	1	0.01087	-4.5218	-0.0491	0.00012
Plectatrypa sp.	1	0.01087	-4.5218	-0.0491	0.00012
Lissatrypa variabilis	1	0.01087	-4.5218	-0.0491	0.00012
Hesperorthis sp.	1	0.01087	-4.5218	-0.0491	0.00012
Eoplectodonta sp.	1	0.01087	-4.5218	-0.0491	0.00012
Meristina sp.	1	0.01087	-4.5218	-0.0491	0.00012
Stegerhynchus ekwanensis	1	0.01087	-4.5218	-0.0491	0.00012
Pentlandina sp.	1	0.01087	-4.5218	-0.0491	0.00012
				H = -1.93	**S = 0.23**

Table 49: Locality HP01A, Attawapiskat Formation

Genus / species	N	p_i	$\ln(p_i)$	$p_i*\ln(p_i)$	$(p_i)^2$
Septatrypa varians	115	0.72327	-0.324	-0.2343	0.52312
Pentameroides septentrionalis	11	0.06918	-2.671	-0.1848	0.00479
Gotatrypa hedei	11	0.06918	-2.671	-0.1848	0.00479

Table 49: Locality HP01A, Attawapiskat Formation (continued)

Genus / species	N	p$_i$	ln(p$_i$)	p$_i$*ln(p$_i$)	(p$_i$)^2
Erilevigatella euthylomata	10	0.06289	-2.7663	-0.174	0.00396
Gypidula akimiskiformis	7	0.04403	-3.123	-0.1375	0.00194
Howellella porcata	3	0.01887	-3.9703	-0.0749	0.00036
Lissatrypa sp.	2	0.01258	-4.3758	-0.055	0.00016
				-1.0453	0.5391

Table 50: Locality HP01B, Attawapiskat Formation

Genus / species	N	p$_i$	ln(p$_i$)	p$_i$*ln(p$_i$)	(p$_i$)^2
Pentameroides septentrionalis	55	0.94828	-0.0531	-0.0504	0.89923
Gypidula akimiskiformis	3	0.05172	-2.9618	-0.1532	0.00268
				H = -0.20	**S = 0.90**

Table 51: Locality A1412, Chicotte Formation

Genus / species	N	p$_i$	ln(p$_i$)	p$_i$*ln(p$_i$)	(p$_i$)^2
Stegerhynchus vicina	1	1	0	0	1
				H = 0	**S = 1**

Table 52: Locality A1413, Chicotte Formation

Genus / species	N	p$_i$	ln(p$_i$)	p$_i$*ln(p$_i$)	(p$_i$)^2
Pentamerus oblongus	4	0.57143	-0.5596	-0.3198	0.32653
Costistricklandia gaspeensis	1	0.14286	-1.9459	-0.278	0.02041
Stegerhynchus vicina	1	0.14286	-1.9459	-0.278	0.02041
Gotatrypa sp.	1	0.14286	-1.9459	-0.278	0.02041
				H = -1.15	**S = 0.39**

Table 53: Locality A1416, Chicotte Formation

Genus / species	N	p$_i$	ln(p$_i$)	p$_i$*ln(p$_i$)	(p$_i$)^2
Stegerhynchus vicina	8	1	0	0	1
				H = 0	S = 1

Table 54: Locality A1421, Chicotte Formation

Genus / species	N	p_i	$\ln(p_i)$	$p_i * \ln(p_i)$	$(p_i)^2$
Clorinda rotunda	15	0.83333	-0.1823	-0.1519	0.69444
Eospirifer sp.	2	0.11111	-2.1972	-0.2441	0.01235
Lissatrypa sp.	1	0.05556	-2.8904	-0.1606	0.00309
				-0.5566	0.70988

Table 55: Locality A1522, Chicotte Formation

Genus / species	N	p_i	$\ln(p_i)$	$p_i * \ln(p_i)$	$(p_i)^2$
Stegerhynchus vicina	133	0.95	-0.0513	-0.0487	0.9025
Gotatrypa sp.	4	0.02857	-3.5553	-0.1016	0.00082
Erilevigatella euthylomata	2	0.01429	-4.2485	-0.0607	0.0002
smooth athyridid	1	0.00714	-4.9416	-0.0353	5.1E-05
				H = -0.25	S = 0.90

Table 56: Locality A1560, Chicotte Formation

Genus / species	N	p_i	$\ln(p_i)$	$p_i * \ln(p_i)$	$(p_i)^2$
Eospirifer sp.	5	0.38462	-0.9555	-0.3675	0.14793
Gotatrypa hedei	3	0.23077	-1.4663	-0.3384	0.05325
Leptaena sp.	2	0.15385	-1.8718	-0.288	0.02367
Costistricklandia gaspeensis	2	0.15385	-1.8718	-0.288	0.02367
Pentamerus oblongus	1	0.07692	-2.5649	-0.1973	0.00592
				H = -1.45	**S = 0.25**

Table 57: Locality A1563, Chicotte Formation

Genus / species	N	p_i	$\ln(p_i)$	$p_i * \ln(p_i)$	$(p_i)^2$
Whitfieldella nitida	15	0.38462	-0.9555	-0.3675	0.14793
Gotatrypa hedei	12	0.30769	-1.1787	-0.3627	0.09467
Leptaena sp.	4	0.10256	-2.2773	-0.2336	0.01052
Linguopugnoides sp.	3	0.07692	-2.5649	-0.1973	0.00592
Stegerhynchus vicina	3	0.07692	-2.5649	-0.1973	0.00592
Stegerhynchus cf. angaciensis	1	0.02564	-3.6636	-0.0939	0.00066
Dicoelosia paralata	1	0.02564	-3.6636	-0.0939	0.00066
				H = -1.55	**S = 0.27**

Table 58: Hartung Quarry, Racine Formation

Genus / species	N	p$_i$	ln(p$_i$)	p$_i$*ln(p$_i$)	(p$_i$)^2
Antirhynchonella ventricosta	469	0.40051	-0.915	-0.3665	0.16041
Reserella canalis	193	0.16482	-1.8029	-0.2972	0.02716
Dicoelosia biloba	151	0.12895	-2.0483	-0.2641	0.01663
Leangella dissiticostellata	125	0.10675	-2.2373	-0.2388	0.01139
Meristina sp.	43	0.03672	-3.3044	-0.1213	0.00135
Reticulatrypa sp.	42	0.03587	-3.3279	-0.1194	0.00129
Atrypina magnaventra	31	0.02647	-3.6316	-0.0961	0.0007
Isorthis clivosa	18	0.01537	-4.1752	-0.0642	0.00024
Dolerorthis sp.	16	0.01366	-4.293	-0.0587	0.00019
Sphaerirhynchia sp.	12	0.01025	-4.5807	-0.0469	0.00011
Cyrtia meta	9	0.00769	-4.8684	-0.0374	5.9E-05
Leptaena depressa	8	0.00683	-4.9862	-0.0341	4.7E-05
Protomegastrophia profunda	7	0.00598	-5.1197	-0.0306	3.6E-05
Skenidioides sp.	7	0.00598	-5.1197	-0.0306	3.6E-05
Nucleospira sp.	6	0.00512	-5.2739	-0.027	2.6E-05
Platystrophia sp.	6	0.00512	-5.2739	-0.027	2.6E-05
Oxoplecia niagarensis	5	0.00427	-5.4562	-0.0233	1.8E-05
Plectodonta sp.	4	0.00342	-5.6793	-0.0194	1.2E-05
Howellella sp.	3	0.00256	-5.967	-0.0153	6.6E-06
Stegerhynchus sp.	3	0.00256	-5.967	-0.0153	6.6E-06
Macropleura eudora	3	0.00256	-5.967	-0.0153	6.6E-06
Orbiculoidea sp.	2	0.00171	-6.3725	-0.0109	2.9E-06
Dictyonella reticulata	1	0.00085	-7.0656	-0.006	7.3E-07
Plectatrypa imbricata	1	0.00085	-7.0656	-0.006	7.3E-07
Dalejina sp.	1	0.00085	-7.0656	-0.006	7.3E-07
Eospirifer radiatus	1	0.00085	-7.0656	-0.006	7.3E-07
Ancillotoechia sp.	1	0.00085	-7.0656	-0.006	7.3E-07
Coolinia subplana	1	0.00085	-7.0656	-0.006	7.3E-07
Craniops sp.	1	0.00085	-7.0656	-0.006	7.3E-07
Striispirifer sp.	1	0.00085	-7.0656	-0.006	7.3E-07
				H = -2.01	**S = 0.22**

Table 59: Currie Park Quarry, Racine Formation

Genus / species	N	p$_i$	ln(p$_i$)	p$_i$*ln(p$_i$)	(p$_i$)^2
Reserella canalis	197	0.32998	-1.1087	-0.3659	0.10889
Antirhynchonella ventricosta	104	0.1742	-1.7475	-0.3044	0.03035
Dicoelosia biloba	85	0.14238	-1.9493	-0.2775	0.02027
Leangella dissiticostellata	65	0.10888	-2.2175	-0.2414	0.01185
Reticulatrypa sp.	46	0.07705	-2.5633	-0.1975	0.00594
Isorthis clivosa	32	0.0536	-2.9262	-0.1568	0.00287
Atrypina magnaventra	12	0.0201	-3.907	-0.0785	0.0004
Dolerorthis sp.	12	0.0201	-3.907	-0.0785	0.0004
Howellella sp.	11	0.01843	-3.994	-0.0736	0.00034
Meristina sp.	7	0.01173	-4.446	-0.0521	0.00014
Plectodonta sp.	6	0.01005	-4.6002	-0.0462	0.0001
Dictyonella reticulata	4	0.0067	-5.0056	-0.0335	4.5E-05
Plectatrypa imbricata	4	0.0067	-5.0056	-0.0335	4.5E-05
Philhedra magnacostata	4	0.0067	-5.0056	-0.0335	4.5E-05
Eospirifer radiatus	3	0.00503	-5.2933	-0.0266	2.5E-05
Cyrtia meta	2	0.00335	-5.6988	-0.0191	1.1E-05
Protomegastrophia profunda	2	0.00335	-5.6988	-0.0191	1.1E-05
Oxoplecia niagarensis	2	0.00335	-5.6988	-0.0191	1.1E-05
Stegerhynchus sp.	2	0.00335	-5.6988	-0.0191	1.1E-05
Conchidium multicostatum	2	0.00335	-5.6988	-0.0191	1.1E-05
Schizoramma sp.	2	0.00335	-5.6988	-0.0191	1.1E-05
Nucleospira sp.	1	0.00168	-6.3919	-0.0107	2.8E-06
Platystrophia sp.	1	0.00168	-6.3919	-0.0107	2.8E-06
Coolinia subplana	1	0.00168	-6.3919	-0.0107	2.8E-06
Craniops sp.	1	0.00168	-6.3919	-0.0107	2.8E-06
Pentlandina glypta	1	0.00168	-6.3919	-0.0107	2.8E-06
				H = -2.17	**S = 0.18**

Table 60: Story Quarry, Racine Formation

Genus / species	N	p_i	$\ln(p_i)$	$p_i * \ln(p_i)$	$(p_i)^2$
Reticulatrypa sp.	5	0.26316	-1.335	-0.3513	0.06925
Reserella canalis	4	0.21053	-1.5581	-0.328	0.04432
Antirhynchonella ventricosta	3	0.15789	-1.8458	-0.2914	0.02493
Protomegastrophia profunda	2	0.10526	-2.2513	-0.237	0.01108
Dolerorthis sp.	2	0.10526	-2.2513	-0.237	0.01108
Plectodonta sp.	1	0.05263	-2.9444	-0.155	0.00277
Nucleospira sp.	1	0.05263	-2.9444	-0.155	0.00277
Dictyonella reticulata	1	0.05263	-2.9444	-0.155	0.00277
				H = -1.91	**S = 0.17**

Table 61: Tunnel Excavation, Racine Formation

Genus / species	N	p_i	$\ln(p_i)$	$p_i * \ln(p_i)$	$(p_i)^2$
Antirhynchonella ventricosta	54	0.58065	-0.5436	-0.3156	0.33715
Reserella canalis	11	0.11828	-2.1347	-0.2525	0.01399
Reticulatrypa sp.	8	0.08602	-2.4532	-0.211	0.0074
Dicoelosia biloba	5	0.05376	-2.9232	-0.1572	0.00289
Leangella dissiticostellata	4	0.04301	-3.1463	-0.1353	0.00185
Cyrtia meta	2	0.02151	-3.8395	-0.0826	0.00046
Ancillotoechia sp.	2	0.02151	-3.8395	-0.0826	0.00046
Isorthis clivosa	1	0.01075	-4.5326	-0.0487	0.00012
Atrypina magnaventra	1	0.01075	-4.5326	-0.0487	0.00012
Nucleospira sp.	1	0.01075	-4.5326	-0.0487	0.00012
Oxoplecia niagarensis	1	0.01075	-4.5326	-0.0487	0.00012
Eospirifer radiatus	1	0.01075	-4.5326	-0.0487	0.00012
Conchidium multicostatum	1	0.01075	-4.5326	-0.0487	0.00012
Dolerorthis sp.	1	0.01075	-4.5326	-0.0487	0.00012
				H = -1.58	**S = 0.37**

Appendix 3: Relative Abundance Data

Appendix 3 contains relative abundance data of the brachiopod fauna from the localities of the Attawapiskat Formation. This data was used in principal components analysis (PCA) and cluster analysis of Chapter 4. All values are the percent (%) of the particular species in the particular locality.

Species Legend:

1. *Septatrypa varians*, 2. *Pentameroides septentrionalis*, 3. *Gypidula akimiskiformis*, 4. *Lissatrypa variabilis*, 5. *Gotatrypa hedei*, 6. *Meifodia discoidalis*, 7. *Trimerella ekwanensis*, 8. *Whifieldella suclatina*, 9. *Eomegastrophia philomena*, 10. *Erilevigatella euthylomata*, 11. *Clorinda tumidula*, 12. Smooth atrypoids, 13. *Eoplectodonta* sp., 14. *Eomegastrophia* sp. A, 15. *Meristina* sp., 16. *Mictospirifer jinii*, 17. *Cyphomenoidea parvula*, 18. *Parastrophinella* sp., 19. *Howellella porcata*, 20. *Clorinda parvolinguifera*, 21. *Eomegastrophia* sp., 22. *Leptaena sp.*, 23. *Hesperorthis* sp., 24. *Eoplectodonta hudsonensis*, 25. *Parmula hemisphaerica*, 26. *Septatrypa severnensis*, 27. *Leangella* sp., 28. *Stegerhynchus ekwanensis*, 29. *Merista rhombiformis*, 30. *Rhytidorhachis guttuliformis*, 31. *Hesperorthis davidsoni*, 32. *Plectatrypa* sp., 33. *Lissatrypa discoidalis*, 34. *Clorinda rotunda*, 35. *Gypidulina* sp., 36. *Whitfieldella pygmaea*, 37. *Coolinia* sp., 38. *Atrypoidea prelingulata*, 39. *Leangella segmentum*, 40. *Atrypoidea lentiformis*, 41. *Lissatrypa* sp., 42. *Clorinda* n. sp., 43. *Dalejina striata*, 44. *Dictyonella* sp., 45. *Didymothyris* sp., 46. *Gypidula rudiplicativa*, 47. *Gypidulina biplicata*, 48. *Isorthis* sp., 49. *Katastrophomena* sp., 50. *Pentandina* sp., 51. Spiriferid indet, 52. *Whitfieldella* sp., 53. Athyridid, 54. *Eocoelia akimiskii*

Locality	1	2	3	4	5	6	7	8	9	10
AK1a	14.7	1.7	2.8	48.4	26.5	0.2	0.2	0	0	1
AK1-01a	51.9	3.9	8.5	0.4	22.5	0.8	0.8	0	0	3.5
AK2a	1.1	15.8	64.6	4.4	4.4	0.5	0.5	0	2.7	0.7
AK2b	20.1	1	1.2	14.8	13.1	3.6	0	14	0	0.6
AK2c	17.8	3.9	35	8.2	5.7	6.9	3.1	0.4	6.7	0.9
AK2-01a	51	9	9.6	0	12.3	7.1	0	0.3	0	1.9
AK3a	46.6	2	3.5	5	11.7	6.4	0	1.5	0	2
AK3b	22.4	19.7	0	0	23.7	9.2	1.3	6.6	0	5.3
AK3-01a	13.2	0.7	0	1.5	52.2	2.2	0	0	0	0
AK4a	0	33	0	0	67	0	0	0	0	0
Ak4b	9.3	75.3	3.3	0	4.7	2.8	0.9	0	0	0.5
AK4c	5.6	7.4	9.3	5.6	55.6	0	0	0	0	1.9
AK5a	8.6	29.4	0.5	0	2.5	0	54.3	0	0	1
AK5b	0	0	0	0	0	0	0	0	0	0
AK5c	0	100	0	0	0	0	0	0	0	0
AK5d	16.5	42.4	9.1	12.3	5.8	3.7	4.5	0	0	0
AK5-01a	5.6	36.6	0	0	0	0	57.7	0	0	0
AK6-01a	42	7.2	2.9	0	20.3	0	1.9	1.4	0	3.4
AK6-01b	6.9	90.3	0	0	2.1	0	0	0	0	0
AK6-01c	2.6	0	0	94.5	1	0	0	0	0	0
AK7-01a	49.4	15.7	0	0	4.5	2.2	0	0	0	4.5
AK7-01b	31	22.1	0	0	18.6	3.5	3.5	0	0	7.1
AK7-01c	11.1	13.9	5.6	0	27.8	0	0	5.6	0	0
AK8-01a	39.2	40.4	3.5	0	4.1	1.8	4.1	0	0	2.3
AK8-01b	14.9	70.6	4.4	2	6	0	0.4	0.4	0	0.8
AK8-01c	32.6	7.6	9.9	0	11.6	18.6	0	0	0	2.9
AK8-01d	0	25	0	0	0	0	0	0	0	0
AK8-01e	10.3	79.5	3.2	0	1.3	0	0	0	0	0
AK9-01a	18.8	48	11.9	0	5.9	2	0	0	0	1
AK9-01b	29.3	37	2.2	1.1	1.1	0	0	0	0	5.4
HP01a	72.3	6.9	4.4	0	6.9	0	0	0	0	6.3
HP01b	0	94.8	5.2	0	0	0	0	0	0	0

Locality	11	12	13	14	15	16	17	18	19	20	21
AK1a	0.6	0	1	0	0.2	0.7	0	0	0.6	0	0.2
AK1-01a	1.2	0	5	0	0.4	0.4	0	0	0	0	0
AK2a	0	0	0	0	0.5	0	0	0.7	0	1.1	0
AK2b	0	8.6	1.8	0	0.9	1.6	0	2.6	1.5	0.5	0.4
AK2c	0	0	0	3.7	1.6	0.8	0	1.3	0.9	0.7	0
AK2-01a	1.1	0	0.5	0	0	1.1	0.3	0.5	1.4	1.4	1.9
AK3a	2	0	2	0	0	0	14.6	0	0.3	0	0.3
AK3b	5.3	0	0	0	0	0	0	0	0	0	3.9
AK3-01a	4.4	0	0.7	0	0.7	1.5	0	0	0.7	5.9	2.2
AK4a	0	0	0	0	0	0	0	0	0	0	0
Ak4b	0	0	0	0	0	0	0	0.5	0	0.5	1.4
AK4c	0	0	0	0	0	3.7	0	0	0	0	3.7
AK5a	1	0	0.5	0	0	0	0	0	0	0.5	0
AK5b	0	0	0	0	0	0	0	0	0	0	0
AK5c	0	0	0	0	0	0	0	0	0	0	0
AK5d	1.6	0	0.8	0	0	0	0	0	0	0	0.4
AK5-01a	0	0	0	0	0	0	0	0	0	0	0
AK6-01a	11.6	0	0	0	1.9	0.5	0	0	1.4	0	0
AK6-01b	0.7	0	0	0	0	0	0	0	0	0	0
AK6-01c	0	0	0	0	0	0	0	0	0	0	0
AK7-01a	20.2	0	0	0	1.1	0	0	0	0	0	1.1
AK7-01b	3.5	0	0	0	0	0	0	0	0	0	1.8
AK7-01c	19.4	0	2.8	0	0	0	0	0	0	0	2.8
AK8-01a	1.8	0	0	0	0.6	0.6	0	0	0	0	1.8
AK8-01b	0.4	0	0	0	0	0	0	0	0	0	0
AK8-01c	4.7	0	3.5	0	1.2	4.1	0	0	0	0	1.7
AK8-01d	0	0	0	0	0	0	0	0	0	0	50
AK8-01e	0	0	3.8	0	0.6	0.6	0	0.6	0	0	0
AK9-01a	1.5	0	1	0	4	1	0	0	1	0	1.5
AK9-01b	6.5	0	1.1	0	1.1	0	0	0	0	0	2.2
HP01a	0	0	0	0	0	0	0	0	1.9	0	0
HP01b	0	0	0	0	0	0	0	0	0	0	0

Locality	22	23	24	25	26	27	28	29	30	31	32
AK1a	0.6	0.1	0	0	0	0.2	0.1	0	0	0	0
AK1-01a	0	0	0	0	0	0	0	0	0	0	0
AK2a	1.6	0.1	0	0	0	0.1	0	0	0	0	0
AK2b	0.6	1.6	0.2	2.6	1.6	1.1	0	4	1.2	0	0
AK2c	0.1	0.4	0.9	0	0	0.1	0.6	0	0	0	0
AK2-01a	0	0	0	0	0	0.3	0.3	0	0	0	0
AK3a	0.6	0.3	0	0	0.6	0	0.3	0	0	0	0
AK3b	0	0	0	0	0	0	0	0	0	0	0
AK3-01a	1.5	0	0	0	0	0.7	0	1.5	0	4.4	5.1
AK4a	0	0	0	0	0	0	0	0	0	0	0
Ak4b	0	0	0	0	0	0	0.5	0	0	0	0
AK4c	0	0	0	0	0	5.6	1.9	0	0	0	0
AK5a	0	0	0	0	0.5	0	0.5	0	0	0.5	0
AK5b	0	0	0	0	0	0	0	0	0	0	0
AK5c	0	0	0	0	0	0	0	0	0	0	0
AK5d	0.4	0.4	0	0	0	0	0	0	0	0	0
AK5-01a	0	0	0	0	0	0	0	0	0	0	0
AK6-01a	0	1.9	1.9	0	0	0	0	1.4	0	0	0
AK6-01b	0	0	0	0	0	0	0	0	0	0	0
AK6-01c	0	0	0	0	0	0	0	0	0	0	0
AK7-01a	0	0	0	0	0	0	0	0	0	0	0
AK7-01b	0	0	0	0	1.8	0	0.9	1.8	0	0.9	0
AK7-01c	0	0	0	0	2.8	0	0	5.6	0	0	0
AK8-01a	0	0	0	0	0	0	0	0	0	0	0
AK8-01b	0	0	0	0	0	0	0	0	0	0	0
AK8-01c	0	0	0	0	0	0	1.7	0	0	0	0
AK8-01d	0	0	25	0	0	0	0	0	0	0	0
AK8-01e	0	0	0	0	0	0	0	0	0	0	0
AK9-01a	0	0	0	0	0	0	0	0.5	0	0	0
AK9-01b	0	1.1	0	0	0	0	1.1	2.2	0	0	1.1
HP01a	0	0	0	0	0	0	0	0	0	0	0
HP01b	0	0	0	0	0	0	0	0	0	0	0

Locality	33	34	35	36	37	38	39	40	41	42	43
AK1a	0	0	0	0	0	0	0	0	0	0	0
AK1-01a	0	0	0	0	0	0	0	0	0	0	0.4
AK2a	0	0	0.7	0	0	0.3	0	0	0	0	0
AK2b	0	0	0	0	0	0	0	0	0	0	0
AK2c	0	0	0	0	0.2	0	0	0	0	0	0
AK2-01a	0	0	0	0	0	0	0	0	0	0	0
AK3a	0	0	0	0	0	0.3	0	0	0	0	0
AK3b	0	0	0	0	0	0	0	0	0	0	0
AK3-01a	0	0	0	0	0	0	0	0	0	0	0
AK4a	0	0	0	0	0	0	0	0	0	0	0
Ak4b	0	0	0.5	0	0	0	0	0	0	0	0
AK4c	0	0	0	0	0	0	0	0	0	0	0
AK5a	0	0	0	0	0	0	0	0	0	0	0
AK5b	0	0	0	0	0	0	0	0	0	0	0
AK5c	0	0	0	0	0	0	0	0	0	0	0
AK5d	0	0	0	0	0	0	0	0.4	1.2	0.4	0
AK5-01a	0	0	0	0	0	0	0	0	0	0	0
AK6-01a	0	0	0	0	0	0	0	0	0	0	0
AK6-01b	0	0	0	0	0	0	0	0	0	0	0
AK6-01c	1.8	0	0	0	0	0	0	0	0	0	0
AK7-01a	0	0	0	0	0	0	0	0	0	0	0
AK7-01b	0	0	0	3.5	0	0	0	0	0	0	0
AK7-01c	0	0	0	0	0	0	0	0	0	0	0
AK8-01a	0	0	0	0	0	0	0	0	0	0	0
AK8-01b	0	0	0	0	0	0	0	0	0	0	0
AK8-01c	0	0	0	0	0	0	0	0	0	0	0
AK8-01d	0	0	0	0	0	0	0	0	0	0	0
AK8-01e	0	0	0	0	0	0	0	0	0	0	0
AK9-01a	0	1.5	0	0	0	0	0	0.5	0	0	0
AK9-01b	0	3.3	0	0	0	0	3.3	0	0	0	0
HP01a	0	0	0	0	0	0	0	0	1.3	0	0
HP01b	0	0	0	0	0	0	0	0	0	0	0

Locality	44	45	46	47	48	49	50	51	52	53	54
AK1a	0	0	0	0	0	0	0	0	0	0.1	0
AK1-01a	0.4	0	0	0	0	0	0	0	0	0	0
AK2a	0	0	0	0	0.1	0	0	0	0.1	0	0
AK2b	0	0	0	0	0	0	0	0.1	0	0	0
AK2c	0	0	0	0	0	0	0	0	0	0	0
AK2-01a	0	0	0	0	0	0	0	0	0	0	0
AK3a	0	0	0	0	0	0	0	0	0	0	0
AK3b	0	0	1.3	0	0	1.3	0	0	0	0	0
AK3-01a	0	0	0	0.7	0	0	0	0	0	0	0
AK4a	0	0	0	0	0	0	0	0	0	0	0
Ak4b	0	0	0	0	0	0	0	0	0	0	0
AK4c	0	0	0	0	0	0	0	0	0	0	0
AK5a	0	0	0	0	0	0	0	0	0	0	0
AK5b	0	0	0	0	0	0	0	0	0	0	100
AK5c	0	0	0	0	0	0	0	0	0	0	0
AK5d	0	0	0	0	0	0	0	0	0	0	0
AK5-01a	0	0	0	0	0	0	0	0	0	0	0
AK6-01a	0	0	0	0	0	0	0	0	0	0	0
AK6-01b	0	0	0	0	0	0	0	0	0	0	0
AK6-01c	0	0	0	0	0	0	0	0	0	0	0
AK7-01a	0	0	0	0	0	0	0	0	0	0	0
AK7-01b	0	0	0	1.1	0	0	0	0	0	0	0
AK7-01c	0	2.8	0	0	0	0	0	0	0	0	0
AK8-01a	0	0	0	0	0	0	0	0	0	0	0
AK8-01b	0	0	0	0	0	0	0	0	0	0	0
AK8-01c	0	0	0	0	0	0	0	0	0	0	0
AK8-01d	0	0	0	0	0	0	0	0	0	0	0
AK8-01e	0	0	0	0	0	0	0	0	0	0	0
AK9-01a	0	0	0	0	0	0	0	0	0	0	0
AK9-01b	0	0	0	0	0	0	1.1	0	0	0	0
HP01a	0	0	0	0	0	0	0	0	0	0	0
HP01b	0	0	0	0	0	0	0	0	0	0	0

Appendix 4: Volumetric Data of the Brachiopod Fauna of the Attawapiskat Formation

Appendix 4 contains the minimum, maximum, and average volumetric measurements for the brachiopods fauna of the Attawapiskat Formation used in Chapter 4.

Table 1: Minimum volumetric values

Table 2: Maximum volumetric values

Table 3: Average volumetric values

N/A signifies data not available. Species or genera represented by one measurable specimen contain an average value, but no minimum or maximum value.

Table 1: Minimum volumetric measurements. Min L = minimum length, Min W = minimum width, Min T = minimum thickness, Min V = minimum volume.

Genus sp.	Min L (mm)	Min W (mm)	Min T (mm)	Min V (mm³)
Septatrypa varians	5.6	6	2.5	**28**
Pentameroides septentrionalis	7.7	6.9	5.2	**92.1**
Gypidula akimiskiformis	7.3	9.2	4.3	**96.3**
Lissatrypa variabilis	2.6	2.3	1.2	**2.4**
Gotatrypa hedei	6.8	6.9	3.3	**51.6**
Eocoelia akimiskii				**N/A**
Meifodia discoidalis	4.6	4.8	2.1	**15.5**
Trimerella ekwanensis	35.7	36.9	19.7	**8650.5**
Whitfieldella sulcatina	1.6	1.6	0.9	**0.8**
Eomegastrophia philomena	13.1	15.6	2.5	**170.3**
Erilevigatella euthylomata	6.5	7.5	4	**65**
Clorinda tumidula	13.6	14.4	9.5	**620.2**
smooth atrypoids	1.8	2	0.9	**1.1**
Eoplectodonta sp.	5.4	7.6	1	**13.7**
Eomegastrophia sp. A	9.2	13.1	2.3	**92.4**
Meristina sp.	7.6	5.1	10.8	**139.5**
Mictospirifer jini	2.2	3.5	1.5	**3.9**
Cyphonenoidea parvula				**N/A**
Parastrophinella sp.	2.8	3	1.1	**3.1**
Howellella porcata	4.1	4.9	3	**20.1**
Clorinda parvolinguifera	13.1	14.2	8.8	**545.7**
Eomegastrophia sp.	12.8	17.4	4.9	**363.8**
Leptaena sp.				**N/A**
Hesperorthis sp.	5.8	7	3	**40.6**
Eoplectodonta hudsonensis	6.8	10.2	2.9	**67**
Parmula hemisphaerica	2.6	2.7	0.8	**1.9**
Septatrypa severnensis	4.6	3.9	2	**12**
Leangella sp.	7.8	8.6	3.5	**78.3**
Stegerhynchus ekwanensis	5.7	6.4	4.2	**51.1**
Merista rhombiformis	3.2	2.3	1.3	**3.2**
Rhytidorhachis guttuliformis	3	3.5	1.7	**6**
Hesperorthis davidsoni	8.7	10.7	6.1	**189.3**
Plectatrypa sp.	6.8	7.4	2.9	**48.6**
Lissatrypa discoidalis				**N/A**

Table 1: Minimum volumetric measurements. Min L = minimum length, Min W = minimum width, Min T = minimum thickness, Min V = minimum volume (continued).

Genus **sp.**	**Min L (mm)**	**Min W (mm)**	**Min T (mm)**	**Min V (mm³)**
Clorinda rotunda	13.8	13.8	8.7	**552.3**
Gypidulina sp.	7.5	11	5.5	**151.3**
Whitfieldella pygmaea	4.8	5.1	2.6	**21.2**
Coolinia sp.	7.2	8.8	2.7	**57**
Atrypoidea prelingulata				**N/A**
Leangella segmentum				**N/A**
Atrypoidea lentiformis				**N/A**
Lissatrypa sp.				**N/A**
Clorinda n. sp.				**N/A**
Dalejina striata				**N/A**
Dictyonella sp.				**N/A**
Didymothyris sp.				**N/A**
Gypidula rudiplicativa				**N/A**
Gypidulina biplicata				**N/A**
Isorthis sp.				**N/A**
Katastrophomena sp.				**N/A**
Pentlandina sp.				**N/A**
spiriferid indet				**N/A**
Whitfieldella sp.				**N/A**
athyridid (minute)				**N/A**

Table 2: Maximum volumetric measurements. Max L = maximum length, Max W = maximum width, Max T = maximum thickness, Max V = maximum volume.

Genus sp.	Max L (mm)	Max W (mm)	Max T (mm)	Max V (mm³)
Septatrypa varians	20.5	25	12.1	**2067.2**
Pentameroides septentrionalis	66.4	62.4	46.8	**64,636.4**
Gypidula akimiskiformis	17.1	21.2	15.1	**1824.7**
Lissatrypa variabilis	8	8.8	4.3	**100.9**
Gotatrypa hedei	12.8	14.4	8.8	**540.7**
Eocoelia akimiskii				
Meifodia discoidalis	8.5	9.6	4.6	**125.1**
Trimerella ekwanensis	69.9	60	31.6	**44,176.8**
Whitfieldella sulcatina	6.9	7.7	4.5	**79.7**
Eomegastrophia philomena	34.9	38	7.4	**3271.3**
Erilevigatella euthylomata	15.31	16.9	11.3	**974.6**
Clorinda tumidula	22.6	26	17.6	**3447.3**
smooth atrypoids	3.9	4.3	1.9	**10.6**
Eoplectodonta sp.	21	26.5	7.1	**1317.1**
Eomegastrophia sp. A	18.1	22.8	6.2	**852.9**
Meristina sp.	26.2	29.8	14.9	**3877.8**
Mictospirifer jini	9.9	11.6	7.3	**279.4**
Cyphonenoidea parvula				**N/A**
Parastrophinella sp.	6	5.9	3.8	**44.8**
Howellella porcata	11.1	14.1	7.6	**396.5**
Clorinda parvolinguifera	20	20.6	15.8	**2169.9**
Eomegastrophia sp.	38.3	46.3	8.7	**5142.5**
Leptaena sp.				**N/A**
Hesperorthis sp.	12.3	13.9	5.6	**319.1**
Eoplectodonta hudsonensis	24.8	26.6	6	**1319.4**
Parmula hemisphaerica	4.4	3.9	2.4	**13.7**
Septatrypa severnensis	9.3	9.1	6.3	**177.7**
Leangella sp.	15.3	19	7	**678.3**
Stegerhynchus ekwanensis	8.4	9.8	7.1	**194.8**
Merista rhombiformis	9.3	8.1	6.6	**165.7**
Rhytidorhachis guttuliformis	9.3	8.2	4.2	**106.8**
Hesperorthis davidsoni	13.7	15.5	7.6	**538**
Plectatrypa sp.	10.8	11.8	6.7	**284.6**
Lissatrypa discoidalis				**N/A**

Table 2: Maximum volumetric measurements. Max L = maximum length, Max W = maximum width, Max T = maximum thickness, Max V = maximum volume (continued).

Genus sp.	Min L (mm)	Min W (mm)	Min T (mm)	Max V (mm³)
Clorinda rotunda	16.7	17.6	13.2	**1293.2**
Gypidulina sp.	12.4	14.8	9.4	**575**
Whitfieldella pygmaea	6.6	6.7	4	**59**
Coolinia sp.	12.1	18.1	3.2	**233.6**
Atrypoidea prelingulata				**N/A**
Leangella segmentum				**N/A**
Atrypoidea lentiformis				**N/A**
Lissatrypa sp.				**N/A**
Clorinda n. sp.				**N/A**
Dalejina striata				**N/A**
Dictyonella sp.				**N/A**
Didymothyris sp.				**N/A**
Gypidula rudiplicativa				**N/A**
Gypidulina biplicata				**N/A**
Isorthis sp.				**N/A**
Katastrophomena sp.				**N/A**
Pentlandina sp.				**N/A**
spiriferid indet				**N/A**
Whitfieldella sp.				**N/A**
athyridid (minute)				**N/A**

Table 3: Average volumetric measurements. Av L = average length, Av W = average width, Av T = average thickness, Av V = average volume.

Genus sp.	Av L (mm)	Av W (mm)	Av T (mm)	Av V (mm³)
Septatrypa varians	13.5	14	8.3	**522.9**
Pentameroides septentrionalis	32.7	32.3	21.6	**7604.7**
Gypidula akimiskiformis	11.4	13.4	8.8	**449**
Lissatrypa variabilis	6.5	5.9	3.1	**39.6**
Gotatrypa hedei	9.5	10.5	5.7	**189.5**
Eocoelia akimiskii				**N/A**
Meifodia discoidalis	7.5	7.1	3.3	**58.6**
Trimerella ekwanensis	49.6	45	21.9	**16,293.6**
Whitfieldella sulcatina	3.9	3.6	2.1	**9.8**
Eomegastrophia philomena	21.1	27.8	5.1	**997.2**
Erilevigatella euthylomata	9.4	11.5	6.2	**223.4**
Clorinda tumidula	18.1	19.1	13.5	**1555.7**
smooth atrypoids	3	3	1.2	**3.6**
Eoplectodonta sp.	10	14.5	4	**193.3**
Eomegastrophia sp. A	13.4	16.7	4.3	**320.8**
Meristina sp.	12.6	9.6	17.5	**705.6**
Mictospirifer jini	5.2	6.4	2.3	**25.5**
Cyphonenoidea parvula				**N/A**
Parastrophinella sp.	4.5	5.2	2.2	**17.2**
Howellella porcata	6.9	9	4.4	**91.1**
Clorinda parvolinguifera	16.1	16.3	9.6	**839.8**
Eomegastrophia sp.	21	28.6	6.8	**1361.4**
Leptaena sp.				**N/A**
Hesperorthis sp.	9.8	10.6	4.3	**148.9**
Eoplectodonta hudsonensis	13.6	18.5	5.8	**486.4**
Parmula hemisphaerica	3.1	3.8	1.4	**5.5**
Septatrypa severnensis	6.6	6	4.5	**59.4**
Leangella sp.	12.5	15.5	5.6	**361.7**
Stegerhynchus ekwanensis	6.7	7.2	3.4	**54.7**
Merista rhombiformis	6.2	4.7	2.6	**25.3**
Rhytidorhachis guttuliformis	5.4	5.8	3.1	**32.4**
Hesperorthis davidsoni	11.3	13.4	6.7	**338.2**
Plectatrypa sp.	8.8	9.4	6	**165.4**
Lissatrypa discoidalis				**N/A**

Table 3: Average volumetric measurements. Av L = average length, Av W = average width, Av T = average thickness, Av V = average volume (continued).

Genus sp.	Av L (mm)	Av W (mm)	Av T (mm)	Av V (mm³)
Clorinda rotunda	14.2	17.1	10.4	**841.8**
Gypidulina sp.	10.4	12.1	7.4	**310.4**
Whitfieldella pygmaea	5	5.6	3.1	**28.9**
Coolinia sp.	9.5	14.4	2.7	**123.1**
Atrypoidea prelingulata	16.3	15	9.6	**782.4**
Leangella segmentum	11.6	14	4.6	**249**
Atrypoidea lentiformis	21.6	21.1	11.7	**1777.5**
Lissatrypa sp.	13.1	14.3	6.3	**393.4**
Clorinda n. sp.	9.9	9.1	7.5	**225.2**
Dalejina striata	14	14.7	7.7	**528.2**
Dictyonella sp.				**N/A**
Didymothyris sp.	16.6	14.7	11.7	**951.7**
Gypidula rudiplicativa	22	21.6	17.3	**2740.3**
Gypidulina biplicata	9.6	10.6	7.2	**244.2**
Isorthis sp.	4.4	5.4	1.8	**14.3**
Katastrophomena sp.				**N/A**
Pentlandina sp.	5.2	10.1	0.7	**12.3**
spiriferid indet	4.2	6.3	2.4	**21.2**
Whitfieldella sp.	9.9	8.8	6.2	**180**
athyridid (minute)	3	2.9	1.7	**4.9**

Curriculum Vitae

Name

Cale A.C. Gushulak

Education

- M. Sc., Geology – University of Western Ontario, 2014–2016
- B.Sc. Hons., Biology – Brandon University, 2010–2014

Honours and Awards

- Ontario Graduate Scholarship (OGS), 2015
- Charles A. Southworth Memorial Prize in Paleontology, 2015
- Western Science Entrance Scholarship, 2014
- H. Stewart Perdue Memorial Scholarship, 2014
- Graduated with Distinction, 2014
- Inducted in Brandon University Honour Society, 2014
- Inducted into President's Honour Society, 2014
- J.Y. Tsukamoto Scholarship in Plant Biology, 2013
- Board of Governors Advanced Early Admissions Scholarship, 2010
- Brandon University Board of Governors Entrance Scholarship, 2010

Publications

- **Gushulak, C.A.C.**, Jin, J., and Rudkin, D.M. 2016. Paleolatitudinal morpho-gradient of the early Silurian brachiopod *Pentameroides* in Laurentia. Canadian Journal of Earth Sciences, 53(7): 680–694, doi: 10.1139/cjes-2015-0183.

- **Gushulak, C.A.C.**, West, C.K., and Greenwood, D.R. 2016. Paleoclimate and precipitation seasonality of the Early Eocene McAbee megaflora, Kamloops Group, British Columbia. Canadian Journal of Earth Sciences, 53(6): 591–604.

Conference Presentations

- **Gushulak, C.A.C.**, Jin, J., and Rudkin, D.M. 2015. Paleolatitudinal morpho-gradient of the early Silurian brachiopod *Pentameroides* in Laurentia. IGCP 591, Quebec City, Quebec, 2015.
- **Gushulak, C.A.C.**, Archibald, S.B., and Greenwood, D.R. 2014. Climate of the Early Eocene McAbee macroflora, British Columbia. GSA, Vancouver, British Columbia, 2014.

Related Work Experience

- Graduate Teaching Assistant, University of Western Ontario, 2014-2015
- Teaching Assistant, Brandon University, 2014